

Dissertation der Fakultät für Physik
der
Ludwig-Maximilians-Universität München

Nonperturbative Type IIB Model Building in the F-Theory Framework

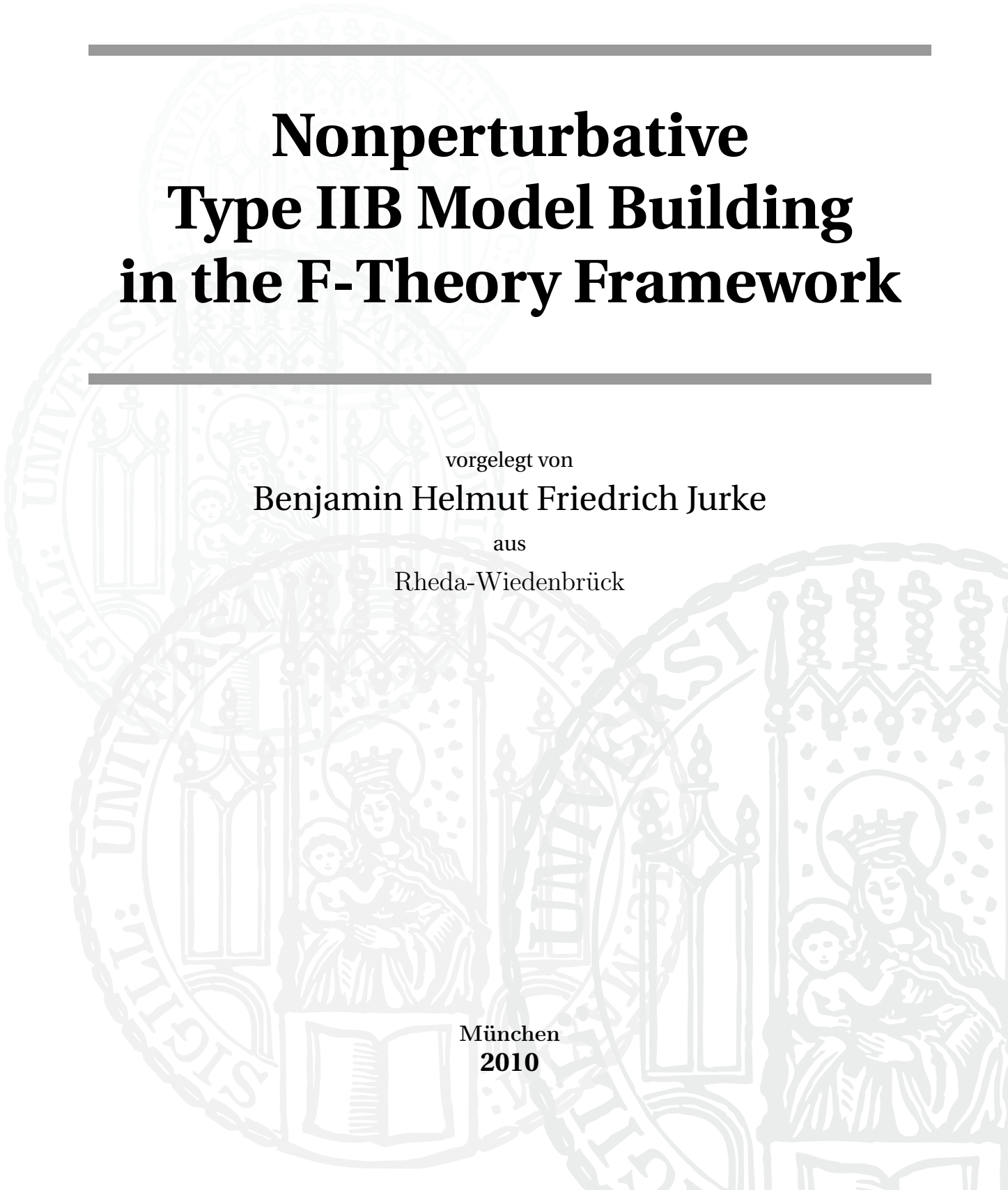
vorgelegt von

Benjamin Helmut Friedrich Jurke

aus

Rheda-Wiedenbrück

München
2010



Benjamin Helmut Friedrich Jurke

**Nonperturbative
Type IIB Model Building
in the F-Theory Framework**



1. *Gutachter:* PD Dr. Ralph Blumenhagen
Max-Planck-Institut für Physik, München, Germany

2. *Gutachter:* Prof. Dr. Ilka Brunner
Ludwig-Maximilians Universität München, Germany

Datum der mündlichen Prüfung: 28. Februar 2011

to whom it may concern...
(and in particular my mother)

Zusammenfassung

Diese Dissertation behandelt das Gebiet der nicht-störungstheoretischen Stringtheorie, die allgemein als vielversprechendster Ansatz zu einer konsistenten Beschreibung der Quantengravitation angesehen wird. Die fünf bekannten zehn-dimensionalen perturbativen Stringtheorien sind durch zahlreiche Dualitäten miteinander verknüpft, sodass eine zugrundeliegende nicht-perturbative elf-dimensionale Theorie, genannt M-Theorie, postuliert wird. Über deren fundamentale Objekte ist aufgrund diverser technischer Schwierigkeiten allerdings nur wenig bekannt.

Zur Typ-IIB-Stringtheorie existiert auch noch ein alternativer nicht-perturbativer Zugang, die F-Theorie. Diese geometrisiert die $SL(2; \mathbb{Z})$ -Selbstdualität der IIB-Theorie in Form einer elliptischen Faserung über der Raumzeit. Darüber hinaus sind auch höherdimensionale Objekte wie etwa 7-Branen als Singularitäten in der geometrischen Beschreibung enthalten. Dieser formal elegante Ansatz erfordert allerdings einen großen technischen Aufwand in der Konstruktion akzeptabler Kompaktifizierungsgeometrien, da sehr viele Aspekte zwangsläufig gleichzeitig behandelt werden müssen. Dafür ist aber eine im Vergleich zur perturbativen Stringtheorie einfachere Erzeugung essenzieller Bausteine für vereinheitlichte Theorien (GUTs) möglich, beispielsweise bestimmte Yukawa-Kopplungen oder Spinor-Darstellung. Ziel der Untersuchungen ist es daher eine vereinheitlichte Theorie innerhalb der F-Theorie zu formulieren, welche gewisse phänomenologische Grundbedingungen erfüllt.

Im Rahmen dieser Arbeit werden zunächst E3-Bran-Instantonen der Typ-IIB-Stringtheorie — also vier-dimensionale Objekte, die sich ausschließlich um die unsichtbaren Dimensionen der Raumzeit wickeln — mit M5-Branen in der F-Theorie in Beziehung gesetzt. Diese Objekte sind von großer Bedeutung für die Erzeugung benötigter Yukawa-Kopplungen oder etwa die Stabilisierung diverser freier Parameter einer Theorie. Bestimmte Eigenschaften der M5-Branen erlauben es dann eine neue Bedingung zu formulieren, wann E3-Branen zum Superpotential beitragen können.

Im Anschluss zu dieser Analyse werden verschiedene Kompaktifizierungsgeometrien konstruiert und ihre prinzipielle Tauglichkeit zur Beschreibung grundlegend realistischer vereinheitlichter Theorien geprüft. Ein entscheidender Punkt ist dabei den Eichfluss auf den enthaltenen 7-Branen korrekt zu beschreiben. Über die Methode der spektralen Überdeckungen — die zunächst noch weiterer Verfeinerungen bedarf — lässt sich

dadurch dann chirale Materie erzeugen und zugleich die vereinheitlichte Eichgruppe zum Standardmodell hin reduzieren. Letztlich gelingt es in dieser Arbeit ein konkretes, vereinheitlichtes Modell mit der Eichgruppe $SU(5)$ im Rahmen der F-Theorie zu konstruieren, welches eine akzeptable Phänomenologie aufzeigt und zudem die beobachteten drei chiralen Materie-Generationen reproduziert.

Summary

This dissertation is concerned with the topic of non-perturbative string theory, which is generally considered to be the most promising approach to a consistent description of quantum gravity. The five known 10-dimensional perturbative string theories are all interconnected by numerous dualities, such that an underlying non-perturbative 11-dimensional theory, called M-theory, is postulated. Due to several technical obstacles, little is known about the fundamental objects in this theory.

There exists an alternative non-perturbative description to type IIB string theory, namely F-theory. Here the $SL(2; \mathbb{Z})$ self-duality of IIB theory is geometrized in the form of an elliptic fibration over the space-time. Moreover, higher-dimensional objects like 7-branes are included via singularities into the geometric picture. This formally elegant description, however, requires significant technical effort for the construction of suitable compactification geometries, as many different aspects necessarily have to be dealt with at the same time. On the other hand, the generation of essential GUT building blocks like certain Yukawa couplings or spinor representations is easier compared to perturbative string theory. The goal of this study is therefore to formulate a unified theory within the framework of F-theory, that satisfies basic phenomenological constraints.

Within this thesis, at first E3-brane instantons in type IIB string theory — 4-dimensional objects that are entirely wrapped around the invisible dimensions of space-time — are matched with M5-branes in F-theory. Such objects are of great importance in the generation of critical Yukawa couplings or the stabilization of the free parameters of a theory. Certain properties of M5-branes then allow to derive a new criterion for E3-branes to contribute to the superpotential.

In the aftermath of this analysis, several compactification geometries are constructed and checked for basic properties that are relevant for semi-realistic unified model building. An important aspect is the proper handling of the gauge flux on the 7-branes. Via the spectral cover description — which at first requires further refinements — chiral matter can be generated and the unified gauge group can be broken to the Standard Model. Ultimately, in this thesis an explicit unified model based on the gauge group $SU(5)$ is constructed within the F-theory framework, such that an acceptable phenomenology and the observed three chiral matter generations are obtained.

Acknowledgments

My particular gratitude goes to my advisor Ralph Blumenhagen, who constantly—in his very own iconic way—encouraged me and let me partake on his numerous insights into string theory and the required mathematics to delve deeper into the subject. I could not have asked for a more stimulating atmosphere in our work group during the countless discussions and research debates. I am also indebted to Dieter Lüst for his constant support and the effort he puts into providing all members of the string theory group with extraordinary opportunities for travel and research.

I am very grateful to my collaborators Andrés Collinucci, Thomas W. Grimm and Timo Weigand, from whom I learned at an unsurpassed pace especially during the first half of my PhD time. It was truly an unique opportunity to work with such a group of gifted people. Likewise, I would also like to thank my later collaborators and (former) office mates Thorsten Rahn and Helmut Roschy for the many productive and humorous hours back in the “cave”, which was recently joined by Andreas Deser. Our time in the office was and still is a constant source of many memorable moments.

Thanks to Oliver Schlotterer for many discussions (and disputes) as well as the occasional shared bottle of wine, a statement which in the same spirit can be extended to my old friend and former office mate Florian Kühnel. For comments on the manuscript of my thesis I would in particular like to thank Florian Kühnel, Thorsten Rahn, Helmut Roschy and Oliver Schlotterer.

Furthermore, I would like to thank—in alphabetical order—Martin Ammon, Volker Braun, Ilka Brunner, James Gray, Michael Haack, James Halverson, Daniel Härtl, Johannes Held, Johanna Knapp, Philipp Kostka, Sebastian Moster, Erik Plauschinn, Felix Rennecke, Maximilian Schmidt-Sommerfeld and Stephan Stieberger for various discussions and the sharing of thoughts and ideas. Moreover, I am grateful to my undergraduate advisor Reinhart Kögerler for pointing me in the right direction.

An important cornerstone for me have always been my longstanding friends from back home, namely Daniel Altemeier, Cathrin and Sebastian Becker, Michael Brockamp, Markus and Martin Menze, Christian Mester and Johannes Röttig. I am looking forward to each opportunity to meet the old circle again. I would also like to mention Philipp Nordhus.

Words seem inadequate for the level of gratitude I have for my mother, who despite

difficult circumstances made my venture into academia possible in the first place and supported me through all those years— thanks, mum! Likewise, I am deeply thankful to my family, in particular my grandmother Gertrud as well as my godfathers Helmut and Friedrich for countless instances of help and support, which also includes my aunt Hannelore. Thanks for all your understanding and encouragement.



This work is part of the String Theory program at the Max Planck Institute of Physics (MPP) in collaboration with the Arnold Sommerfeld Center (ASC) of the Ludwig-Maximilians-Universität München (LMU) and supported by the International Max Planck Research School (IMPRS) on Elementary Particle Physics (EPP) of the Max Planck Society in Munich, Germany.

Publications

During the preparation of this thesis the following five research projects — in collaboration with the indicated authors — and their respective results were published in peer-reviewed journals, listed in chronological order of publication:

Global F-theory GUT model building and related matters:

- Ralph Blumenhagen, Thomas W. Grimm, Benjamin Jurke, Timo Weigand:
“***F-Theory Uplifts and GUTs***”;
JHEP 09 (2009) 053; arXiv:0906.0013 [hep-th], 25+4pp., 2009.
- Ralph Blumenhagen, Thomas W. Grimm, Benjamin Jurke, Timo Weigand:
“***Global F-theory GUTs***”;
Nucl. Phys. B 829 (2010) 325-369; arXiv:0908.1784 [hep-th], 53+5pp., 2009.
- Ralph Blumenhagen, Andrés Collinucci, Benjamin Jurke:
“***On Instanton Effects in F-Theory***”;
JHEP 08 (2010) 079; arXiv:1002.1894 [hep-th], 47+5pp., 2010.

Mathematical algorithm for sheaf cohomology of line bundles:

- Ralph Blumenhagen, Benjamin Jurke, Thorsten Rahn, Helmut Roschy:
“***Cohomology of Line Bundles: A Computational Algorithm***”;
J. Math. Phys. 51 (2010) 103525; arXiv:1003.5217 [hep-th], 10+1pp., 2010.
Subsequent development and support of the C++ implementation **cohomCalc**.
- Ralph Blumenhagen, Benjamin Jurke, Thorsten Rahn, Helmut Roschy:
“***Cohomology of Line Bundles: Applications***”;
arXiv:1010.3717 [hep-th], 53+3pp., 2010.

The material presented in this thesis concerns primarily the first three publications on global F-theory GUT model building and related geometrical issues. The basics of the two mathematical project are summarized in the appendix and are applied in suitable passages of the main text.

Contents

<i>Summary</i>	<i>ix</i>
<i>Acknowledgments</i>	<i>xi</i>
<i>Publications</i>	<i>xiii</i>

Part I Prologue 21

Chapter 1. Stringy Unification of the Standard Model and General Relativity	23
1.1 The Road to Unification	23
1.2 Problems of the Standard Model and General Relativity	25
1.2.1 Theory versus experiment	25
1.2.2 Conceptual inconsistencies	26
1.3 Supersymmetry, Grand Unification and Locality	29
1.4 Overview of String Theory	32
1.4.1 The bosonic string	32
1.4.2 The superstring	33
1.4.3 D-branes	34
1.4.4 Recovering gravity and quantum gauge theory	34
1.4.5 Dealing with higher-dimensional space-time	35
1.4.6 Dualities and M-theory	36
1.4.7 F-theory	37
1.5 Motivation and Outline	38

Part II Preliminaries 41

Chapter 2. Orientifold Compactification of Type II String Theory	43
2.1 Type II Superstring Theory	43
2.1.1 Worldsheet action	43
2.1.2 Mode expansion, quantization and massless closed string spectrum	45
2.1.3 Effective 10d $\mathcal{N}=2$ Type IIB Supergravity	47
2.2 D-branes and Gauge Theory	49
2.3 Four-dimensional Calabi-Yau Compactification	51
2.4 Orientifolds	54
2.5 Intersecting D-branes, O-planes and Chiral Matter	56
2.6 D-brane Instantons	59

2.6.1	General aspects	59
2.6.2	Fermionic zero-modes	61
2.6.3	$U(1)$ -instantons and $O(1)$ -instantons	62
2.7	Flux Compactifications	63
2.8	Phenomenological Aspects and Consistency Conditions	64
2.8.1	Tadpoles	64
2.8.2	Freed-Witten Anomalies	66
2.8.3	K-theory	67
Chapter 3. F-theory as a Non-perturbative Type IIB Framework		69
3.1	Geometrization of Type IIB self-duality	69
3.2	Monodromies and (p,q) -strings	71
3.3	Elliptic Singularities and 7-branes	73
3.4	F-theory via Dualities	76
3.4.1	F-theory and M-theory	76
3.4.2	Elliptic degenerations and M2/M5-brane wrappings	78
3.4.3	Fluxes	79
3.4.4	Other dualities and definitions	81
3.4.5	F-theory and the heterotic string	81
3.5	The Spectral Cover Construction	83
3.6	Consistency Conditions	86
3.7	Weak-coupling Sen Limit	87
3.8	Local vs. Global Model Building	88
3.8.1	The Decoupling Principle	89
3.8.2	Local F-theory GUT model building	90
3.8.3	$U(1)_Y$ -hypercharge flux GUT group breaking	92
3.8.4	Global issues	92
Part III Results & Developments		95
Chapter 4. M5-brane F-theory Instantons and E3-brane Type IIB Instantons		97
4.1	Octic Toy Model Orientifold Geometry	98
4.2	Generic D7-Brane Structure in the Sen Limit	100
4.3	Uncharged Zero-Mode Counting	102
4.3.1	Self-Invariant $O(1)$ E3-brane instantons	102
4.3.2	Non-Self-Invariant $U(1)$ E3/E3'-brane pair instantons	104
4.3.3	Uplifting to vertical M5-branes	105
4.3.4	Interpretation and Analysis	106

4.4	Charged Matter Zero-Mode Counting	107
4.4.1	Matter zero-modes from smooth 7-branes	108
4.4.2	Generalized matter zero-mode counting for non- $SU(n)$ branes	110
4.4.3	Matter zero-modes from the singular remainder component	111
4.5	Relating M5-brane and E3-brane Hodge Diamonds	114
4.6	Phenomenological Implications	117
Chapter 5. GUT Model Geometries in Type IIB and F-theory		121
5.1	Euler Characteristic for Singular O-plane Intersections	122
5.2	Single del Pezzo Transition of the Quintic	123
5.2.1	Type IIB orientifold geometry	123
5.2.2	Uplift Calabi-Yau 4-fold geometry	125
5.2.3	Interpretation of the Euler characteristics	127
5.2.4	Minimal and maximal gauge groups	128
5.2.5	Non-perturbative O7-plane splitting	131
5.2.6	Exceptional gauge groups and absence of $SO(10)$ spinor representations	131
5.3	Double del Pezzo Transition of the Quintic	133
5.3.1	Type IIB orientifold geometry	133
5.3.2	Uplift Calabi-Yau 4-fold geometry	135
5.3.3	Minimal and maximal gauge groups	136
5.3.4	GUT related representations and Yukawa couplings	137
5.4	Non-Generic del Pezzo Transition of the Quartic 3-fold	138
5.4.1	Fano 3-fold bases and non-generic del Pezzo transitions	138
5.4.2	Gauge group enhancements and $SU(5)$ GUT ingredients	141
5.4.3	The $SO(10)$ matter curve	143
Chapter 6. Semi-Realistic Global F-theory GUT Model Building		145
6.1	F-theory Spectral Covers without Heterotic Duals	146
6.1.1	Generic spectral cover construction	146
6.1.2	$SU(5)$ specifics	147
6.2	Global $SU(5)$ GUT Models with Spectral Cover Fluxes	148
6.2.1	Matter curves in the spectral cover description	148
6.2.2	Gauge flux on the $SU(5)$ GUT and matter branes	150
6.2.3	Chiral matter	150
6.2.4	GUT group breaking via hypercharge flux	152
6.3	Split Spectral Cover Refinements	154
6.3.1	$S[U(4)_X \times U(1)_X]$ split spectral cover construction	154
6.3.2	Factorization of matter curves and intersections	157

6.3.3	Chiral matter	158
6.3.4	GUT group breaking via hypercharge flux	161
6.3.5	Computing the Euler characteristic and 3-brane tadpole	162
Chapter 7. A Global F-theory $SU(5)$ GUT with Three Chiral Matter Generations		165
7.1	Construction of the Calabi-Yau 4-fold	165
7.1.1	Transversality of intersecting hypersurfaces	165
7.1.2	Hypersurface constraints and monomials	167
7.1.3	Resolving the $SU(5)$ GUT brane singularity	168
7.2	Gauge fluxes for three chiral matter generations	170
7.2.1	Realizing the split spectral cover	170
7.2.2	Tuning of three chiral matter generations	171
7.2.3	Tuning of the GUT breaking hypercharge flux	172
7.3	Evaluating the Consistency Conditions	173
7.3.1	D-term condition	173
7.3.2	3-brane tadpole condition	174
7.4	Phenomenological Properties	175
Chapter 8. Summary and Outlook		179
8.1	Obtained Results	179
8.2	Future Outlook and Open Questions	182
Part IV Appendices		185
Chapter A. Toric Geometry and Algorithmic Cohomology Computations		187
A.1	Toric Varieties and Fans	187
A.2	Dimensions of Sheaf Cohomology Groups for Line Bundles	189
A.2.1	Computation of multiplicity factors	189
A.2.2	Counting monomials	190
A.3	Using Exactness for Computations	191
A.4	Hypersurfaces and Complete Intersections	192
A.5	Equivariant Cohomology	193
Part Backmatter		cxcvii
<i>Figures & Tables</i>		<i>cxcix</i>
<i>Curriculum Vitæ</i>		<i>cci</i>
<i>Bibliography</i>		<i>cciii</i>

*The greatest obstacle to discovery is
not ignorance —
it is the illusion of knowledge.*

Daniel J. Boorstin
(American historian and writer)

I Prologue

Chapter 1

Stringy Unification of the Standard Model and General Relativity

1.1 The Road to Unification

UNDERSTANDING the laws of nature has relied on the principle of unification from the earliest time man tried to grasp its mysterious ways and workings. In the history of modern mathematical science, classical mechanics and Newtonian gravity unified the seemingly distinct and unrelated motion of objects both in the sky—the wandering of the moon and the planets on the firmament—and down on earth, like the movement of the (in)famous falling apple. It is for this insight and the precise mathematical formulation that Sir Isaac Newton’s book *Philosophiæ Naturalis Principia Mathematica*, of which the first part of three was published in the year 1687, ranks among the most influential texts in history. Roughly two centuries later, in 1864, James Clerk Maxwell’s differential equations of electrodynamics brought together the prior discoveries of Ørsted (magnetism of electric currents), Ampère (magnetic force and circuital law), Faraday (induction of electricity) and others. Those two pillars of classical pre-20th century physics are generally deemed to be *the* groundbreaking discoveries in fundamental science. Only the laws of thermodynamics formulated during the late 19th century—which however are of statistical and emergent nature—could be compared in terms of importance for the future development of physics.

Physics in the 20th century took off with two further instances of unification that led to an explosive growth in knowledge and understanding: Based on Maxwell’s conjecture that electromagnetic waves are traveling with the speed of light and the Galilean principle of relativity, Einstein formulated the theory of special relativity. It was published in 1905 along with three other major discoveries during his *annus mirabilis*. This led

to such fundamental insights like the mass-energy equivalence $E = mc^2$ and eliminated the concept of absolute space and time. Later he combined this theory with Newtonian gravity into the general theory of relativity, whose unified perspective removes the apparent distinction between the effects of gravity and accelerated reference frames. It uses the concept of a curved space-time to encapsulate gravity and showed that movement follows geodesic paths instead of straight lines. The space-time deformation caused by the sun and the planets allowed to understand the perihelion precession of Mercury.

Around the same time, right on the verge of the century in 1900, Max Planck successfully combined Maxwell's electrodynamics with the principles of thermodynamics in order to describe the puzzling black body radiation spectrum by postulating that energy is emitted in discrete quanta instead of a continuous distribution. This unification laid the groundwork for quantum mechanics, which was later combined with special relativity by Dirac and yielded the framework of quantum field theory.

If one carefully traces back all the major and minor unification processes up to the late mid-20th century, two results remain: the theory of general relativity—a successful description of gravity on the large macroscopic scale—as well as the concept of quantum fields that characterizes the effects of forces at the sub-atomic scale. The Standard Model of particle physics is formulated in the latter framework and itself originates from unification processes, bringing together the theory of quantum electrodynamics (QED), the subsequent Glashow-Salam-Weinberg electroweak theory and quantum chromodynamics (QCD). General relativity and the Standard Model provide the foundation of modern theoretical physics.

Naturally, the unification of both theories is expected to be the next logical step in the progress of physical understanding. A unified theory of quantum gravity and Standard Model phenomenology is expected to have the potential to answer a number of substantial questions (like the microscopic details of black hole physics or the origin and fate of the universe). It also seems necessary to remedy numerous conceptual inconsistencies contained in both theories and to explain several curious experimental findings of somewhat younger date.

1.2 Problems of the Standard Model and General Relativity

1.2.1 Theory versus experiment

On the experimental side the Standard Model of particle physics has been confirmed countless times. During its development the existence of a third matter generation was predicted along with the masses of the contained quarks that were indeed found decades later. So far only the postulated Higgs particle— which is responsible for the mass generation within the Standard Model— has eluded its detection. The Standard Model makes no predictions for the Higgs mass,¹ but by LEP experiments it is known at high confidence level that it has to be heavier than 114.4 GeV [1]. In fact, the Standard Model could (at least conceptually) remain valid up to the Planck scale if the Higgs mass is between 115 to 180 GeV. The Tevatron further excluded the mass range of 158 to 175 GeV, and by indirect means a Higgs mass above 185 GeV seems rather unlikely. Theoretically the Higgs mass could be as high as 1.4 TeV, beyond that certain inconsistencies with electroweak symmetry breaking appear. Most indirect theoretical predictions seem to favor a rather light Higgs of about 120 GeV [2]. Much hope is placed on the Large Hadron Collider (LHC) experiment, which is currently in the early stages of data gathering.

The Higgs mass is deeply related to the hierarchy problem of particle physics, which asks why the weak interaction is about 10^{32} times stronger than gravity. Within the Standard Model this can be rephrased to the question why the Higgs mass is so much lighter than the Planck mass

$$m_{\text{Pl}} = \sqrt{\frac{\hbar c}{G}} \approx 1.22 \cdot 10^{19} \frac{\text{GeV}}{c^2} \approx 22 \mu\text{g}.$$

Since any measured mass parameter has to be renormalized in order to remove the radiative loop corrections of virtual particles, an incredible amount of fine-tuning (about 30 orders of magnitude) is required to reach the experimental bounds. One would clearly like to have a better understanding of this process.

Another discrepancy appears in the naive computation of the vacuum energy and the measured value of the cosmological constant— here the mismatch between theory and experiment is as high as 120 orders of magnitude. However, as the Standard Model does not include gravity, this can be interpreted as a strong hint for the missing quantum effects of gravity in the vacuum energy computation. The lack of understanding of

¹In the context of the MSSM (see section 1.3) the supersymmetric Higgs mass can be predicted and the lower range has already been excluded. This does not invalidate the MSSM, but a Higgs mass above 125 GeV would strongly hint at new physics beyond the MSSM.

the cosmological constant is also seen in the accelerated expansion of the universe. Not only does it continuously grow, but according to high-precision measurements of distant supernovae it does so faster and faster. Understanding those effects from the QFT framework requires to cure an energy scale which is much below the electron mass without screwing up all the well-established physics of the Standard Model.

Neither non-accelerated nor the accelerated expansion have been understood at a fundamental level, which together with the observation of galactic rotational curves led to the postulation of dark matter and energy. Those only gravitationally interacting and purely hypothetical forms of energy supposedly make up more than 95% of today's universe. Clearly, both the Standard Model and the theory of general relativity fail to explain significant portions of our universe—both on the microscopic and macroscopic scale.

On the other hand, one has to keep in mind that gravity is very difficult to test experimentally on small scales due to its comparative weakness to the other forces. At the time of writing, the squared-inverse dependence on distances is verified only down to lengths of about $1 \mu\text{m}$.^{II} It therefore cannot be ruled out that the laws of gravity simply are different on small scales with the corresponding implications for particle physics. Conversely, general relativity is also only well tested up to the scale of the solar system. Dark matter and dark energy may also be hints (in disguise) to a different gravitational law at galactic scales. Deviations from the established gravitational law that are extremely small and experimentally very hard to identify on our scale may have drastic effects thousands of light-years away from us. Generalized gravitational theories like “Modified Newtonian Dynamics” (MOND) [4–6] and “Modified Gravity” (MOG) [7] have been considered to bring theory and experiment closer together, but those attempts violate well-established and (apparently) fundamental principles like Lorentz invariance and energy-momentum conservation.

1.2.2 Conceptual inconsistencies

In addition to the unexplained phenomena, both theories suffer from a number of unresolved conceptual shortcomings and are known not to be truly fundamental. Most obviously, they are mutually exclusive—with the Standard Model not including gravity, whereas on the other hand Einstein's theory is not handling the other three forces.

General relativity's range of validity is reached when a massive object's size becomes smaller than its Schwarzschild radius, i.e. when it collapses to a black hole under its own gravity. Mathematically this is described by a point-like singularity in space-time

^{II}Quite recently an experiment based on dielectric microspheres has been proposed, which could improve this value significantly in the near future [3].

that in the simplest case is usually visualized as an infinite funnel. While a limited scope is a generic feature to all theories in natural science, the truly problematic aspect here is that initially well-defined and smooth settings may dynamically propagate into such a singular situation. The life cycle of a star with a huge mass, which ultimately evolves into a black hole, is a prime example of this shortcoming. However, in the case of general relativity the problematic aftermath of the resulting point-like singularity is hidden inside an event horizon that serves as a communication and observation barrier, effectively cutting off access to the regions where the theory breaks down. It is therefore reasonable to assume— if one would like to avoid drastic topology changes of space during the progression of time— that nature obeys a different gravitational law, where e.g. the central black hole singularity is smeared to a smooth solution by quantum effects.

Furthermore, as a classical black hole is characterized only by its mass, charge and angular momentum one might wonder what happens to the information encoded in the particles falling into it, which due to the event horizon is apparently lost to the external observer. While this may be fine in a classical theory, it is a strong contradiction to quantum mechanics. This issue is closely related to the missing microscopic explanation of the Bekenstein-Hawking black hole entropy formula, which was computed using approximative methods that are only valid in situations of low curvature at the event horizon. But this leaves out the important case of microscopic black holes which may account for a significant amount of the mass and in particular the entropy in the universe [8].

A kind of validity protection has to be employed in quantum field theory as well, which already breaks down at the computation of the most basic 1-loop level contributions for any interacting theory. Here self-interactions between charged matter particles and the gauge bosons of the sourced field quickly lead to infinite values and make it necessary to introduce a cutoff at high energy, despite the fact that those contributions in principle have to be considered in the computation of the amplitudes as well. Besides this so-called regularization procedure more involved renormalization techniques are available to deal with several other sources of infinities. Even worse, following an old argument by F. Dyson, the radius of convergence of many perturbation series (in particular the QED one) is actually zero. All those problems were first observed in quantum electrodynamics— still one of the best tested and precisely verified descriptions in physics— and continue to trouble in the subsequently constructed theories leading to the Standard Model. Nevertheless, from a conceptual point of view one has to admit that even the apparently trivial situation of a single electron is not correctly understood within the theory.

Aside from the aforementioned problems there is the issue of arbitrariness, much more prominently found in the Standard Model with its (at least) 19 unrestricted parameters that have to be tuned from empirical data. Clearly, one would like to understand the relations between the values of particle masses and interaction strengths from the theory itself—unfortunately, this insight is completely lacking at the moment. In fact, there is not even a guiding principle that singles out the Standard Model Lagrangian or its gauge group $SU(3)_C \times SU(2)_W \times U(1)_Y$ in the space of anomaly-free, renormalizable quantum gauge field theories other than the observation that it remarkably well seems to reproduce the experimental data and is reasonably simple at the same time. General relativity on the other hand has at least an elegant geometrical origin arising uniquely from a very limited number of input postulates posed by Einstein, which is very much in the spirit of Newton’s theory. It is the only classical theory that captures the effects of a massless spin-2 particle in four space-time dimensions.

Ignoring the individual problems of either theory, one may nevertheless go on with the unification process, which results in a fully unified “theory of everything”, meaning that all four known fundamental interactions are described in a common framework. Considering that general relativity is a classical theory without any kind of fundamental discretization, the traditional approach—which was very fruitful in turning other established theories into their quantum version—rewrites the gravitational interaction into a field theory of its supposed exchange particle, the graviton. But the canonical attempt to quantize gravity fails dramatically. If one naively tries to introduce a spin-2 particle as the gravitational exchange boson in the established quantum field theory framework, one ends up with a non-renormalizable theory where every computation of physically meaningful quantities diverges.

Before one can proceed at all, it is therefore necessary to look closer at the generic fundamental properties of either theory. There are several conceptual key differences: Whereas general relativity is a classical theory with strictly deterministic character, quantum fields are of intrinsically probabilistic nature—as exhibited by the built-in uncertainty principle. Furthermore, the background independence underlying general relativity is incompatible with the framework of quantum field theory, which requires a fixed stage in order to define the fields. A critical aspect is the fact that gravity in contrast to the other three forces introduces a natural scale. Via the mass-energy equivalence gravity couples to all objects while at the same time setting the stage in which those objects propagate and in which the spreading of information is limited by the speed of light. The energy scales of the Standard Model are determined by the masses of the gauge bosons, i.e. the coupling to the Higgs boson, which are not understood at a more fundamental level.

Pushing the energy level further and further up, one expects the effects of quantum gravity at the latest to become important around the Planck scale. Whereas in plain quantum field theory in principle virtual particles of any mass and momentum have to be considered, the inclusion of gravity naturally introduces a cutoff at the energy level, where via the mass-energy equivalence the Schwarzschild radius becomes equal to the Compton wavelength. At this point the notion of a point particle necessarily collapses and a classical black hole is obtained. While the microscopic details of this setting are very speculative, it is clear that from a unified perspective a not too drastic “transition” instead of two completely different descriptions is to be expected. Ultimately, the necessary modifications anticipated from a fundamental theory of quantum gravity are therefore assumed to take care of the rather artificial regularization and renormalization techniques as well as the point-like black hole singularity.

Taking all this into account it does not really seem too surprising that many attempts of the past century have failed to incorporate both gravity and quantum field theory. Einstein himself spent the later decades of his life in search for a unified theory. Both the conceptual foundations of quantum theory and gravity appear to be mutually incompatible, which strongly suggests a more revolutionary approach to the problem.

1.3 Supersymmetry, Grand Unification and Locality

Following the failed attempt to quantize the graviton field in a consistent manner, the discovery of supersymmetry and the subsequently developed supergravity approach again gave reason to hope for a unified theory during the 1970s and 80s. The idea of supersymmetry arises from adding fermionic (anti-commuting) generators to the symmetry algebra, which mathematically corresponds to a \mathbb{Z}_2 -grading of the Poincaré symmetry. This allows to bypass the Coleman-Mandula “no-go theorem” [9] which states that in order to obtain non-trivial scattering amplitudes in any interacting quantum field theory (under reasonable assumptions) there are no other groups than the product of the Poincaré group and some internal group. Its supersymmetric generalization is the Haag-Lopuszański-Sohnius theorem [10], which includes the aforementioned fermionic symmetry generators.

From the resulting representation theory of the Poincaré supergroup one derives a near doubling of the particles expected in the spectrum, i.e. every ordinary particle is supposed to have a supersymmetric partner particle. The theoretical benefit of this approach is a huge cancellation of the diverging contributions in the loop amplitudes, which originally seemed to keep the results finite. In the computation of the vacuum energy the presence of supersymmetry leads to a reduction of 60 orders of magnitude—which unfortunately is still vastly off the expected value.

Supergravity is then the quantum field theory of the spin-2 graviton exchange boson which forms a SUSY multiplet with the spin- $\frac{3}{2}$ gravitino fermion. Unfortunately, for the natural case of minimal $\mathcal{N}=1$ supersymmetry in four space-time dimensions, supersymmetry only manages to cure the divergences at the lower loop levels — for higher loop orders one is still left with the original problem of non-renormalizable divergences. Some specific maximally supersymmetric (and therefore non-chiral) supergravity theories that have been computed to higher orders still have the potential to be finite at all orders [11, 12]. Overall, the supergravity approach is nowadays rather considered to be an effective description of the graviton field at low energies and almost flat space-time curvature, which is suffering from the same conceptual problems like the Standard Model.

The concept of supersymmetry on the other hand is still widely used in modern theories, which makes it necessary to reflect upon its implications. Whereas the theoretical properties of supersymmetry are strikingly elegant — it sparked the very fruitful field of supergeometry in pure mathematics — one has to realize that up to this date no one ever observed any direct hints of supersymmetry. Due to the fact that exact supersymmetry implies the same mass for both supersymmetry partner particles — which would have been observed in experiments a long time ago — it can safely be assumed that supersymmetry is broken at low energies. This is in stark contrast to other examples of progress in physics, where one usually tries to find the underlying symmetry for a seemingly random collection of experimental data. For supersymmetry instead one proposes a symmetry and at the same time has to explain why it is not observed in nature. The usual approach to this problem is to use a spontaneous symmetry breaking like in the Higgs mechanism, where a symmetry is broken below a certain energy scale. This saves the regulatory properties for the troublesome high energy regime and at the same time provides an explanation for our non-observation of supersymmetry. The canonical extension of the Standard Model that includes supersymmetry is called the Minimal Supersymmetric Standard Model (MSSM). Despite its formally elegant properties, one has to keep in mind that the MSSM contains much more free parameters as the Standard Model, such that the problem of arbitrariness is even worse.

Another relevant feature for a so-called “theory of everything” is the concept of grand unification. In the Standard Model of particle physics each one of the three fundamental interactions has its own coupling constant that determines the relative strength and provides a value for the loop expansion. However, the notion of a coupling ‘constant’ is actually a misnomer, since the respective values are varying with the energy scale. Somewhat surprisingly, all three couplings appear almost to intersect at a very high energy scale, which suggests that they are actually low-energy artifacts of an underlying

ing symmetry. If one adds supersymmetry to this thought, one actually finds a perfect intersection of the running couplings at high energies. The idea of embedding the Standard Model gauge group $SU(3)_C \times SU(2)_W \times U(1)_Y$ into a higher dimensional simple group like $SU(5)$ or $SO(10)$ has therefore become rather important [13, 14]. Again, one aims to employ a spontaneous symmetry breaking in order to make contact with the established physics. And again one also has to interject that no experimental data exists to justify or rule out this particular approach — it is only an extrapolation of the running behavior observed and computed at comparatively low energy scales. Furthermore, as the grand unification approach also stays within the established quantum field framework, it is equally doomed not to solve the really troubling conceptual issues, but becomes a useful guide in constructing theories supposedly valid at high energies.

Supersymmetry also offers a potential solution for the hierarchy problem, provided that it exists close to the TeV scale. The radiative quantum corrections to the mass of the Higgs boson — which make it extremely large — tend to cancel out in a supersymmetric theory, thus keeping a relatively small value. However, as there is also no understanding of the Higgs mass itself — the μ -problem — and no natural breaking process of the supersymmetry so far below the GUT scale is known, one effectively replaces the original hierarchy problem by the new problem of (low-energy) supersymmetry breaking.

Depending on one's point of view, all the aforementioned ultra-violet infinities arising in interacting quantum fields can be traced back to the point-like and artificial interaction vertices underlying the framework of interacting quantum fields. Ignoring the quest to include gravity for the moment, a reasonable step is therefore to “smear out” such interaction points, i.e. to introduce a limited level of non-locality in the theory. The principle of locality in quantum field theory is required for causality. The proposed approach also makes it necessary to replace the concept of point particles by some kind of extended fundamental object. Nevertheless, conceptually this can still be interpreted as a rather conservative attempt at generalizing the quantum field concept.

Considering that points are of dimension zero, the goal is therefore to find a theory of extended objects that effectively reproduces the key properties found in the quantum field approach. However, finding such a consistent quantum theory of extended objects proves to be extremely difficult and has in fact only succeeded in dimension one — yielding a theory of quantized strings.

1.4 Overview of String Theory

A proper formulation of string theory that takes all of the aforementioned concepts manifestly into account is still missing. So far there is no background independent description of string theory available, which was originally invented to describe the confinement properties associated to the strong nuclear interaction before the asymptotic freedom underlying quantum chromodynamics was discovered. Instead of a fully dynamical string field theory with intrinsic mechanisms to handle a variable number of fundamental string objects, the current perturbative string theory descriptions rely on considering fixed string topologies inside a fixed space-time. However, this already suffices for the computation of e.g. scattering amplitudes with direct analogies to the QFT framework's summation over different Feynman diagrams. In the following a brief and informal overview of string theory is presented, following the standard references on the subject [15–26].

1.4.1 The bosonic string

The perturbative description of a string is based on a non-linear σ -model for the embedding of a two-dimensional surface into a higher-dimensional target space-time. The surface is called the string worldsheet and combines the one-dimensional spatial extension of the string plus the temporal dimension. It is therefore the canonical generalization of a point particle's worldline. On top of this worldsheet surface lives a conformal field theory (CFT) [27–31]. The conformal symmetry allows for stretching and deforming of the worldsheet as long as local angles are preserved — basically, one ignores all kinds of length information. The only CFTs that have been solved exactly so far and can be quantized are two-dimensional CFTs, which is the major obstacle when attempting to generalize to higher-dimensional objects. The string worldsheet CFT falls precisely into this category of exactly solvable CFTs.

But in general the CFT yields a conformal anomaly from the quantization of the Weyl rescaling symmetry, which is exactly canceled using a 26-dimensional target space-time for the embedding of the worldsheet.^{III} Thus, one ends up with the 26-dimensional bosonic string theory discovered in the late 1960s.

Due to its extended nature a string can have vibrational excitation modes that result in an infinite tower of particle states, each of which gets more massive the higher the

^{III}One can also consider a non-critical string theory, where the dimension is $d \neq 26$. As the conformal anomaly is proportional to the central charge, the non-zero value can be corrected by enabling a non-trivial expectation value for the dilaton. However, this generally violates the Lorentz invariance, which makes non-critical string theory an unsuitable candidate for a theory of quantum gravity.

excitation mode is. However, for the typical values of the string length the mass gap between adjacent modes already is so enormous (determined by $\frac{1}{\ell_s} = \frac{1}{\sqrt{\alpha'}}$ — where α' is the stringy Regge slope — and typically assumed to be of the order of the Planck mass) that only the massless particle spectrum needs to be considered. Nevertheless, certain corrections from massive states to potentially observable scattering amplitudes can be obtained under the assumption of a low string scale [32–34].

The original bosonic string theory suffers from a number of shortcomings: As implied by the name only bosonic states of integer spin are contained in the spectrum, whereas all known fundamental matter particles are of fermionic nature. Even worse, a destabilizing tachyon state of imaginary mass and energy is found as well, ruling out all hopes of this being a physically viable theory.

Nevertheless, the perhaps most surprising aspect of string theory is that from the sole attempt to construct a well-defined quantum theory of one-dimensional extended objects — which is highly constrained by consistency requirements of both physical and mathematical nature — one apparently gets out gravity at the other end. The fact that the bosonic string contains a well-defined spin-2 particle state in its massless spectrum came as a big surprise. It corresponds to the hypothetical graviton interaction boson that eluded all prior attempts of quantization in the ordinary QFT framework.

1.4.2 The superstring

With the inclusion of supersymmetry the two main problems of the bosonic string theory can be dealt with. Supersymmetry by definition implies the presence of fermionic partner states and an appropriate superconformal field theory (SCFT) can be solved and quantized much like in the non-supersymmetric case, providing a supersymmetric worldvolume theory. The troublesome tachyon state is projected out by the GSO projection [35, 36] which ultimately turns the σ -model into its supersymmetric version, yielding target space supersymmetry [37–40]. However, now one has to deal with a superconformal anomaly, which (for the critical theory) cancels only in a 10-dimensional target space-time.

Following this supersymmetrization procedure, one ultimately arrives at the perturbative 10d $\mathcal{N}=2$ type II superstring theory, which comes in a non-chiral IIA and chiral IIB variant. If orientation of the string worldsheet is neglected the 10d $\mathcal{N}=1$ type I superstring can be constructed in the same fashion. The hybrid heterotic string theory is obtained by combining half of the type II superstring with half of the bosonic string. Rolling up all of the mismatching 16 dimensions to a higher-dimensional torus provides the internal gauge group $SO(32)$ or $E_8 \times E_8$, yielding the heterotic $SO(32)$ and $E_8 \times E_8$ theory. In all cases one is left with a theory depending only on a single free parameter:

the string length ℓ_s which is related to α' and T_s .

1.4.3 D-branes

Whereas a point particle has no intrinsic properties, the one-dimensional string can be either of open or closed topology. Due to conservation of internal momentum on the string worldsheet, the endpoints of an open string in type II theory are confined to the worldvolumes of D-branes, which are named for the Dirichlet boundary condition of the string.

D-branes are higher-dimensional objects in string theory, which acquire a dynamical structure due to the open strings ending on them [41]. It should be emphasized that not the D-brane itself is quantized as a fundamental object but rather the open strings on top of it. This effectively equips D-branes with a super-Yang-Mills gauge theory on the worldvolume. By assigning an appropriate background flux to the brane this gauge group can be broken. As spatially extended objects D-branes can intersect. This allows open strings to connect the two branes and produce new massless states along the intersection. Together with an appropriate background flux chiral matter is usually engineered from intersecting brane models [42, 43].

In the type IIA string theory D-branes have even spatial dimension (D0, D2, D4, D6, D8), whereas in type IIB one encounters odd spatial dimensions (D1, D3, D5, D7, D9). The special case of D9-branes effectively allows for freely moving open strings.

1.4.4 Recovering gravity and quantum gauge theory

Closed strings on the other hand are completely unrestricted in their movement through the space-time. As the massless closed string spectrum contains the aforementioned spin-2 particle state, this sector is usually associated with the gravitational aspects of string theory. It also houses the dilaton field that dynamically determines the string coupling g_s .

It is certainly surprising that the only two smooth topologies of a one-dimensional object — the string — can be associated to a gauge sector (open strings) and gravity (closed strings). From this point of view the extended nature of the fundamental object in string theory serves as the means of bridging the gap between general relativity and quantum gauge field theory [44, 45].

Hailed as one of the most important breakthroughs of the string framework, the theory manages via certain wrappings of D-branes to reproduce the Bekenstein-Hawking entropy formula for extremal black holes [46], which has the minimal mass for a given charge and angular momentum. Furthermore, with the fuzzball proposal [47, 48] — where the entire region inside the black hole's event horizon is filled by a dense ball of

interacting strings—a candidate for a general microscopic quantum description of black holes exists [49].

However, despite the apparent elegance of this construction, the perturbative nature of the current formulation does not provide an entirely unified perspective, in particular on general relativity. The fact that we are considering closed strings moving in a fixed space-time introduces a conceptual splitting in the treatment of gravity, which is in contrast to the intrinsically captured back-reaction between energy, matter and the dynamically curved space-time in general relativity. Likewise, the second important property of background independence cannot be manifestly recovered from the perturbative description.

1.4.5 Dealing with higher-dimensional space-time

There exists an obvious mismatch between the number of four dimensions we experience in our everyday world (as well as in all experiments conducted at the microscopic scale so far) and the ten dimensions predicted by perturbative superstring theory. Several approaches have been developed in order to deal with this issue [50, 51].

For once, the world that we experience mostly through the interactions described by gauge theories could be associated to the worldvolume of a D3-brane. As the open strings—the building blocks of the gauge sector—are fixed to this brane, one cannot detect the higher dimensions of space-time from electromagnetic, weak and strong interactions. Furthermore, this approach would also provide an explanation for the relative weakness of gravity measured from our four-dimensional perspective as the closed strings may propagate away from the brane without any restrictions. Our gravitational law would then be a remnant of a higher-dimensional gravitational effect whose suppression with distance is much stronger in ten space-time dimensions [52].

The more conservative approach goes back to an early attempt at unifying general relativity and electromagnetism by considering a five-dimensional space-time and rolling up the fifth dimension to a compact circle of some finite—supposedly very tiny—radius [53]. As one can in principle generalize this idea in order to get effectively rid of an arbitrary number of dimensions, the compactification on a six-dimensional torus was considered much earlier to explain the dimensional mismatch. However, compactifying some dimensions also implies an inversely size-related discretization of the momentum in this direction. For extremely small compact dimensions states of higher momentum are then automatically of much higher energy, such that those higher Kalazu-Klein modes are usually ignored similarly to the higher vibrational string excitation modes, i.e. one once again only considers the effective theory (of lower dimension) obtained from the massless spectrum.

The shape and structure of the compact dimensions has a direct influence on the effective theory. In order to recover the Standard Model phenomenology at some point, one therefore has to find a suitable compactification space. For example, as chiral theories are only possible for $\mathcal{N}=1$ supersymmetry one needs to compactify on Calabi-Yau manifolds [54] and use further ingredients like orientifold symmetries as well as D-branes to obtain 4d $\mathcal{N}=1$ effective theories. In this light the arbitrariness of the Standard Model and the tuning of its parameters is partially found again in terms of geometric moduli that describe the internal geometry of a higher-dimensional string theory.

1.4.6 Dualities and M-theory

The original hope of unveiling a unique theory of gravity and quantum gauge fields is spoiled due to the existence of five perturbative string theories (type I, type IIA and IIB, heterotic $SO(32)$ and $E_8 \times E_8$). However, the subsequent discovery of dualities between those theories suggests again the existence of a single unique underlying theory, called M-theory [55].

In 1995 E. Witten observed that the type IIA superstring seems to “grow” an additional spatial dimension when going into the non-perturbative strong coupling limit $g_s \rightarrow \infty$. A corresponding observation can be made from the heterotic $E_8 \times E_8$ theory, where two completely space-time filling “boundary branes” are pulled apart. Suddenly the one-dimensional string seems to spread out an entire two-dimensional membrane—the M2-brane. By considering different wrappings of the M2-brane together with the dualities, all five perturbative string theories can be recovered from M-theory. Furthermore, its effective low-energy theory precisely corresponds to the 11d $\mathcal{N}=1$ supergravity, which is the unique supergravity theory of maximal dimension and maximal level of supersymmetry that can be constructed. Many indirect arguments therefore strongly suggest that M-theory provides a more unified non-perturbative perspective on the merger of gravity and quantum gauge theory [25, 56–58].

Unfortunately, as M2-branes in M-theory take the place of the fundamental object of the theory, this takes one back to the still unresolved problem of finding a consistent quantum theory of extended higher-dimensional objects—M2-branes are of dimension three (two spatial plus one temporal dimension). Therefore only indirect descriptions of M-theory are available which prohibits direct computation of e.g. M2-brane scattering amplitudes.

Due to the dimensional mismatch between 11d M-theory and the observed 4d world one has to employ the compactification procedure again. The non-perturbative perspective offered by M-theory allows to define a potential on the moduli space of compacti-

fication geometries, which is called the string landscape. Despite the fact that no truly physically realistic selection mechanism is explicitly known, string theory possesses the right ingredients to stabilize the moduli and single out the parameters of the theory. The uniqueness and moduli stabilization possibility inherited by the perturbative string theory limits of M-theory are the main conceptual advantages over the Standard Model or more generally the quantum field theory framework.

1.4.7 F-theory

A technically more accessible treatment of non-perturbative aspects originates from the type IIB superstring. The strong-weak coupling duality that maps g_s to its inverse $\frac{1}{g_s}$ and relates the heterotic $SO(32)$ string to the type I theory is part of a larger self-duality group of the type IIB superstring. In other words, the IIB theory itself already contains the means to represent non-perturbative strong coupling situations via its own perturbative weak coupling description.

C. Vafa first noted that the enhanced self-duality group $SL(2; \mathbb{Z})$ actually corresponds to the reparametrization group of a two-dimensional torus and came up with the idea of using the value of the string coupling-related dilaton ϕ and the D7-brane-sensitive axion C_0 to describe the shape of a torus [59]. This gives rise to an elliptic fibration over the 10d space-time of type IIB and the theory on top of the 12d elliptically-fibered total space is called F-theory.

Further study reveals that much more information is actually stored in this fibration, like for example the location and worldvolume gauge group of non-standard 7-branes with a non-perturbative origin. For example, one can easily obtain exceptional gauge group representations from intersecting branes in the F-theory framework, which are highly relevant for the reproduction of Standard Model phenomenology from GUT theories. In the IIB theory those groups can only be described by considering complicated networks of (p, q) -strings between (p, q) -branes mapped under the $SL(2; \mathbb{Z})$ self-duality [60–65]. Ultimately, the geometrization of F-theory elegantly captures 7-branes and their back-reaction on the ambient geometry in a unified fashion and therefore provides a more proper description of those objects.

In comparison to M-theory one does not create a new fundamental object in F-theory (like the M2-brane) but rather uses a clever geometrization of the innate non-perturbative objects in type IIB theory to provide an alternative non-perturbative perspective on superstrings and 7-branes. As it turns out, the non-perturbative regime of large string coupling g_s almost inevitably becomes relevant in generic type IIB settings.

1.5 Motivation and Outline

At the low energy scale string theory must reproduce the phenomenology described by the Standard Model. One of the numerous branches of string phenomenology discusses type IIB model building using the F-theory framework. After the initial wave of interest in the years following Vafa's original idea, F-theory widely vanished from the list of actively pursued topics. Quite recently (in 2008) a series of papers renewed interest in this framework and introduced the idea of local F-theory GUT model building [66–69]. This was largely motivated by the fact that one can easily realize exceptional gauge groups to generate certain Yukawa couplings in GUT models that require D3-brane instanton corrections in the perturbative type IIB theory [70].

In order to analyze the generic properties of this approach a considerable amount of effort has been spent on local F-theory GUT model building [71–85], where the task of constructing an appropriate compact elliptically-fibered Calabi-Yau 4-fold is neglected. But many consistency and stability conditions can only be evaluated in a fully global model. Sooner or later one is therefore forced to attack the more involved problem of global F-theory GUT model building [86] to check if the promising local effects can actually be realized appropriately and within the same model.

Structure of results

This thesis is concerned with several aspects of global F-theory GUT model building and the correspondence of this non-perturbative framework to perturbative type IIB superstring setups. A small part deals with the development of an efficient algorithm utilized in the zero-mode counting of instantons, which is a result of purely mathematical interest as well.

The following research results are discussed in part III, which are not in chronological order of their development [87–91]:

- **Chapter 4:** Before turning to more sophisticated GUT models, the correspondence between E3-brane instantons in type IIB and M5-brane instanton effects in F-theory is investigated. After matching the zero-mode structures, this allows to study instanton effects in F-theory settings away from the perturbative Sen limit. A new sufficient criterion to generate a nowhere vanishing, uncharged superpotential is derived [89].
- **Chapter 5:** As a first step in the direction of global F-theory GUT building the uplifting of type IIB orientifold GUT model geometries to the corresponding F-theory model is considered to get a better understanding of the non-perturbative

effects on 7-branes and gauge groups [87]. Some of those are usually invisible in the perturbative IIB theory or are extremely difficult to obtain.

- **Chapter 6:** Chiral matter requires the presence of non-trivial gauge flux on the branes, which at the moment can only be described via the spectral cover description borrowed from heterotic theory. Using a split spectral cover construction for an appropriate tuning of gauge fluxes on the GUT 7-brane, many phenomenological conditions can be satisfied in global $SU(5)$ F-theory GUT models [88].
- **Chapter 7:** Ultimately, based on the geometry obtained from a non-generic del Pezzo transition of the quartic $\mathbb{P}^4[4]$, an explicit global F-theory $SU(5)$ GUT model with three chiral matter generations and semi-realistic GUT phenomenology is described [88].

Furthermore, some separate mathematical research results used primarily in chapter 4 are summarized in the appendix part IV:

- **Chapter A:** Counting zero-modes technically requires computing the dimension of certain sheaf cohomology groups, which is in general a rather laborious process. A newly developed algorithm and efficient implementation thereof significantly simplifies this step for future investigations [90, 91].

II Preliminaries

Chapter 2

Orientifold Compactification of Type II String Theory

IN this chapter the first prerequisites needed for the proper definition of the F-theory framework and the subsequent building of semi-realistic GUT models are introduced. Beginning with the effective 10-dimensional $\mathcal{N} = 2$ type IIB supergravity theory that arises from the massless spectrum of the IIB superstring and describes the gravitational closed string sector, D-branes are added to include the open string sector for gauge theory. The subsequent compactification to four space-time dimensions on Calabi-Yau 3-folds has to be enhanced by orientifolding in order to break the effective 4d supersymmetry down to the chiral $\mathcal{N} = 1$ level of the MSSM. Intersecting D-branes, the chiral index as well as D-brane instantons and their zero-mode structure are introduced as well. Briefly mentioned are background fluxes in Calabi-Yau settings. The chapter closes with a summary of the consistency conditions that are to be imposed on any stable and viable model. The exposition follows the standard literature [15–26].

2.1 Type II Superstring Theory

2.1.1 Worldsheet action

The perturbative bosonic string theory is described by a non-linear σ -model.¹ On a (Riemannian) surface Σ for the string worldsheet several scalars are defined whose dynamical values provide an embedding of the worldsheet into the target space-time.

¹In general terms, a non-linear σ -model describes a field theory where the fields take values in a specific target space. This can naturally be interpreted as an embedding of the space (where the fields are defined) into this target space.

This worldsheet theory is described by the Nambu-Goto action

$$S_{\text{NG}} = -T \int_{\Sigma} d\sigma d\tau \sqrt{\left(\dot{X} \cdot X'\right)^2 - \dot{X}^2 X'^2}, \quad (2.1)$$

where $X = (X^0, \dots, X^N)$ is a vector of all scalar fields X^μ with the partial derivatives

$$\dot{X}^\mu := \frac{\partial X^\mu}{\partial \tau} \quad \text{and} \quad X'^\mu := \frac{\partial X^\mu}{\partial \sigma} \quad (2.2)$$

in the two directions on the worldsheet. Classically it is equivalent to the string σ -model Polyakov action

$$S_{\text{P}} = -\frac{T}{2} \int_{\Sigma} d\sigma d\tau \sqrt{-h} h^{\alpha\beta} g_{\mu\nu}(X) \partial_\alpha X^\mu \partial_\beta X^\nu \quad \text{for } \alpha, \beta = 1, 2, \quad (2.3)$$

where h is the auxiliary metric on the string worldsheet Σ . Using an appropriate (local) change of worldsheet coordinates $(\tau, \sigma) \rightarrow (z, \bar{z})$ where $z := e^{\tau+i\sigma}$, one can effectively perform a Wick rotation $\tau \rightarrow -i\tau$ to obtain an Euclidean signature worldsheet metric that is positive definite. The Polyakov action can then be written as

$$S_{\text{P}} = -T \int_{\Sigma} d^2z g_{\mu\nu}(X) \partial X^\mu \bar{\partial} X_\nu. \quad (2.4)$$

The two-dimensional field theory on the string worldsheet has a conformal symmetry that exhibits an anomaly upon quantization. In the presence of 26 scalars X^μ the conformal anomaly precisely cancels, yielding a 26-dimensional space-time for the embedding of the string worldsheet (for bosonic string theory as described by the Polyakov action).

Due to the lack of fermions and the presence of a tachyon state in the bosonic string one opts for a supersymmetric version of the previous approach. The fermionic superpartners $\Psi^\mu = (\psi^\mu, \tilde{\psi}^\mu)^{\text{T}}$ are included in the worldsheet action via

$$S_{\text{RNS}} = -T \int_{\Sigma} d^2z g_{\mu\nu}(X) \left(\partial X^\mu \bar{\partial} X^\nu + \frac{\alpha'}{2} \left(\psi^\mu \bar{\partial} \psi^\nu + \tilde{\psi}^\mu \partial \tilde{\psi}^\nu \right) \right), \quad (2.5)$$

which describes a supersymmetric non-linear σ -model. Here the corresponding superconformal anomaly is canceled in the presence of 10 fields and their respective superpartners, i.e. the target space-time has 10 dimensions into which the superstring worldsheet is embedded by the fields X^μ , $\mu = 0, \dots, 9$. This is usually referred to as the Ramond-Neveu-Schwarz description of the supersymmetric string theory.

2.1.2 Mode expansion, quantization and massless closed string spectrum

Strings can be either open or closed, i.e. topologically equivalent to an interval or a circle. In order to conserve momentum and energy on the open string worldsheet, appropriate boundary conditions have to be imposed:

$$\begin{aligned} \text{von Neumann: } & \partial_\sigma X^r(\tau, \sigma)|_{\sigma=0, 2\pi} = 0 \quad \text{for } r = 0, \dots, p, \\ \text{Dirichlet: } & \delta X^s(\tau, \sigma)|_{\sigma=0, 2\pi} = 0 \quad \text{for } s = p + 1, \dots, 9. \end{aligned} \quad (2.6)$$

In order to preserve full target-space Poincaré invariance, the choice of von Neumann boundary conditions for all dimensions (i.e. $p = 9$) is required. Open strings will be considered further in section 2.2.

Closed strings, on the other hand, require the periodicity $X^\mu(\tau, \sigma + 2\pi) = X^\mu(\tau, \sigma)$. In terms of the complex coordinates z, \bar{z} this periodicity is automatically provided due to $e^{\tau+i(\sigma+2\pi)} = e^{\tau+i\sigma}$, which corresponds to mapping the closed string worldsheet “tube” to an annulus in the complex plane [21]. Together with the equations of motion one obtains a splitting of the fields

$$\begin{aligned} X^\mu(z, \bar{z}) &= X_L^\mu(z) + X_R^\mu(\bar{z}), \\ \psi^\mu(z, \bar{z}) &= \psi^\mu(z), \\ \tilde{\psi}^\mu(z, \bar{z}) &= \tilde{\psi}^\mu(\bar{z}), \end{aligned} \quad (2.7)$$

into independent left- and right-moving (bosonic) as well as chiral and anti-chiral (fermionic) components, which in turn are of strictly holomorphic or anti-holomorphic dependency on the (complex) worldsheet coordinates. Furthermore, the periodicity condition for the fermionic superpartners is only determined up to sign, which leads to the choice

$$\psi^\mu(z + 2\pi) = \begin{cases} +\psi^\mu(z) & \text{Ramond (R)} \\ -\psi^\mu(z) & \text{Neveu-Schwarz (NS)} \end{cases} \quad (2.8)$$

of periodicity conditions. The subsequent splitting into left- and right-moving components reveals the analogous correspondence to (anti)holomorphicity found for the bosons in (2.7). Due to the different periodicity sign the fermions of the Ramond sector and the Neveu-Schwarz sector possess a different mode expansion

$$\begin{aligned} \text{Ramond:} & \quad \psi_L^\mu(z) = \sum_{n \in \mathbb{Z}} d_n^\mu z^{-n-\frac{1}{2}}, & \tilde{\psi}_R^\mu(\bar{z}) &= \sum_{n \in \mathbb{Z}} \tilde{d}_n^\mu \bar{z}^{-n-\frac{1}{2}}, \\ \text{Neveu-Schwarz:} & \quad \psi_L^\mu(z) = \sum_{r \in \mathbb{Z} + \frac{1}{2}} b_r^\mu z^{-r-\frac{1}{2}}, & \tilde{\psi}_R^\mu(\bar{z}) &= \sum_{r \in \mathbb{Z} + \frac{1}{2}} \tilde{b}_r^\mu \bar{z}^{-r-\frac{1}{2}}, \end{aligned} \quad (2.9)$$

whereas the Fourier mode expansion of the bosonic fields takes the form

$$\begin{aligned} X_L^\mu(z) &= \frac{x_0^\mu}{2} - i\frac{\alpha'}{2}p_{0,L}^\mu \ln(z) + i\sqrt{\frac{\alpha'}{2}} \sum_{0 \neq n \in \mathbb{Z}} \frac{\alpha_n^\mu}{n} z^{-n}, \\ X_R^\mu(\bar{z}) &= \frac{x_0^\mu}{2} - i\frac{\alpha'}{2}p_{0,R}^\mu \ln(\bar{z}) + i\sqrt{\frac{\alpha'}{2}} \sum_{0 \neq n \in \mathbb{Z}} \frac{\tilde{\alpha}_n^\mu}{n} \bar{z}^{-n}, \end{aligned} \quad (2.10)$$

where x_0^μ and p_0^μ are the center position and momentum of the string. In order to turn the (so far) classical theory into its quantum version, the canonical (anti-)commutation relations of harmonic oscillators are used:

$$\begin{aligned} \text{bosons:} \quad & [\alpha_m^\mu, \alpha_n^\nu] = [\tilde{\alpha}_m^\mu, \tilde{\alpha}_n^\nu] = m\delta_{m+n,0}\eta^{\mu\nu}, \\ & [x_0^\mu, p_0^\nu] = i\eta^{\mu\nu}, \\ \text{Ramond fermions:} \quad & \{d_m^\mu, d_n^\nu\} = \{\tilde{d}_m^\mu, \tilde{d}_n^\nu\} = \delta_{m+n,0}\eta^{\mu\nu}, \\ \text{Neveu-Schwarz fermions:} \quad & \{b_r^\mu, b_s^\nu\} = \{\tilde{b}_r^\mu, \tilde{b}_s^\nu\} = \delta_{r+s,0}\eta^{\mu\nu}. \end{aligned} \quad (2.11)$$

The quantization of the superstring therefore effectively produces a system of coupled harmonic oscillators. All states can be constructed by acting with the creation and annihilation operators on the ground state. In the Ramond-Neveu-Schwarz formalism this is done in the light-cone gauge, where after an appropriate change of coordinates the dynamical degrees of freedom correspond to the 8 transverse directions $\mu = 2, \dots, 9$ of the embedded string worldsheet. For both the left- and right-moving components of the closed string there is a Ramond and Neveu-Schwarz ground state. Whereas the Neveu-Schwarz sector is tachyonic and therefore unstable, the Ramond sector ground state $|0\rangle_R$ is degenerate and corresponds to a $16_{\mathbb{C}}$ -component Dirac spinor that cannot be supersymmetric to the $8_{\mathbb{R}}$ bosonic components X^μ . Both shortcomings are handled by the GSO projection induced from the G -parity operator [35, 36]

$$G = \begin{cases} \Gamma_{11}(-1)^{F_L} & \text{Ramond (R)} \\ (-1)^{F_L+1} & \text{Neveu-Schwarz (NS)} \end{cases} \quad (2.12)$$

that uses the left-moving fermion excitation number F_L . Together with the equations of motion it truncates the Neveu-Schwarz sector $b_{-\frac{1}{2}}^\mu |0\rangle_{\text{NS}}$ to include only states of positive G -parity,^{II} effectively discarding the tachyon state,^{II} and leaves in the degenerate Ramond sector the choice of chirality for an $8_{\mathbb{R}}$ -component Majorana-Weyl spinor ground state $|\alpha\rangle_R$.

^{II}On the Ramond sector the GSO projection implies a choice of chirality due to the operator Γ_{11} , effectively turning the $16_{\mathbb{C}}$ Dirac spinor into an $8_{\mathbb{C}}$ Weyl spinor. The equation of motion, i.e. the on-shell condition, then halves the degrees of freedom again and effectively give an $8_{\mathbb{R}}$ Majorana-Weyl spinor — a reduction that is only possible in $2 + 8k$ space-time dimensions for $k \in \mathbb{N}$.

bosons:	NS-NS:	$\tilde{b}_{-\frac{1}{2}}^\mu 0\rangle_{\text{NS}} \otimes b_{-\frac{1}{2}}^\nu 0\rangle_{\text{NS}}$	dilaton ϕ (1b) B -field $B_{\mu\nu}$ (28b) graviton $g_{\mu\nu}$ (35b)
	R-R:	$ \alpha\rangle_{\text{R}} \otimes \alpha\rangle_{\text{R}}$	IIA: C_1 (8b), C_3 (56b) IIB: C_0 (1b), C_2 (28b), C_4 (35b)
fermions:	NS-R:	$\tilde{b}_{-\frac{1}{2}}^\mu 0\rangle_{\text{NS}} \otimes \alpha\rangle_{\text{R}}$	dilatino (8f) gravitino (56f)
	R-NS:	$ \alpha\rangle_{\text{R}} \otimes b_{-\frac{1}{2}}^\nu 0\rangle_{\text{NS}}$	dilatino (8f) gravitino (56f)

Table 2.1.: Massless closed string spectrum of type II superstring theory, corresponding to a 10d $\mathcal{N}=2$ supergravity multiplet. The IIB 4-form R-R field C_4 is subject to a self-duality condition of its field strength, which halves the number of the naively expected degrees of freedom for a 4-form field.

Since the closed type II superstring has a left- and right-moving component for all fields, altogether four combinations have to be considered: NS-NS, R-NS, NS-R, R-R. The choice of chirality for both the left- and right-moving Ramond state leads to either the non-chiral type IIA (different chiralities) or the chiral type IIB (same chiralities) superstring theory. Ultimately, the massless spectrum obtained in this construction is given by the states in table 2.1. It can be shown that the resulting states left over after the GSO projection indeed have a 10d $\mathcal{N}=2$ target space-time supersymmetry, as suggested by the agreeing number of bosonic and fermionic degrees of freedom.

2.1.3 Effective 10d $\mathcal{N}=2$ Type IIB Supergravity

Due to the huge mass gap between string states of different excitation levels, only the massless spectrum of table 2.1 is relevant in the effective quantum field theory. This corresponds to the limit $T \rightarrow \infty$ of infinite string tension, where the string length ℓ_s shrinks to zero—yielding a point particle—and the mass gap goes to infinity. The states found in the massless type II spectrum are expected from a supergravity theory, of which there are precisely two in 10d at $\mathcal{N}=2$ supersymmetry level: the type IIA and type IIB supergravity. Conversely, the type IIA and IIB superstring theory is usually interpreted as the ultraviolet (high-energy) completion of the respective supergravities.

One problematic aspect of the type IIB superstring theory is the 4-form R-R field C_4 , which is subject to a self-duality of the associated field strength. Unfortunately, no

effective supergravity formulation is known that manifestly incorporates this condition. The bosonic part of the type IIB supergravity action (in Einstein frame) [26]

$$S_{\text{IIB}} = \frac{1}{2\kappa_{10}^2} \int d^{10}x \sqrt{-g} R - \frac{1}{4\kappa_{10}^2} \int \left[\frac{|d\tau|^2}{(\text{Im } \tau)^2} + \frac{|G_3|^2}{\text{Im } \tau} + \frac{|\tilde{F}_5|^2}{2} + C_4 \wedge H_3 \wedge F_3 \right] \quad (2.13)$$

in the democratic formulation therefore has to be supplied with the self-duality constraint $\tilde{F}_5 = \star \tilde{F}_5$. Here $|F|^2 = F \wedge \star \bar{F}$ is used. In the above formulation the following field redefinitions are used:

$$\begin{aligned} \text{complex axion-dilaton: } & \tau := C_0 + i e^{-\phi}, \\ \text{NS-NS field strength: } & H_3 := dB_2, \\ \text{R-R field strengths: } & F_p := dC_{p-1} \quad \text{for } p = 1, 3, 5, \\ \text{mixed fields: } & \tilde{F}_5 := F_5 - \frac{1}{2} C_2 \wedge H_3 + \frac{1}{2} B_2 \wedge F_3, \\ & G_3 := F_3 - \tau H_3. \end{aligned} \quad (2.14)$$

Non-trivial background fluxes will be discussed further in section 2.7.

A central aspect of the type IIB theory is the $SL(2; \mathbb{R})$ symmetry of the (classical) action, which is reduced to $SL(2; \mathbb{Z})$ in the quantum theory. The transformation takes the form

$$\begin{aligned} \text{axio-dilaton: } & \tau \mapsto \frac{a\tau + b}{c\tau + d}, \\ \text{metric: } & g_{\mu\nu} \mapsto g_{\mu\nu}, \\ \text{\textit{p}-form fields: } & \begin{pmatrix} H_3 \\ F_3 \end{pmatrix} \mapsto \begin{pmatrix} d & c \\ b & a \end{pmatrix} \begin{pmatrix} H_3 \\ F_3 \end{pmatrix} \quad \text{for } \begin{pmatrix} a & b \\ c & d \end{pmatrix} \in SL(2; \mathbb{R}), \\ & G_3 \mapsto \frac{G_3}{c\tau + d}, \\ & \tilde{F}_5 \mapsto \tilde{F}_5, \end{aligned} \quad (2.15)$$

and provides the basis for the construction of F-theory later on. The non-perturbative properties essentially originate in this extended strong-weak coupling self-duality, which is special among all string theories.

bosons:	NS:	$\psi_{-\frac{1}{2}}^\mu 0\rangle_{\text{NS}}$	gauge vector A_μ (8b)
fermions:	R:	$ \alpha\rangle_{\text{R}}$	gaugino (8f)

Table 2.2.: Massless open string spectrum of type II superstring theory with a single D-brane and a single open string, corresponding to a 10d $\mathcal{N}=1$ vector multiplet.

2.2 D-branes and Gauge Theory

Aside from closed strings, one can also consider open strings, which are subject to the boundary conditions (2.6). The Dirichlet boundary condition requires a vanishing of the field's variation at the string endpoints, i.e. the string motion at the endpoints is restricted to a p -dimensional plane. The number p counts the remaining dimensions of unrestricted spatial movement — the non-Dirichlet dimensions — and the plane of movement is called a Dirichlet brane or Dp -brane for short.

A D-brane is not a static object in string theory. Instead it receives its dynamics indirectly from the attached open strings. With respect to the changed boundary conditions the mode expansions (2.9) and (2.10) and subsequent canonical quantization procedure (2.11) can be worked out again for an open string starting and ending on the same brane. This leads to the massless open string spectrum in table 2.2. The 10d $\mathcal{N}=1$ vector multiplet adds a supersymmetric gauge sector to the theory. The $9 - p$ components of the vector A_μ normal to the D-brane are deformation scalars and describe fluctuations of the D-brane. The remaining components give rise to an Abelian $U(1)$ worldvolume gauge theory on the D-brane. Those dynamical properties and the subsequent coupling to the closed string background fields are described by the Dirac-Born-Infeld action

$$S_{\text{DBI}} = -\mu_p \int_W d^{p+1}\xi e^{-\phi(X)} \sqrt{-\det \left(g_{\mu\nu}(X) + B_{\mu\nu} + 2\pi\alpha' F_{\mu\nu}(X) \right)}, \quad (2.16)$$

where μ_p is the Dp -brane tension, ξ are the coordinates on the $(p + 1)$ -dimensional worldvolume and F is the gauge field strength of the vector field A_μ . Nontrivial gauge fluxes for F will be considered later in section 2.5.

The presence of a D-brane breaks several symmetries of the bulk closed string vacuum, e.g. translational invariance. For a stable $\frac{1}{2}$ -BPS brane half of the original supersymmetries are broken, leaving a 10d $\mathcal{N}=1$ superstring theory. Furthermore, D-branes carry an R-R charge which due to charge conservation turns D-branes into stable objects [41]. The even/odd difference in the R-R fields between type IIA and IIB theory is therefore

found in the dimension of the D-branes as well:

$$\begin{aligned} \text{IIA theory: } & \text{D0, D2, D4, D6, D8,} \\ \text{IIB theory: } & \text{D(-1), D1, D3, D5, D7, D9,} \end{aligned} \quad (2.17)$$

where the D(-1)-branes in type IIB theory — a single point in space-time — are a somewhat special case. The coupling to the R-R background fields is described by the Chern-Simons action

$$S_{\text{CS}} = -\mu_p \int_W \text{ch}(2\pi\alpha' F) \wedge \sqrt{\frac{\hat{\mathcal{A}}(R_T)}{\hat{\mathcal{A}}(R_N)}} \wedge \sum_q C_q, \quad (2.18)$$

where $\hat{\mathcal{A}}(R_T)$ and $\hat{\mathcal{A}}(R_N)$ are the $\hat{\mathcal{A}}$ -genera of the worldvolume's tangent and normal bundle. Note that via the Hodge duality of the associated field strengths one distinguishes between electric and magnetic couplings to the R-R potentials, which is incorporated in the formulation above. A potential C_{p+1} couples “electrically” to a D p -brane with the associated field strength $F_{p+2} = dC_{p+1}$. Magnetic couplings analogous to classical electrodynamics are introduced by considering the Hodge dual field strength:

$$F'_{10-p-2} := \star F_{p+2} = \star dC_{p+1}. \quad (2.19)$$

Assuming that this dual field strength F'_{10-p-2} also arises from a R-R potential via $F'_{10-p-2} = dC_{10-p-3}$ it follows for the coupling that a

$$\text{D}p\text{-brane couples } \left\{ \begin{array}{l} \text{electrically to } C_{p+1} \\ \text{magnetically to } C_{7-p}. \end{array} \right. \quad (2.20)$$

For $p = 3$ this gives rise to the aforementioned self-duality constraint $\star \tilde{F}_5 = \tilde{F}_5$ as electrical and magnetical coupling are identical. This gives the following coupling for all D-branes:

$$\begin{array}{ll} \text{Type IIA: D0: } & C_1 \quad C_7 \\ & \text{D2: } C_3 \quad C_5 \\ & \text{D4: } C_5 \quad C_3 \\ & \text{D6: } C_7 \quad C_1 \\ & \text{D8: } C_9 \\ \text{Type IIB: D(-1): } & C_0 \quad C_8 \\ & \text{D1: } C_2 \quad C_6 \\ & \text{D3: } C_4 \quad C_4 \text{ (self-dual)} \\ & \text{D5: } C_6 \quad C_2 \\ & \text{D7: } C_8 \quad C_0 \\ & \text{D9: } C_{10} \end{array} \quad (2.21)$$

Stacks of coincident D-branes lead to an enhancement of the worldvolume theory's gauge group. The open string that produces the vector multiplet can now have end-points on different D-branes, leading to an $U(n)$ gauge group for n coincident D-branes.

Non-coincident parallel D-branes contribute to the massive spectrum— with the mass determined by the spatial separation— and therefore are irrelevant for the massless spectrum considered in effective theories. Intuitively the gauge enhancement for stacks of D-branes can be treated as n parallel mutually approaching D-branes with $U(1)^n$ gauge group that is enhanced to $U(n)$ when the strings stretching between different branes become massless upon collision. Furthermore, one can also consider non-coincident intersecting D-branes, which will be discussed in section 2.5.

2.3 Four-dimensional Calabi-Yau Compactification

The type II superstring requires a 10-dimensional target space-time for anomaly cancellation. In order to make contact with the apparently flat 4d space-time the usual approach is to compactify 6 spatial dimensions to small size, which makes them invisible to low-energy physics. In general, with respect to basic symmetries like Poincaré invariance, the target space-time \mathcal{M}_{10} is in fact fibered over the flat space-time $\mathbb{R}^{1,3}$, which leads to a warped space-time metric

$$ds^2 = \underbrace{e^{A(y)} g_{\mu\nu} dx^\mu dx^\nu}_{\text{flat 4d coordinates}} + \underbrace{e^{-A(y)} g_{mn} dy^m dy^n}_{\text{internal space}}. \quad (2.22)$$

for the most general ansatz. The term $A(y)$, which only depends on the internal space to preserve homogeneity and isotropy in the flat 4d space-time, can be used to describe back-reactions of fluxes that are potentially present in the setting. However, for many types of compactification the warp factor $e^{A(y)}$ is neglected for reasons of simplicity. The assumption is therefore to consider a product target space-time

$$\mathcal{M}_{10} = \mathbb{R}^{1,3} \times \mathcal{X}, \quad (2.23)$$

where \mathcal{X} is the compact 6d internal space and $A(y) = 0$. A non-zero warp factor would also affect the Calabi-Yau condition discussed below.

One of the most restrictive phenomenological requirements is the presence of low-energy minimal supersymmetry. Since only minimally supersymmetric $\mathcal{N}=1$ theories allow for chiral matter, the bulk $\mathcal{N}=2$ supersymmetry— which yields an effective 4d $\mathcal{N}=8$ theory in the absence of supersymmetry breaking like for T^6 -compactifications— must be partially broken during the compactification. On the other hand any presence of supersymmetry requires the existence of at least one supersymmetry-generating spinor in the 10d space-time, which decomposes in the product space-time to the existence of a parallel^{III} spinor (i.e. $w_2(\mathcal{X}) = 0$) on the non-trivial compact space. One can show

^{III}A parallel spinor is a covariantly constant, nowhere vanishing spinor.

that for the case of 6 dimensions the internal space therefore has to be a Calabi-Yau manifold [54]. This requires the following equivalent properties:

- The first integral Chern class of the tangent bundle vanishes, i.e. $c_1(\mathcal{X}) = 0 \in H^2(\mathcal{X}; \mathbb{Z})$.
- The manifold has $SU(3)$ -holonomy.
- The canonical line bundle $K_{\mathcal{X}} = \det(\Omega^{1,0}(\mathcal{X})) = \Omega^{3,0}(\mathcal{X})$ is trivial.
- The manifold admits a nowhere vanishing holomorphic volume form $\Omega_3 \in \Omega^{3,0}(\mathcal{X})$.

Unfortunately, without any further ingredients the Calabi-Yau compactification of the 10d $\mathcal{N}=2$ type II superstring yields a 4d $\mathcal{N}=2$ effective theory. The necessary further breaking to chiral $\mathcal{N}=1$ supersymmetry level via e.g. D-branes will be discussed in the next subsection. One can then derive an effective 4d $\mathcal{N}=1$ theory from the Calabi-Yau compactification [92–94].

Despite the phenomenological “no-go” of pure type II Calabi-Yau settings they serve as an excellent toy model to study general compactification issues. Due to the assumption of extremely small internal dimensions and the related high momentum / energy / mass gap, one is ultimately interested in the massless 4d spectrum. The general idea is to expand all fields into the (generalized) Fourier modes and discard excited modes. Due to the product structure of the space-time the wave operators split into a corresponding 4d wave operator times a 6d Laplacian differential operator:

$$\square_{10} = \square_4 + \Delta_6. \quad (2.24)$$

The Laplacian Δ_6 appears due to the Euclidean signature metric on the internal space. A 10d field Φ is then expanded into harmonics of the internal space, i.e. one performs a generalized Fourier expansion where the modes are given as eigenfunctions:

$$\Phi = \sum_k \phi_k(x) Y_k(y) \quad \text{where} \quad \begin{aligned} \Delta_6 Y_k(y) &= -\lambda_k Y_k(y), \\ (\square_4 - \lambda_k) \phi_k(x) &= 0. \end{aligned} \quad (2.25)$$

Each $\phi_k(x)$ is then a 4d field with mass $\sqrt{\lambda_k}$. The massless 4d modes with $\square_4 \phi_k(x) = 0$ arise from the modes with $\lambda_k = 0$, such that one needs to count the number of $Y_k(y)$ satisfying $\Delta_6 Y_k(y) = 0$. The number of 4-dimensional massless fields is therefore determined by the number of harmonic functions supported on the internal compactification manifold with the corresponding extension to harmonic (p, q) -form fields. Dolbeault’s generalization of the Hodge theorem provides the isomorphism

$$H^{p,q}(\mathcal{X}) := H_{\bar{\partial}}^{p,q}(\mathcal{X}) \cong \mathcal{H}^{p,q}(\mathcal{X}), \quad (2.26)$$

such that harmonic (p, q) -forms in $\mathcal{H}^{p,q}(\mathcal{X})$ are counted by the Dolbeault cohomology groups. The number of massless 4d fields arising from a 10d (p, q) -form field is then

		$h^{0,0}$				1					
		$h^{1,0}$	$h^{0,1}$			0	0				
Hodge	↑ ↓	$h^{2,0}$	$h^{1,1}$	$h^{0,2}$			0	$h^{1,1}$	0		
		$h^{3,0}$	$h^{2,1}$	$h^{1,2}$	$h^{0,3}$	\rightsquigarrow	1	$h^{1,2}$	$h^{1,2}$	1	
		$h^{3,1}$	$h^{2,2}$	$h^{1,3}$			0	$h^{1,1}$	0		
		$h^{3,2}$	$h^{2,3}$					0	0		
		$h^{3,3}$							1		
		\longleftrightarrow				$\underbrace{\hspace{10em}}_{\text{Calabi-Yau 3-fold}}$					
		complex conjugation									

Table 2.3.: Hodge diamond of a Calabi-Yau 3-fold.

given by the Hodge numbers $h^{p,q} = \dim H^{p,q}(\mathcal{X})$, which are subject to a number of symmetries corresponding to isomorphisms of the respective cohomology groups on a compact n -dimensional Kähler manifold:

- The Hodge \star -operator induces $H^{p,q}(\mathcal{X}) \cong H^{n-p,n-q}(\mathcal{X})$.
- The complex conjugation induces $H^{p,q}(\mathcal{X}) \cong H^{q,p}(\mathcal{X})$.

Since cohomology groups are topological invariants, the massless 4d spectrum—often called the zero-mode structure—is entirely determined by the topology of the internal space.

The set of all Hodge numbers is referred to as the Hodge diamond, which for a 3-dimensional Calabi-Yau manifold takes a rather restricted form (see table 2.3) that leaves only 2 independent numbers $h^{1,1} = h^{2,2}$ and $h^{1,2} = h^{2,1}$, which are related to the Euler characteristic by

$$\chi(\mathcal{X}) = 2(h^{1,1} - h^{1,2}). \tag{2.27}$$

In the four-dimensional spectrum the massless scalars are usually called moduli fields and are associated to the degrees of freedom in choosing the geometrical structure (Kähler structure and complex structure) on the internal space. More precisely, after choosing a Calabi-Yau 3-fold \mathcal{X} there are

$$\begin{aligned} h^{1,1} & \text{ Kähler moduli } T^A, \\ h^{1,2} & \text{ complex structure moduli } U^k, \end{aligned} \tag{2.28}$$

on the smooth 6-dimensional (real) manifold underlying \mathcal{X} . Note that any Calabi-Yau 3-fold is equipped with the following nowhere-vanishing differential forms:

$$\begin{aligned} \text{Kähler form:} & \quad J \in \Omega^{1,1}(\mathcal{X}), \\ \text{holomorphic volume form:} & \quad \Omega_3 \in \Omega^{3,0}(\mathcal{X}). \end{aligned} \tag{2.29}$$

After an appropriate choice of bases for the (1,1)- and (1,2)-forms as well as their respective Hodge-duals, one can decompose the fields found in the type IIB string theory and derive the effective 4d $\mathcal{N}=2$ theory. In addition to the supergravity multiplet and a double-tensor multiplet, it contains $h^{1,1}$ hypermultiplets and $h^{1,2}$ vector multiplets depending on the topology of the Calabi-Yau 3-fold \mathcal{X} .

2.4 Orientifolds

The non-chiral $\mathcal{N}=2$ supersymmetry in Calabi-Yau compactifications has to be broken at least to $\mathcal{N}=1$ for any attempt of semi-realistic model building, which can be achieved by adding D-branes. In order to properly satisfy several consistency conditions discussed in section 2.8 this requires orientifold settings [43, 95–97]. For the process of orientifolding a space-time symmetry is required and combined with an orientation reversal on the string, such that the physical theory lives on the invariant coset space. Key objects are so-called orientifold planes (O-planes) introduced by this procedure. O-planes are the fixpoint sets of the orientifold involution. While they have no dynamical properties like D-branes, they carry charge and tension that is used to cancel the respective D-brane quantities. The dimensional counting for O_p -planes is analogous to Dp -branes — the p gives the number of spatial dimensions — and the 4d flat space-time is entirely invariant, i.e. $p \geq 3$.

More precisely, let \mathcal{X} be a compact Calabi-Yau 3-fold and $\sigma : \mathcal{X} \rightarrow \mathcal{X}$ be a self-inverse (i.e. $\sigma^2 = \text{id}$) isometric involution, which induces a \mathbb{Z}_2 -action on the 10d space-time that acts as the identity on the additional four flat dimensions. For type IIB orientifolds the induced mapping σ^* on differential forms leaves the Kähler form J invariant, but $\sigma^2 = \text{id}$ implies the choice of sign in the action on the holomorphic volume form, i.e.

$$\sigma^* J = J, \quad \sigma^* \Omega_3 = \pm \Omega_3. \quad (2.30)$$

The choice of positive sign requires to leave an odd number of complex coordinates (1 or 3) invariant, which leads to O5- and O9-planes of fixpoints. Likewise a negative sign keeps an even number of coordinates (0 or 2) invariant, yielding O3- and O7-planes. Furthermore, let $\Omega_{\mathbb{P}}$ be the worldsheet parity operator that reverses the orientation on the string worldsheet. Often a sign $(-1)^{F_L}$ depending on the fermion number in the left-moving sector is added. The entire orientifold mapping then takes the form

$$O = \begin{cases} \Omega_{\mathbb{P}}(-1)^{F_L} \sigma & \text{for } \sigma^* \Omega_3 = -\Omega_3 \text{ (O3/O7 case)} \\ \Omega_{\mathbb{P}} \sigma & \text{for } \sigma^* \Omega_3 = +\Omega_3 \text{ (O5/O9 case)}. \end{cases} \quad (2.31)$$

The fields contained in the type IIB superstring have the signs listed in table 2.4 under

a different perspective, one basically removes the additional component fields in the non-orientifolded $\mathcal{N}=2$ theory and obtains chiral $\mathcal{N}=1$ by adding a certain space-time symmetry.

2.5 Intersecting D-branes, O-planes and Chiral Matter

D-branes in string theory provide the gauge sector due to the states of the massless open string spectrum, where stacks of D-branes give rise to a non-Abelian $U(n)$ gauge group. As objects inside space-time the D-brane worldvolume is affected by the orientifold action, which makes it subject to the decomposition into invariant and anti-invariant parts. Geometrically one has to consider the cases where the D-brane intersects the O-plane, coincides with the O-plane or is in a non-intersecting invariant position. Let $[D_a] \in H^{6-n}(\mathcal{X})$ be the (Poincaré-dual) cohomology class^V of a (stack of) D(3+n)-brane(s) wrapping $D_a \subset \mathcal{X}$. Let $D'_a := OD_a$ be the image under the orientifold mapping—called the image brane (stack)—whose presence is required in order for the D-brane to be invariant and to survive the orientifold projection. Then there are three cases to distinguish:

- $D_a = D'_a$: Brane and image brane are identical.
- $[D_a] = [D'_a]$, but $D_a \neq D'_a$: Cohomological equivalence of brane and image brane, i.e. both wrap the same cycles of the internal geometry.
- $[D_a] \neq [D'_a]$: Brane and image brane are different and wrap different cycles of the internal geometry.

Focusing on the case of D7-branes and O7-planes, the first two cases where brane and image brane are equivalent imply an intersection of the brane with the orientifold plane. In the third case an intersection with the O7-plane is possible, but not necessary, e.g. brane and image brane can be in a non-intersecting position parallel to the O7-plane. Due to the symmetrization performed by the orientifold projection a stack of D-branes intersecting the O-plane has the reduced gauge group $SO(n) \subset U(n)$ or $Sp(n) \subset U(n)$, depending on the details of the intersection and orientifold projection. Together with the $U(n)$ group for D7-branes not intersecting the O7-plane, orientifold settings therefore provide the gauge groups

$$U(n), \quad SO(n), \quad Sp(n). \quad (2.34)$$

^VFor each n -dimensional submanifold D of the internal geometry \mathcal{X} the Poincaré-dual cohomology class $[D] = \star\rho_D \in H^{\dim \mathcal{X}-n}(\mathcal{X})$ to the corresponding homology class $\rho_D \in H_n(\mathcal{X})$ is considered. Using the representation of cohomology classes via (harmonic) differential forms this convention allows for direct computation with the symbol $[D]$. Note that this notation is different from the mathematical standard, where $[D]$ refers to the homology class ρ_D instead of the Poincaré-dual.

setting	multiplicity	representation	bundle
brane a / brane b :	I_{ab}	$(\bar{\square}_{-1}^a, \square_{1}^b)$	$E_a^* \otimes E_b$
image brane a' / brane b :	$I_{a'b}$	$(\square_{1}^a, \square_{1}^b)$	$E_a \otimes E_b$
brane / image brane:	$\frac{1}{2}I_{a'a} + I_{aO7}$	\square_{2}^a	$\Lambda^2 E_a$
	$\frac{1}{2}I_{a'a} - I_{aO7}$	\boxplus_{2}^a	$S^2 E_a$

Table 2.5.: Multiplicities, bundles and representations arising from a D-brane, image brane and O-plane intersection. The subscripts denote the respective Abelian $U(1)$ charges.

An important further degree of freedom for D-branes are possible non-trivial gauge fluxes for the Yang-Mills gauge field strength F that appears both in the DBI action (2.16) and the CS action (2.18). Those can be mathematically described by stable holomorphic vector bundles defined over the D-brane worldvolume. The structure group of the bundle is then embedded into the gauge bundle of the D-brane (stack) and breaks down the plain gauge group to the commutator of the embedded group. In the following only Abelian $U(1)$ background fluxes are considered.

For example, take a stack of 5 D-branes with the gauge group $U(5)$. By activating a $U(1)$ background flux—a holomorphic line bundle over the worldvolume of the stack—that is embedded diagonally as $U(1) \subset U(5)$, the gauge group is reduced to $SU(5) \times U(1)$. A second line bundle L_Y with a specifically chosen embedding matrix corresponding to the hypercharge generator T_Y then breaks the $SU(5)$ further down to (almost) the Standard Model gauge group, i.e.

$$U(5) \xrightarrow{L} SU(5) \times U(1) \xrightarrow{L_Y} SU(3) \times SU(2) \times U(1)_Y \times U(1). \quad (2.35)$$

This basic idea is used later in the breaking of the GUT group and the generation of chiral matter.

One can also consider intersections of D-branes with other D-branes. For example, two space-time-filling D7-branes always intersect along a complex 1d curve for dimensional reasons (if they are not coincident). The open strings that stretch between the two branes become massless along the intersection curve and therefore contribute additional representations to the effective spectrum. Due to the presence of orientifold planes in consistent compactifications involving D-branes, one has to distinguish between the intersections with the D-branes and the corresponding image D-branes. In table 2.5 the potential intersections between two stacks of D7-branes $D_a, D_b \subset \mathcal{X}$, the image brane $D_{a'} \subset \mathcal{X}$ as well as an orientifold plane $O7 \subset \mathcal{X}$ are listed. The central

quantity that determines the multiplicity of the additional representations is the chiral index^{VI} [43, 99]

$$\begin{aligned} I_{ab} &= \sum_{n=0}^3 (-1)^n \dim \text{Ext}^n(\iota_* L_a, \iota_* L_b) \\ &= - \int_{\mathcal{X}} [D_a] \wedge [D_b] \wedge (c_1(L_a) - c_1(L_b)), \end{aligned} \quad (2.36)$$

where $c_1(L_a), c_1(L_b) \in H^2(\mathcal{X})$ are the first Chern classes of the flux line bundles over the respective D-brane worldvolumes and $[D_a], [D_b] \in H^2(\mathcal{X})$ are the Poincaré-dual 2-forms corresponding to the wrapped 4-cycles $D_a, D_b \subset \mathcal{X}$, for which ι_* is the push-forward induced from the inclusion mappings into the space-time. Note that for the brane/image brane intersections the actual intersection with the O-plane (i.e. $D_a \cap O7 = D'_a \cap O7$) determines the asymmetry in the number of symmetric and anti-symmetric representations. The corresponding chiral index is computed via

$$I_{aO7} = \int_{\mathcal{X}} [D_a] \wedge [O7] \wedge c_1(L_a). \quad (2.37)$$

From the intersections of two different D-branes the bi-fundamental representations $(\square_{-1}^a, \square_1^b)$ and $(\square_1^a, \square_1^b)$ are obtained, which for the special case of D_b being just a single brane (instead of a stack) provides $(\square_{-1}^a, \mathbf{1}^b)$ and $(\square_1^a, \mathbf{1}^b)$. The D-brane intersections therefore provide the building blocks of chiral matter content. Obviously, by (2.36) non-trivial gauge fluxes are required in order to obtain non-vanishing chiral indices and therefore chiral matter representations, see table 2.5.

^{VI}The extension groups $\text{Ext}^i(A; B)$ arise as derived functors in homological algebra and basically measure the failure of the functor $\text{Hom}(A, \bullet)$ to keep an injective resolution

$$0 \longrightarrow B \hookrightarrow I^0 \longrightarrow I^1 \longrightarrow I^2 \longrightarrow \dots,$$

which is a long exact sequence, exact. The groups $\text{Ext}^i(A, B)$ therefore are the cohomology groups of the sequence

$$0 \longrightarrow \text{Hom}(A, B) \longrightarrow \text{Hom}(A, I^0) \longrightarrow \text{Hom}(A, I^1) \longrightarrow \dots$$

The structure of intersecting D-branes with non-trivial line bundles can be understood in terms of extension groups [98] and usually one can find isomorphisms relating them to regular cohomology groups, for example later in chapter 6.

2.6 D-brane Instantons

2.6.1 General aspects

In a generic setting D-branes are always assumed to fill out the flat 4d space-time dimensions first, i.e. a Dp -brane wraps a $(p - 3)$ -dimensional internal space. Instead one can also consider D-branes exclusively wrapping around the internal geometry, which then appear as a single point in the 4d space-time. Since all internal dimensions are spatial, i.e. of Euclidean signature, such branes are appropriately called Euclidean branes or E-branes for short. The dimensional counting is carried over directly from Dp -brane dimensions (p spatial plus 1 temporal), such that an E_p -brane is actually of spatial dimension $p + 1$, i.e. an E3-instanton is a $4_{\mathbb{R}}$ -dimensional complex surface wrapped around 4-cycles of the internal geometry \mathcal{X} . In particular, from the perspective of the 4d theory the instanton brane is therefore localized at a single point space and time—thus the name “instanton”. Such D-brane instantons have become an important aspect in string model building [100].

The terminus “instanton” refers to the fact that E-branes have a similar effect on the correlation functions like instantons in quantum field theory [101]. Instantons contribute a highly suppressed, non-perturbative factor [102]:

$$\text{instanton contribution: } \propto \exp\left(-\frac{1}{g_s^2}\right), \quad (2.38)$$

which only becomes truly important when certain non-renormalizability statements effectively eliminate the perturbative contributions—effectively turning the instanton term into the leading order contribution. Those non-perturbative contributions can be used to adjust hierarchies and generate mass terms as well as certain Yukawa couplings. In particular, the top quark Yukawa coupling in $SU(5)$ GUT models can— as a non-perturbative effect — only be introduced via E-brane instantons into a perturbative type II setting [70, 99].^{VII} The discovery how to construct those states from the unified perspective of F-theory was one of the major arguments for the renewed interest in this approach to non-perturbative type IIB model building.

^{VII}In perturbative D-brane models the gauge group $SO(10)$ arises from intersections of a D-brane stack with its image brane stack, i.e. along the intersection with the O-plane. The absence of the top-quark Yukawa coupling, which derives from the $\mathbf{10} \cdot \mathbf{10} \cdot \mathbf{5}_H$ coupling in the $SU(5)$ GUT, can therefore roughly be understood as an— perturbatively impossible — intersection of O-planes. The non-perturbative F-theory framework, on the other hand, does not particularly distinguish O-planes from D-branes, as will be shown in chapter 3. From this point of view it is not particularly surprising that it is rather unproblematic to obtain such couplings in F-theory.

Ultimately, one is again interested in the effective 4d theory arising from a setting involving E-brane instantons. Here four kinds of massless zero-modes are distinguished.

- *Universal zero-modes*: Those are the zero-modes arising from open strings starting and ending on the same instanton E-brane, completely analogous to the case of ordinary space-time filling D-branes. From the perspective of the 4d effective field theory those zero-modes correspond to Goldstone bosons from the breakdown of the translational invariance, since the instanton distinguishes a single point in the 4d space-time. The presence of a D-brane also leads to a (partial) breakdown of supersymmetries, which appear as the Goldstino fermions and are called universal fermionic zero-modes, see section 2.6.2.
- *Deformation zero-modes*: They are analogous to the transversal deformations of an ordinary D-brane and originate in the modes of the open string normal to the brane worldvolume, see section 2.2. The number of such deformations is determined by the topology of the cycle in the internal geometry wrapped by the instanton. For the specific case of an E3-instanton $E \subset \mathcal{X}$ —which will be the most relevant in this work—there are two relevant topological numbers:

$$\begin{aligned} b_1 &= \dim H^1(E; \mathcal{O}) : \text{ number of Wilson-line moduli,} \\ b_2 &= \dim H^2(E; \mathcal{O}) : \text{ number of normal deformations.} \end{aligned} \tag{2.39}$$

If the instanton brane wraps a rigid cycle no deformations are present. Those additional zero-modes have to be lifted by fluxes or soaked up to actually contribute to the superpotential [103–105].

- *Charged (matter) zero-modes*: Given an additional D-brane wrapping $D \subset \mathcal{X}$ in the setting, one can consider the zero-modes arising from the intersection with the instanton E-brane $E \subset \mathcal{X}$, which are also counted by the chiral index I_{ED} defined in (2.36). Those zero-modes are charged under the effective 4d gauge group of the D-brane stack the instanton is intersecting—hence the name.
- *Multi-instanton zero-modes*: Likewise one can consider intersections of several instanton E-branes, which again leads to massless states originating from open strings localized along the intersection.

As will be discussed later in chapter 4, the zero-mode structure is not the only possible source of superpotential contributions, in particular in the context of charged (matter) zero-modes. For the moment, however, only the zero-mode structure will be considered.

2.6.2 Fermionic zero-modes

In orientifold settings the E-brane E has to be invariant under the orientifold symmetry like an ordinary D-brane, which—depending on the wrapped cycle relative to the O-plane—necessitates the introduction of an image E-brane E' . The instanton branes then locally perceive the full $\mathcal{N}=2$ supersymmetry allowed by the Calabi-Yau manifold which is generated by the supercharges $Q_1^\alpha, \bar{Q}_1^{\dot{\alpha}}, Q_2^\alpha, \bar{Q}_2^{\dot{\alpha}}$. The orientifold projection only preserves the $\mathcal{N}=1$ subalgebra generated by the supercharges $Q^\alpha, \bar{Q}^{\dot{\alpha}}$. The orthogonal complement generated by $Q'^\alpha, \bar{Q}'^{\dot{\alpha}}$ is the $\mathcal{N}=1'$ copy which is broken in the effective 4d theory. Whereas a space-time filling D-brane preserves the $\mathcal{N}=1$ copy of unprimed $Q^\alpha, \bar{Q}^{\dot{\alpha}}$, the localization of the instanton along a $\frac{1}{2}$ -BPS cycle in the internal dimensions—preserving exactly half of the supersymmetry and leading to four fermionic Goldstino modes—instead preserves the off-diagonal combination $Q'^\alpha, \bar{Q}'^{\dot{\alpha}}$ of supercharges. Let $\theta^\alpha, \bar{\theta}^{\dot{\alpha}}$ denote the four Goldstino modes associated to the breaking of $Q^\alpha, \bar{Q}^{\dot{\alpha}}$ and $\tau^\alpha, \bar{\tau}^{\dot{\alpha}}$ likewise for the primed $Q'^\alpha, \bar{Q}'^{\dot{\alpha}}$, i.e.

$$\mathcal{N}=2 \rightsquigarrow \begin{array}{l} \mathcal{N}=1 : \quad Q^\alpha, \bar{Q}^{\dot{\alpha}} \rightsquigarrow \text{Goldstinos } \theta^\alpha, \bar{\theta}^{\dot{\alpha}}, \\ \mathcal{N}=1' : \quad Q'^\alpha, \bar{Q}'^{\dot{\alpha}} \rightsquigarrow \text{Goldstinos } \tau^\alpha, \bar{\tau}^{\dot{\alpha}}. \end{array} \quad (2.40)$$

The preservation of the off-diagonal $Q'^\alpha, \bar{Q}'^{\dot{\alpha}}$ combination (or equivalently the breaking of $Q^\alpha, \bar{Q}^{\dot{\alpha}}$) then yields the four fermionic (Goldstino) zero-modes $\theta^\alpha, \bar{\tau}^{\dot{\alpha}}$. In order to potentially contribute to a (chiral) 4d $\mathcal{N}=1$ F-term of the form $F(x) \theta^1 \theta^2$ the $\mathcal{N}=1'$ associated fermionic zero-modes $\bar{\tau}^{\dot{\alpha}}$ have to be effectively removed from the massless spectrum, which is the main condition for instantons to contribute to the theory.

The easiest way to get rid of the fermionic extra zero-modes $\bar{\tau}^{\dot{\alpha}}$ is to place the instanton directly on top of a D-brane, i.e. the D-brane and the E-instanton wrap the same cycle in the internal geometry. This configuration also allows to recover the field theoretic ADHM description of gauge instantons [101] for the worldvolume gauge theory on the D-brane. Further cases are discussed below in section 2.6.3

Likewise, deformation and charged zero-modes only contribute if the fermionic extra zero-modes are lifted by fluxes or soaked up. For the case of charged fermionic zero-modes λ_{Ea} from the intersection of an E-brane with the D-brane stack D_a , couplings of the form $\lambda_{Ea_i} \Phi_{a_i b_i} \lambda_{b_i E}$ in the interaction part of the effective instanton action “pull down” the charged matter fields Φ , such that terms of the form

$$W = \prod_i \Phi_{a_i b_i} e^{-S_E} \quad (2.41)$$

appear in the holomorphic superpotential. The total charge of all those matter fields can be canceled by the total charge

$$Q_a(E) = N_a(I_{ED_a} - I_{ED'_a}) \quad (2.42)$$

	zero-modes	statistics	number
universal:	X_μ	bose	1
$\mathcal{N}=1$ SUSY:	θ_α	fermi	1
$\mathcal{N}=1'$ SUSY:	$\bar{\tau}_{\dot{\alpha}}$	fermi	1
Wilson lines:	$(w, \gamma_\alpha, \bar{\gamma}_{\dot{\alpha}})$	(bose, fermi)	$H^{1,0}(E)$
deformations:	$(c, \chi_\alpha, \bar{\chi}_{\dot{\alpha}})$	(bose, fermi)	$H^{2,0}(E)$

Table 2.6.: Zero-modes of an (isolated, non-intersected) $U(1)$ -instanton.

	zero-modes	statistics	number
universal / $\mathcal{N}=1$ SUSY:	(X_μ, θ_α)	(bose, fermi)	1
$\mathcal{N}=1'$ SUSY:	$\bar{\tau}_{\dot{\alpha}}$	fermi	0
invariant Wilson lines:	γ_α	fermi	$H_+^{1,0}(E)$
anti-invariant Wilson lines:	$(w, \bar{\gamma}_{\dot{\alpha}})$	(bose, fermi)	$H_-^{1,0}(E)$
invariant deformations:	χ_α	fermi	$H_+^{2,0}(E)$
anti-invariant deformations:	$(c, \bar{\chi}_{\dot{\alpha}})$	(bose, fermi)	$H_-^{2,0}(E)$

Table 2.7.: Zero-modes of an (isolated, non-intersected) $O(1)$ -instanton.

of the brane/image brane and instanton/image instanton, i.e. only when the gauge invariance is guaranteed by the condition

$$\sum_i Q_a(\Phi_{a_i b_i}) = -Q_a(E) \quad (2.43)$$

can a superpotential term of the form (2.41) be generated and contribute to the superpotential W . In general, the different methods of removing certain fermionic zero-modes are most important for E-brane instantons.

2.6.3 $U(1)$ -instantons and $O(1)$ -instantons

If the E-brane is not on top of a D-brane, the orientifold action itself can take care of the extra zero-modes if the instanton is in an invariant position. Let E be the instanton brane and E' the image under the orientifold action. E-branes in the generic non-invariant position $E \neq E'$ are referred to as $U(1)$ -instantons.

For an E-brane in the invariant $E = E'$ position on top of the orientifold plane the symmetrization and anti-symmetrization analogous to ordinary D-branes has to be distinguished—however the role of $SO(n)$ and $Sp(n)$ is switched compared to D-branes.

The number of remaining fermionic universal zero-modes is

$$\begin{aligned} Sp(n)\text{-instanton:} & \quad \frac{n(n-1)}{2} \times \theta^\alpha + \frac{n(n+1)}{2} \times \bar{\tau}^{\dot{\alpha}}, \\ (S)O(n)\text{-instanton:} & \quad \frac{n(n+1)}{2} \times \theta^\alpha + \frac{n(n-1)}{2} \times \bar{\tau}^{\dot{\alpha}}. \end{aligned} \quad (2.44)$$

The special case of a so-called $O(1)$ -instanton then has precisely the desired θ^α zero-modes, but no $\bar{\tau}^{\dot{\alpha}}$ s. Such instantons therefore generically provide the primary contributions to the superpotential. Both $U(1)$ - and $O(1)$ -instantons will be investigated further in chapter 4.

2.7 Flux Compactifications

Type IIB superstring theory supports several different background fluxes, i.e. non-trivial values for the p -form fields G_3 and F_5 appearing in the effective action (2.13). Here only the special case of Calabi-Yau compactifications involving fluxes is considered, which leads to a significant simplification compared to the general case, since the Calabi-Yau condition requires F_5 to vanish due to the absence of supporting 5-cycles, cf. $b_5 = h^{3,2} + h^{2,3} = 0$ in table 2.3.

Given an orientifold setting, the 3-form fields F_3 and H_3 appearing in the G_3 -flux also have to be split into invariant and anti-invariant components in $H_\pm^3(\mathcal{X})$. For $G_3 = G_3^+ + G_3^-$ the G_3 -term proportional to $|G_3|^2$ in (2.13) can be rewritten as

$$-\frac{1}{4\kappa_{10}^2} \int \frac{|G_3|^2}{\text{Im } \tau} = \frac{1}{2\kappa_{10}^2} \int_{\mathcal{X}} \frac{1}{\text{Im } \tau} \left(G_3^+ \wedge \star_6 \bar{G}_3^+ - \frac{i}{2} G_3 \wedge \bar{G}_3 \right), \quad (2.45)$$

of which the second term is topological and summarized by $\mu_3 N_{\text{flux}}$, where μ_3 is the D3-brane tension and N_{flux} an integer value. This quantity contributes to the C_4 potential tadpole^{VIII} cancellation condition discussed in section 2.8.1.

For the case of a type IIB orientifold the contribution of the G_3 -flux to the effective low-energy 4d supergravity theory is described by the Gukov-Vafa-Witten superpotential term [107]

$$\text{O3/O7: } W = \frac{1}{\kappa_{10}^2} \int_{\mathcal{X}} G_3 \wedge \Omega, \quad \text{O5/O9: } W = \frac{1}{\kappa_{10}^2} \int_{\mathcal{X}} F_3 \wedge \Omega. \quad (2.46)$$

Via those superpotential contributions the presence of background fluxes potentially breaks supersymmetry. Aside from the σ -eigenvalue splitting of G_3 , one has to study

^{VIII}Tadpoles were first considered by Sidney Coleman [106], who also invented the word ‘‘tadpole’’ for this particular type of Feynman diagram. Rumor has it, that the editor was at first not satisfied, but he soon changed his mind once Sidney Coleman proposed ‘‘spermion’’ instead.

the naive (p, q) -form decomposition of a 3-form and check for the absence of F-terms—chiral terms of the form $F\theta^1\theta^2$ —in the 4d effective theory. The F-term conditions arise from the covariant derivatives of the superpotential involving the G_3 -flux, where the variations with respect to the Kähler structure, axio-dilaton and complex structure moduli are considered:

$$\begin{aligned}
\text{Kähler structure: } D_{T^A}W &= \frac{\partial K}{\partial T^A} \int_{\mathcal{X}} G_3 \wedge \Omega_3 = 0 && \rightsquigarrow G_3^{0,3} = 0, \\
\text{axio-dilaton: } D_{\tau}W &= \frac{1}{\tau - \bar{\tau}} \int_{\mathcal{X}} \bar{G}_3 \wedge \Omega_3 = 0 && \rightsquigarrow G_3^{3,0} = 0, \\
\text{complex structure: } D_{U^k}W &= \int_{\mathcal{X}} G_3 \wedge \chi_k = 0 && \rightsquigarrow G_3^{1,2} = 0,
\end{aligned} \tag{2.47}$$

which follows since $\Omega_3 \in H^{3,0}(\mathcal{X})$ and $\chi_k \in H^{2,1}(\mathcal{X})$. Therefore, 4d $\mathcal{N}=1$ supersymmetry in fact only allows for a non-trivial $G_3^{2,1}$ -component of the G_3 -flux. Only specifically tuned configurations on Calabi-Yau manifolds therefore allow any flux at all. More general approaches to flux compactification relax the Calabi-Yau condition and use generalized complex geometry [108, 109].

2.8 Phenomenological Aspects and Consistency Conditions

There are several generic consistency conditions that any well-defined orbifold compactification setting has to fulfill [43, 110].

2.8.1 Tadpoles

D-branes carry an R-R charge and couple to the R-R background potentials C_q by means of the Chern-Simons action (2.18). In order to preserve the validity of Gauß’s law — which generalizes to Stokes’ theorem for general differential forms — the total charge within the compact dimensions has to vanish, much like the electric charge in electrodynamics on compact spaces. The same conditions can also be derived from the equations of motion for the R-R potentials C_q and are referred to as “tadpole cancellation conditions”. Nonzero tadpoles manifest as divergences in the 1-loop open string (disk) amplitude, which from the perspective of the 4d effective field theory can be interpreted as quadratic ultraviolet divergences for the corresponding massless field at 1-loop level, i.e. the cancellation of such divergences is crucial.

Aside from artificially defined anti-D-branes of opposite charge to the normal ones — which however result in mostly unstable configurations — the primary source of negative R-R charge comes from orientifold planes. This underlines the mutual dependency of D-branes and orientifold settings in order to satisfy the global consistency conditions.

Note that due to the Chern-Simons action the higher-dimensional objects (Dp -branes and Op -planes) couple to all C_q fields of lower rank $q < p$. For the case of type IIB orientifolds with O3/O7-planes three non-trivial conditions arise:

- *C_4 potential / D3-brane tadpole condition:* Let N_{D3} and N_{O3} denote the number of D3-branes and O3-planes in the setting. An effective gauge bundle V_a is defined on a stack of N_a D7-branes wrapping the 4-cycle $D_a \subset \mathcal{X}$ of the internal geometry. The general condition

$$\begin{aligned} N_{D3} + N_{\text{flux}} - \sum_a N_a \int_{D_a} \text{ch}_2(V_a) \\ = \frac{N_{O3}}{4} + \sum_a \frac{N_a}{24} \int_{D_a} c_2(T_{D_a}) + \frac{1}{12} \int_{O7} c_2(T_{O7}) \end{aligned} \quad (2.48)$$

also involves contributions from fluxes and the 7-brane/plane sector. Here the term $\text{ch}_2(V_a) = \frac{1}{2}c_1(V_a)^2 - c_2(V_a) \in H^4(\mathcal{X}; \mathbb{Z})$ refers to the second level term in the Chern character of the gauge bundle. T_{D_a} and T_{O7} are the tangent bundles of the D7-brane and O7-plane worldvolume, respectively.

- *C_6 potential tadpole condition:* The C_6 field condition does not involve any D5-branes, but due to the lower-rank coupling of D7-branes there is the condition

$$\sum_a \text{ch}_1(V_a) \wedge D_a \wedge \omega_a = 0, \quad (2.49)$$

where the $\omega_a \in H_-^{1,1}(\mathcal{X})$ form a basis. Naturally, if the internal manifold supports no anti-invariant (1,1)-forms (or respectively 2-cycles) this condition is trivial. It is often referred to as the D5-brane tadpole condition due to the canonical coupling to the C_6 potential. Even in the absence of D5-branes in a setting, this condition is quite important for the absence of chiral anomalies [111, 112] that arise from the couplings to other R-R potentials.

- *C_8 potential / D7-brane tadpole condition:* The condition for the C_8 field corresponds precisely to the naively expected charge conservation:

$$\sum_a \left([D_a] + [D'_a] \right) = 8 \cdot [O7]. \quad (2.50)$$

This is in fact the condition for the “upstairs” geometry. In the “downstairs” coset space $\mathcal{B} = \mathcal{X}/\sigma$ the brane and image brane are identified, such that the corresponding “downstairs” tadpole condition reads

$$\sum_a N_a [D_a] = 4 \cdot [O7]. \quad (2.51)$$

Note that an O7-plane has -8 times the R-R charge of an “upstairs” D7-brane. The cancellation happens at topological level, i.e. the charge within each wrapped cycle has to cancel individually.

If one neglects to satisfy the tadpole conditions, numerous anomalies appear in the effective theory, for example the C_6 and C_8 tadpole cancellation conditions are related to a cubic non-Abelian anomaly.

2.8.2 Freed-Witten Anomalies

A Dp -brane wrapped around an internal cycle that supports a non-trivial NS-NS 3-form flux H_3 , i.e. any $p \geq 6$, potentially suffers from the Freed-Witten anomaly [113]. Those are found when the wrapped cycle is not spin — obstructed by $w_2(D_a) \neq 0 \in H^2(D_a; \mathbb{Z}_2)$ — but instead supports a $\text{spin}^{\mathbb{C}}$ structure, to which the integral third Stiefel-Whitney class is the corresponding obstruction. The H_3 -flux sort of shifts this condition. Like any other anomaly this has to be canceled for the quantum theory to be consistent, which in this case requires the H_3 -flux restricted to the internally wrapped cycle to be equal to the integral third Stiefel-Whitney class:

$$H_3|_{D_a} = W_3(D_a) \in H^3(D_a; \mathbb{Z}). \quad (2.52)$$

For the case of a Calabi-Yau manifold any 4-cycle is always $\text{spin}^{\mathbb{C}}$, such that from $W_3(D_a) = 0$ it follows

$$H_3|_{D_a} = 0 \quad (2.53)$$

for the H_3 -flux on D7-branes $D_a \subset \mathcal{X}$ in type IIB O3/O7 orientifold settings. This particular condition can also be interpreted as the Bianchi identity for the gauge bundle on the D-brane.

Furthermore, by the same line of reasoning a D-brane with a non-trivial gauge flux F wrapping a non-spin cycle D_a is also subject to the anomaly. In a situation with an Abelian gauge flux F_a that is represented by a holomorphic line bundle over D_a , the cancellation is guaranteed if the gauge flux obeys the integrality condition

$$\int_{\omega} F_a + \frac{1}{2} \int_{\omega} K_{D_a} \in \mathbb{Z} \quad \text{for all 2-cycles } \omega \in H_2(D_a; \mathbb{Z}). \quad (2.54)$$

This ties the internal gauge flux directly to the obstruction $c_1(D_a) = -c_a(K_{D_a}) \not\equiv 0 \pmod{2}$ of the wrapped divisor to be spin. This will be observed at the end of section 6.3.1.

2.8.3 K-theory

There are additional consistency conditions, which arise from the fact that D-brane wrappings and the associated charges are not entirely classified by the concept of (co)homology. Instead it has been conjectured that K-theory and twisted K-theory are in fact the right mathematical tools to describe D-branes and the gauge bundles they carry [114–116]. The missing special cases are related to the Witten anomaly of global $SU(2)$ s.

Lacking truly applicable means to work with K-theory directly, one relies on a probe brane argument, which effectively ensures that the number of 4d chiral fermions in the fundamental $Sp(2N)$ representation is even, leading to the condition

$$\sum_a N_a I_{a(\text{probe})} \in 2\mathbb{Z}, \quad (2.55)$$

where $I_{a(\text{probe})}$ is the chiral index between the (for dimensional reasons always intersecting) probe D7-brane and the D7-brane D_a of the considered setting. It has been shown that those conditions imply the fulfillment of the conjectured K-theory constraints.

Chapter 3

F-theory as a Non-perturbative Type IIB Framework

F-THEORY is a description of the strong coupling regime of type IIB superstring theory. It is based on a geometrization of the (enhanced) IIB strong-weak coupling self-duality, which is summarized in the beginning of this chapter. An elliptic fibration is introduced on top of the 10d space-time, where degenerations encode the location and worldvolume gauge group of non-perturbative 7-branes that for example allow direct access to exceptional gauge groups. In the IIB string theory those objects can be recovered by using $SL(2; \mathbb{Z})$ -mapped D7-branes and non-perturbative string networks. The Sen limit of F-theory is then briefly summarized as the only known method to make contact with true orientifold settings. This raises the issue of corresponding consistency conditions on the F-theory side. At the end of the chapter different aspects of the “pragmatic” local F-theory GUT model building approach like the decoupling principle and basics of $SU(5)$ GUTs are discussed and the need for a “conceptually sound” global model is explained. This chapter summarizes several standard introductions on the subject [85, 117–119].

3.1 Geometrization of Type IIB self-duality

The starting point is a type IIB orientifold setting with O3/O7-planes on a Calabi-Yau 3-fold \mathcal{X} , which was introduced in chapter 2 [43]. A central quantity in F-theory is the complex axio-dilaton scalar field

$$\tau = C_0 + ie^{-\phi}, \quad (3.1)$$

combining the R-R 0-form field C_0 and the dilaton scalar ϕ that corresponds to the string coupling

$$g_s = e^\phi = \frac{1}{\text{Im } \tau}. \quad (3.2)$$

Via birational (Möbius) transformations the $SL(2; \mathbb{Z})$ self-duality acts on τ , where the naive strong-weak duality $S : \tau \mapsto -\frac{1}{\tau}$ corresponds to $\begin{pmatrix} 0 & 1 \\ -1 & 0 \end{pmatrix} \sim \begin{pmatrix} 0 & -1 \\ 1 & 0 \end{pmatrix} \in SL(2; \mathbb{Z})$. The $SL(2; \mathbb{Z})$ group is also well-known from modular transformations on the torus, i.e. the value of $\tau \in \mathbb{C}$ can be used to parameterize the geometry and complex structure on a torus $T^2 = \mathbb{C}/(\mathbb{Z} \operatorname{Re} \tau + i\mathbb{Z} \operatorname{Im} \tau)$. Naively, by assigning such a τ -dependent torus to each point of \mathcal{X} one obtains a fibration on top of the 10d space-time. However, this picture is only sensible in the absence of orientifold planes and D-branes—phenomenologically somewhat trivial situations in type IIB theory.

Consider a D7-brane inside the 10d space-time [120]. The 2-dimensional transverse space can locally be parameterized by a complex coordinate z , such that the D7-brane is located at z_0 . From the Laplacian equation $\partial_{\bar{z}} \tau(z, \bar{z}) = 0$ of the axio-dilaton on the transverse space it follows that τ must be a purely holomorphic function. Using the modular invariant j -function¹

$$j(\tau) = \frac{\left(\vartheta_3^8(\tau) + \vartheta_4^8(\tau) + \vartheta_2^8(\tau)\right)^3}{8\eta^{24}(\tau)} \approx e^{-2\pi i \tau} + 744 + 196884e^{2\pi i \tau} + \dots, \quad (3.3)$$

that maps the $SL(2; \mathbb{Z})$ fundamental region of τ to the entire complex plane, it can be shown that close to the location of the D7-brane the axio-dilaton field behaves like

$$j(\tau(z)) \propto \frac{1}{z - z_0} \quad \rightsquigarrow \quad \tau(z) \propto \frac{1}{2\pi i} \log(z - z_0), \quad (3.4)$$

which due to the singularity at z_0 gives rise to the monodromy $\tau \rightarrow \tau + 1$ in the field when the brane is encircled [121]. The monodromy originates from the magnetic coupling of a 7-brane to the C_0 potential, cf. (2.21). In strict mathematical terms this requires the introduction of a branch cut from the logarithm singularity to infinity, which upon crossing yields the monodromy action. In the same fashion the 2-form fields are affected by the same $SL(2; \mathbb{Z})$ monodromy:

$$\begin{array}{l} \tau \rightarrow \tau + 1 \\ B_2 \rightarrow B_2 \text{ (invariant)} \\ C_2 \rightarrow C_2 + B_2 \\ C_4 \rightarrow C_4 \text{ (invariant)} \end{array} \quad \text{corresponding to} \quad \underbrace{\begin{pmatrix} 1 & 1 \\ 0 & 1 \end{pmatrix}}_{\text{monodromy matrix}} \in SL(2; \mathbb{Z}). \quad (3.5)$$

In the neighborhood of the D7-brane (3.2) and the approximation (3.4) imply a weak coupling behavior

$$g_s \propto -\frac{2\pi}{\log(|z - z_0|)} \xrightarrow{z \rightarrow z_0} 0. \quad (3.6)$$

¹Klein's j -function incorporates the modular symmetries $j(\tau + 1) = j(\tau)$ and $j(-\frac{1}{\tau}) = j(\tau)$. It can be explicitly stated in terms of Jacobi's ϑ -functions, which are quasi-periodically and related to elliptic functions. Its usage here is primarily the removal of the $SL(2; \mathbb{Z})$ redundancy of τ .

However, due to the holomorphicity of τ even a small non-zero value in any other region necessarily implies the existence of a true strong coupling region somewhere else. The divergence g_s of (3.6) for $z - z_0 \rightarrow 1$ can be treated as an indicator for the back-reaction of the 7-brane on the geometry that cannot be neglected in a proper treatment of 7-branes.

The singularities in the axio-dilaton naturally give rise to singularities of the associated torus fibration over the space-time. It is therefore called an elliptic fibration, where the fiber is described as a potentially degenerate degree-6 hypersurface in $\mathbb{C}\mathbb{P}_{231}^2$. In strict mathematical terms the geometrization of the axio-dilaton field τ in a type IIB orientifold setting with D7-branes and O7-planes is therefore given by a $\mathbb{C}\mathbb{P}_{231}^2[6]$ -bundle over the orientifold coset “downstairs” geometry \mathcal{X}/σ .

3.2 Monodromies and (p,q) -strings

The type IIB self-duality also affects D-branes contained in the setting. If ordinary D7-branes are identified as $(1,0)$ -branes, more general (p,q) 7-branes are defined as images under the $SL(2; \mathbb{Z})$ transformation such that

$$\begin{pmatrix} p \\ q \end{pmatrix} = \begin{pmatrix} p & r \\ q & s \end{pmatrix} \begin{pmatrix} 1 \\ 0 \end{pmatrix} \quad \text{for} \quad \begin{pmatrix} p & r \\ q & s \end{pmatrix} \in SL(2; \mathbb{Z}) \quad (3.7)$$

holds [60–65, 122]. In the same fashion one introduces the notion of (p,q) -strings as images of the fundamental open $(1,0)$ -string under $SL(2; \mathbb{Z})$, which is p times charged under the NS-NS B_2 potential and q times under the R-R C_2 -potential [123]. A string with charges (p,q) can only end on an equally charged (p,q) -brane. It can be understood as a bound state of p fundamental strings and q D1-branes, which opens up the possibility of forming networks of strings as long as charge conservation at the 3-junctions is respected— analogous to Kirchoff’s junction rule for electrical circuits. The $SL(2; \mathbb{Z})$ transformation also affects the corresponding monodromy matrix of a 7-brane^{II} via

$$M_{p,q} = g_{p,q} \begin{pmatrix} 1 & 1 \\ 0 & 1 \end{pmatrix} g_{p,q}^{-1} = \begin{pmatrix} 1 - pq & p^2 \\ -q^2 & 1 + pq \end{pmatrix}, \quad (3.8)$$

i.e. it is the matrix adjoint to the original $(1,0)$ D7-brane monodromy matrix (3.5). Note that in the computation of the total monodromy of several 7-branes the order is relevant. If a (p,q) -string passes through the branch cut of a 7-brane its charges are affected by the monodromy. One can then consider complex networks of (p,q) -strings encircling different 7-branes.

^{II}Note that there are several conventions for the monodromy matrices used throughout the literature. In particular note $K_{p,q} = M_{p,q}^{-1}$.

7-branes	number	total monodromy
A	1	$M_A = \begin{pmatrix} 1 & 1 \\ 0 & 1 \end{pmatrix}$
B	1	$M_B = \begin{pmatrix} 2 & 1 \\ -1 & 0 \end{pmatrix}$
C	1	$M_C = \begin{pmatrix} 0 & 1 \\ -1 & 2 \end{pmatrix}$
A^n	n	$M_A^n = \begin{pmatrix} 1 & n \\ 0 & 1 \end{pmatrix}$
AB	2	$M_A M_B = \begin{pmatrix} 1 & 1 \\ -1 & 0 \end{pmatrix}$
$A^2 B$	3	$M_A^2 M_B = \begin{pmatrix} 0 & 1 \\ -1 & 0 \end{pmatrix}$
$A^2 B A$	4	$M_A^2 M_B M_A = \begin{pmatrix} 0 & 1 \\ -1 & -1 \end{pmatrix}$
$A^n B C$	$n + 2$	$M_A^n M_B M_C = \begin{pmatrix} -1 & -n+4 \\ 0 & -1 \end{pmatrix}$
$A^5 B C B$	8	$M_A^5 M_B M_C M_B = \begin{pmatrix} -1 & -1 \\ 1 & 0 \end{pmatrix}$
$A^6 B C B$	9	$M_A^6 M_B M_C M_B = \begin{pmatrix} 0 & -1 \\ 1 & 0 \end{pmatrix}$
$A^6 B C B A$	10	$M_A^6 M_B M_C M_B M_A = \begin{pmatrix} 0 & -1 \\ 1 & 1 \end{pmatrix}$

Table 3.1.: Monodromies arising from combinations of non-perturbative A , B and C 7-branes.

The usage of (p, q) -strings and 7-branes allows to capture many non-perturbative aspects of type IIB theory. Let

$$A := (1, 0), \quad B := (1, -1), \quad C := (1, 1) \quad (3.9)$$

be a choice of charges for (p, q) 7-branes, whose corresponding monodromy matrices are

$$M_A = \begin{pmatrix} 1 & 1 \\ 0 & 1 \end{pmatrix} = M_{D7}, \quad M_B = \begin{pmatrix} 2 & 1 \\ -1 & 0 \end{pmatrix}, \quad M_C = \begin{pmatrix} 0 & 1 \\ -1 & 2 \end{pmatrix}. \quad (3.10)$$

Those are the building blocks for stacks of non-perturbative 7-branes, which are described by an ordered set of A , B and C branes together with the relevant string networks before the clashing of the worldvolumes. If the monodromies of two (p, q) 7-branes do not commute the branes are said to be mutually non-local, which implies that their degrees of freedom are not independent and the brane system is generically strongly coupled. Unlike for ordinary D7-brane stacks one therefore has to keep all the information of the individual brane positions and wrappings due to the different monodromies. Ultimately the massless states originating from such non-perturbative 7-brane stacks and string networks give rise to further gauge groups and representations. A list of relevant 7-brane stacks and their respective total monodromy is found in table 3.1.

A particularly important case is the 7-brane pair BC with the total monodromy

$$M_B M_C = \begin{pmatrix} -1 & 4 \\ 0 & -1 \end{pmatrix}. \quad (3.11)$$

It is canceled by 4 ordinary A -branes (i.e. D7-branes) since $M_A^4 M_B M_C = -\mathbb{1}$. This can be interpreted as the downstairs clashing of 4 D7-branes and an O7-plane, since the effect of the total monodromy due to $M_{-p,-q} = M_{p,q}$ implies a flip of orientation on the (p, q) -string [124–126]. The non-perturbative characteristics therefore allow to “resolve” the O7-plane from the plain type IIB picture into a bound state of two non-perturbative (p, q) 7-branes. Note that the choice of charges in (3.9) is not unique—other pairs of branes also allow to produce the O7-plane monodromy (3.11). The relationship to type IIB orientifold settings will be further discussed in section 3.7.

3.3 Elliptic Singularities and 7-branes

Using the quantization of the $SL(2; \mathbb{Z})$ self-duality and the geometrization of the axio-dilaton field τ in the form of an elliptically-fibered $8d_{\mathbb{R}}$ total space \mathcal{Z} , i.e.

$$\begin{array}{ccc} \mathbb{E} \hookrightarrow \mathcal{Z} & & \\ \downarrow & \mathbb{E} = \text{elliptic curve, i.e.} & \\ \mathcal{B} = \mathcal{X}/\sigma, & \text{potentially singular } T^2 & \end{array} \quad (3.12)$$

the 7-brane monodromies of table 3.1 can be recovered [127–129]. A generic elliptic curve can be described as a non-singular projective algebraic curve of genus 1 and in its most general form is given by the equation

$$y^2 + a_1xyz + a_3yz^3 = x^3 + a_2x^2z^2 + a_4xz^4 + a_6z^6 \quad (3.13)$$

for $(x, y, z) \in \mathbb{C}\mathbb{P}_{231}^2$, which is called the Tate form [130–133]. This describes the most generic degree-6 hypersurface in \mathbb{P}_{231}^2 and due to the projective weights has vanishing first Chern class, i.e. the elliptic curve is Ricci-flat. Since the characteristic of the underlying field of complex numbers \mathbb{C} is neither 2 or 3, every elliptic curve (3.13) can in fact be reduced to the simpler Weierstrass form

$$y^2 = x^3 + fxz^4 + gz^6 \quad \text{where} \quad \begin{cases} f = \frac{1}{48}(24b_4 - b_2^2), \\ g = \frac{1}{864}(216b_6 - 36b_4b_2 + b_2^3), \end{cases} \quad (3.14)$$

for $\begin{cases} b_2 := a_1^2 + 4a_2, \\ b_4 := a_1a_3 + 2a_4, \\ b_6 := a_3^2 + 4a_6, \end{cases}$

which is still a $\mathbb{P}_{231}^2[6]$ curve. Alternative representations of elliptic curves are the hypersurfaces $\mathbb{P}_{112}^2[4]$ and $\mathbb{P}^2[3]$, which are more restricted [134].

The extension of elliptic curves to a global elliptic fibration over \mathcal{B} is not entirely straightforward. Following Deligne, every elliptic fibration with a global section can be represented by a global Weierstrass model—called an E_8 -fibration due to the maximal obtainable singularity type—which means that f and g in the Weierstrass form (3.14) are promoted to global sections

$$\begin{aligned} f &\in \Gamma(K_{\mathcal{B}}^{-4}) = H^0(\mathcal{B}; K_{\mathcal{B}}^{-4}), \\ g &\in \Gamma(K_{\mathcal{B}}^{-6}) = H^0(\mathcal{B}; K_{\mathcal{B}}^{-6}). \end{aligned} \tag{3.15}$$

The global variants of the $\mathbb{P}_{112}^2[4]$ and $\mathbb{P}^2[3]$ parameterizations—called E_7 - and E_6 -fibrations, respectively—are bi-rationally equivalent to the corresponding singularities in an E_8 -parameterization. However, for a generic elliptic fibration the Tate form (3.13) can only be obtained locally since the transformation of f and g to global Tate coefficients $a_i \in \Gamma(K_{\mathcal{B}}^{-i})$ may involve branch cuts. Global Tate parameterizations are therefore a particularly convenient subclass of all elliptic fibrations, as the gauge group can be directly read off from the vanishing degrees of the Tate coefficients, see table 3.6. However, they do not give rise to the most general singularity structure an elliptic fibration can describe.

An important quantity in the description of elliptic curves is the elliptic discriminant

$$\begin{aligned} \Delta &= 4f^3 + 27g^2 \\ &= -\frac{1}{16} \left(-\frac{1}{4}b_2^2(b_2b_6 - b_4^2) - 8b_4^3 - 27b_6^2 + 9b_2b_4b_6 \right), \end{aligned} \tag{3.16}$$

whose zeros correspond to degenerations of the elliptic curve in the fiber.^{III} This can be seen in the explicit description of the j -function

$$j(\tau) = \frac{4(24f)^3}{\Delta} \tag{3.17}$$

with infinities where Δ vanishes. Following section 3.1 the locations of 7-branes are therefore given by the discriminant locus

$$\{\Delta = 0\} \subset \mathcal{B} = \mathcal{X}/\sigma. \tag{3.18}$$

Mathematically one can now proceed with the systematic Kodaira classification of all singularities that can potentially appear in an elliptic fibration, see table 3.2. Note that

^{III}The somewhat unorthodox prefactor $-\frac{1}{16}$ in (3.16) has been added for the convenience of the reader to simplify direct comparison with most of the literature. As one usually considers the vanishing locus $\Delta = 0$, the often neglected (or redefined) prefactor has no effect on any results.

$\deg(f)$	$\deg(g)$	$\deg(\Delta)$	fiber	singularity	comp.	local geometry	monod.
≥ 0	≥ 0	0	I_0	smooth	1		$\begin{pmatrix} 1 & 0 \\ 0 & 1 \end{pmatrix}$
0	0	1	I_1	dbl. point	1	$y^2 = x^2 + z$	$\begin{pmatrix} 1 & 1 \\ 0 & 1 \end{pmatrix}$
0	0	n	I_n	A_{n-1}	n	$y^2 = x^2 + z^n$	$\begin{pmatrix} 1 & n \\ 0 & 1 \end{pmatrix}$
≥ 1	1	2	II	cusp	1		$\begin{pmatrix} 1 & 1 \\ -1 & 0 \end{pmatrix}$
≥ 1	≥ 2	3	III	A_1	2	$y^2 = x^2 + z^2$	$\begin{pmatrix} 0 & 1 \\ -1 & 0 \end{pmatrix}$
≥ 2	2	4	IV	A_2	3	$y^2 = x^2 + z^3$	$\begin{pmatrix} 0 & 1 \\ -1 & -1 \end{pmatrix}$
2	3	6	I_0^*	D_4	5	$y^2 = x^2 z + z^3$	$\begin{pmatrix} -1 & 0 \\ 0 & -1 \end{pmatrix}$
2	≥ 3	$n+6$	I_n^*	D_{n+4}	$n+5$	$y^2 = x^2 z + z^{n+3}$	$\begin{pmatrix} -1 & -n \\ 0 & -1 \end{pmatrix}$
≥ 2	3						
≥ 3	4	8	IV*	E_6	7	$y^2 = x^3 + z^4$	$\begin{pmatrix} -1 & -1 \\ 1 & 0 \end{pmatrix}$
3	≥ 5	9	III*	E_7	8	$y^2 = x^3 + xz^3$	$\begin{pmatrix} 0 & -1 \\ 1 & 0 \end{pmatrix}$
≥ 4	5	10	II*	E_8	9	$y^2 = x^3 + z^5$	$\begin{pmatrix} 0 & -1 \\ 1 & 1 \end{pmatrix}$

Table 3.2.: The original Kodaira classification of singular fibers in analytic surfaces [135, 136]. The local geometry of the elliptic surface around such a singularity is modeled in terms of projective coordinates $(x, y, z) \in \mathbb{C}^3$. In the last column the elliptic monodromy of the singular fiber is given in terms of an $SL(2, \mathbb{Z})$ -matrix, cf. table 3.6.

the majority of elliptic monodromies corresponds precisely to the 7-brane monodromies in table 3.1 and the vanishing degree $\deg(\Delta)$ agrees with the number of (p, q) 7-branes. For the agreeing cases one can therefore conclude that a certain elliptic degeneration describes the location of a collapsed (p, q) 7-brane stack of the corresponding total brane monodromy. This effectively introduces non-perturbative 7-brane stacks with e.g. exceptional gauge groups at the location of the corresponding type of elliptic degeneration in the fibration, which cannot be realized from ordinary D7-brane stacks and O-plane intersections.

It should be noted that the total discriminant of an elliptic fibration generically factorizes as

$$\Delta = \Delta_R \cdot \prod_{a=1}^n \Delta_a^{\delta_a}, \quad (3.19)$$

where δ_a is the respective vanishing degree. Here $\Delta_a^{\delta_a}$ is supposed to vanish over a smooth divisor $\mathcal{D}_a := \{\Delta_a = 0\} \subset \mathcal{B}$, such that one obtains according to the Kodaira

classification in table 3.2 the gauge group G_a over \mathcal{D}_a . A closer inspection of the Calabi-Yau condition $c_1(\mathcal{Z}) = 0$ for elliptically-fibered 4-folds can be reformulated as

$$[\{\Delta = 0\}] = [\mathcal{D}_R] + \sum_{a=1}^n \delta_a [\mathcal{D}_a] = 12c_1(\mathcal{B}) \in H^2(\mathcal{B}; \mathbb{Z}), \quad (3.20)$$

which resembles a 7-brane tadpole condition in the F-theory base. It encodes the fact that the discriminant is a section of $K_{\mathcal{B}}^{-12}$, hence the prefactor [136]. Just like the (non-trivial) type IIB D7-brane tadpole condition (2.51), the discriminant locus is not unconstrained either — the structure of the 7-branes in F-theory is just intrinsically restricted by the Calabi-Yau condition on the 4-fold \mathcal{Z} . In order to satisfy this condition there is usually also a factor Δ_R in the discriminant, that generically corresponds to an I_1 type singularity of the fibers over a singular divisor $\mathcal{D}_R := \{\Delta_R = 0\} \subset \mathcal{B}$. The simplest example is a totally generic Weierstrass model with no further non-Abelian gauge enhancements, such that $\Delta = \Delta_R = 4f^3 + 27g^2$. The divisor \mathcal{D}_R in this case becomes singular over the so-called cusp curve

$$\mathcal{C}_{\text{cusp}} := \{f = g = 0\} \subset \mathcal{D}_R \subset \mathcal{B}. \quad (3.21)$$

While this remainder component of the discriminant handles the 7-brane tadpole, it adds additional 7-branes in a global setting that have to be taken into account.

3.4 F-theory via Dualities

3.4.1 F-theory and M-theory

The entirety of the previously discussed properties and the geometrization of the axio-dilaton together with the correspondence between 7-branes and elliptic degenerations is called F-theory — a name that was coined by Vafa in the original paper from 1996 [59]. To summarize: F-theory is a conjectured auxiliary theory defined on an elliptically-fibered 12-dimensional space \mathcal{Z} that describes strongly coupled type IIB superstring theory on the fibration base \mathcal{B} . The theory provides a unified perspective on several non-perturbative aspects of type IIB theory. However, the two additional dimensions of the fibration are not analogous to the 10d space-time base \mathcal{B} . Instead they are auxiliary constructions from the geometrization of the $SL(2; \mathbb{Z})$ self-duality of IIB and the axio-dilaton τ . There is no directly corresponding low-energy field theory due to the absence of a 12d supergravity with metric signature (11,1).

Nevertheless, one can find a more precise definition of F-theory when starting from M-theory [102, 117, 137–139], which is the 11-dimensional theory describing non-perturbative type IIA string theory. In M-theory all 11 dimensions are equivalent and constitute a

“real” space-time with a uniquely corresponding 11d $\mathcal{N}=1$ supergravity at low energies. Via the T-duality between IIA and IIB one comes into contact with F-theory, which can therefore be defined via a chain of dualities as an M-theory compactification on T^2 in the vanishing fiber size limit $\text{vol}(T^2) \rightarrow 0$.

In order to make this correspondence more precise consider the space-time $M_9 \times T^2$ with coordinates (\vec{w}, x, y) , which is given by the metric

$$ds_M^2 = ds_9^2 + \frac{V}{\tau_2(\vec{w})} \left((dx + \tau_1(\vec{w}) dy)^2 + \tau_2(\vec{w})^2 dy^2 \right). \quad (3.22)$$

The second part of this metric corresponds to the torus T^2 with volume (area) V and the complex structure modulus $\tau = \tau_1 + i\tau_2 \in \mathbb{C}$. Due to the holomorphic dependency of τ on the coordinates \vec{w} of M_9 this describes a fibration instead of a product, i.e. (3.22) describes an elliptically-fibered 11d space-time. Due to $\dim H^1(T^2) = 2$ there are 2 independent cycles for the torus. Let the α -cycle be in the direction of x and the β -cycle in the direction of the coordinate y . Upon the reduction along the α -cycle in the weak coupling limit of M-theory one obtains 10d type IIA string theory, which is related to the 11d M-theory metric by

$$ds_M^2 = L^2 e^{\frac{4x}{3}} (dx + C_1)^2 + e^{-\frac{2x}{3}} ds_{\text{IIA}}^2. \quad (3.23)$$

The coordinate x has periodicity 1 and C_1 describes the connection on the S^1 -bundle of the α -cycle over the IIA space-time $M_9 \times S_\beta^1$. Furthermore, L is a length scale for the M-theory α -cycle. Comparing with (3.22) allows to express C_1 , χ and in particular the type IIA metric

$$ds_{\text{IIA}}^2 = \frac{\sqrt{V}}{L\sqrt{\tau_2}} (V\tau_2 dy^2 + ds_9^2) \quad (3.24)$$

in terms of the elliptic fibration volume V and modulus τ . Along the remaining β -cycle of the original torus fibration one can now perform the T-duality in order to obtain type IIB string theory. In the Einstein frame the metric then takes the form

$$ds_{\text{IIB}} = \frac{\sqrt{V}}{L} \left(\frac{L^2 \ell_s^4}{V^2} dy^2 + ds_9^2 \right) \quad (3.25)$$

and only depends on V , τ_2 , L and the string scale ℓ_s . Now consider the case of a 3d compactification with $M_9 = \mathbb{R}^{1,2} \times \mathcal{B}$, where \mathcal{B} is a compact internal 6d $_{\mathbb{R}}$ Kähler manifold. The holomorphic dependency of the elliptic fibration on M_9 keeps the volume V of the fiber torus constant, such that by taking the scale $L = \sqrt{V}$ the type IIB metric simplifies to

$$ds_{\text{IIB}} = -(dx^0)^2 + (dx^1)^2 + (dx^2)^2 + \frac{\ell_s^4}{V} dy^2 + ds_{B_6}^2. \quad (3.26)$$

- M2-branes: A space-time filling M2-brane is mapped to a space-time filling D3-brane.
- M5-branes (4-cycle wrapping): If a 4-cycle $\Sigma_4 \subset \mathcal{Z}$ is wrapped in addition to 1+1 flat dimensions of the 11d space-time, the following cases are possible:
 - Σ_4 completely transversal to fiber: This yields a Kaluza-Klein monopole along Σ_4 and the two flat directions.
 - Σ_4 wraps the cycle $p\alpha + q\beta$ of the elliptic fiber, giving rise to a S^1 -fibration over a 3-dimensional subspace Σ_3 in the base \mathcal{B} of \mathcal{Z} . If Σ_3 is closed, this gives a (p, q) 5-brane wrapping the 3-cycle Σ_3 . When Σ_3 has a boundary on a degeneration locus of the elliptic fibration it maps to a (p, q) 5-brane ending on a (p, q) 7-brane.
 - Σ_4 completely wraps the fiber: This gives a D3-brane wrapping a 2-cycle in the fibration base \mathcal{B} and appears as a string from the 4d flat perspective.
- M5-branes (entirely internal): If the M5-brane entirely wraps a 6-cycle Σ_6 of the internal space \mathcal{Z} two cases have to be distinguished:
 - If only one cycle of the fiber is wrapped or the 6-cycle is entirely transversal to the fiber, the action becomes non-finite in the vanishing fiber volume limit that is implied for the duality to F-theory.
 - An internal M5-brane that entirely wraps the elliptic fiber is mapped to a D3-brane instanton. This case will be discussed in chapter 4.

In principle one can understand the additional gauge groups appearing in the Kodaira classification (cf. table 3.2) in terms of M2-branes wrapping collapsed 2-cycles in the fibration, whose intersections determine the enhanced gauge group.

3.4.3 Fluxes

Fluxes in F-theory are defined via the M/F-theory duality by fluxes and potentials of M-theory, which has just the sole \hat{C}_3 potential such that only a non-trivial 4-form flux

$$G_4 := d\hat{C}_3 \tag{3.27}$$

on the elliptically-fibered 4-fold \mathcal{Z} can be turned on [138, 140, 141]. This requires relaxing the geometry structure to a conformal Calabi-Yau type due to the back-reactions. Analogous to (2.47) one can then derive that in order to preserve supersymmetry $G_4^{4,0} = G_4^{0,4} = 0$ is required. The G_4 -flux is also subject to a self-duality condition

$$G_4 = \star_{\mathcal{Z}} G_4 \tag{3.28}$$

on the internal space \mathcal{Z} to ensure that there are no flux contributions to the effective tree-level moduli potential on the flat space-time, which has runaway direction towards large volume of the internal space [117]. On a 4-fold this also implies that $G_4^{3,1} = G_4^{1,3} = 0$ and therefore only leaves the $G_4^{2,2}$ component of the G_4 flux. In fact, on a 4-fold \mathcal{Z} a primitive (2,2)-form is in particular self-dual, such that the gauge flux actually is specified by

$$\begin{aligned} \text{primitivity: } & G_4 \wedge J = 0, \\ (2,2)\text{-form: } & G_4 = G_4^{2,2} \in H^{2,2}(\mathcal{Z}). \end{aligned} \tag{3.29}$$

Furthermore, there is a certain integrality condition described in section 3.6. The part of the G_4 -flux compatible with 4d Poincaré invariance in the type IIB picture is of the form

$$G_4 = H_3 \wedge L dx + F_3 \wedge L dy. \tag{3.30}$$

However, this parametrization in terms of the IIB R-R and NS-NS 3-form fluxes H_3 and F_3 is only a small subset of all valid fluxes as $H_3, F_3 \in H^3(\mathcal{B}; \mathbb{Z})$ is not directly related to $G_4 \in H^4(\mathcal{Z}; \mathbb{Z})$. Often the number of suitable 4-cycles in \mathcal{Z} goes into the thousands, whereas 3-cycles in the base can be rather rare. Furthermore, in the context of F-theory compactifications it is still unknown how to describe G_4 -fluxes properly for general settings that involve singularities due to non-perturbative, non-Abelian 7-branes in the total space \mathcal{Z} of the fibration.

The fact that type IIB “bulk fluxes” only provide a small fraction of all G_4 -fluxes is related to the non-trivial $SL(2; \mathbb{Z})$ monodromy of the H_3 and F_3 -fluxes in the presence of 7-branes, cf. (2.15) and (3.5). The G_4 -flux not only encodes background fluxes on \mathcal{Z} but contains brane worldvolume fluxes as well. Locally around a 7-brane, i.e. where at least one cycle $S^1 \subset T^2$ of the elliptic fiber shrinks to zero size and causes a zero in the elliptic discriminant, the Calabi-Yau 4-fold geometry is similar to a Taub-NUT space. It supports a harmonic (1,1)-form ω that peaks over the discriminant locus and allows to decompose the 3-form potential to

$$\hat{C}_3 = A \wedge \omega. \tag{3.31}$$

This A corresponds to the $U(1)$ open string gauge fields on the 7-brane worldvolume. Similarly, an internal gauge flux F on the 7-brane worldvolume is encoded via

$$G_4 = F \wedge \omega. \tag{3.32}$$

The non-perturbative F-theory framework and the G_4 flux from M-theory therefore provide an unified perspective on all types of fluxes that can be accommodated. Lacking general methods to construct all G_4 -fluxes, one has to use the spectral cover approach

introduced in section 3.5 to describe such fluxes. This is used in the construction of chiral matter content via intersecting 7-branes in the presence of non-trivial G_4 -flux backgrounds following the basic approach of section 2.5.

3.4.4 Other dualities and definitions

Aside from the duality between F-theory and M-theory with vanishing fiber volume, one can also show a duality to $E_8 \times E_8$ heterotic string theory — which is particularly interesting as heterotic models in the absence of D-branes and open strings only contain the intrinsically global closed string sector. While this duality will be a guide for certain constructions in chapter 6, it is less general than the M/F-theory duality described so far in section 3.4.1. For example, it can be shown that the class of local F-theory GUT models with $U(1)_Y$ -hypercharge flux GUT symmetry breaking — considered primary in recent years — does not have an appropriate heterotic dual.

Ultimately, there are three known dualities — or definitions, depending on one’s point of view — for the particular class of non-perturbative string theory models described by F-theory [117, 119]:

1. The geometrization of the varying axio-dilaton τ in type IIB models with 7-branes.
2. The limit of M-theory on an elliptically-fibered space with vanishing fiber volume.
3. The duality to heterotic $E_8 \times E_8$ string theory.

In the following the focus will be almost exclusively on the first and second definition of (or rather duality to) F-theory, but the spectral cover construction discussed in section 3.5 requires a basic understanding of the third duality.

3.4.5 F-theory and the heterotic string

The F-theory description via M-theory is a proper description for all models. In contrast, the heterotic/F-theory duality only applies to a small class of F-theory compactifications, but allows to carry over some useful constructions developed for the heterotic string.

The duality states that F-theory compactified on an elliptically-fibered $K3$ surface is dual to the heterotic string on T^2 . The mapping between the two geometrical settings is called a Fourier-Mukai transform [66, 69, 119, 142–148]. More specifically, in the context of $\mathcal{N}=1$ supersymmetric compactifications the internal space has to be a $K3$ -fibered Calabi-Yau \mathcal{Z}_{n+2} on the F-theory side and where each $K3$ is itself elliptically-fibered over a \mathbb{P}^1 :

$$\begin{aligned} K3 &\hookrightarrow \mathcal{Z}_{n+2} \twoheadrightarrow \mathcal{B}_n \\ \mathbb{E} &\hookrightarrow K3 \twoheadrightarrow \mathbb{P}^1. \end{aligned} \tag{3.33}$$

The elliptic fibration of the $K3$ naturally descends to an elliptic fibration of \mathcal{Z}_{n+2} with the base \mathcal{B}_{n+1} . This elliptic base is itself \mathbb{P}^1 -fibered over the $K3$ base \mathcal{B}_n . The heterotic/F-theory duality therefore asserts the existence of an elliptically-fibered Calabi-Yau space \mathcal{Y}_{n+1} over the $K3$ base \mathcal{B}_n . This duality is technically established by comparing the moduli spaces of both theories. In particular, the volume of the base \mathbb{P}^1 is dual to the heterotic string coupling $g_{\text{het}} = e^{2\phi}$. All those fibrations can be summarized in a diagram

$$\begin{array}{ccc}
 \mathbb{E} & \xrightarrow{\text{wavy}} & \mathcal{Y}_{n+1} \\
 \downarrow & \searrow & \downarrow \\
 K3 & \xrightarrow{\quad} & \mathcal{Z}_{n+2} \longrightarrow \mathcal{B}_n \\
 \downarrow & \searrow & \downarrow \\
 \mathbb{P}^1 & \dashrightarrow & \mathcal{B}_{n+1}
 \end{array}
 \quad \text{where } \begin{array}{l} \mathcal{Y}_{n+1} \text{ heterotic compact. space,} \\ \mathcal{Z}_{n+2} \text{ F-theory compact. space,} \end{array} \quad (3.34)$$

such that $\text{vol}(\mathbb{P}^1) \xleftarrow{\text{dual}} g_{\text{het}}$,

that shows how the space \mathcal{Y}_{n+1} intertwines the double fibration structures (3.33) from the F-theory side. Naturally, this particular geometric setting is rather constrained and not generic to all F-theory models.

For the case of four flat dimensions—corresponding to $n = 1$ in the above outline—one can be more explicit about the involved spaces. The base \mathcal{B}_2 of an elliptically-fibered Calabi-Yau 3-fold \mathcal{Y}_3 on the heterotic side can only be a del Pezzo surface dP_n , a (blowup of a) Hirzebruch surface \mathbb{F}_k or the Enriques surface $K3/\mathbb{Z}_2$. For the dual F-theory Calabi-Yau 4-fold \mathcal{Z}_4 the elliptic base \mathcal{B}_3 is a \mathbb{P}^1 -fibration over this surface \mathcal{B}_2 . It can be characterized cohomologically by a line bundle \mathcal{T} over \mathcal{B}_2 , i.e. via $t := c_1(\mathcal{T})$. The base \mathcal{B}_3 can then be constructed as the total space of the projectivization of the rank-2 vector bundle $\mathcal{O} \oplus \mathcal{T}$ over \mathcal{B}_2 , i.e. $\mathcal{B}_3 = \mathbb{P}(\mathcal{O} \oplus \mathcal{T})$ where each fiber is a $\mathbb{P}(\mathbb{C} \oplus \mathbb{C}) = \mathbb{P}^1$. In summary, we therefore have the geometric situation

$$\begin{array}{ccc}
 \mathbb{E} & \xrightarrow{\text{wavy}} & \mathcal{Y}_3 \\
 \downarrow & \searrow & \downarrow \\
 K3 & \xrightarrow{\quad} & \mathcal{Z}_4 \longrightarrow \mathcal{B}_2 = \begin{cases} dP_n \\ \mathbb{F}_k \\ B(\mathbb{F}_k) \\ K3/\mathbb{Z}_2 \end{cases} \\
 \downarrow & \searrow & \downarrow \\
 \mathbb{P}^1 & \dashrightarrow & \mathcal{B}_3 = \mathbb{P}(\mathcal{O} \oplus \mathcal{T})
 \end{array} \quad (3.35)$$

for compactifications to four dimensions. The construction of F-theory models with heterotic duals can therefore be restated in terms of constructing vector bundles. Furthermore, the value t can be interpreted as a generalized instanton number related to 6d compactifications.

3.5 The Spectral Cover Construction

In the absence of space-time singularities the gauge group G_{het} of the heterotic string is either $E_8 \times E_8$ or $SO(32)$. Given a holomorphic vector bundle V with structure group H on the internal space \mathcal{Y}_3 , the gauge group is broken to the commutator $G = H^\perp \subset G_{\text{het}}$ after embedding H into G_{het} . Under the heterotic / F-theory duality one therefore expects the vector bundle to map to a singular geometry of \mathcal{Z}_4 and a non-trivial gauge flux G_4 . In the context of the duality, \mathcal{Y}_3 is assumed to be elliptically-fibered over \mathcal{B}_2 . The underlying idea of the spectral cover construction is to split up the information contained in the vector bundle V into two structures that can be entirely characterized by their respective topological data: the spectral surface $\mathcal{C}^{(n)}$ and the spectral line bundle \mathcal{N} . In the F-theory dual $\mathcal{C}^{(n)}$ then determines the singularity structure of the base \mathcal{B}_3 of \mathcal{Z}_4 , whereas \mathcal{N} specifies the G_4 flux [144, 149].

The construction of the spectral surface discussed here originates from generic properties of a rank- n vector bundle W with structure group $U(n)$ or $SU(n)$ over an elliptic curve \mathbb{E} . It can be shown that such a vector bundle decomposes into the direct sum of line bundles

$$W = L_1 \oplus \cdots \oplus L_n \quad \text{over } \mathbb{E}. \quad (3.36)$$

Each L_i has to be of zero degree, which implies that there exists a meromorphic section of each L_i that has exactly one zero in the point $q_i \in \mathbb{E}$ and a single pole at the point p that corresponds to the origin of the elliptic curve. The line bundle is therefore explicitly given by

$$L_i = \mathcal{O}_{\mathbb{E}}(q_i - p) \quad (3.37)$$

for a vector bundle W with structure group $U(n)$. For the $SU(n)$ structure group the additional constraint of a trivial determinant is imposed, i.e.

$$\bigotimes_{i=1}^n L_i = \mathcal{O}_{\mathbb{E}} \quad \rightsquigarrow \quad \sum_{i=1}^n (q_i - p) = 0. \quad (3.38)$$

The entire vector bundle W over \mathbb{E} is therefore determined by the collection of n points q_i on the elliptic curve.

Coming back to the original heterotic setting of a vector bundle V over the elliptically-fibered 3-fold \mathcal{Y}_3 , one considers the restriction

$$V|_{(\mathcal{Y}_3)_b} = \bigoplus_{i=1}^n \mathcal{O}(q_i(b) - p) \quad (3.39)$$

to the elliptic fiber $(\mathcal{Y}_3)_b \cong \mathbb{E}$ over $b \in \mathcal{B}_2$. This associates a set of n points $q_i(b)$ to each point of the base \mathcal{B}_2 and therefore uniquely defines an n -sheeted covering $\mathcal{C}^{(n)}$ of \mathcal{B}_2 —

the spectral cover surface. Since each $q_i(b)$ lies in the fiber over $b \in \mathcal{B}_2$, the spectral surface is a hypersurface inside \mathcal{Y}_3 , i.e.

$$\{1, \dots, n\} \hookrightarrow \mathcal{C}^{(n)} \xrightarrow{\pi_n} \mathcal{B}_2 \quad \text{such that} \quad \mathcal{C}^{(n)} \cap (\mathcal{Y}_3)_b = \bigcup_{i=1}^n q_i(b). \quad (3.40)$$

In order to describe $\mathcal{C}^{(n)}$ topologically, let σ be the section of the elliptic fibration of \mathcal{Y}_3 that embeds the base $\mathcal{B}_2 \subset \mathcal{Y}_3$. It has the property

$$\sigma \cdot \sigma = -\sigma c_1(\mathcal{B}_2) \in H^4(\mathcal{Y}_3; \mathbb{Z}), \quad (3.41)$$

such that the Poincaré-dual cohomology class of $\mathcal{C}^{(n)} \subset \mathcal{Y}_3$ can be written as

$$[\mathcal{C}^{(n)}] = n\sigma + \pi^*\eta \in H^2(\mathcal{Y}_3; \mathbb{Z}), \quad (3.42)$$

where $\eta \in H^2(\mathcal{B}_2; \mathbb{Z})$ is some effective class and $\pi : \mathcal{Y}_3 \rightarrow \mathcal{B}_2$ the elliptic fibration's projection mapping. In summary, one has

$$\begin{array}{ccc} \mathbb{E} & \hookrightarrow & \mathcal{Y}_3 \xrightarrow{\pi} \mathcal{B}_2 \\ \cup & & \cup \nearrow \pi_n \\ \{1, \dots, n\} & \hookrightarrow & \mathcal{C}^{(n)} \end{array} \quad (3.43)$$

i.e. the spectral cover is a discrete sub-fibration of the elliptic fibration of \mathcal{Y}_3 over \mathcal{B}_2 .

The restriction of the vector bundle V to the elliptic fibers in (3.39) naturally discards information on the global structure of the bundle. By introducing the spectral cover line bundle \mathcal{N} on $\mathcal{C}^{(n)}$ with the property

$$(\tilde{\pi}_n)_*\mathcal{N} = V|_{\mathcal{B}_2} \quad (3.44)$$

the missing information can be restored. Here $(\tilde{\pi}_n)_*$ essentially takes the line bundle fiber of \mathcal{N} over each of the n points in $(\pi_n)^{-1}(b)$ in order to reconstruct^V the rank- n vector bundle V over $b \in \mathcal{B}_2$. This reformulation in terms of a line bundle allows to describe the data by the first Chern class $c_1(\mathcal{N}) \in H^2(\mathcal{C}^{(n)}; \mathbb{Z})$, which is decomposed as

$$c_1(\mathcal{N}) = \frac{r}{2} + \gamma \quad \text{where} \quad \begin{aligned} r &= -c_1(\mathcal{C}^{(n)}) + (\pi_n)^*c_1(\mathcal{B}_2), \\ \gamma &= \frac{1}{n}(\pi_n)^*c_1(V) + \gamma_u. \end{aligned} \quad (3.45)$$

^VThe tilde in the mapping $(\tilde{\pi}_n)_*$ highlights that the rank- n vector bundle is decomposed into a direct sum of n line bundles that are distributed to the n sheets of the spectral cover $\mathcal{C}^{(n)}$. Due to this decomposition (or Whitney-summing for the inverse mapping) the mapping $(\tilde{\pi}_n)_*$ is therefore not the ordinary push-forward of a line bundle.

The part γ_u is chosen such that $(\pi_n)_*\gamma_u = 0$, which yields

$$\gamma_u = \lambda \left(n\sigma - (\pi_n)^*\eta + n(\pi_n)^*c_1(\mathcal{B}_2) \right) \in H^2(\mathcal{C}^{(n)}; \mathbb{Z}) \quad (3.46)$$

for a number $\lambda \in \mathbb{Q}$, that is chosen appropriately to satisfy the integrality conditions in the cohomology groups. Ultimately, one obtains

$$\begin{aligned} c_1(\mathcal{N}) = & -\sigma + n \left(\frac{1}{2} + \lambda \right) \sigma + \left(\frac{1}{2} - \lambda \right) (\pi_n)^*\eta \\ & + \left(-\frac{1}{2} + n\lambda \right) (\pi_n)^*c_1(\mathcal{B}_2) + \frac{1}{n}(\pi_n)^*c_1(V) \end{aligned} \quad (3.47)$$

for the spectral line bundle. Together the spectral cover surface $\mathcal{C}^{(n)}$ and the spectral line bundle \mathcal{N} provide the topological description for the vector bundle V over the elliptically-fibered 3-fold \mathcal{Y}_3 .

Using the spectral cover description of the gauge breaking vector bundle V in the heterotic string theory, one can explicitly formulate the dual F-theory description. Let $\eta_1, \eta_2 \in H^2(\mathcal{B}_2; \mathbb{Z})$ be the classes of $V = V_1 \oplus V_2$ embedded into $E_8^{(1)} \times E_8^{(2)}$ as defined in (3.42). The remaining heterotic gauge group $G = G_1 \times G_2 = H_1^\perp \times H_2^\perp \subset E_8^{(1)} \times E_8^{(2)}$ then appears in the \mathbb{P}^1 -fibered base \mathcal{B}_3 of the F-theory 4-fold \mathcal{Z}_4 . More precisely, the gauge groups G_1 and G_2 are respectively localized on the divisors of \mathcal{B}_3 that correspond to the north and south pole of the \mathbb{P}^1 in the fibration.

Following the “projectivization description” of \mathcal{B}_3 in (3.35), the relationship to the line bundle \mathcal{T} on \mathcal{B}_2 is given by

$$\begin{aligned} \eta_1 = 6c_1(\mathcal{B}_2) - c_1(\mathcal{T}) \\ \eta_2 = 6c_1(\mathcal{B}_2) + c_1(\mathcal{T}) \end{aligned} \quad \rightsquigarrow \quad c_1(\mathcal{T}) = \frac{1}{2}(\eta_2 - \eta_1), \quad (3.48)$$

i.e. the spectral surface $\mathcal{C}^{(n)}$ determines the geometry of the base \mathcal{B}_3 and therefore — with the duality-inherited elliptic fibration structure — the F-theory 4-fold \mathcal{Z}_4 .

The gauge flux G_4 on the resolved 4-fold $\tilde{\mathcal{Z}}_4$ is governed by the γ_u piece defined in (3.45) and (3.46), i.e.

$$\int_{\tilde{\mathcal{Z}}_4} G_4 \wedge G_4 = - \int_{\mathcal{B}_2} (\pi_n)_* \left((\gamma_1)^2 + (\gamma_2)^2 \right). \quad (3.49)$$

It should be noted, that the entire discussion here only applies to vector bundles V with structure group $U(n)$ or $SU(n)$, otherwise certain modifications in the decomposition (3.36) and the form (3.37) are necessary. In section 6.1 the construction will be generalized to F-theory settings without a heterotic dual.

3.6 Consistency Conditions

The consistency conditions of F-theory models are comparable to the type IIB conditions in section 2.8. Since several conditions are intrinsically encoded in the geometry of the elliptically-fibered 4-fold \mathcal{Z} —like a 7-brane tadpole condition one might expect—far less explicit conditions actually remain [110]:

- *D3-brane tadpole condition:* The number of D3-branes, the G_4 -flux and the elliptically-fibered 4-fold are related by

$$N_{\text{D3}} + \frac{1}{2} \int_{\mathcal{Z}} G_4 \wedge G_4 = \frac{\chi(\mathcal{Z})}{24}. \quad (3.50)$$

As the 4-fold \mathcal{Z} becomes singular in the presence of certain non-perturbative 7-brane stacks and configurations, one has to resolve the space or generalize the Euler characteristic appropriately.

Supersymmetry requires the 4-fold \mathcal{Z} to be of Calabi-Yau type—a condition which in the presence of fluxes has to be relaxed somewhat. In order to obtain 4d $\mathcal{N}=1$ supersymmetry and stability in the effective theory, it was already discussed in section 3.4.3 that an analysis similar to (2.47) shows that upon splitting $G_4 = G_{4,0} + G_{3,1} + G_{2,2} + G_{1,3} + G_{0,4}$ the following components have to vanish:

$$G_{4,0} = G_{3,1} = G_{1,3} = G_{0,4} = 0. \quad (3.51)$$

The remaining non-vanishing component $G_{2,2} \in \Omega^{2,2}(\mathcal{Z})$ has to satisfy the primitivity condition

$$G_{2,2} \wedge J = 0, \quad (3.52)$$

such that ultimately the allowable G_4 -fluxes in the context of M/F-theory are

$$G_4 \in \Omega_{\text{primitive}}^{2,2}(\mathcal{Z}), \quad (3.53)$$

which according to (3.28) have to be self-dual on the internal space. Furthermore, one has to deal with the quantization of the G_4 -form flux [117, 141]. A shift leads to the integrality condition

$$[G_4] - \frac{c_2(\mathcal{Z})}{2} \in H^4(\mathcal{Z}; \mathbb{Z}). \quad (3.54)$$

In general, compared to the type II conditions in section 2.8 all those conditions are rather difficult to evaluate and apply in non-trivial settings, which is mostly due to technical difficulties in handling the singularities of \mathcal{Z} .

3.7 Weak-coupling Sen Limit

In section 3.1 it was observed that non-trivial F-theory settings involving 7-branes are intrinsically of strong coupling. On the other hand, the perturbative type IIB origin of the theory necessarily implies the existence of weakly coupled regions. This raises the question of how one can see such weakly coupled, perturbative regions in F-theory. According to (3.2) this means to search for regions where $\text{Im } \tau$ is rather large and ideally constant. In this context the idea was first discussed by Sen [124–126, 150, 151]—hence the name Sen limit.

A generic setting can be constructed by introducing a parameter ε for rescaling the Tate coefficients

$$\begin{aligned} a_3 &\rightarrow \varepsilon a_3 & f &= \frac{1}{48}(24\varepsilon b_4 - b_2^2), \\ a_4 &\rightarrow \varepsilon a_4 & g &= \frac{1}{864}(215\varepsilon^2 b_6 - 36\varepsilon b_4 b_2 + b_2^3), \\ a_6 &\rightarrow \varepsilon^2 a_6 \end{aligned} \quad \rightsquigarrow \quad (3.55)$$

such that in the limit $\varepsilon \rightarrow 0$ the fraction $\frac{f^3}{g^2}$ is constant. A slight rescaling of the coefficient functions brings those terms in a more accessible form:

$$\begin{aligned} h &:= -\frac{1}{4}b_2 & f &= -3h^2 + \varepsilon\eta, \\ \eta &:= \frac{1}{2}b_4 & g &= -2h^3 + \varepsilon h\eta - \varepsilon^2 \frac{\chi}{12}, \\ \chi &:= -\frac{215}{72}b_6, \end{aligned} \quad \rightsquigarrow \quad (3.56)$$

The leading ε -order of the elliptic discriminant and the j -function take the form

$$\begin{aligned} -16\Delta &\approx -\frac{\varepsilon^2}{4}b_2^2(b_2 b_6 - b_4^2) + \mathcal{O}(\varepsilon^2) = -9\varepsilon^2 h^2(\eta^2 - h\chi), \\ j(\tau) &\propto \frac{b_2^4}{\varepsilon^2(b_2 b_6 - b_4^2)} \propto \frac{h^4}{\varepsilon^2(\eta^2 - h\chi)}. \end{aligned} \quad (3.57)$$

Via (3.3) it then follows that in the limit $\varepsilon \rightarrow 0$ the type IIB coupling constant vanishes almost everywhere except $h = 0$:

$$g_s \propto -\frac{1}{\log|\varepsilon|} \xrightarrow{\varepsilon \rightarrow 0} 0. \quad (3.58)$$

A detailed analysis of the monodromies shows that in the limit $\varepsilon \rightarrow 0$ the discriminant locus can be identified with an O7-plane and D7-brane located at

$$\begin{aligned} \text{O7: } & h(u) = 0, \\ \text{D7: } & \eta(u)^2 = h(u)\chi(u), \end{aligned} \quad (3.59)$$

where $u \in \mathcal{B}$ are the coordinates on the base. This brings the Sen limit into direct contact with a type IIB orientifold setting. Away from the $\epsilon \rightarrow 0$ limit the factorization of the discriminant and subsequent identification of the perturbative O7-plane and D7-brane is lost. The non-perturbative effects included via the F-theory description essentially smoothen out the singular BC -type orientifold locus. Note that the particular form of (3.59) generically can give rise to self-intersecting D7-brane configurations in global models, which will be explicitly investigated later in section 4.2 [87, 111, 152, 153].

However, it should be emphasized that the limit itself has no direct meaning as all non-trivial content is eliminated for $\epsilon = 0$ due to $a_3 = a_4 = a_6 = 0$, cf. table 3.6. It rather provides the means to parameterize the corresponding type IIB coupling constant and use the parameter to go arbitrarily far into the weakly-coupled regime—the limit being the no-coupling special case of no direct interest. Having such a weakly coupled region in the setting allows to compare to the perturbative theory and justifies the description in terms of a type IIB orientifold setting. In a more general context, having a Sen limit in an F-theory setting therefore corresponds to the existence of a parameter that allows for a global tuning of the elliptic fibration—the complex structure of the torus—that smoothly connects the strong coupling and weak coupling region.

3.8 Local vs. Global Model Building

After the initial surge of developments in F-theory following the original paper from 1996 [59], the publication of several papers in 2008 on local F-theory GUT models [66–69] stirred the interest in this approach anew. This is mostly due to the realization that the F-theory framework easily accommodates exceptional gauge groups necessary for GUT model building and the discovery of the decoupling principle. The existence of exceptional groups in F-theory was already known in the early stages, but technical difficulties in engineering suitable Calabi-Yau 4-folds prohibited extensive model building in the late '90s—and except for certain special cases still do.

In stringy IIB GUT theories [99] a stack of 7-branes wrapping the internal 4-cycle $\mathcal{S}_{\text{GUT}} \subset \mathcal{B}$ of the base carries the GUT gauge group, e.g. $SU(5)$ or $SO(10)$. Further 7-branes $\mathcal{S}, \mathcal{S}' \subset \mathcal{B}$ in the setting necessarily intersect the GUT brane along 1-dimensional curves $\mathcal{S}_{\text{GUT}} \cap \mathcal{S}$ of the internal geometry, where matter states localize—hence the name “matter curves”. When multiple 7-branes (or equivalently multiple matter curves) meet in a point, Yukawa couplings and superpotential contributions arise. Intersection angles, volumes of the wrapped cycles and topology of the intersection curves all determine the resulting interaction strengths and other phenomenologically relevant properties. Generically, however, the numerous back-reactions between the branes and the geometry easily becomes unmanageable.

3.8.1 The Decoupling Principle

In order to deal with the back-reactions the natural idea is to focus on a local neighborhood of the GUT brane. Basically, one would like to work just on the effective 8d worldvolume gauge theory of the GUT brane. From this perspective one only sees the matter curves and triple intersection points, but ignores the global structure of the branes that gives rise to those curves and points. In the local F-theory GUT model building approach one completely neglects therefore the tedious task of constructing suitable elliptically-fibered Calabi-Yau 4-folds and instead engineers intersections with the GUT-brane only locally in a small neighborhood [67, 68]. This necessarily raises the question whether the global structure and its gravitational back-reactions can be neglected at all. The existence of a decoupling limit essentially demands that all gravitational interactions can be made parametrically small — which has obvious similarities to the coupling-parametrically Sen limit discussed in section 3.7. This implies to be able to increase the Planck mass arbitrarily while keeping the gauge theory parameters finite.

On a technical level the existence of a decoupling limit implies a significant simplification due to the geometric dependence of the Planck scale M_{Pl} , the GUT coupling α and the GUT scale M_{GUT} [67, 154]. Via the dimensional reduction of the 10d Einstein-Hilbert action on $\mathbb{R}^{1,3} \times \mathcal{B}$ one finds

$$M_{\text{Pl}} \propto \text{vol}(\mathcal{B}), \quad (3.60)$$

i.e. the 4d Planck scale depends on size of the inner dimensions. The GUT coupling, which arises from the reduction of the 8d super-Yang-Mills theory on the GUT-brane worldvolume, is similarly dependent on the geometrical size of the wrapped GUT-brane divisor

$$\alpha \propto \text{vol}(\mathcal{S})^{-1}, \quad (3.61)$$

and one can determine by dimensional analysis that the GUT scale dependency is

$$M_{\text{GUT}} \propto \text{vol}(\mathcal{S})^{-\frac{1}{4}}. \quad (3.62)$$

Ultimately, the gauge parameters α and M_{GUT} depend on the size of the GUT brane divisor, whereas the Planck mass is proportional to the total volume of the compact inner dimensions.

The existence of a decoupling limit therefore requires a geometry, where in the gravitational decoupling limit $\text{vol}(\mathcal{B}) \rightarrow \infty$ the GUT-brane divisor volume $\text{vol}(\mathcal{S})$ remains at a fixed finite value. As a mathematical alternative one can also consider the limit where $\text{vol}(\mathcal{S}) \rightarrow 0$ while $\text{vol}(\mathcal{B})$ remains finite, even if there are subtle differences between those

$\mathbb{CP}^1 \times \mathbb{CP}^1$:	1	\mathbb{CP}^2 :	1	dP_n :	1
	0 0		0 0		0 0
	0 2 0		0 1 0		0 $n+1$ 0
	0 0		0 0		0 0
	1		1		1

Table 3.4.: Hodge diamonds of the del Pezzo surfaces, where the number of \mathbb{CP}^2 -blowups is $n = 1, \dots, 8$.

limits. For this reason one usually wraps the GUT 7-brane around a del Pezzo surface \mathcal{S} inside the Kähler 3-fold base $\mathcal{B} = \mathcal{X}/\sigma$ of the elliptically-fibered Calabi-Yau 4-fold \mathcal{Z} in typical F-theory GUT models. Such del Pezzo surfaces are $\mathbb{CP}^1 \times \mathbb{CP}^1$, \mathbb{CP}^2 and blowups of \mathbb{CP}^2 at $n = 1, \dots, 8$ distinct points, denoted dP_n . The Hodge diamonds in table 3.4 clearly show that all del Pezzo surfaces have no deformation moduli as $b_1 = 0$, which makes them rigid with the overall volume being the only parameter.

3.8.2 Local F-theory GUT model building

The typical setting in a local F-theory GUT model involves a GUT 7-brane with gauge group $SU(5)$ or $SO(10)$, that would supposedly wrap a del Pezzo surface in the corresponding global model [67, 68]. Following the Georgi-Glashow $SU(5)$ GUT models [13], the Standard Model gauge group $SU(3)_C \times SU(2)_W \times U(1)_Y$ is embedded in $SU(5)$ such that the generator of the Abelian $U(1)_Y$ -factor is identified with the generator^{VI}

$$Y = \left(-\frac{1}{6}\right) \text{diag}(2, 2, 2, -3, -3) \quad (3.63)$$

of the $SU(5)$ -algebra and the matter content of the $\mathcal{N}=1$ (minimal) supersymmetric Standard Model (MSSM) is organized in the $SU(5)$ -multiplets listed in table 3.5. The gauge bosons arise from the decomposition of the adjoint representation

$$\mathbf{24} \rightarrow \underbrace{(\mathbf{8}, \mathbf{1})_0 \oplus (\mathbf{1}, \mathbf{3})_0 \oplus (\mathbf{1}, \mathbf{1})_0}_{\text{Standard Model gauge bosons}} \oplus \underbrace{(\mathbf{3}, \mathbf{2})_{-\frac{5}{6}} \oplus (\bar{\mathbf{3}}, \mathbf{2})_{\frac{5}{6}}}_{\text{exotic bosons}} \quad (3.64)$$

yielding two exotic representations that have to be taken care of in realistic models. The $SU(5)$ GUT also suffers from the doublet-triplet splitting problem, which in addition to the required Higgs representations yields unwanted color triplets in the decomposition of $\mathbf{5}_H$ and $\bar{\mathbf{5}}_H$.

^{VI}Note that the factorized prefactor $-\frac{1}{6}$ in (3.63) is often omitted in the literature. Between the different embedding matrices only the hypercharge flux of the decomposed representations changes. The convention chosen here gives the fractional charges usually found in the Standard Model.

10	$(\mathbf{3}, \mathbf{2})_{\frac{1}{6}}$	Q_L	left-handed quark doublet
	$(\bar{\mathbf{3}}, \mathbf{1})_{-\frac{2}{3}}$	$\bar{u}_L = (u_R)^c$	left-handed up-type anti-quark
	$(\mathbf{1}, \mathbf{1})_1$	$\bar{e}_L = (e_R)^c$	left-handed anti-lepton
$\bar{\mathbf{5}}_m$	$(\mathbf{3}, \mathbf{1})_{\frac{1}{3}}$	$\bar{d}_L = (d_R)^c$	left-handed down-type anti-quark
	$(\mathbf{1}, \mathbf{2})_{-\frac{1}{2}}$	L_L	left-handed lepton doublet
1	$(\mathbf{1}, \mathbf{1})_0$	$\bar{\nu}_L = (\nu_R)^c$	left-handed anti-neutrino
$\mathbf{5}_H$	$(\mathbf{3}, \mathbf{1})_{-\frac{1}{3}}$	T_u	up-type color triplet (GUT remnant)
	$(\mathbf{1}, \mathbf{2})_{\frac{1}{2}}$	H_u	up-type Higgs doublet
$\bar{\mathbf{5}}_H$	$(\bar{\mathbf{3}}, \mathbf{1})_{\frac{1}{3}}$	T_d	down-type color triplet (GUT remnant)
	$(\mathbf{1}, \mathbf{2})_{-\frac{1}{2}}$	H_d	down-type Higgs doublet

Table 3.5.: Standard Model representations in $SU(5)$ GUTs. A single generation of left-handed matter is contained in the $\mathbf{10} \oplus \bar{\mathbf{5}}_m \oplus \mathbf{1}$ representation.

As mentioned earlier, in a local GUT model the matter representations and couplings originate from (multiple) intersections of the GUT-brane with further 7-branes, leading to enhancements of the singularity type in the elliptic fibration over the intersection curve or point. For correspondence with the MSSM states this requires at least the presence of three matter curves of type $\mathbf{10}$, $\bar{\mathbf{5}}_m$ and $\mathbf{1}$ as well as a single Higgs curve of type $\mathbf{5}_H$ and $\bar{\mathbf{5}}_H$ each. Over triple intersections of matter curves (i.e. quadruple intersections of 7-branes) the elliptic degeneration gets worse which leads to Yukawa couplings [66, 67, 72, 77, 155]. For example, over the triple intersection of two $\mathbf{10}$ matter curves with the $\mathbf{5}_H$ Higgs curve the singularity enhances according to table 3.6 to exceptional type E_6 . The decomposition then yields the $\mathbf{10} \cdot \mathbf{10} \cdot \mathbf{5}_H$ Yukawa coupling — which is of strictly non-perturbative origin and is generated in perturbative type II orientifold models by D-brane instantons. One of the major appealing arguments for the usage of the F-theory framework is the entirely unified and natural origin of this crucial coupling. In terms of MSSM fields the relevant Yukawa couplings are

$$\begin{aligned}
 \mathbf{10} \cdot \mathbf{10} \cdot \mathbf{5}_H &\rightarrow Q_L (u_R)^c H_u, \\
 \mathbf{10} \cdot \bar{\mathbf{5}}_m \cdot \bar{\mathbf{5}}_H &\rightarrow L_L (e_R)^c H_d + Q_L (d_R)^c H_d.
 \end{aligned}
 \tag{3.65}$$

The localization of the up- and down-type Higgs on distinct matter curves helps solving the doublet-triplet splitting problem in specific models. Further refinements on e.g. interaction strengths can then be tuned directly in the geometry of the intersections and the matter curves.

3.8.3 $U(1)_Y$ -hypercharge flux GUT group breaking

Any viable GUT model requires the breaking of the unification symmetry at low energies in order to reproduce the Standard Model gauge group. Three approaches are known to achieve this breaking in generic string models: Using adjoint Higgs fields or Higgses in large representations, breaking via Wilson lines and the activation of a non-trivial Abelian background flux on the GUT 7-brane [69, 156]. As it turns out, only the last method is actually applicable to F-theory GUT models if one aims to preserve certain phenomenological aspects—like solutions for the double-triplet splitting problem and rapid proton decay—and to avoid singular branes.

The basic idea of the hypercharge flux GUT breaking is to turn on a non-trivial $U(1)_Y$ -hypercharge flux on $\mathcal{S}_{\text{GUT}} \subset \mathcal{B}$. One specifies a line bundle L on \mathcal{S}_{GUT} , which is embedded via the matrix (3.63) into the GUT group $SU(5)$. A non-zero value of $c_1(L) \in H^2(\mathcal{S}_{\text{GUT}})$ corresponds to a non-trivial background flux. This background flux on the worldvolume can be encoded into the M/F-theory G_4 -flux via

$$G_4 \propto c_1(L) \wedge (\omega^Y - \omega_2) = -c_1(L^{\frac{5}{6}}) \wedge \omega_3 \quad (3.66)$$

where ω^Y is a specific 2-form that can be understood as a δ -function localized on \mathcal{S}_{GUT} and ω_2 as well as ω_3 are non-trivial shifts required to eliminate the unacceptable exotic gauge bosons found in (3.64). Ultimately, this requires both $L^{\frac{5}{6}}$ and L to be well-defined line bundles over \mathcal{S}_{GUT} . A further constraint arises from the Stückelberg mechanism that could potentially give a mass to the $U(1)_Y$ field. Since $\mathcal{S}_{\text{GUT}} \subset \mathcal{B}$ has codimension 1, the vanishing of the hypercharge Stückelberg masses Π_M^Y requires that the Poincaré-dual 2-cycle $\Xi := \text{PD}(c_1(L)) \in H_2(\mathcal{S}_{\text{GUT}})$ is trivial as a 2-cycle $\iota_*\Xi \in H_2(\mathcal{B})$ of the base, i.e. $\Xi \in \ker(\iota_*)$ for the embedding $\iota : \mathcal{S}_{\text{GUT}} \hookrightarrow \mathcal{B}$. This yields a somewhat non-trivial topological condition for the base and the embedded GUT-brane divisor \mathcal{S}_{GUT} .

3.8.4 Global issues

The possibility to work in geometrically simple settings while benefiting from the strong-coupling properties of F-theory in local GUT models—like exceptional gauge symmetries—led to the successful reproduction of several phenomenological aspects within this unified perspective. Unfortunately, the key consistency conditions enumerated in section 3.6 can only be evaluated in global settings where the full elliptically-fibered Calabi-Yau 4-fold is explicitly known. As it turns out, the stepping-up from local to global F-theory models is highly non-trivial at a technical level and so far has only been successful at isolated instances. This puts the results of local F-theory models in the awkward situation of being somewhat speculative, as there may be severe global

restriction that prohibit the assumed specific configurations of 7-branes, intersections and fluxes to be realized in truly global models [86, 88, 157–162].

The remainder of this work therefore deals with several aspects of constructing global F-theory models from known type IIB settings and local F-theory models.

sing. type	discr. deg(Δ)	gauge enhancement		coefficient vanishing degrees					f	g
		type	group	a_1	a_2	a_3	a_4	a_6		
I_0	0		—	0	0	0	0	0	0	0
I_1	1		—	0	0	1	1	1	0	0
I_2	2	A_1	$SU(2)$	0	0	1	1	2	0	0
I_{2k}^{ns}	$2k$	C_{2k}	$SP(2k)$	0	0	k	k	$2k$	0	0
I_{2k}^{s}	$2k$	A_{2k-1}	$SU(2k)$	0	1	k	k	$2k$	0	0
I_{2k+1}^{ns}	$2k+1$		[unconv.]	0	0	$k+1$	$k+1$	$2k+1$	0	0
I_{2k+1}^{s}	$2k+1$	A_{2k}	$SU(2k+1)$	0	1	k	$k+1$	$2k+1$	0	0
II	2		—	1	1	1	1	1	1	1
III	3	A_1	$SU(2)$	1	1	1	1	2	1	1
IV^{ns}	4		[unconv.]	1	1	1	2	2	1	1
IV^{s}	4	A_2	$SU(3)$	1	1	1	2	3	1	1
$I_0^{*\text{ns}}$	6	G_2	G_2	1	1	2	2	3	2	3
$I_0^{*\text{ss}}$	6	B_3	$SO(7)$	1	1	2	2	4	2	3
$I_0^{*\text{s}}$	6	D_4	$SO(8)$	1	1	2	2	4	2	3
$I_1^{*\text{ns}}$	7	B_4	$SO(9)$	1	1	2	3	4	2	3
$I_1^{*\text{s}}$	7	D_5	$SO(10)$	1	1	2	3	5	2	3
$I_2^{*\text{ns}}$	8	B_5	$SO(11)$	1	1	3	3	5	2	3
$I_2^{*\text{s}}$	8	D_6	$SO(12)$	1	1	3	3	5	2	3
$I_{2k-3}^{*\text{ns}}$	$2k+3$	B_{2k}	$SO(4k+1)$	1	1	k	$k+1$	$2k$	2	3
$I_{2k-3}^{*\text{s}}$	$2k+3$	D_{2k+1}	$SO(4k+2)$	1	1	k	$k+1$	$2k+1$	2	3
$I_{2k-2}^{*\text{ns}}$	$2k+4$	B_{2k+1}	$SO(4k+3)$	1	1	$k+1$	$k+1$	$2k+1$	2	3
$I_{2k-2}^{*\text{s}}$	$2k+4$	D_{2k+2}	$SO(4k+4)$	1	1	$k+1$	$k+1$	$2k+1$	2	3
$IV^{*\text{ns}}$	8	F_4	F_4	1	2	2	3	4	3	4
$IV^{*\text{s}}$	8	E_6	E_6	1	2	2	3	5	3	4
III*	9	E_7	E_7	1	2	3	3	5	3	5
II*	10	E_8	E_8	1	2	3	4	5	3	5
non-min	12		—	1	2	3	4	6	4	6

Table 3.6.: Refined Kodaira classification resulting from Tate’s algorithm. In order to distinguish the “semi-split” case $I_{2k}^{*\text{ss}}$ from the “split” case $I_{2k}^{*\text{s}}$ one has to work out a further factorization condition which is part of the aforementioned algorithm, see §3.1 of [132].

III Results & Developments

Chapter 4

M5-brane F-theory Instantons and E3-brane Type IIB Instantons

THE importance of the non-perturbatively generated Yukawa couplings and other effects for semi-realistic model building via E-brane instantons in perturbative string theory [42, 70, 100, 103, 163–168] — introduced in section 2.6 — requires a better understanding of the underlying structure of instantons. In fact, considering that the F-theory framework provides a manifestly unified non-perturbative perspective on type IIB theory, it is highly suggestive to match ordinary Euclidean D3-brane instantons to their respective counterparts. Those were identified as so-called vertical M5-branes, i.e. six-dimensional Euclidean surfaces that magnetically couple to the 3-form potential \hat{C}_3 and entirely wrap the elliptic fiber [102].

Instead of dealing with M5-brane instantons from first principles, one can compare the zero-mode structure of F-theory M5-brane instantons to IIB E3-brane instantons in a basic toy model geometry. F-theory then allows to move away from the weak-coupling Sen limit to the truly non-perturbative regime, such that one can study for example the non-perturbative stability of type IIB $U(1)$ vs. $O(1)$ instantons and the lifting of the troublesome $\bar{\tau}_{\hat{\alpha}}$ zero-modes. In fact, $U(1)$ instantons naturally recombine to the generic self-invariant $O(1)$ brane arrangement, unless the elliptic fiber does not experience the $O7$ -plane monodromy.

The non-perturbative perspective obtained from the zero-mode matching also reveals that on the F-theory side charged (matter) zero-modes pair up if one moves away from the weak-coupling Sen limit. Most importantly, charged zero-modes on the F-theory side are not counted by the holomorphic Euler characteristic, as suggested by an old argument of Witten [102, 169] that in the absence of fluxes $\chi(\mathcal{M}; \mathcal{O}_{\mathcal{M}}) = 1$ is required for a M5-brane to contribute to the superpotential. His argument was based on counting the fermionic zero-modes of the Dirac operator on the M5-brane. The precise matching of the E3-brane and M5-brane Hodge diamonds will be used to find a new criterion to

generate such an uncharged, nowhere vanishing superpotential [89].

4.1 Octic Toy Model Orientifold Geometry

The well-established basics of type II E-brane instantons as well as the zero-mode structure [100] were already introduced in section 2.6. The Euclidean D3-branes wrap 4-cycles of the “upstairs” Calabi-Yau geometry \mathcal{X} , which usually requires the inclusion of the corresponding mirror E3-branes in order to be invariant under the orientifold projection. Let E and E' be such an E3-brane/image brane pair in \mathcal{X} , which is projected onto $\mathcal{E} \subset \mathcal{B} = \mathcal{X}/\sigma$ in the “downstairs” orientifold geometry. This space also serves as the base of the F-theory elliptically-fibered Calabi-Yau 4-fold geometry \mathcal{Z} , and by adding the two fiber dimensions over \mathcal{E} , one naively obtains the M5-brane $\mathcal{M} \subset \mathcal{Z}_4$. This generic geometric setting is shown in figure 4.1.

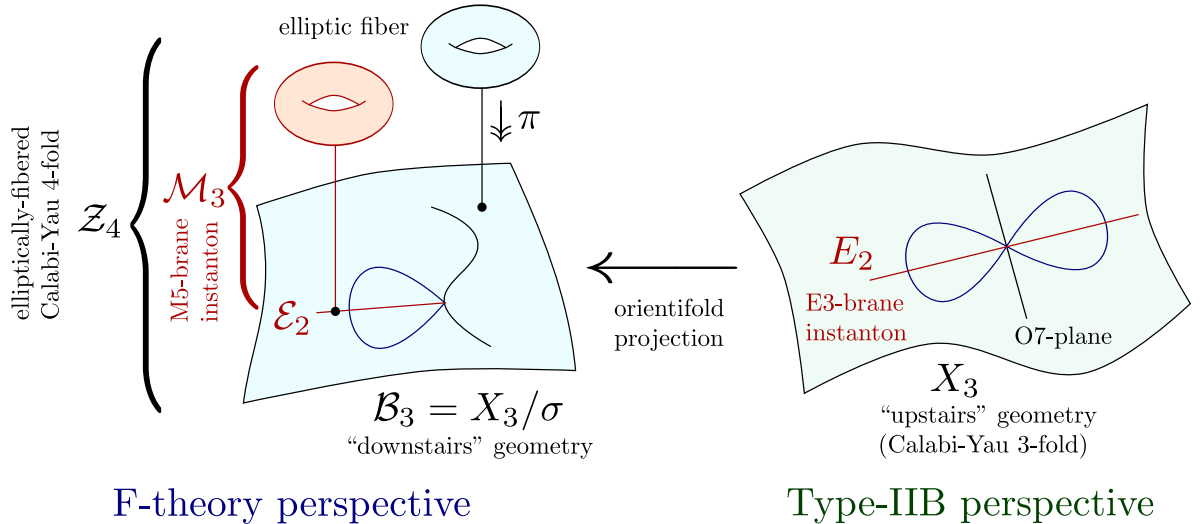


Figure 4.1.: Generic geometric setting of E3-branes E in the “upstairs” type IIB Calabi-Yau geometry and the corresponding vertical (fiber-wrapping) M5-branes \mathcal{M} in F-theory.

In order to have an explicit geometry, the octic Calabi-Yau 3-fold [111] will be used for the type IIB “upstairs” geometry. It is given by a degree-8 hypersurface in the weighted projective space \mathbb{P}_{11114}^4 with homogeneous coordinates (x_1, \dots, x_4, ξ) . A suitable orientifold involution mapping is the sign flip of the weight-4 coordinate ξ , i.e. the orientifold data is given by

$$\mathcal{X} := \mathbb{P}_{11114}^4[8] \quad \text{and} \quad \begin{aligned} \sigma : \mathcal{X} &\longrightarrow \mathcal{X} \\ \xi &\mapsto -\xi \end{aligned} \quad (4.1)$$

vertices of the polyhedron / fan	coords	GLSM charges		divisor class
		Q^1	Q^2	
$\rho_1 = (0, 0, 0, 1, 0)$	x	2	0	$2\sigma + 8H$
$\rho_2 = (0, 0, 0, 0, 1)$	y	3	0	$3\sigma + 12H$
$\rho_3 = (0, 0, 0, -2, -3)$	z	1	-4	σ
$\rho_4 = (-1, -1, -1, -8, -12)$	u_1	0	1	H
$\rho_5 = (1, 0, 0, 0, 0)$	u_2	0	1	H
$\rho_6 = (0, 1, 0, 0, 0)$	u_3	0	1	H
$\rho_7 = (0, 0, 1, 0, 0)$	u_4	0	1	H
conditions:		6	0	

intersection form: $-64\sigma^4 + 16\sigma^3H - 4\sigma^2H^2 + \sigma H^3$
 Stanley-Reisner ideal: $\langle xyz, u_1u_2u_3u_4 \rangle$

Table 4.1.: Toric data for the F-theory uplift 4-fold over \mathbb{P}^3 .

serves as the space involution. Note that this constrains the degree-8 polynomial somewhat in order for the hypersurface to be compatible with the involution, i.e. only even powers of ξ are allowed. The orientifold fixpoint plane is obviously located along the divisor

$$O7 = D_\xi := \{\xi = 0\}, \quad (4.2)$$

which is cohomologically given by $[O7] = 4H \in H^4(\mathcal{X}; \mathbb{Z})$, where H is the class of any other coordinate divisor D_{x_i} . The Stanley-Reisner ideal of the ambient space corresponds to the removal of the origin of \mathbb{C}^5 , i.e.

$$\text{SR}(\mathbb{P}_{11114}^4) = \langle x_1x_2x_3x_4\xi \rangle, \quad (4.3)$$

which specifies the relevant toric data entirely. Using the computational method described in appendix A, one can compute the relevant cohomology group dimensions. The upstairs geometry has $h^{1,1}(\mathcal{X}) = 1$ Kähler moduli and $h^{1,2}(\mathcal{X}) = 149$ complex structure moduli, such that by (2.27)

$$\chi(\mathcal{X}) = 2(h^{1,1} - h^{1,2}) = -296 \quad (4.4)$$

is the Euler characteristic. This simple yet sufficiently rich orientifold setting will serve as the stage for the remainder of this chapter.

The corresponding “downstairs” geometry $\mathcal{B} = \mathcal{X}/\sigma$ is simply given by the projective space \mathbb{P}^3 , which serves as the base of the F-theory uplift, whose elliptically-fibered Calabi-Yau 4-fold \mathcal{Z} is constructed by adding a $\mathbb{P}_{231}^2[6]$ -bundle. The toric data for \mathcal{Z} is summarized in table 4.1, and the simplicity of the chosen toy geometry lies in the fact that both the “upstairs” geometry \mathcal{X} as well as the corresponding F-theory uplift geometry are described by hypersurfaces (instead of e.g. complete intersections) in a toric variety. One can then determine the topology of \mathcal{Z} , which has non-trivial and non-zero Hodge numbers

$$\begin{aligned} h^{1,1}(\mathcal{Z}) &= 15564 \quad (\text{Kähler moduli}) \\ h^{3,1}(\mathcal{Z}) &= 3874 \quad (\text{complex structure moduli}) \end{aligned} \tag{4.5}$$

such that using the relations from table 3.3 the Euler characteristic is $\chi(\mathcal{Z}) = 23328$.

4.2 Generic D7-Brane Structure in the Sen Limit

The orientifold plane induces a tadpole of $8[\text{O7}] = 32H$, which has to be canceled by adding D7-branes of the same total cohomological charge [43]. In the strict sense of the Sen limit, generically only a single D7-brane is present in the setting, which—rather surprisingly—is not entirely generic but has a double point intersection with the O7-plane [111, 121]. This can be seen from the D7-brane equation in (3.59), which for the case at hand reduces to

$$\begin{aligned} \text{O7: } & h_8(x_1, \dots, x_4, \xi) := \xi^2 = 0, \\ \text{D7: } & (\eta_n)^2 = h_8 \chi_{2n-8} = (\eta_n)^2 - \xi^2 \chi_{2n-8} \end{aligned} \tag{4.6}$$

for $n = 16$, where the homogeneous degrees in the subscripts of the mappings η_n and χ_{2n-8} have been kept free for later reference. Clearly, along the O7-plane locus $\xi = 0$ the D7-brane $(\eta_n)^2 = \xi^2 \chi_{2n-8} \rightarrow 0$ shows a double point type of singularity, depicted in figure 4.2.

For the specific choice $\chi_{2n-8} = (\psi_{n-4})^2$ with $n \geq 4$ the entire D7-brane equation factorizes to

$$(\eta_n)^2 - \xi^2 \chi_{2n-8} = (\eta_n + \xi \psi_{n-4})(\eta_n - \xi \psi_{n-4}), \tag{4.7}$$

which describes a brane/image brane pair D7/D7' intersecting on the O7-plane. This intersecting brane pair carries a $U(1)$ gauge group, whereas the necessarily self-intersecting (generic) single D7-brane of the Sen limit has a trivial $SO(1) \cong \{1\}$ gauge group, see section 2.5. By giving a non-trivial vacuum expectation value to the massless fields localized on the $\text{D7} \cap \text{D7}'$ intersection one can initiate a D7-brane recombination that

gives back the single (generic) brane. However, the D3-brane tadpole condition requires adding non-trivial line bundles [111]

$$\begin{aligned} \text{D7: } \quad L &:= \mathcal{O}\left(\frac{n-4}{2}\right), \\ \text{D7': } \quad L' &:= \mathcal{O}\left(-\frac{n-4}{2}\right). \end{aligned} \tag{4.8}$$

For later reference it is relevant to investigate the moduli spaces of both brane configurations. For the generic $SO(1)$ case the moduli space consists of the number of deformations that preserve (4.6), i.e.

$$\begin{aligned} N_{SO(1)} &= \binom{n+3}{3} + \binom{2n-8+3}{3} - \binom{n-8+3}{3} - 1 \\ &= \frac{4}{3}n^3 - 8n^2 + \frac{59}{3}n. \end{aligned} \tag{4.9}$$

Following the earlier argument, this number is expected to be the same for the $U(1)$ brane/image brane pair after the brane recombination has been taken into account [105].

The moduli space for the brane/image brane system has a more involved structure. The number of transverse deformations is given by

$$\begin{aligned} N_{\text{D7/D7'}} &= \binom{n+3}{3} + \binom{n-1}{3} - 1 \\ &= \frac{n}{3}(n^2 + 11) - 1. \end{aligned} \tag{4.10}$$

The brane recombination moduli are localized on the intersection curve $C := \text{D7} \cap \text{D7}'$. Due to the orientifold involution, only the invariant (i.e. symmetric) states are relevant—the anti-symmetric ones are entirely projected out. Mathematically, the orientifold involution induces a splitting

$$H^i(\mathcal{X}; V) = H_+^i(\mathcal{X}; V) \oplus H_-^i(\mathcal{X}; V) \tag{4.11}$$

of the cohomology, see section A.5 for details. Due to the lifted action of the involution σ to the bundle, the role of the (mathematically) invariant and anti-invariant subspaces of $H^i(\mathcal{X}; V)$ may be exchanged. For the case at hand the relevant zero-modes are counted by the groups $H^i(C; L^2 \otimes K_C^{-\frac{1}{2}})$. In fact, the symmetric modes are all located on the part of the intersection curve away from the O7-plane, i.e.

$$\tilde{C} := C - \text{O7}, \tag{4.12}$$

which becomes singular in $R = \int_{\mathcal{X}} [D] \cdot [\text{O7}] \cdot ([\text{D7}] - [\text{O7}])$ ramification points. Using the isomorphisms

$$\begin{aligned} H_-^i(C; L^2 \otimes K_C^{-\frac{1}{2}}) &\cong H^i(\tilde{C}/\sigma; \tilde{L}|_{\tilde{C}/\sigma}), \\ \text{where } c_1(\tilde{L})|_{\tilde{C}/\sigma} &= c_1(L \otimes K_{\text{D7}}^{\frac{1}{2}})|_{\tilde{C}} - \frac{R}{2}, \end{aligned} \quad (4.13)$$

both cohomology group dimensions can be computed to

$$\begin{aligned} h_-^0(C; L^2 \otimes K_C^{-\frac{1}{2}}) &= n(n-4)^2 + 1, \\ h_-^1(C; L^2 \otimes K_C^{-\frac{1}{2}}) &= 1, \end{aligned} \quad (4.14)$$

such that the total number of recombination modes is $N_{\text{D7/D7}'}^{\text{recomb}} = n(n-4)^2 + 2$. Together with (4.9) and (4.10) one obtains the relation

$$N_{SO(1)} = N_{\text{D7/D7}'} + N_{\text{D7/D7}'}^{\text{recomb}} - 1, \quad (4.15)$$

where the extra -1 stems from the $U(1)$ gauge symmetry D-term condition that eliminates one modulus. Therefore, despite the somewhat surprising geometrical arrangement of the D7-brane and brane/image brane pair in the Sen limit prototype parametrization of the octic geometry, the D7-brane moduli counting is fully understood if one takes recombination moduli properly into account.

4.3 Uncharged Zero-Mode Counting

Since 3-branes are unlike 7-branes not directly seen in the F-theory geometry and not constrained, a generic E3-brane does not have a singular self-intersection like the D7-branes. One can now distinguish the two cases shown in figure 4.3, i.e. the self-invariant $O(1)$ instanton and the $U(1)$ instanton E3/E3' pair that were both introduced in section 2.6.3.

4.3.1 Self-Invariant $O(1)$ E3-brane instantons

In order to study the uncharged zero-mode structure of $O(1)$ instantons it is useful to consider an explicit example. Let $E_n \subset \mathcal{X}$ be a generic degree- n divisor in the Calabi-Yau geometry, such that the intersection form reduces to $I(E_n) = 2nH^2$. Using the Koszul sequence

$$0 \longrightarrow \mathcal{O}_{\mathcal{X}}(-n) \hookrightarrow \mathcal{O}_{\mathcal{X}} \longrightarrow \mathcal{O}_{E_n} \longrightarrow 0 \quad (4.16)$$

introduced in section A.4, one is able to derive the cohomology on E_n from the cohomology of \mathcal{X} . This in turn is derived from the (known) cohomology of the weighted

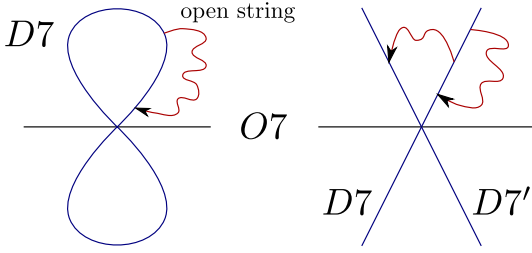


Figure 4.2.: Generically self-intersecting D7-brane in the Sen limit and factorized D7-brane/image brane pair.

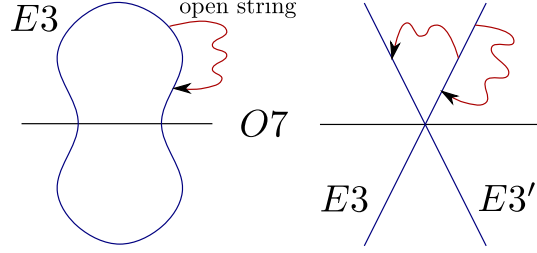


Figure 4.3.: Generic self-invariant $O(1)$ instanton E3-brane and $U(1)$ instanton E3/E3' instanton brane pair.

projective ambient space $\mathcal{A} := \mathbb{P}_{11114}^4$ via a second (twisted) Koszul sequence

$$0 \longrightarrow \mathcal{O}_{\mathcal{A}}(-n-8) \hookrightarrow \mathcal{O}_{\mathcal{A}}(-n) \twoheadrightarrow \mathcal{O}_{\mathcal{X}}(-n) \longrightarrow 0. \quad (4.17)$$

Using the computational algorithm described in appendix A.2, one can show that the only non-trivial contributions to the ambient space cohomology are counted by rational functions of the form

$$\begin{aligned} h^4(\mathcal{A}; \mathcal{O}_{\mathcal{A}}(-n)) &= \# \left\{ \frac{1}{x_1 x_2 x_3 x_4 \xi \cdot P_{n-8}(x_1, \dots, x_4, \xi)} \right\} \\ h^4(\mathcal{A}; \mathcal{O}_{\mathcal{A}}(-n-8)) &= \# \left\{ \frac{1}{x_1 x_2 x_3 x_4 \xi \cdot P_n(x_1, \dots, x_4, \xi)} \right\} \end{aligned} \quad (4.18)$$

where P_n denotes a degree- n polynomial in the homogeneous coordinates. The number p_n of such polynomials that respect the weight 4 of ξ is given by

$$p_n := \sum_{k=0}^{\lfloor \frac{n}{4} \rfloor} \binom{n-4k+3}{3}, \quad (4.19)$$

such that following section A.3 one can derive the cohomology group dimensions

$$\begin{aligned} h^\bullet(E_n; \mathcal{O}_{E_n}) &= (1, 0, p_n - p_{n-8} - 1) \\ &= \left(1, 0, \frac{n}{3}(n^2 + 11) - 1\right) \end{aligned} \quad (4.20)$$

for the E3-brane divisor. Due to $h^1(E_n; \mathcal{O}_{E_n}) = 0$ there are no non-trivial Wilson lines and the holomorphic Euler characteristic is

$$\chi(E_n; \mathcal{O}_{E_n}) = \frac{n}{3}(n^2 + 11). \quad (4.21)$$

As before, it is necessary to split the cohomology group dimensions into the σ -invariant and σ -anti-invariant part. For the known O7-plane fixpoint set $\{\xi = 0\}$ the holomorphic Lefschetz theorem (A.27) can be computed to be

$$\chi^\sigma(E_n; \mathcal{O}_{E_n}) = -2n^2, \quad (4.22)$$

and using (A.32) one can deduce

$$\begin{aligned} h_+^\bullet(E_n; \mathcal{O}_{E_n}) &= \left(1, 0, \frac{1}{6}(n^3 + 11n) - n^2 - 1\right), \\ h_-^\bullet(E_n; \mathcal{O}_{E_n}) &= \left(0, 0, \frac{1}{6}(n^3 + 11n) + n^2 - 1\right) \end{aligned} \quad (4.23)$$

for the cohomology of the $O(1)$ instanton. This will later be matched to the cohomology of the corresponding vertical M5-brane divisor in the F-theory uplift.

4.3.2 Non-Self-Invariant $U(1)$ E3/E3'-brane pair instantons

For the factorized case of a Euclidean 3-brane pair let $n = 2m$ be even for $m \geq 4$. The divisors are specified by the same equation (4.7) like a space-time filling D7-brane pair—only that E3-branes are purely wrapping the internal compact dimensions. The Euclidean 3-branes likewise have to carry different line-bundles in order to have the same C_0 and C_4 tadpole contribution as the recombined $O(1)$ instanton previously discussed:

$$\begin{aligned} \text{E3} : \quad E_m &:= \{\eta_m + \xi\psi_{m-4} = 0\} \quad \text{with} \quad L = \mathcal{O}\left(-\frac{m}{2}\right), \\ \text{E3}' : \quad E'_m &:= \{\eta_m - \xi\psi_{m-4} = 0\} \quad \text{with} \quad L' = \mathcal{O}\left(\frac{m}{2}\right). \end{aligned} \quad (4.24)$$

This choice of gauge flux also cancels the Freed-Witten anomaly if m is odd. As before, one can compute the cohomology

$$h_\pm^\bullet(E_m; \mathcal{O}_{E_m}) = \left(1, 0, \frac{1}{3}(m^3 + 11m) - 1\right), \quad (4.25)$$

which in this case splits symmetrically into σ -invariant and σ -anti-invariant parts. The extra universal zero-mode $h_-^0(E_m; \mathcal{O}_{E_m}) = 1$ indicates the $\bar{\tau}_\alpha$ zero-mode of the $U(1)$ instanton in contrast to the $O(1)$ instanton in (4.23).

One naturally expects additional zero-modes to be localized on the intersection curve $C := \text{E3} \cap \text{E3}'$ of the brane pair, where $K_C = \mathcal{O}(2m)$. The computation of those recombination zero-modes is analogous to the factorized D7-brane case discussed in section 4.2, i.e. the relevant cohomology groups are

$$H_\pm^i(C; L^2 \otimes K_C^{\frac{1}{2}}) \cong H_\pm^i(C; \mathcal{O}_C) \quad \text{for } i = 0, 1. \quad (4.26)$$

	zero-modes	statistics	Type IIB	F-theory
universal / $\mathcal{N}=1$ SUSY:	(X_μ, θ_α)	(bose, fermi)	$H_+^{0,0}(E)$	$H^{0,0}(\mathcal{M})$
$\mathcal{N}=1'$ SUSY:	$\bar{\tau}_{\dot{\alpha}}$	fermi	$H_-^{0,0}(E)$	$H^{1,0}(\mathcal{M})$
invariant Wilson lines:	γ_α	fermi	$H_+^{1,0}(E)$	
anti-invariant Wilson lines:	$(w, \bar{\gamma}_{\dot{\alpha}})$	(bose, fermi)	$H_-^{1,0}(E)$	$H^{2,0}(\mathcal{M})$
invariant deformations:	χ_α	fermi	$H_+^{2,0}(E)$	
anti-invariant deformations:	$(c, \bar{\chi}_{\dot{\alpha}})$	(bose, fermi)	$H_-^{2,0}(E)$	$H^{3,0}(\mathcal{M})$

Table 4.2.: Type IIB and F-theory zero-modes for an $O(1)$ instanton, compare to the general instanton zero-mode structure in table 2.7.

Using the algorithm for equivariant line bundle cohomologies described in appendix A.5 one can compute

$$\begin{aligned} h_+^\bullet(C; \mathcal{O}_C) &= (1, m^3 + 4m^2 + 1), \\ h_-^\bullet(C; \mathcal{O}_C) &= (0, m^3 - 4m^2). \end{aligned} \quad (4.27)$$

Like for the $SO(1)$ and $U(1)$ D7-brane moduli spaces in section 4.2, one finds an agreement between the $O(1)$ and $U(1)$ instanton moduli spaces as well. More precisely,

$$N_\pm(E_{2m}^{O(1)}) = N_\pm(E_m^{U(1)}) + N_{\mp}(C) \quad (4.28)$$

holds for N_\pm being the sum of the respective cohomology group dimensions $\sum_i h_\pm^i$ in (4.23), (4.25) and (4.27). To summarize, both the D7- and E3-brane structure for $(S)O(1)$ as well as $U(1)$ arrangements is fully understood if recombination moduli are properly taken into account.

4.3.3 Uplifting to vertical M5-branes

The next step now is to consider the uplift to a vertical M5-brane divisor in the elliptically-fibered Calabi-Yau 4-fold \mathcal{Z} summarized in table 4.1 and compare the zero-mode counting. Let

$$\pi : \mathcal{Z} \longrightarrow \mathcal{B} = \mathbb{P}^3 \quad (4.29)$$

be the projection mapping of the elliptic fibration. As mentioned earlier, a vertical M5-brane is entirely wrapping the elliptic fiber, i.e. one actually considers preimages $\mathcal{M} = \pi^{-1}(\mathcal{E})$ of complex surfaces $\mathcal{E} \subset \mathcal{B}$. Since the base $\mathcal{B} = \mathcal{X}/\sigma$ is the downstairs geometry of the previously considered type IIB Calabi-Yau \mathcal{X} and due to the simplicity

of both geometries, the correspondence between the M5-brane divisor on the F-theory side and the E3-brane on the type IIB side is given by

$$\underbrace{\mathcal{M}_n := \pi^{-1}(\mathcal{E}_n)}_{\text{M5-brane divisor}} \subset \mathcal{Z} \quad \text{where} \quad \underbrace{\mathcal{E}_n := E_n/\sigma}_{\text{“downstairs” E3-brane divisor}} \subset \mathcal{B}, \quad (4.30)$$

such that $[\mathcal{M}_n] = nH \in H^2(\mathcal{Z}; \mathbb{Z})$ is the M5-brane divisor class. Using the by now familiar algorithm from appendix A.2, and the Koszul sequence

$$0 \longrightarrow \mathcal{O}_{\mathcal{Z}}(-nH) \hookrightarrow \mathcal{O}_{\mathcal{Z}} \longrightarrow \mathcal{O}_{\mathcal{M}_n} \longrightarrow 0 \quad (4.31)$$

as well as $h^i(\mathcal{Z}; \mathcal{O}_{\mathcal{Z}}) = h^{i,0}(\mathcal{Z}) = (1, 0, 0, 0, 1)$ due to the Calabi-Yau property of \mathcal{Z} , one can determine the M5-brane cohomology and the holomorphic Euler characteristic

$$\begin{aligned} h^\bullet(\mathcal{M}_n; \mathcal{O}_{\mathcal{M}_n}) &= \left(1, 0, \binom{n-1}{3}, \binom{n+3}{3} - 1\right), \\ \chi(\mathcal{M}_n; \mathcal{O}_{\mathcal{M}_n}) &= \sum_{i=0}^3 h^i(\mathcal{M}_n; \mathcal{O}_{\mathcal{M}_n}) = -2n^2. \end{aligned} \quad (4.32)$$

Note that this $\chi(\mathcal{M}_n; \mathcal{O}_{\mathcal{M}_n})$ precisely agrees with the Lefschetz number $\chi^\sigma(E_n; \mathcal{O}_{E_n})$ for $O(1)$ instantons from (4.22). A closer inspection actually reveals

$$\underbrace{h^\bullet(\mathcal{M}_n; \mathcal{O}_{\mathcal{M}_n})}_{\text{M5-brane cohomology}} = \underbrace{\left(h_+^0, h_-^0 + h_+^1, h_-^1 + h_+^2, h_-^2\right)}_{O(1) \text{ instanton E3-brane cohomology}}, \quad (4.33)$$

i.e. the σ -invariant and σ -anti-invariant zero-modes $h_\pm^i(E_n; \mathcal{O}_{E_n})$ of the $O(1)$ instanton pairwise combined exactly yield the cohomology of the vertical M5-brane divisor. Therefore this rather non-trivial agreement of the computations convincingly shows the (universal) E3/M5-brane instanton zero-mode correspondence listed in table 4.2.

4.3.4 Interpretation and Analysis

In order to understand the arrangement of the E3-brane cohomology groups in the M5-brane uplift, one has to take the monodromy of the O7-plane into account. As shown (partially) by the O7-plane monodromy matrix (3.11), the net effect of the O7-plane here is a sign flip

$$(\alpha, \beta) \mapsto (-\alpha, -\beta) \quad (4.34)$$

in the homology of the elliptic fiber for $\alpha, \beta \in H_1(T^2; \mathbb{Z})$. This implies that an $(i, 0)$ -form of the “upstairs” E3-brane in \mathcal{X} must be σ -odd in order to combine with the $(1, 0)$ -form of the elliptic fiber into an even $(i + 1, 0)$ -form that survives the orientifolding process.

The second observation one can take away from table 4.2 is that only universal and deformation zero-modes contribute to $h^{i,0}(\mathcal{M})$, i.e. the information contained in the open strings starting and ending on the instanton E3-brane. Matter zero-modes that arise from the intersection with other 7-branes will be investigated in the next section.

As a third point, one can observe in the discussed toy model that only the $O(1)$ instanton gets truly uplifted. If the factorized E3/E3' brane pair setting is uplifted to the corresponding divisors

$$(\eta_m)^2 \pm h(\psi_{m-4})^2 = 0, \quad (4.35)$$

one finds a singularity at $\eta = \psi = 0$. However, even after resolving this singularity one does not find the additional $\bar{\tau}_\alpha$ zero-mode identified in (4.25) that should be expected from a $U(1)$ instanton compared to the $O(1)$ instanton. Apparently, a non-perturbative effect forces the $U(1)$ brane pair to recombine into the corresponding (generic) $O(1)$ instanton, which also smooths out the singularity from (4.35).

This raises the question whether F-theory contains any $U(1)$ instantons from type IIB at all that do not automatically recombine into $O(1)$ instantons. It is necessary for the E3-brane to wrap a divisor that does not intersect the O7-plane in order to avoid this recombination — a condition that cannot be satisfied within the simple \mathbb{P}^3 toy model base considered here. However, based on a non-standard geometrical phase (i.e. arising as a flop transition from the standard phase discussed in section 5.3) of the double del Pezzo transition of the quintic Calabi-Yau 3-fold $\mathbb{P}^4[5]$ that contains two non-intersecting dP_6 divisors, one can indeed construct a $U(1)$ instanton that uplifts accordingly to the non-perturbative F-theory framework [89]. The two dP_6 surfaces are identified by the orientifold mapping and are projected onto a single dP_6 divisor $\mathcal{E} \subset \mathcal{B}$ of the base. Here one finds that both the fermionic zero-mode θ_α counted by $h_+^{0,0}(E) = 1$ and the $\bar{\tau}_\alpha$ mode counted by $h_-^{0,0}(E)$ survive in the F-theory uplift. One concludes therefore that it is indeed possible to have non-recombining “genuine” $U(1)$ instantons in F-theory, even if the framework non-perturbatively aims to protect from such settings if allowed by the geometry. This completes the analysis of the zero-mode structure formed on isolated, non-intersecting E3-brane instantons.

4.4 Charged Matter Zero-Mode Counting

Intersections between E3-branes with D7-branes add charged (matter) zero-modes to the instanton properties on the perturbative type IIB side [100]. Those are counted by $h^i(C; L \otimes K_C^{\frac{1}{2}})$, where $C := D7 \cap E3$ is the intersection curve and L a line bundle encoding internal gauge flux on the D7-brane worldvolume. Naturally, one expects corresponding structures on the F-theory side, i.e. when the vertical M5-brane intersects

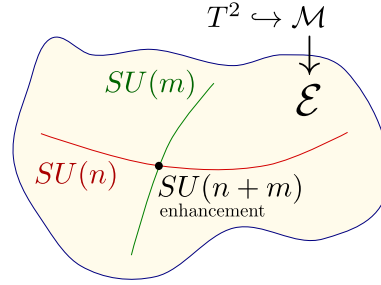


Figure 4.4.: The base surface $\mathcal{E} \subset \mathcal{B}$ of an vertical M5-brane $\mathcal{M} = \pi^{-1}(\mathcal{E}) \subset \mathcal{Z}$ intersects two $SU(n)$ degenerations of the fiber, which gives rise to $SU(n)$ matter zero-modes and Yukawa-type interactions in the triple intersection point.

the discriminant locus that encodes the location of the 7-branes. The big obstacle here comes in the form of various singularities: As the elliptic fiber degenerates along the 7-brane locus, the intersecting M5-brane is effectively wrapping a singular vertical divisor that has to be treated accordingly. Furthermore, as the generic remainder component \mathcal{D}_R of the discriminant (3.19) is often singular, one may encounter both singularities in the intersection curve as well as the elliptic fibration. It is therefore helpful to treat those two cases — the intersection of \mathcal{M} with smooth branes \mathcal{D}_a or the generically singular \mathcal{D}_R remainder — separately.

4.4.1 Matter zero-modes from smooth 7-branes

First consider the intersection with a smooth D7-brane divisor $D_a \subset \mathcal{X}$ in the upstairs type IIB geometry. As a typical situation take a D7/D7' brane stack pair and a single $O(1)$ instanton E . If D_a is intersected by another D7-brane stack wrapping $D_b \subset \mathcal{X}$, the corresponding number of zero-modes in the bi-fundamental $(\mathbf{n}_a, \bar{\mathbf{n}}_b)$ representation of $U(n_a) \times U(n_b)$ is counted by

$$\text{D7/D7' intersection: } h^i(C_{ab}; L_a \otimes L_b^\vee \otimes K_{C_{ab}}^{\frac{1}{2}}) \quad \text{for } i = 0, 1, \quad (4.36)$$

where L_a and L_b are line bundles over D_a and D_b and $C_{ab} := C_a \cap C_b$ is the intersection curve of both divisors. As mentioned before, given an E3-brane $E \subset \mathcal{X}$ the charged matter zero-modes $\lambda_{\mathbf{n}_a}$ are localized on the curve $C_{ae} := D_a \cap E$ and are counted by

$$\text{D7/E3 intersection: } h^i(C_{ae}; L_a \otimes K_{C_{ae}}^{\frac{1}{2}}) \quad \text{for } i = 0, 1. \quad (4.37)$$

Moreover, Yukawa-type interactions of the form $\Phi_{(\mathbf{n}_a, \bar{\mathbf{n}}_b)} \lambda_{\mathbf{n}_a} \lambda_{\bar{\mathbf{n}}_b}$ arise from triple intersection points $D_a \cap D_b \cap E$.

vertices of the polyhedron / fan	coords	GLSM charges			divisor class
		Q^1	Q^2	Q^3	
$\nu_1 = (1, 0, 0, 0, 0)$	x	2	0	1	$3\sigma + 12H - S$
$\nu_2 = (0, 1, 0, 0, 0)$	y	3	0	1	$2\sigma + 8H - S$
$\nu_3 = (-2, -3, 0, 0, 0)$	z	1	-4	0	σ
$\nu_4 = (-8, -12, -1, -1, -1)$	u_1	0	1	0	H
$\nu_5 = (0, 0, 1, 0, 0)$	u_2	0	1	0	H
$\nu_6 = (0, 0, 0, 1, 0)$	u_3	0	1	0	H
$\nu_6 = (0, 0, 0, 0, 1)$	u_4	0	1	1	$H - S$
$\nu_7 = (1, 1, 0, 0, 1)$	v	0	0	-1	S
conditions:		6	0	2	

Stanley-Reisner ideal: $\langle xyz, u_1u_2u_3u_4, zv, xyu_4, u_1u_2u_3v \rangle$

Table 4.3.: Toric data for the resolution of the $SU(2)$ -enhancement singularity along $\{u_4 = 0\} \subset \mathcal{B} = \mathbb{P}^3$ in table 4.1.

In the F-theory uplift let $\mathcal{D}_a, \mathcal{D}_b \subset \mathcal{B}$ be the corresponding smooth downstairs divisors, where the elliptic fibration degenerates to give the $SU(n_a)$ and $SU(n_b)$ gauge groups, respectively. The disappearance of the $U(1) \subset U(n_a)$ from the perturbative setting can be understood due to an F-theoretic kind of Stückelberg mechanism that makes this Abelian factor massive [170]. The matter fields arise from the gauge enhancements to $SU(n_a + n_b)$ along the intersection curve $\mathcal{C}_{ab} := \mathcal{D}_a \cap \mathcal{D}_b$. If the M5-brane instanton wraps both the fiber and $\mathcal{E} \subset \mathcal{B}$, one basically encounters the geometric setting depicted in figure 4.4. The matter zero-modes $\lambda_{\mathbf{n}_a}$ are then localized on the intersection curve $\mathcal{C}_{ae} := \mathcal{D}_a \cap \mathcal{E} \subset \mathcal{B}$ of the $SU(n)$ 7-brane divisor \mathcal{D}_a and the instanton base surface \mathcal{E} . The expectation is now that similar to the earlier finding the number of such zero-modes is counted by

$$SU(n) \text{ 7-brane/M5 intersection: } \quad h^i(\mathcal{C}_{ae}; K_{\mathcal{C}_{ae}}^{\frac{1}{2}}) \quad \text{for } i = 0, 1, \quad (4.38)$$

i.e. the upstairs formula (4.37) where $L_a = \mathcal{O}$. One can indeed show for various examples that this claim seems to hold and gives the correct number of charged matter zero-modes for vertical M5-branes intersecting the smooth 7-brane components.

At this point one might be concerned about the counting of uncharged and deformation zero-modes from section 4.3, as the M5-brane divisor $\mathcal{M} \subset \mathcal{Z}$ clearly is singular along all intersections \mathcal{C}_{ae} with 7-branes. Technically, the quantities $h^i(\mathcal{M}; \mathcal{O}_{\mathcal{M}})$ used

earlier are therefore ill-defined, despite the fact that the computational algorithm from appendix A is still applicable. In order to check the validity of those results, one has to explicitly resolve the non-Abelian singularity in the fiber and compute the holomorphic cohomology of the smoothed M5-brane divisor. Consider the octic $\mathbb{P}_{11114}^4[8]$ geometry with the \mathbb{P}^3 downstairs base from section 4.1 again and assume the factorization of the discriminant to the form

$$\Delta = \Delta_R \cdot \Delta_{u_4}^{\delta=2} \xrightarrow{\text{Sen}} \underbrace{h^2}_{O7} \cdot \underbrace{((\eta_{15})^2 - h\chi_{22})}_{\text{remainder } \mathcal{D}_R} \cdot \underbrace{(u_4)^2}_{\mathcal{D}_{u_4}}, \quad (4.39)$$

such that over the divisor $\mathcal{D}_{u_4} = \{u_4 = 0\} \subset \mathcal{B} = \mathbb{P}^3$ a $SU(2)$ degeneration is localized. Since the singularity is found both in the fibration and the total space \mathcal{Z} itself, the entire Calabi-Yau 4-fold has to be resolved. Fortunately, for the (rather simple) case of an $SU(2)$ singularity this can be done using toric methods, such that the resolved 4-fold $\tilde{\mathcal{Z}}$ is specified in table 4.3. However, this space no longer has a Weierstrass fibration, but the resolved M5-brane divisor $\tilde{\mathcal{M}}_n$ can be identified as

$$[\tilde{\mathcal{M}}_n] = nH \in H^2(\tilde{\mathcal{Z}}; \mathbb{Z}). \quad (4.40)$$

The $H^i(\tilde{\mathcal{M}}_n; \mathcal{O}_{\tilde{\mathcal{M}}_n})$ cohomology groups are now well-defined and one can compute

$$h^\bullet(\tilde{\mathcal{M}}_n; \mathcal{O}_{\tilde{\mathcal{M}}_n}) = \left(1, 0, \binom{n-1}{3}, \binom{n+3}{3} - 1\right) \quad (4.41)$$

in perfect agreement to the earlier result (4.32) obtained under the assumption of an entirely smooth elliptic fibration. It therefore appears that an explicit resolution of the (for matter zero-modes generically) singular M5-brane divisor \mathcal{M} to $\tilde{\mathcal{M}}$ is not necessary.

4.4.2 Generalized matter zero-mode counting for non- $SU(n)$ branes

Aside from $SU(n)$ gauge groups, the non-perturbative F-theory description allows for numerous other types of singularities. One is therefore forced to ask what happens if the instanton M5-brane \mathcal{M} intersects a generic smooth 7-brane divisor $\mathcal{D}_a \subset \mathcal{B}$ that is not of $SU(n)$ singularity type. It is helpful to use a setting which is also K3-fibered and therefore has a heterotic dual. Under the Fourier-Mukai transformation the vertical M5-brane divisor $\mathcal{M} \subset \mathcal{Z}$ is mapped by the duality to a worldsheet instanton wrapping the curve Σ . The gauge group due to singularities in the elliptic fiber on the F-theory side can be captured via the spectral cover description introduced in section 3.5 for the heterotic string. The gauge breaking vector bundle V , whose structure group is embedded into $E_8 \times E_8$, is encoded in the spectral line bundle \mathcal{N} by virtue of (3.44) over the spectral surface $\mathcal{C}^{(n)}$. The left-moving fermionic zero-modes of the aforementioned

dual worldsheet instanton along Σ are then counted by

$$h^i(\Sigma; V|_{\Sigma} \otimes K_{\Sigma}^{\frac{1}{2}}) \quad \text{for } i = 0, 1 \quad (4.42)$$

and transform in the singlet representation of the associated gauge group G . This counting corresponds to the earlier finding (4.38), as one basically considers the intersection of the M5-brane with the spectral surface $\mathcal{C}^{(n)}$ instead of the 7-brane itself.

4.4.3 Matter zero-modes from the singular remainder component

Handling the generically singular remainder component \mathcal{D}_R of the discriminant locus is substantially more difficult. Not only does one encounter the usually elliptic degeneration over a 7-brane, but the divisor \mathcal{D}_R itself becomes singular [111]—which also implies that the corresponding D7-brane in the perturbative “upstairs” type IIB picture is singular. One has therefore to deal with singularities (and the unavoidable ambiguities in their removal) on both sides one aims to compare. Here one sees for the first time a non-perturbative effect at work that effectively removes some of the matter zero-modes on the F-theory side.

With respect to the octic toy model from section 4.1, the singular D7-brane in the “upstairs” geometry is given by $\{\eta^2 = \xi^2 \chi\} \subset \mathcal{X}$ according to the generic findings of section 4.2. Let the $O(1)$ E3-brane instanton be described by $\{Q_{E3} = 0\} \subset \mathcal{X}$, such that the charged matter zero-modes of interest are localized on the intersection curve

$$C := D7 \cap E3 = \{\eta^2 = \xi^2 \chi\} \cap \{Q_{E3} = 0\} \subset \mathcal{X}, \quad (4.43)$$

which exhibits double point singularities at the points

$$\eta = \xi = Q_{E3} = 0. \quad (4.44)$$

Those singularities can be handled by a (relatively) straightforward blowup that defines a resolved curve \tilde{C} , which makes the computation on the type IIB side reasonably safe. For a homogeneous polynomial Q_{E3} of degree n , which describes an E3-brane instanton $E_n \subset \mathcal{X}$ as before, one can then determine

$$\begin{aligned} h_+^0(\tilde{C}; K_{\tilde{C}}^{\frac{1}{2}}) &= \mathfrak{N}(14 + \frac{n}{2}) - \mathfrak{N}(14 - \frac{n}{2}) - \mathfrak{N}(\frac{n}{2} - 18) \\ &= \begin{cases} \frac{1}{24}n(n^2 + 3068) & \text{if } 0 \leq n < 36, \\ 4(n^2 + 340) & \text{if } n \geq 36, \end{cases} \end{aligned} \quad (4.45)$$

for the σ -invariant matter zero-modes and likewise for the σ -anti-invariant modes

$$\begin{aligned}
h_-^0(\tilde{C}; K_{\tilde{C}}^{\frac{1}{2}}) &= \mathfrak{N}(10 + \frac{n}{2}) - \mathfrak{N}(10 - \frac{n}{2}) - \mathfrak{N}(\frac{n}{2} - 6) \\
&\quad + \mathfrak{N}(2 + \frac{n}{2}) - \mathfrak{N}(2 - \frac{n}{2}) - \mathfrak{N}(\frac{n}{2} - 14) \\
&= \begin{cases} \frac{1}{12}n(n^2 + 956) & \text{if } 0 \leq n \leq 4, \\ \frac{1}{16}(n^3 + 8n^2 + 1212n + 160) & \text{if } 4 < n < 12, \\ \frac{1}{24}n^3 + n^2 + \frac{431}{6}n + 20 & \text{if } 12 \leq n \leq 20, \\ \frac{1}{48}(n^3 + 120n^2 + 1724n + 14688) & \text{if } 20 < n < 28, \\ 4(n^2 + 148) & \text{if } 28 \geq n, \end{cases} \quad (4.46)
\end{aligned}$$

where $\mathfrak{N}(n)$ counts the number of global sections of $\mathcal{O}_{\mathcal{B}}(n)$, i.e.

$$\mathfrak{N}(n) := h^0(\mathcal{B}; \mathcal{O}_{\mathcal{B}}(n)) = \binom{n+3}{3} \theta(n) \quad (4.47)$$

with $\theta(n)$ being the Heaviside function given by $\theta(x) = 1$ for $x \geq 0$ and zero otherwise. The expected total number of matter zero-modes is then

$$\text{IIB matter zero-modes:} \quad h_+^0(\tilde{C}; K_{\tilde{C}}^{\frac{1}{2}}) + h_-^0(\tilde{C}; K_{\tilde{C}}^{\frac{1}{2}}) \quad (4.48)$$

in correspondence to (4.37) for $L_a = \mathcal{O}$, as from the open string perspective an E3 \rightarrow D7 string is mapped to a D7 \rightarrow E3 string, i.e. both have to be present in order to survive the orientifold projection.

The computation of the total number can be confirmed by considering the non-generic $U(1)$ instanton that arises from the factorization of the single invariant D7-brane into a brane/image brane pair with line bundles $L = \mathcal{O}(6)$. Here the D7-brane is smooth and one can consider the equally smooth intersection curve

$$\Sigma := \{\eta + \xi\psi = 0\} \cap \{Q_{\text{E3}} = 0\} \subset \mathcal{X}. \quad (4.49)$$

Indeed the subsequently computed number of matter zero-modes from the $U(1)$ instantons agrees as expected with the previously obtained $O(1)$ computation

$$\underbrace{h^0(\Sigma; L \otimes K_{\Sigma}^{\frac{1}{2}}) + h^0(\Sigma; L^{\vee} \otimes K_{\Sigma}^{\frac{1}{2}})}_{\text{brane/image brane}} = \underbrace{h_+^0(\tilde{C}; K_{\tilde{C}}^{\frac{1}{2}}) + h_-^0(\tilde{C}; K_{\tilde{C}}^{\frac{1}{2}})}_{\text{recombined brane}}. \quad (4.50)$$

This result adds a reasonable level of confidence to the earlier blowup procedure to desingularize the singular intersection curve C of the D7-brane and the E3-brane.

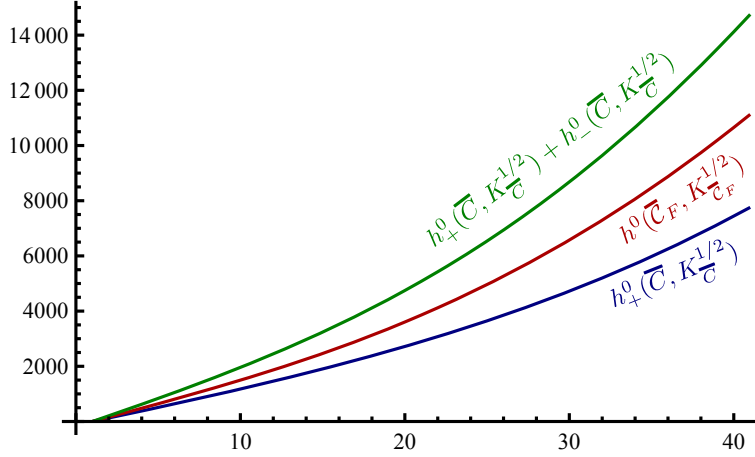


Figure 4.5.: The different numbers of matter zero-modes (σ -invariant IIB / F-theory / IIB) from (4.54) are plotted depending on the E3-brane divisor degree n .

On the F-theory side one encounters the generic D7-brane locus $\mathcal{D}_R = \{f^3 = g^2\} \subset \mathcal{B}$. Given an appropriate “downstairs” base surface $\mathcal{E} := \{Q_{\mathcal{E}} = 0\} \subset \mathcal{B}$ of the associated vertical M5-brane divisor, the generic intersection curve

$$\mathcal{C} := \mathcal{D}_R \cap \mathcal{E} = \{f^3 = g^2\} \cap \{Q_{\mathcal{E}} = 0\} \subset \mathcal{B} \quad (4.51)$$

houses the matter zero-modes. As mentioned in (3.21), the generic smooth Weierstrass model discriminant locus becomes singular over a cusp curve, such that singularities appear in

$$\mathcal{C} \cap \mathcal{C}_{\text{cusp}} = \{f = g = Q_{\mathcal{E}} = 0\}. \quad (4.52)$$

Those kind of singularities can be dealt with analogous to the ones on the type IIB intersection curve C , yielding the smooth blown-up intersection curve \tilde{C} . The number of zero-modes is then

$$\begin{aligned} h^0(\tilde{C}; K_{\tilde{C}}^{\frac{1}{2}}) &= \mathfrak{N}(14 + \frac{n}{2}) - \mathfrak{N}(14 - \frac{n}{2}) - \mathfrak{N}(\frac{n}{2} - 18) \\ &\quad + \mathfrak{N}(6 + \frac{n}{2}) - \mathfrak{N}(6 - \frac{n}{2}) - \mathfrak{N}(\frac{n}{2} - 10), \end{aligned} \quad (4.53)$$

which differs from the earlier IIB result in (4.48). However, the first line of (4.53) is equal to the type IIB result (4.46) for the σ -invariant matter zero-modes. One therefore finds the relation

$$\underbrace{h_+^0(\tilde{C}; K_{\tilde{C}}^{\frac{1}{2}})}_{\text{IIB orientifold}} < \underbrace{h^0(\tilde{C}; K_{\tilde{C}}^{\frac{1}{2}})}_{\text{F-theory}} < \underbrace{h_+^0(\tilde{C}; K_{\tilde{C}}^{\frac{1}{2}}) + h_-^0(\tilde{C}; K_{\tilde{C}}^{\frac{1}{2}})}_{\text{IIB orientifold}} \quad (4.54)$$

between the zero-modes, which is also plotted in figure 4.5 for higher values n of the E3-brane divisor E_n . Under the assumption that the performed blowup treatment of the cusp curve is the right way to proceed, the results indicate a partial pairing up (i.e. effective elimination) of some of the matter zero-modes when moving away from the perturbative type IIB orientifold limit.

Surprisingly, the discrepancy between the σ -invariant matter zero-modes from the IIB computation to the F-theory value can be expressed by the “matter zero-modes” on an auxiliary curve \mathcal{C}_A , which arises from the intersection of a degree- n and degree-16 hypersurface in the base $\mathcal{B} = \mathbb{P}^3$ of the toy model geometry. One then obtains

$$\underbrace{h^0(\tilde{\mathcal{C}}; K_{\tilde{\mathcal{C}}}^{\frac{1}{2}})}_{\text{F-theory}} = \underbrace{h^0_+(\tilde{\mathcal{C}}; K_{\tilde{\mathcal{C}}}^{\frac{1}{2}})}_{\text{IIB orientifold}} + h^0(\mathcal{C}_A; K_{\mathcal{C}_A}^{\frac{1}{2}}), \quad (4.55)$$

and the auxiliary curve can be interpreted as the intersection of the vertical M5-brane divisor \mathcal{M} with a component that can be related to the O7-plane in the strict weak-coupling Sen limit. However, the general underlying structure of this observation remains unclear at this point. Nevertheless, one clearly sees non-perturbative effects in the counting of matter zero-modes occurring in the intersection with singular (generic) components of the discriminant locus. This completes the discussion of the charged matter zero-mode structure with the result that instanton zero-modes from the M5-brane perspective are not properly recognized by the perturbative type IIB counting.

4.5 Relating M5-brane and E3-brane Hodge Diamonds

After gathering the information on the instanton zero-mode structure in the previous sections, one can in fact go further and relate the entire Hodge diamond [121] of the vertical M5-brane divisor \mathcal{M} to the E3-brane divisor E for the octic toy model. Considering the prior computation of $h^{i,0}(\mathcal{M}) \cong h^i(\mathcal{M}; \mathcal{O}_{\mathcal{M}})$, this basically leaves $h^{1,1}(\mathcal{M})$ and $h^{2,1}(\mathcal{M})$. In fact, using the Euler characteristic

$$\chi(\mathcal{M}) = -48n(n+20) \quad (4.56)$$

that is easily computed using the Riemann-Roch-Hirzebruch theorem (A.28), one has

$$h^{2,1}(\mathcal{M}) - h^{1,1}(\mathcal{M}) = \frac{n^3}{6} + 21n^2 + \frac{2891n}{6} - 1, \quad (4.57)$$

such that in fact only one independent Hodge number remains. Using the Lefschetz theorem, the Euler characteristic and the known values of $h^{i,0}(E) \cong h^i(E; \mathcal{O}_E)$ one can

determine the σ -invariant and σ -anti-invariant “center” Hodge numbers

$$\begin{aligned} h_+^{1,1}(E) &= \frac{2n^3}{3} - 2n^2 + \frac{7n}{3}, \\ h_-^{1,1}(E) &= \frac{2n^3}{3} + 2n^2 + \frac{103n}{3} \end{aligned} \quad (4.58)$$

of the “upstairs” E3-brane divisor $E \subset \mathcal{X}$. Together with (4.23) this gives the Euler characteristic

$$\chi(E) = 2n(n^2 + 22). \quad (4.59)$$

Since all Kähler classes of \mathcal{M} are inherited from σ -invariant Kähler classes of E except for the elliptic fiber, one obtains

$$\begin{aligned} h^{1,1}(\mathcal{M}) &= h_+^{1,1}(E) + 1 \\ &= \frac{2n^3}{3} - 2n^2 + \frac{7n}{3} + 1, \end{aligned} \quad (4.60)$$

which using (4.57) also gives the number of non-trivial 3-cycles

$$h^{2,1}(\mathcal{M}) = \frac{5n^3}{6} + 19n^2 + \frac{2905n}{6}. \quad (4.61)$$

Numerically this completes the computation of the Hodge diamond $h^{p,q}(\mathcal{M})$, but one actually aims to better understand the number $h^{2,1}(\mathcal{M})$ in terms of the E3-brane Hodge diamond.

Similar to the observation for the zero-modes — the outer edge of the Hodge diamond — the O7-plane monodromy (4.34) acting on the σ -anti-invariant cohomology groups $H_-^{0,2}(E)$, $H_-^{1,1}(E)$ and $H_-^{2,0}(E)$ likewise gives rise to 3-cycles of the M5-brane, i.e.

$$\begin{aligned} H_-^{2,0}(E) &\rightarrow \begin{cases} H^{3,0}(\mathcal{M}) \\ H^{2,1}(\mathcal{M}) \end{cases} \\ H_-^{0,2}(E) &\rightarrow \begin{cases} H^{1,2}(\mathcal{M}) \\ H^{0,3}(\mathcal{M}) \end{cases} \end{aligned} \quad H_-^{1,1}(E) \rightarrow \begin{cases} H^{2,1}(\mathcal{M}) \\ H^{1,2}(\mathcal{M}) \end{cases} . \quad (4.62)$$

It is already known from table 4.2 that the “edge Hodge number” $h^{3,0}(\mathcal{M})$ is equal to $h_-^{2,0}(E)$. But for $h^{2,1}(\mathcal{M})$ one finds in fact

$$\begin{aligned} \mathfrak{h}^{2,1}(\mathcal{M}) &:= h^{2,1}(\mathcal{M}) - h_-^{1,1}(E) - h_-^{2,0}(E) \\ &= 16n(n + 28) \end{aligned} \quad (4.63)$$

1			
$h_+^{1,0}(E)$		$h_+^{0,1}(E)$	
$h_+^{2,0}(E) + h_-^{1,0}(E)$	$h_+^{1,1}(E) + 1$	$h_+^{0,2}(E) + h_-^{0,1}(E)$	
$h_-^{2,0}(E)$	$h_-^{2,0}(E) + h_-^{1,1}(E) + \frac{g(\tilde{C})-1}{2}$	$h_-^{0,2}(E) + h_-^{1,1}(E) + \frac{g(\tilde{C})-1}{2}$	$h_-^{0,2}(E)$

Table 4.4.: Matching of the M5-brane Hodge diamond to the “upstairs” E3-brane topology and the resolved matter curve \tilde{C} .

extra elements which seem to have an unclear origin. A closer inspection reveals that those contain topological information of the charged matter zero-modes. More precisely, the genus $g(\tilde{C})$ of the (resolved) intersection curve \tilde{C} is encoded via

$$\mathfrak{h}^{2,1}(\mathcal{M}) + \mathfrak{h}^{1,2}(\mathcal{M}) = -\frac{1}{2}\chi(\tilde{C}) = g(\tilde{C}) - 1. \quad (4.64)$$

One can confirm this result by analyzing how involution-odd 1-cycles in \tilde{C} give rise to 3-cycles of \mathcal{M} , i.e.

$$\mathfrak{h}^{2,1}(\mathcal{M}) + \mathfrak{h}^{1,2}(\mathcal{M}) = b_-^1(\tilde{C}) \quad (4.65)$$

and conclude via the Lefschetz fixpoint theorem that indeed

$$b_-^1(\tilde{C}) = -\frac{1}{2}\chi(\tilde{C}) = g(\tilde{C}) - 1, \quad (4.66)$$

confirming (4.64). Therefore, one can entirely relate the Hodge diamond of \mathcal{M} to the (σ -split) Hodge diamond of E and the genus of the (resolved) generic D7/E3 intersection curve \tilde{C} , as shown in table 4.4.

In the more generic case of a discriminant locus that splits into several components and where the fiber degenerates to non-Abelian type—yielding singularities in the 4-fold \mathcal{Z} —one has to keep in mind that resolving \mathcal{M} to $\tilde{\mathcal{M}}$ as done in section 4.4.1 leaves $h^{i,0}(\tilde{\mathcal{M}}) = h^{i,0}(\mathcal{M})$ unchanged, but each blow-up increases the size of the Picard group and therefore the number of Kähler parameters. For the $SU(2)$ singularity blowup in table 4.2 one therefore expects $h^{1,1}(\tilde{\mathcal{M}}) = h^{1,1}(\mathcal{M}) + 1$. This is consistent with the previously identified relationship to the genera of (resolved) matter curves.

4.6 Phenomenological Implications

Coming back to the beginning of this chapter, a clear observation that can be drawn from the previous analysis of the zero-mode structure is that in F-theory one encounters charged matter zero-modes, which are not counted by the holomorphic Euler characteristic $\chi(\mathcal{M}; \mathcal{O}_{\mathcal{M}})$ of the M5-brane. Nevertheless, those have carefully to be taken into account for a proper determination to which 4-dimensional effective couplings the M5-brane instanton can make a contribution. Due to the generic intersection of vertical M5-branes with 7-brane components of the discriminant locus, only a careful zero-mode analysis reveals the actual presence of non-perturbative effects — e.g. Polonyi-type supersymmetry breaking or KKLT moduli stabilization [171] due to corrections to the closed string superpotential. A corresponding study of such properties in F-theory [172–174] is therefore quite important for model building.

In fact, the full instanton-generated contribution does not only involve the plain zero-modes, but — at least for holomorphic $\mathcal{N}=1$ couplings — the 1-loop determinant for the fluctuations around the instanton solution. In type IIB this corresponds to the open string 1-loop amplitudes, i.e. the annulus or Möbius strip worldsheet with at least one boundary on the instanton E3-brane. For F-theory one expects open (Euclidean) M2-branes ending on the instanton M5-brane to take this role. Aside from completing the mathematical matching of the E3-brane to the M5-brane topology, the computation of the full Hodge diamond in table 4.4 allows to determine the potential 1-loop contributions explicitly.

More precisely, the presence of non-trivial 3-cycles $H^3(\mathcal{M})$ in the M5-brane can lead to cancellations in the 1-loop determinant contributions. In the effective theory of an M5-brane one finds a sort of chiral 2-form field β_2 propagating on the worldvolume, whose associated field strength T_3 is self-dual. As detailed in section 3.4.3, the M5-brane also couples [169] to the 11d bulk supergravity 3-form \hat{C}_3 with the field strength G_4 . In a consistent setting this forces the G_4 flux to satisfy

$$G_4|_{\mathcal{M}} = dT_3, \quad (4.67)$$

i.e. cohomologically the restriction of G_4 to the M5-brane worldvolume is trivial. The moduli space of appropriate 3-form fields \hat{C}_3 restricted to \mathcal{M} is topologically a torus

$$J_{\mathcal{M}} := H^3(\mathcal{M}; \mathbb{R}) / H^3(\mathcal{M}; \mathbb{Z}) \cong T^{b^3(\mathcal{M})}, \quad (4.68)$$

called the intermediate Jacobian. Witten showed that the β_2 partition function is described by a section of a holomorphic line bundle \mathcal{L} over this moduli space, i.e.

$$\mathcal{L} \xrightarrow{\pi} J_{\mathcal{M}} \quad \rightsquigarrow \quad \beta_2 \text{ partition function } Z(\beta_2) \in \Gamma(\mathcal{L}). \quad (4.69)$$

This partition function mainly governs the 1-loop contributions and potential cancellations. Being a section of a line bundle over a torus, the partition function will vanish over a codimension-2 $_{\mathbb{R}}$ locus of the base $J_{\mathcal{M}}$. Due to (4.68) the presence of 3-cycles in the M5-brane divisor can therefore lead to cancellations — which requires a better geometric understanding of their E3-brane origin.

Using the explicit dictionary between the E3-brane and M5-brane Hodge diamond in table 4.4, the intermediate Jacobian (4.68) can in fact be rewritten as

$$J_{\mathcal{M}} = \frac{(H_{-}^2(E; \mathbb{R}))^2 \times H_{-}^1(\tilde{C}; \mathbb{R})}{(H_{-}^2(E; \mathbb{Z}))^2 \times H_{-}^1(\tilde{C}; \mathbb{Z})} \cong T^{2b_{-}^2(E) + b_{-}^1(\tilde{C})}, \quad (4.70)$$

which allows to understand the different contributions from another perspective.

Obviously, $H_{-}^1(\tilde{C})$ is the contribution from matter zero-modes arising from D7/E3 intersections. Due to $b_{-}^1(\tilde{C}) = g(\tilde{C}) - 1$ this contribution vanishes if the desingularized intersection curve \tilde{C} is either a torus (genus 1) or a \mathbb{P}^1 (genus 0).

The double factor $H_{-}^2(E)$ contains the invariant geometric moduli $h_{-}^{0,2}(E)$ from the E3-brane, but also contains the $h_{-}^{1,1}(E)$ Hodge number that is usually not considered in the standard instanton zero-mode counting. This number basically counts the number of NS-NS B_2 -field moduli, that are allowed due to the presence of the E3-brane. More precisely, from the M-theory perspective the field B_2 arises from a dimensional reduction of \hat{C}_3 and it has to be σ -anti-invariant under the orientifold projection, cf. table 2.4. In orientifold models with $b_{-}^2(\mathcal{X}) = 0$, which is the case for the octic toy model considered here, the NS-NS 2-form field therefore gets projected out. However, if an E3-brane instanton with $b_{-}^2(E) > 0$ is present, the B_2 field can still take configurations that are cohomologically non-trivial in the E3-brane, but vanish in the bulk Calabi-Yau 3-fold geometry.

Ultimately, this analysis is of key value in the context of moduli stabilization: in order to determine whether an $\mathcal{N}=1$ supersymmetric string compactification is non-perturbatively unstable, one needs to look for instantons which do not contain any charged matter zero-modes at all. From the (restricted) perspective of the M5-brane zero-mode structure the existence of such a destabilizing instanton is given provided that:

- The M5-brane is rigid, i.e. $h^{i,0}(\mathcal{M}) \cong h^i(\mathcal{M}; \mathcal{O}_{\mathcal{M}}) = 0$ for $i = 1, 2, 3$.
- All intersections of the M5-brane with smooth components \mathcal{D}_a of the discriminant locus occur over curves of genus zero — a \mathbb{P}^1 — such that the gauge breaking vector bundle V_a from section 4.4.2 restricts trivially on it.

The second condition has a direct analogue in the heterotic theory, namely that a

world-sheet instanton on a rational curve Σ can only contribute to the uncharged superpotential, if the vector bundle restricts trivially on it.

The intrinsically non-perturbative M5-brane statements can then be translated back to the perturbative “upstairs” E3-brane instanton. Note that $g(\tilde{C}) = 0$ also implies the vanishing of the $H^1(\tilde{C})$ contribution to the intermediate Jacobian $J_{\mathcal{M}}$ in (4.70). The previous analysis of this space now allows to improve the above zero-mode conditions by the considerations of the 1-loop contribution. In order for $J_{\mathcal{M}}$ to become entirely trivial—which also implies a nowhere vanishing partition function of the worldvolume 2-form β_2 due to the lower-dimensional vanishing locus—one also needs:

- The E3-brane must not contain any σ -anti-invariant 2-cycles, i.e. $b_-^2(E) = 0$.

This provides a sufficient criterion to have a nowhere vanishing, uncharged superpotential. Ultimately, one learns that E3-brane instantons have in fact more potentially harmful moduli than meet the eye.

Chapter 5

GUT Model Geometries in Type IIB and F-theory

THE discovery of generating the crucial top-quark Yukawa coupling $\mathbf{10} \cdot \mathbf{10} \cdot \mathbf{5}_H$ via D-brane instantons together with the idea of local F-theory GUT model building stirred a search for GUT models in perturbative type IIB string theory [42, 99]. This program led to a number of geometries that are compatible with the decoupling principle and the hypercharge flux GUT symmetry breaking, which implies that the GUT brane is wrapping del Pezzo surfaces containing 2-cycles with trivial relative homology [67, 69, 175].

Those IIB models use orientifolds with more than one component in the fixpoint set. The “upstairs” Calabi-Yau geometries are constructed via del Pezzo transitions of the quintic 3-fold hypersurface $\mathbb{P}^4[5]$. For the construction of global F-theory GUT models it is therefore natural to uplift such orientifold geometries to F-theory — which requires to explicitly construct the “downstairs” orientifold quotient base $\mathcal{B} = \mathcal{X}/\sigma$ of the geometries — and analyze their properties from the non-perturbative perspective this framework offers. Indeed, a tuning of certain moduli of the uplifted geometry reveals several useful properties (like exceptional gauge enhancements) in the truly strongly coupled region that no longer has a direct type IIB orientifold analogue.

Based on those findings one can then obtain an improved geometry directly for F-theory models without prior consideration of a corresponding type IIB setting. Instead of the quintic $\mathbb{P}^4[5]$, the non-Calabi-Yau quartic hypersurface $\mathbb{P}^4[4]$ — a Fano 3-fold [154, 158] and therefore the higher-dimensional counterpart to del Pezzo surfaces — is used as the starting point. Via a non-generic del Pezzo transition that blows up an entire curve instead of an isolated point, the required rigid GUT brane divisor is generated. The subsequent investigation of the enhancement properties and divisor intersections shows that this indeed provides a suitable geometry for further phenomenological study.

5.1 Euler Characteristic for Singular O-plane Intersections

In section 3.7 the ε -parametrization of the Tate coefficients revealed that in the canonical Sen limit the generic D7-brane is of the form $\eta^2 = h\chi$, where $h = 0$ determines the location of the O7-plane within the base $\mathcal{B} = \mathcal{X}/\sigma$. For generic η and χ the D7-brane worldvolume therefore has double point intersections with the O7-plane, as explicitly seen in section 4.2. A closer analysis shows that on the perturbative IIB side this particular structure stems from the Dirac quantization condition and is equivalent to the Whitney umbrella singularity prototype

$$x^2 = zy^2 \quad \text{for } (x, y, z) \in \mathbb{C}^3. \quad (5.1)$$

The aftermath of this situation is that any D7-brane intersecting an O7-plane in the Sen limit necessarily is a self-intersecting, singular space and requires an appropriate treatment. Whereas the induced D3-brane charge on a smooth O7-plane is given by

$$\chi(\text{O7}) = \int_{\mathcal{X}} [\text{O7}]^3 + c_2(\mathcal{X})[\text{O7}], \quad (5.2)$$

the Sen limit's double point intersections of the D7-brane complicate the correct computation. Via computations of the R-R charges on the brane one can argue that

$$\chi_o(D) = \int_{\mathcal{X}} \left([D]^3 + c_2(\mathcal{X})[D] + 3[D][\text{O7}]([[\text{O7}] - [D]]) \right) \quad (5.3)$$

computes the correct Euler characteristic [111, 176] for a D7-brane divisor $D \subset \mathcal{X}$. This newly defined Euler characteristic for D7/O7-intersections can be understood as

$$\chi_o(D) = \chi(\Sigma) - n_{\text{pp}}, \quad (5.4)$$

where Σ is the blown-up non-singular surface corresponding to the D7-brane divisor D and n_{pp} the number of pinch points where the Whitney umbrella of the singularity pinches off.

This is related to the singularities appearing in the elliptically-fibered Calabi-Yau 4-fold \mathcal{Z} along codimension-2 loci of 7-branes with non-Abelian gauge groups. Here similar techniques have to be applied in order to take care of the singularities — which is in general a difficult task due to the numerous types of singularities one potentially encounters.¹ Via the F-theory D3-brane tadpole formula (3.50) one can derive the relation

$$2\chi(\mathcal{Z}) = \chi_o(\text{D7}) + 4\chi(\text{O7}) \quad (5.5)$$

¹This is one of the reasons why the explicit construction of global G_4 -fluxes in non-trivial settings remains elusive.

vertices of the polyhedron / fan	coords	GLSM charges		divisor class
		Q^1	Q^2	
$\nu_1 = (-1, -1, -1, -1)$	u_1	1	0	H
$\nu_2 = (1, 0, 0, 0)$	u_2	1	0	H
$\nu_3 = (0, 1, 0, 0)$	u_3	1	0	H
$\nu_4 = (0, 0, 1, 0)$	u_4	1	0	H
$\nu_5 = (0, 0, 0, 1)$	v	1	1	$H + X = \tilde{H}$
$\nu_6 = (0, 0, 0, -1)$	w	0	1	X
conditions:		5	2	

intersection form: $2H^3 + 3H^2X - 3HX^2 + 3X^3 = 5\tilde{H}^3 + 3X^3$
Stanley-Reisner ideal: $\langle u_1u_2u_3u_4, vw \rangle$

Table 5.1.: Toric data for the single del Pezzo transition of the quintic Calabi-Yau 3-fold $\mathbb{P}^4[5]$.

between the F-theory Calabi-Yau 4-fold \mathcal{Z} and the corresponding type IIB D7-brane/O7-plane configuration in the Sen limit. This formula will later be used in reverse as a non-trivial check on the proposed uplift geometries, which are constructed from known IIB GUT orientifolds.

5.2 Single del Pezzo Transition of the Quintic

5.2.1 Type IIB orientifold geometry

The starting point [87] is the quintic Calabi-Yau 3-fold hypersurface $\mathbb{C}\mathbb{P}^4[5]$ with the homogeneous coordinates x_1, \dots, x_5 . When the degree-5 polynomial of the quintic takes the special form

$$Q := (x_5)^2 P_3(x_1, \dots, x_4) + x_5 P_4(x_1, \dots, x_4) + P_5(x_1, \dots, x_4) = 0 \quad (5.6)$$

the hypersurface becomes singular at the point $(0, 0, 0, 0, 1)$ as dQ vanishes. At this point a del Pezzo singularity of the form $dP_6 = \mathbb{P}^3[3]$ is generated, which can be blown-up to finite size. In the toric description of the resulting Calabi-Yau 3-fold this new dP_6 -divisor $D_w = \{w = 0\}$ appears like a common blowup, see the toric data in table 5.1.

For the proposed holomorphic involution on this single del Pezzo transition of the quintic, the sign flip mapping

$$\sigma : v \mapsto -v \quad (5.7)$$

is considered, i.e. in the new degree-(5,2) Calabi-Yau hypersurface constraint only even powers of the coordinate v are allowed. From the projective equivalences it follows

$$(u_1, \dots, u_4, v, -w) \sim (u_1, \dots, u_4, -v, w) \sim (-u_1, -u_2, -u_3, -u_4, v, w) \quad (5.8)$$

and since D_v and D_w are non-intersecting divisors — according to their product appearing in the Stanley-Reisner ideal generators — it follows that the fixpoint set of the involution is

$$O7 = D_v \cup D_w \quad (5.9)$$

without isolated fixpoints. Whereas D_w is the blowup dP_6 divisor, the D_v divisor is smooth, non-rigid and has $\chi(D_v) = 55$.

The splitting of the O7-plane into a rigid dP_6 divisor and a non-rigid surface is therefore asymmetrical and has to be taken into account in the prediction of the Euler characteristic for the supposed uplift 4-fold \mathcal{Z} . The naive expectation of a single D7-brane wrapping the divisor $8[O7] = 8H + 16X$ yields

$$\text{single D7:} \quad \chi^*(\mathcal{Z}) = \left(\frac{\chi_o(8D_v) + \chi_o(8D_w)}{2} + 2\chi(O7) \right) = 1728, \quad (5.10)$$

which keeps an Abelian gauge group that should not give rise to any 4-fold singularities in the subsequent uplifting.

However, since the two components of the O7-plane are not equivalent one has to cancel the charges separately: As $D_w \cong dP_6$ is rigid, in order to obtain the topological charge $8H + 16X$ it is necessary to consider a single brane wrapping $8[D_v] = 8H + 8X$ and a stack of 8 D7-branes wrapping $[D_w] = X$ each. This gives the gauge group $SO(8)$ and the corresponding prediction for the Euler characteristic is

$$\begin{array}{l} \text{D7-brane and} \\ \text{SO(8) stack:} \end{array} \quad \chi(\mathcal{Z}) = \left(\frac{\chi_o(8D_v) + 8 \cdot \chi_o(D_w)}{2} + 2\chi(O7) \right) = 1224, \quad (5.11)$$

which can be treated as the least-enhanced consistent configuration that saturates the tadpole conditions. Note that this directly implies that the 4-fold \mathcal{Z} is expected to be singular due to the non-Abelian gauge group. Both computed values $\chi^*(\mathcal{Z})$ and $\chi(\mathcal{Z})$ are relevant for the corresponding uplift geometry, as will become clearer in section 5.2.3.

vertices of the polyhedron / fan	coords	GLSM charges		divisor class	type / $\chi(D)$
		Q^1	Q^2		
$\nu_1 = (-1, -1, -1, -2)$	u_1	1	0	P	18
$\nu_2 = (1, 0, 0, 0)$	u_2	1	0	P	18
$\nu_3 = (0, 1, 0, 0)$	u_3	1	0	P	18
$\nu_4 = (0, 0, 1, 0)$	u_4	1	0	P	18
$\nu_5 = (0, 0, 0, 1)$	\tilde{v}	2	1	$2P + X = \tilde{P}$	55
$\nu_6 = (0, 0, 0, -1)$	\tilde{w}	0	1	X	9 (dP_6)
conditions:		5	1		

intersection form: $P^3 + 12X^3 + 3P^2X - 6PX^2 = 20\tilde{P}^3 + 12X^3$
Stanley-Reisner ideal: $\langle u_1u_2u_3u_4, \tilde{v}\tilde{w} \rangle$

Table 5.2.: Toric data for the downstairs Kähler 3-fold base $\mathcal{B} = \mathcal{X}/\sigma$ of the quintic’s single del Pezzo transition, cf. table 5.1.

5.2.2 Uplift Calabi-Yau 4-fold geometry

The next step is the construction of the corresponding elliptically-fibered Calabi-Yau 4-fold geometry \mathcal{Z} . A systematic approach first requires the explicit construction of the “downstairs” coset geometry $\mathcal{B} = \mathcal{X}/\sigma$, i.e. the base of the 4-fold [87, 111, 152, 153]. Working exclusively on the base, the additional constraints implied by the global geometry of \mathcal{Z} are not present, such that an additional constraint arises. Similar to the D7-tadpole condition in type IIB string theory, the purely topological condition (3.20) in the base arises, which is effectively a condition on the 7-brane wrapping.

In order to describe the coset space \mathcal{B} of the Calabi-Yau 3-fold \mathcal{X} that arises from the single del Pezzo transition of $\mathbb{P}^4[5]$ by the orientifold involution $\sigma : v \mapsto -v$, the mapping

$$\tilde{\sigma} : (u_1, \dots, u_4, v, w) \mapsto (u_1, \dots, u_4, v^2, w^2) \quad (5.12)$$

is used, which squares the two coordinates corresponding to the two non-intersecting components of the fixpoint set, i.e. the two O7-planes. If the squares are treated as new coordinates

$$\tilde{v} := v^2, \quad \tilde{w} := w^2, \quad (5.13)$$

this leads to the base geometry shown in table 5.2. This is no longer a Calabi-Yau manifold due to $c_1(\mathcal{B}) = P + X$ but still has the structure of a complex Kähler 3-fold.

In the base geometry the topology of the O7-planes remains unchanged compared to

vertices of the polyhedron / fan	coords	GLSM charges			divisor class
		Q^1	Q^2	Q^3	
$\nu_1 = (1, 0, 0, 0, 0, 0)$	x	2	0	0	$2(\sigma + P + X)$
$\nu_2 = (0, 1, 0, 0, 0, 0)$	y	3	0	0	$3(\sigma + P + X)$
$\nu_3 = (-2, -3, 0, 0, 0, 0)$	z	1	-1	-1	σ
$\nu_4 = (-2, -3, -1, -1, -1, -2)$	u_1	0	1	0	P
$\nu_5 = (0, 0, 1, 0, 0, 0)$	u_2	0	1	0	P
$\nu_6 = (0, 0, 0, 1, 0, 0)$	u_3	0	1	0	P
$\nu_7 = (0, 0, 0, 0, 1, 0)$	u_4	0	1	0	P
$\nu_8 = (0, 0, 0, 0, 0, 1)$	\tilde{v}	0	2	1	$2P + X$
$\nu_9 = (-2, -3, 0, 0, 0, -1)$	\tilde{w}	0	0	1	X
conditions:		6	0	0	
		0	5	1	

$$\text{intersection form: } P^3\sigma + 3P^2X\sigma - 6PX^2\sigma + 12X^3\sigma - 4P^2\sigma^2 \\ + 3PX\sigma^2 - 6X^2\sigma^2 + P\sigma^3 + 3X\sigma^3 - 4\sigma$$

$$\text{Stanley-Reisner ideal: } \langle xyz, u_1u_2u_3u_4, \tilde{v}\tilde{w} \rangle$$

Table 5.3.: Toric data for the elliptically-fibered Calabi-Yau 4-fold \mathcal{Z} arising from the quintic's single del Pezzo transition, cf. table 5.1.

the upstairs geometry of table 5.1, i.e. one still finds a del Pezzo-6 surface for $\mathcal{D}_{\tilde{w}}$ as well as the $\chi = 55$ surface $\mathcal{D}_{\tilde{v}}$. The Calabi-Yau 4-fold is then defined by the Weierstrass model (3.14) over the base, i.e. by adding the projective coordinates (x, y, z) of \mathbb{CP}_{231}^2 which are subject to the degree-6 equation

$$y^2 = x^3 + xz^4f(\vec{u}, \tilde{v}, \tilde{w}) + z^6g(\vec{u}, \tilde{v}, \tilde{w}) \quad (5.14)$$

that specifies the elliptic fiber. As mentioned in section 3.3 the base \mathcal{B} is embedded into \mathcal{Z} as the divisor \mathcal{D}_z of the additional coordinates. The toric data of the total elliptically-fibered Calabi-Yau 4-fold \mathcal{Z} is found in table 5.3. Within this total space the surface $\{z = \tilde{v} = 0\}$ again corresponds to the $\chi = 55$ component of the O7-plane and $\{z = \tilde{w} = 0\}$ is the dP_6 surface.

5.2.3 Interpretation of the Euler characteristics

The described Calabi-Yau 4-fold is highly singular, which prohibits ad-hoc computations of geometrical and topological invariants. Considering the discussion regarding the $SO(8)$ brane stack arrangement to cancel the tadpole, this is to be expected. However, one can simply ignore the singularity for the moment and derive the total Chern class $c^*(\mathcal{Z})$ by expanding the formal fraction^{II} of the (also singular) ambient space total Chern class divided by the hypersurface constraints to compute the naive Euler characteristic

$$\chi^*(\mathcal{Z}) = \int_{\mathcal{Z}} e^*(\mathcal{Z}) = \int_{\mathcal{Z}} c_4^*(\mathcal{Z}) = 1728, \quad (5.15)$$

which is in perfect agreement with the naive prediction (5.10) from the type IIB orientifold setting in section 5.2.1. Furthermore, the general relation [110, 128]

$$\chi^*(\mathcal{Z}) = 12 \int_{\mathcal{B}} c_1(\mathcal{B})c_2(\mathcal{B}) + 360 \int_{\mathcal{B}} c_1(\mathcal{B})^3 \quad (5.16)$$

for smooth elliptically-fibered Calabi-Yau 4-folds, i.e. where only I_1 degenerations of the fibration (but not singularities in the total space \mathcal{Z}) are present, also yields the same result, indicating that the “smooth” phase of the uplift geometry holds some merit.

The correct Euler characteristic that takes the non-Abelian singularity into account, instead is of the general form

$$\chi(\mathcal{Z}) = \chi^*(\mathcal{Z}) - \delta, \quad (5.17)$$

where δ is a correction term that takes care of the singularities in the total space \mathcal{Z} and depends on the discriminant locus. For example, if the fiber degenerates only over a divisor \mathcal{D} of the base with the non-Abelian gauge group G —producing a codimension-2 singularity in \mathcal{Z} —the corrected Euler characteristic can be described by [86, 177]

$$\chi(\mathcal{Z}) = \chi^*(\mathcal{Z}) - r_G c_G (c_G + 1) \int_{\mathcal{D}} c_1(\mathcal{D})^2, \quad (5.18)$$

where r_G and c_G are the rank and dual Coxeter number of the group, respectively.

According to the analysis in section 5.2.1, an $SO(8)$ singularity is located along the O7-brane divisor $\mathcal{D}_{\bar{w}}$ of the base geometry in table 5.2, which is of Dynkin type D_4 and has rank $r_{SO(8)} = 4$ as well as dual Coxeter number $c_{SO(8)} = 6$, such that it follows

$$\begin{aligned} \int_{\mathcal{D}_{\bar{w}}} c_1(\mathcal{D}_{\bar{w}})^2 &= \int_{\mathcal{D}_{\bar{w}}} P^2 = \int_{\mathcal{B}} P^2 X = 3 \\ \rightsquigarrow \chi(\mathcal{Z}) &= \chi^*(\mathcal{Z}) - 4 \cdot 6 \cdot (6 + 1) \cdot 3 = 1224. \end{aligned} \quad (5.19)$$

^{II}The asterisk here indicates that those quantities are derived from formal expressions applied to a singular setting — which is in general false.

This is precisely the result anticipated in (5.11) from the different stacking of 7-branes. In accordance with the structure of the “group-corrected” uplift Euler characteristic (5.18), this suggests to view the smooth case Euler characteristic $\chi^*(\mathcal{Z})$ as a leading order contribution to the actual Euler characteristic $\chi(\mathcal{Z})$ one obtains after a proper treatment of the brane arrangements and the resulting singularities in the 4-fold’s total space.

Whereas on the type IIB side the rigidity of the del Pezzo divisor $D_w \subset \mathcal{X}$ prohibits the splitting of the branes to dissolve the non-Abelian gauge enhancement, the Calabi-Yau 4-fold \mathcal{Z} on the F-theory side possesses no complex structure deformations to remove the non-Abelian singularity while preserving the Weierstrass form (5.14) of the elliptic fibration. This is reflected in the general mapping of IIB D7-brane deformations to complex structure deformation of the F-theory Calabi-Yau 4-fold. It is on the other hand indeed striking to see the direct correspondence between the naive brane arrangement derived from the D7-brane tadpole cancellation condition (5.10) and the naive Euler characteristic of the singular 4-fold as well as the equality of the rigidity-enforced IIB D7-brane configuration to the corrected computation of $\chi(\mathcal{Z})$.

5.2.4 Minimal and maximal gauge groups

After specifying the geometry on the perturbative type IIB side and the subsequent uplifting to elliptically-fibered Calabi-Yau 4-fold, it remains to analyze which additional insights one can obtain from the F-theory description [132]. In order to analyze gauge groups the equivalent Tate description (3.13) of the elliptic fibration is much more suitable than the Weierstrass model. Note that via

$$K_{\mathcal{B}}^{-n} = \mathcal{O}(c_1(K_{\mathcal{B}}^{-n})) = \mathcal{O}(nc_1(K_{\mathcal{B}}^{-1})) = \mathcal{O}(nc_1(\mathcal{B})) \quad (5.20)$$

one can give a rather explicit representation of the coefficient sections $a_n \in H^0(\mathcal{B}; K_{\mathcal{B}}^{-n})$ appearing in the Tate parametrization.

As mentioned in section 5.2.2, the base 3-fold \mathcal{B} of the single del Pezzo transition has $c_1(\mathcal{B}) = P + X$, such that the coefficients are sections $a_n \in H^0(\mathcal{B}; \mathcal{O}(n(P + X)))$. In accordance with the divisor classes of the coordinates in table 5.2, the general parametrization of the coefficients is then of the form

$$\left. \begin{aligned} a_1 &= P_{(1,0)}\tilde{w}, & a_3 &= P_{(3,1)}\tilde{w}^2, \\ a_2 &= P_{(2,1)}\tilde{w}, & a_4 &= P_{(4,2)}\tilde{w}^2, \\ & & a_6 &= P_{(6,3)}\tilde{w}^3, \end{aligned} \right\} G_2 \quad (5.21)$$

where $P_{(n,m)}$ is a polynomial with divisor class degree $nH + mP$. From this one can easily identify the minimal non-Abelian gauge group of the configuration. Due to the common

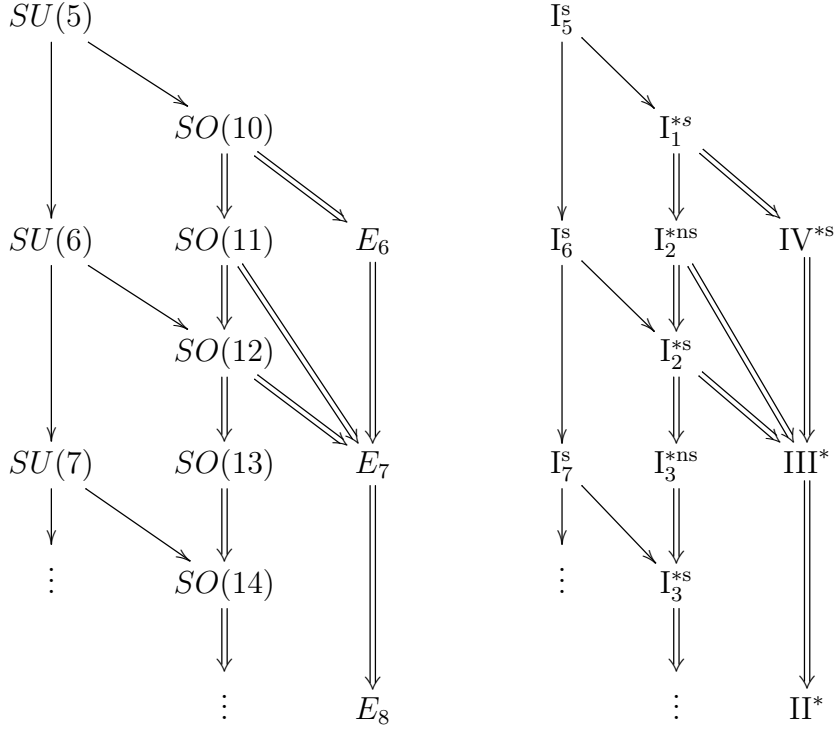


Table 5.4.: Enhancement pattern for an $SU(5)$ (single lines) and $SO(10)$ (double lines) gauge group based on [132], also see the Tate classification table 3.6. Note that this does not take any further consistency conditions into account, e.g. the maximum discriminant vanishing degree.

appearance of \tilde{w} with powers $(1, 1, 2, 2, 3)$, the Tate list (cf. table 3.6) shows that along $\mathcal{D}_{\tilde{w}}$ one finds at least the non-Abelian gauge group G_2 . Since the minimal perturbative type IIB gauge group $SO(8)$ was already identified, the full F-theory—capturing non-perturbative effects—allows for the smaller minimal gauge group $G_2 \subset SO(8)$.

According to (3.14), (3.56) and (3.59), the O7-plane corresponds to the vanishing locus $\{h = 0\} = \{b_2 = (a_1)^2 + 4a_2 = 0\}$. Both coefficients can be described by polynomials

$$\begin{aligned} a_1 &= P_1(\vec{u})\tilde{w}, \\ a_2 &= C_0\tilde{v}\tilde{w} + P_2(\vec{u})\tilde{w}^2, \end{aligned} \tag{5.22}$$

where $P_n(\vec{u})$ is a degree- n polynomial in u_1, u_2, u_3 and $C_0 \in \mathbb{C}$ a complex structure modulus. In the uplifting some of the complex structure moduli can be fixed, such that the O7-plane is located at $\tilde{v}\tilde{w} = 0$, and from the generic O7-plane location $(a_1)^2 + 4a_2 = 0$ this implies $P_2(\vec{u}) = -\frac{1}{4}P_1(\vec{u})^2$ for the used parametrization.

One can now go on and systematically analyze which gauge groups can be obtained. The simplest D7-brane configuration to cancel the tadpole places a stack of 8 D7-branes over each of the divisors D_v and D_w , i.e. a total of 16 D7-branes. This setting differs from the configuration discussed in section 5.2.1, where the primary goal was to use the least number of branes in order to reduce singularities from non-Abelian gauge groups. Due to the two stacks of 8 D7-branes wrapped around D_v and D_w in \mathcal{X} , respectively, the non-Abelian gauge group $SO(8) \times SO(8)$ arises in the setting considered here and the expected Euler characteristic of the singular Calabi-Yau 4-fold is

$$\begin{array}{l} \text{two } SO(8) \\ \text{stacks:} \end{array} \quad \chi(\mathcal{Z}) = \left(\frac{8 \cdot \chi_o(D_v) + 8 \cdot \chi(D_w)}{2} + 2\chi(O7) \right) = 384. \quad (5.23)$$

Considering the earlier predictions (5.10) and (5.11), one observes the trend that stacks of D7-branes significantly reduce the (predicted) Euler characteristic of the 4-fold as more and more complex structure moduli are fixed to describe the necessary degenerations in the elliptic fibration. The corresponding Tate coefficients for this brane configuration are^{III}

$$\left. \begin{array}{l} a_1 = 0, \\ a_2 = \tilde{v}\tilde{w}, \\ a_3 = 0, \\ a_4 = C'_0 \tilde{v}^2 \tilde{w}^2, \\ a_6 = 0, \end{array} \right\} SO(8) \times SO(8) \quad (5.24)$$

in order to reach the required vanishing degrees $(1, 1, 2, 2, 4)$ of $SO(8)$ along $\mathcal{D}_{\tilde{v}}$ and $\mathcal{D}_{\tilde{w}}$, which shows that the simple IIB brane configuration can indeed be uplifted and realized as an F-theory model with $SO(8) \times SO(8)$ gauge group.

Next the maximal possible gauge group, that can be consistently obtained within the single del Pezzo transition setting of the quintic, is to be determined. As the total charge $8H + 16X$ has to be canceled, one can consider the wrapping of a stack of 8 D7-branes around $D_{u_1} = H$ and a stack of 16 D7-branes around $D_w = X$ —yielding the maximal number of branes the model can accommodate. In the absence of any gauge flux the total of those 24 D7-branes give rise to the gauge group $Sp(8) \times SO(16)$ and the prediction for the singular 4-fold is

$$\begin{array}{l} Sp(8) \text{ stack \&} \\ SO(16) \text{ stack:} \end{array} \quad \chi(\mathcal{Z}) = \left(\frac{8 \cdot \chi_o(D_{u_1}) + 16 \cdot \chi_o(D_w)}{2} + 2\chi(O7) \right) = 312. \quad (5.25)$$

^{III}In order to see this quickly one has to realize that there are no non-trivial entries in the Tate classification list (table 3.6) that have non-zero values for a_2 and a_4 , i.e. vanishing degree-0 for both those coefficients. All enhancements are therefore localized on $\tilde{v}\tilde{w} = 0$, i.e. the two O7-plane components $\{\tilde{v} = 0\}$ and $\{\tilde{w} = 0\}$.

However, since the divisors D_{u_1} and D_w are intersecting, there exists also non-chiral matter on the intersection curve. On the F-theory side the Calabi-Yau 4-fold can indeed be tuned to this gauge group using the Tate coefficients

$$\left. \begin{aligned} a_1 &= P_1(\vec{u})\tilde{w}, & a_3 &= 0, \\ a_2 &= \tilde{v}\tilde{w} - \frac{1}{4}P_1(\vec{u})^2\tilde{w}^2, & a_4 &= C_0''(u_1)^4\tilde{w}^4, \\ & & a_6 &= 0, \end{aligned} \right\} Sp(8) \times SO(16) \quad (5.26)$$

yielding again the non-Abelian gauge group $Sp(8)$ along \mathcal{D}_{u_1} and $SO(16)$ on $\mathcal{D}_{\tilde{w}}$. Further gauge enhancements — which however lack a directly corresponding perturbative description — are considered in section 5.2.6.

5.2.5 Non-perturbative O7-plane splitting

On the F-theory side the non-perturbative effects influence the O7-plane geometry as well. Consider again the “maximal branes” setting parameterized in (5.26). In the Sen rescaling (3.55) of the Tate coefficients one can effectively turn off the non-zero coefficient a_4 , such that in direct comparison one finds

$$\begin{aligned} \text{Sen limit: } \Delta_{\text{Sen}} &= 16(C_1)^2(u_1)^8\tilde{w}^{10}\tilde{v}^2, \\ \text{full F-theory: } \Delta_{\text{F}} &= 16(C_1)^2(u_1)^8\tilde{w}^{10}\left(\tilde{v}^2 - 4C_0''(u_1)^4\tilde{w}^2\right), \end{aligned} \quad (5.27)$$

i.e. the higher correction terms in the full F-theory are responsible for splitting up the O7-plane component $\{\tilde{v} = 0\}$ from the perturbative IIB side into two objects:

$$\text{Sen limit: } \{\tilde{v} = 0\} \rightsquigarrow \text{full F-theory: } \left\{ \tilde{v} = \pm 2\sqrt{C_0''(u_1)^4\tilde{w}^2} \right\}. \quad (5.28)$$

This is a first indication for the direct influence of non-perturbative effects on apparently “innocent” type IIB orientifold models. From the perturbative perspective, O-planes are always static objects of the geometry, whereas F-theory treats them as dynamical objects (cf. section 3.2) not much different from regular 7-branes [124–126].

5.2.6 Exceptional gauge groups and absence of $SO(10)$ spinor representations

Besides the classical gauge group $Sp(8)$ and $SO(8)$, it was already observed from the appearance of the G_2 group in section 5.2.4 that also exceptional gauge groups can arise in the F-theory description. It remains to determine which other exceptional gauge groups the geometry supports.

By setting $C_0 = 0$ in (5.22) the general parametrization (5.21) of the Tate coefficients

specializes to

$$\left. \begin{aligned} a_1 &= P_{(1,0)}\tilde{w}, & a_3 &= P_{(3,1)}\tilde{w}^2, \\ a_2 &= P_{(2,0)}\tilde{w}^2, & a_4 &= P_{(4,1)}\tilde{w}^3, \\ & & a_6 &= P_{(6,1)}\tilde{w}^5, \end{aligned} \right\} E_6 \quad (5.29)$$

which gives the vanishing degrees $(1, 2, 2, 3, 5)$ for \tilde{w} —yielding an E_6 singularity on $\mathcal{D}_{\tilde{w}}$. Furthermore, whenever the vanishing of $P_{(3,1)}$ increases the vanishing of a_3 to at least degree 3, the singularity is enhanced further to E_7 type. And if in addition $P_{(4,1)} = 0$ increases $\deg(a_4)$ to at least 3, one finds the E_8 singularity. In summary, with respect to the specialized parametrization (5.29) one finds

$$\begin{aligned} E_6 &: \{\tilde{w} = 0\}, \\ E_7 &: \{\tilde{w} = P_{(3,1)} = 0\}, \\ E_8 &: \{\tilde{w} = P_{(3,1)} = P_{(4,1)} = 0\}. \end{aligned} \quad (5.30)$$

The E_7 curve (as the intersection of two generic constraints) gives rise to matter in the fundamental $\mathbf{27}$ representation. On the (generically) point-like E_8 enhancement one finds the Yukawa coupling $\mathbf{27} \cdot \mathbf{27} \cdot \mathbf{27}$ and the number of those E_8 points is given by the intersection number

$$\int_{\mathcal{B}} [D_{\tilde{w}}] \cdot [P_{(3,1)}] \cdot [P_{(4,1)}] = \int_{\mathcal{B}} X(3P + X)(4P + X) = 6. \quad (5.31)$$

One can therefore conclude that the uplift of the $\mathbb{P}^4[5]$'s del Pezzo transition indeed gives rise to exceptional gauge groups when moving away from the original orientifold setting in the complex structure moduli space.

The generic G_2 parametrization (5.21) also allows for an alternative enhancement to $SO(10)$ instead of E_6 by increasing the a_4 vanishing degree, i.e. the specialized parametrization

$$\left. \begin{aligned} a_1 &= P_{(1,0)}\tilde{w}, & a_3 &= P_{(3,1)}\tilde{w}^2, \\ a_2 &= P_{(2,1)}\tilde{w}, & a_4 &= P_{(4,1)}\tilde{w}^3, \\ & & a_6 &= P_{(6,1)}\tilde{w}^5, \end{aligned} \right\} SO(10) \quad (5.32)$$

localizes an $SO(10)$ gauge group on $\mathcal{D}_{\tilde{w}}$. Over the curve $\{\tilde{w} = P_{(2,1)} = 0\}$ this would be enhanced to E_6 , but the geometry does not support any such intersections as the base intersection form (see table 5.2) has no cross-term involving $X(2P + X) = X\tilde{P}$. This can be traced back to the non-intersection of the two O7-plane components.

Ultimately, with the results of section 5.2.6 this allows to conclude that one can indeed find the exceptional E_n groups and derived Yukawas, but no interactions between $SO(10)$ and E_6 are possible. One could in principle use $U(1)$ fluxes similar to the GUT

breaking mechanism described in section 3.8.3 to break E_6 down to $SO(10)$, but this would inevitably also introduce exotic matter states. Nevertheless, the findings show that even rather simple type IIB geometries gain a lot of additional properties from a proper non-perturbative treatment in the F-theory framework.

5.3 Double del Pezzo Transition of the Quintic

5.3.1 Type IIB orientifold geometry

The second geometry is defined by a further del Pezzo transition—yielding two intersecting $dP_7 = \mathbb{P}^3_{1112}[4]$ surfaces—via restricting the degree-5 hypersurface polynomial of the quintic to contain only monomials where $(x_4)^k$, $k \leq 1$ and $(x_5)^m$, $m \leq 1$. The toric data of the blowup geometry with divisors of finite size is summarized in table 5.5.

vertices of the polyhedron / fan	coords	GLSM charges			divisor class
		Q^1	Q^2	Q^3	
$\nu_1 = (-1, -1, -1, -1)$	u_1	1	0	0	H
$\nu_2 = (1, 0, 0, 0)$	u_2	1	0	0	H
$\nu_3 = (0, 1, 0, 0)$	u_3	1	0	0	H
$\nu_4 = (0, 0, 1, 0)$	v_1	1	0	1	$H + Y$
$\nu_5 = (0, 0, 0, 1)$	v_2	1	1	0	$H + X$
$\nu_6 = (0, 0, 0, -1)$	w_1	0	1	0	X
$\nu_7 = (0, 0, -1, 0)$	w_2	0	0	1	Y
conditions:		5	2	2	

$$\text{intersection form: } 2(H^2X - HX^2 + X^2 + H^2Y - HY^2 + Y^3) + HXY - X^2Y - XY^2$$

$$\text{Stanley-Reisner ideal: } \langle u_1u_2u_3, v_1w_2, v_2w_1 \rangle$$

Table 5.5.: Toric data for the double del Pezzo transition of the quintic Calabi-Yau 3-fold $\mathbb{P}^4[5]$.

The general Calabi-Yau hypersurface constraint for this geometry can be written as

$$Q_{\mathcal{X}} := \sum_{m=0}^2 \sum_{n=0}^2 P_{5-m-n}(\vec{u}) \cdot (v_1)^m (w_2)^{2-m} (v_2)^n (w_1)^{2-n} = 0, \quad (5.33)$$

where $P_k(\vec{u})$ is a degree- k polynomial in u_1, u_2, u_3 . Both dP_7 -divisors D_{w_1} and D_{w_2} have

$\chi(D_{w_i}) = 10$ and intersect over a complex curve

$$C := D_{w_1} \cap D_{w_2} \cong \mathbb{P}^1 \quad (5.34)$$

as indicated by $\chi(C) = -D_{w_1} \cdot D_{w_2} \cdot (D_{w_1} + D_{w_2}) = 2$. Whereas the single del Pezzo transition produced an orientifold plane consisting of two components, the second setting involves the exchange of the dP_7 divisors by the orientifold mapping

$$\sigma : \begin{cases} v_1 \leftrightarrow v_2 \\ w_1 \leftrightarrow w_2. \end{cases} \quad (5.35)$$

Using the projective equivalences Q^2 and Q^3 of the toric space it follows

$$(\vec{u}, v_1, v_2, w_1, w_2) \sim \left(\vec{u}, \frac{v_1}{w_2}, \frac{v_2}{w_1}, 1, 1 \right) \xrightarrow{\sigma} \left(\vec{u}, \frac{v_2}{w_1}, \frac{v_1}{w_2}, 1, 1 \right), \quad (5.36)$$

such that the fixpoint locus is found at $\frac{v_1}{w_2} = \frac{v_2}{w_1} \iff v_1 w_1 = v_2 w_2$ and the O7-plane is given by

$$[\text{O7}] = [\{v_1 w_1 - v_2 w_2 = 0\}] = H + X + Y \in H^2(\mathcal{X}; \mathbb{Z}) \quad (5.37)$$

with $\chi(\text{O7}) = 56$. Note that the explicit equation defining the O7-plane in (5.37) is not the most generic one in the divisor class $H + X + Y$, since a term $P_1(\vec{u})w_1 w_2$ could be added. The intersection with the Calabi-Yau hypersurface constraint of class $5H + 2X + 2Y$ reveals two curves embedded inside the geometry:

$$\begin{aligned} \text{genus-0 curve } \mathbb{P}^1: & \quad \mathcal{X} \cap \text{O7} \cap \{w_i = 0\}, \\ \text{genus-6 curve:} & \quad \mathcal{X} \cap \{v_i = 0\}. \end{aligned} \quad (5.38)$$

The \mathbb{P}^1 curve is the intersection curve C of both dP_7 divisors from (5.34).

In this setting the O7-plane only consists of a single component, whose charges are canceled by a single D7-brane wrapping the divisor $8[\text{O7}] = 8(H + X + Y)$. The prediction for the uplift geometry 4-fold is then

$$\text{single D7:} \quad \chi^*(\mathcal{Z}) = \left(\frac{\chi_o(8(H + X + Y))}{2} + 2\chi(H + X + Y) \right) = 1008, \quad (5.39)$$

which is once again the configuration containing the minimal number of D7-branes that cancels the tadpole. In contrast to the earlier model considered in section 5.2, this brane configuration indeed suggests a smooth uplift Weierstrass model.

5.3.2 Uplift Calabi-Yau 4-fold geometry

vertices of the polyhedron / fan	coords	GLSM charges		divisor class	type / $\chi(D)$
		Q^1	Q^2		
$\nu_1 = (-1, -1, -2, -1)$	u_1	1	0	P	13
$\nu_2 = (1, 0, 0, 0)$	u_2	1	0	P	13
$\nu_3 = (0, 1, 0, 0)$	u_3	1	0	P	13
$\nu_4 = (0, 0, 1, 0)$	\tilde{v}	2	1	$2P + X = \tilde{P}$	46
$\nu_5 = (0, 0, 0, 1)$	\tilde{h}	1	1	$P + X$	24 (K3)
$\nu_6 = (0, 0, -1, -1)$	\tilde{w}	0	1	X	10 (dP_7)
conditions:		5	2		

$$\begin{aligned} \text{intersection form: } & 2P^2X - PX^2 - X^3 \\ & = 37\tilde{P}^3 + 3\tilde{P}X - 3\tilde{P}X^2 + 19X^3 \end{aligned}$$

$$\text{Stanley-Reisner ideal: } \langle u_1u_2u_3, \tilde{v}\tilde{h}\tilde{w} \rangle$$

Table 5.6.: Toric data for the downstairs Kähler 3-fold base $\mathcal{B} = \mathcal{X}/\sigma$ of the quintic’s double del Pezzo transition, cf. table 5.5.

In the uplifting of the described orientifold one proceeds analogous to section 5.2.2. In this case the orientifold mapping (5.35) exchanges the two dP_7 surfaces and is represented by the projection mapping

$$\begin{aligned} \tilde{\sigma} : (u_1, u_2, u_3, v_1, v_2, w_1, w_2) &\mapsto (u_1, u_2, u_3, \tilde{v}, \tilde{h}, \tilde{w}), \\ \text{where } \begin{cases} \tilde{v} := v_1v_2, \\ \tilde{h} := v_1w_1 + v_2w_2, \\ \tilde{w} := w_1w_2, \end{cases} & \end{aligned} \quad (5.40)$$

that is 2-to-1 away from the orientifold locus $v_1w_1 = v_2w_2$. In this projection one coordinate is dropped and the resulting “downstairs” geometry that serves as the base \mathcal{B} of the uplift 4-fold is described by the toric data in table 5.6.

The divisor $\mathcal{D}_{\tilde{w}}$ has $\chi(\mathcal{D}_{\tilde{w}}) = 10$ and can be identified as the invariant dP_7 surface, whereas $\mathcal{D}_{\tilde{h}}$ is the divisor of the O7-plane. The full Calabi-Yau 4-fold \mathcal{Z} is constructed in the same fashion as before, i.e. one adds homogeneous coordinates $(x, y, z) \in \mathbb{P}_{231}^2$ intertwined appropriately such that the divisor $\mathcal{D}_z = \{z = 0\}$ embeds the base \mathcal{B} into the 4-fold \mathcal{Z} . The degree-6 Weierstrass model equation

$$y^2 = x^3 + xz^4f(\vec{u}, \tilde{v}, \tilde{h}, \tilde{w}) + z^6g(\vec{u}, \tilde{v}, \tilde{h}, \tilde{w}), \quad (5.41)$$

is imposed and \mathcal{Z} is once again described by a complete intersection of two hypersurfaces. In accordance to the perturbative type IIB prediction (5.39) of section 5.3.1, one finds that $\chi^*(\mathcal{Z}) = 1008$ when computing the naive Euler characteristic by evaluating the top Chern class of the 4-fold or (ab)using the I_1 singularity relation (5.16). Again, this provides the leading order contribution to the Euler characteristic, that has to be corrected in the presence of non-Abelian singularities.

5.3.3 Minimal and maximal gauge groups

The analysis of the available gauge groups is analogous to the one carried out in section 5.2.4, but technically more complicated due to the third coordinate contributing cohomologically to the divisor class X . In this geometry one finds $c_1(\mathcal{B}) = P + X$, such that $a_n \in H^0(\mathcal{B}; \mathcal{O}(n(P + X)))$. The first two Tate coefficients can now have more terms

$$\begin{aligned} a_1 &= C_h \tilde{h} + P_1(\vec{u}) \tilde{w}, \\ a_2 &= C_0 \tilde{v} \tilde{w} + C_{h^2} \tilde{h}^2 + Q_1(\vec{u}) \tilde{h} \tilde{w} + P_2(\vec{u}) \tilde{w}^2 \end{aligned} \quad (5.42)$$

in their most generic form and likewise for a_3 , a_4 and a_6 . The location of the O7-plane is given by

$$b_2 = \rho(\tilde{h}^2 - 4\tilde{v}\tilde{w}) = 0, \quad (5.43)$$

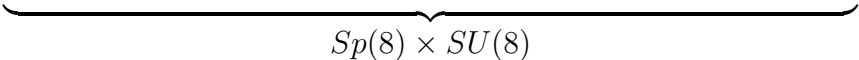
where $\rho \neq 0$ is some non-zero constant. The generic expression $b_2 = (a_1)^2 + 4a_2$ for the O7-plane term restricts the Tate coefficient a_2 of (5.42) to take the form

$$a_2 = -\rho \tilde{v} \tilde{w} + \frac{\rho - C_{h^2}}{4} \tilde{h}^2 - \frac{C_h}{2} P_1(\vec{u}) \tilde{h} \tilde{w} - \frac{1}{4} P_1(\vec{u})^2 \tilde{w}^2. \quad (5.44)$$

Due to the single D7-brane that cancels the tadpole in this setting, no singularities are expected except over the rigid curve \mathbb{P}^1 from the original intersection of the two dP_7 surfaces in the ‘‘upstairs’’ Calabi-Yau geometry \mathcal{X} . The curve $C \subset \mathcal{X}$ is mapped to $\mathcal{D}_{\tilde{w}} \cap \mathcal{D}_{\tilde{h}} \cong \mathbb{P}^1$ and on this locus the combined vanishing of \tilde{w} and \tilde{h} is of degrees $(1, 1, 2, 2, 3)$ —yielding a G_2 singularity over the genus-0 curve.

In the type IIB orientifold the maximal perturbative gauge group $Sp(8) \times SU(8)$ is obtained from two stacks of 8 D7-branes wrapping D_{u_1} and D_{w_1} , respectively. One can show that this configuration can be realized in the uplift 4-fold via the Tate parametrization

$$\begin{aligned} a_1 &= C_h \tilde{h} + P_1(\vec{u}) \tilde{w}, & a_3 &= 0, \\ a_2 &= -C_h \tilde{v} \tilde{w} - \frac{C_h}{2} P_1(\vec{u}) \tilde{h} \tilde{w} - \frac{1}{4} P_1(\vec{u})^2 \tilde{w}^2, & a_4 &= C_d (u_1)^4 \tilde{w}^4, \\ & & a_6 &= 0, \end{aligned} \quad (5.45)$$


 $Sp(8) \times SU(8)$

which reveals the same kind of non-perturbative O7-plane splitting observed in section 5.2.5 for the single del Pezzo transition orientifold.

5.3.4 GUT related representations and Yukawa couplings

It remains to determine the properties of the uplift model away from the orientifold locus, more specifically the GUT model ingredients one can obtain in this geometry. For $C_h = C_{h^2} = 0$ the group $SO(10)$ with vanishing degrees $(1, 1, 2, 3, 5)$ can be arranged along the del Pezzo divisor $\mathcal{D}_{\tilde{w}}$. This sets the basic stage for an $SO(10)$ GUT model. The restriction of the Tate coefficients to the form (5.32)—which was used to show the absence of $SO(10)$ spinors in section 5.2.6—now reveals an enhancement to E_6 along $\{\tilde{w} = P_{(2,1)} = 0\}$ since in the exchange geometry the two divisors indeed intersect, i.e. $X(2P + X) = X\tilde{P}$ restricts to a non-trivial intersection form on the E_6 -curve according to table 5.6. Furthermore, a Higgs field in the **10** representation can be localized along the genus-4 curve $\{\tilde{w} = P_{(3,1)} = 0\}$, and a closer inspection reveals 6 mutual intersection points of both curves. In summary, one finds

$$\begin{aligned} E_6 &\rightsquigarrow & \mathbf{16} & SO(10) \text{ spinor} & \{\tilde{w} = P_{(2,1)} = 0\}, \\ SO(12) &\rightsquigarrow & \mathbf{10}_H & \text{Higgs field} & \{\tilde{w} = P_{(3,1)} = 0\}, \\ E_7 &\rightsquigarrow & \mathbf{16} \cdot \mathbf{16} \cdot \mathbf{10}_H & \text{Yukawa coupling} & \{\tilde{w} = P_{(2,1)} = P_{(3,1)} = 0\}. \end{aligned} \quad (5.46)$$

The exchange orientifold geometry therefore provides just the right ingredients to build a basic $SO(10)$ GUT model.

One can also consider an $SU(5)$ GUT in this geometry, which follows from the specific parametrization

$$\left. \begin{aligned} a_1 &= P_{(1,1)}, & a_3 &= P_{(3,1)}\tilde{w}^2, \\ a_2 &= P_{(2,1)}\tilde{w}, & a_4 &= P_{(4,1)}\tilde{w}^3, \\ & & a_6 &= P_{(6,1)}\tilde{w}^5, \end{aligned} \right\} SU(5) \quad (5.47)$$

of the Tate coefficients. The overall vanishing degree along the divisor $\mathcal{D}_{\tilde{w}}$ is $(0, 1, 2, 3, 5)$ and provides the $SU(5)$ GUT group. Along the \mathbb{P}^1 curve where $P_{(1,1)}$ vanishes as well, the singularity type enhances further to $SO(10)$. This provides matter in the **10** representation from the subsequent decomposition of representations. Further matter in the **5** representation is obtained from an $SU(6)$ enhancement along the intersection with

$$Q_{(8,3)} := P_{(3,1)}^2 P_{(2,1)} - P_{(4,1)} P_{(3,1)} P_{(1,1)} + P_{(6,1)} P_{(1,1)}^2 = 0. \quad (5.48)$$

This particular polynomial is derived from the leading orders in \tilde{w} of the discriminant, a procedure that will be shown in detail for the upcoming geometry in section 5.4. Of particular interest is the triple intersection of $\mathcal{D}_{\tilde{w}}$ with $P_{(1,1)} = P_{(3,1)} = 0$. Here

one finds a single point of enhancement to $SO(12)$ that precisely yields the bottom-quark Yukawa coupling $\mathbf{10} \cdot \bar{\mathbf{5}} \cdot \bar{\mathbf{5}}_H$. For the basic $SU(5)$ GUT one therefore obtains the following enhancements:

$$\begin{aligned}
SO(10) &\rightsquigarrow \mathbf{10} \text{ matter} && \{\tilde{w} = P_{(1,1)} = 0\}, \\
SU(6) &\rightsquigarrow \mathbf{5} \text{ matter / Higgs field} && \{\tilde{w} = Q_{(8,3)} = 0\}, \\
SO(12) &\rightsquigarrow \mathbf{10} \cdot \bar{\mathbf{5}} \cdot \bar{\mathbf{5}}_H \text{ Yukawa coupling} && \{\tilde{w} = P_{(1,1)} = Q_{(8,3)} = 0\}.
\end{aligned} \tag{5.49}$$

Unfortunately, the triple intersection $\{\tilde{w} = P_{(1,1)} = P_{(2,1)} = 0\}$ to the group E_6 is non-existent, such that top-quark Yukawas of type $\mathbf{10} \cdot \mathbf{10} \cdot \mathbf{5}_H$ are not supported in the F-theory $SU(5)$ model of the double del Pezzo transition of the quintic.

5.4 Non-Generic del Pezzo Transition of the Quartic 3-fold

5.4.1 Fano 3-fold bases and non-generic del Pezzo transitions

The promising success in uplifting the “upstairs” del Pezzo transitions of the quintic hypersurface $\mathbb{P}^4[5]$ suggests to follow this approach further. However, a noteworthy observation of the toric data for the “downstairs” geometries is that the hypersurface degree of the non-Calabi-Yau spaces is the sum of all coordinate charges minus one in each GLSM charge vector Q^i . This particular structure can be observed for the hypersurface del Pezzo surfaces

$$\begin{aligned}
dP_6 &= \mathbb{P}^3[3], \\
dP_7 &= \mathbb{P}_{1112}^3[4], \\
dP_8 &= \mathbb{P}_{1123}^3[6],
\end{aligned} \tag{5.50}$$

all of which are 2-dimensional Fano surfaces. Mathematically, a Fano variety \mathcal{B} is a non-singular complete variety whose anti-canonical bundle $K_{\mathcal{B}}^{-1}$ is very ample, which roughly speaking means that \mathcal{B} admits an embedding into a projective space $\mathbb{C}\mathbb{P}^n$. This is a sufficient criterion for the existence of global elliptic fibrations over \mathcal{B} , such that the total 4-fold \mathcal{Z} is non-singular.

Smooth Fano 3-folds therefore provide an important class of suitable bases for F-theory model building geometries [154, 158, 160], which have been classified by Iskovskih and Mori-Mukai [178–181]. The simplest candidate in three dimensions that follows the observed “total coordinate GLSM charge minus one” scheme of the prior examples and (5.50) is the Fano 3-fold quartic hypersurface $\mathbb{P}^4[4]$. Other examples are $\mathbb{P}^4[3]$ and $\mathbb{P}^4[2]$.

In order to obtain del Pezzo surfaces for the GUT brane inside this base space, the del Pezzo transition is used again. One can generate a dP_6 singularity in $\mathbb{P}^4[4]$ by tuning

vertices of the polyhedron / fan	coords	GLSM charges		divisor class	type / $\chi(D)$
		Q^1	Q^2		
$\nu_1 = (-1, -1, -1, -1)$	u_1	1	0	P	12
$\nu_2 = (1, 0, 0, 0)$	u_2	1	0	P	12
$\nu_3 = (0, 1, 0, 0)$	u_3	1	0	P	12
$\nu_4 = (0, 0, 1, 0)$	u_4	1	1	$P + X = \tilde{P}$	24 (K3)
$\nu_5 = (0, 0, 0, 1)$	u_5	1	1	$P + X = \tilde{P}$	24 (K3)
$\nu_6 = (0, 0, -1, -1)$	w	0	1	X	10 (dP_7)
conditions:		4	2		

intersection form: $2P^2X - 2X^3 = 4\tilde{P}^3 - 2\tilde{P}X^2 - 2X^3$

total Chern class: $1 + (P + X) + (6P^2 + X^2 + 7PX) - 18P^2X - 14P^3 - 7PX^2 - X^3$

Stanley-Reisner ideal: $\langle u_1u_2u_3, u_4u_5w \rangle$

Table 5.7.: Toric data for the downstairs Kähler 3-fold base \mathcal{B} of the quartic’s non-generic del Pezzo transition along a curve \mathbb{P}^1 .

the degree-4 hypersurface condition to the form

$$u_5F_3(u_1, \dots, u_4) + F_4(u_1, \dots, u_4) = 0, \tag{5.51}$$

where F_d is a polynomial of degree d in the first four \mathbb{P}^4 coordinates u_1, \dots, u_4 . Note that $F_3(u_1, \dots, u_4) = 0$ precisely describes a dP_6 singularity at $(0, 0, 0, 0, 1) \in \mathbb{P}^4$, cf. (5.50). The standard toric blowup procedure used in sections 5.2 and 5.3 then adds a further coordinate w , such that the blowup constraint becomes

$$u_5F_3(u_1, \dots, u_4) + wF_4(u_1, \dots, u_4) = 0. \tag{5.52}$$

The toric data for this geometry is shown in table 5.1 of the earlier studied single del Pezzo transition of the quintic—aside from the intersection form due to the different hypersurface constraint degree. Unfortunately, this geometry would therefore also suffer from the absence of $SO(10)$ enhancement, analogous to the discussion back in section 5.2.6.

The idea is therefore to consider a non-generic del Pezzo transition. Instead of producing an isolated singularity in $\mathbb{P}^4[4]$, one tunes the coefficients such that an entire curve \mathbb{P}^1 parameterized by

$$(0, 0, 0, u_4, u_5) \sim (0, 0, 0, \lambda u_4, \lambda u_5) \quad \text{for } \lambda \in \mathbb{C}^\times \tag{5.53}$$

vertices of the polyhedron / fan	coords	GLSM charges			divisor class
		Q^1	Q^2	Q^3	
$\nu_1 = (1, 0, 0, 0, 0, 0)$	x	2	0	0	$2(\sigma + P + X)$
$\nu_2 = (0, 1, 0, 0, 0, 0)$	y	3	0	0	$3(\sigma + P + X)$
$\nu_3 = (-2, -3, 0, 0, 0, 0)$	z	1	-1	-1	σ
$\nu_4 = (-2, -3, -1, -1, -1, -1)$	u_1	0	1	0	P
$\nu_5 = (0, 0, 1, 0, 0, 0)$	u_2	0	1	0	P
$\nu_6 = (0, 0, 0, 1, 0, 0)$	u_3	0	1	0	P
$\nu_7 = (0, 0, 0, 0, 1, 0)$	u_4	0	1	1	$P + X$
$\nu_8 = (0, 0, 0, 0, 0, 1)$	u_5	0	1	1	$P + X$
$\nu_9 = (-2, -3, 0, 0, -1, -1)$	w	0	0	1	X
conditions:		6	0	0	
		0	4	2	

Stanley-Reisner ideal: $\langle xyz, u_1u_2u_3, u_4u_5w \rangle$

Table 5.8.: Toric data for the elliptically-fibered Calabi-Yau 4-fold \mathcal{Z} arising from the quartic's non-generic del Pezzo transition, cf. table 5.7.

becomes singular. The corresponding blowup of this curve generates a dP_7 of finite size. The toric data for this base geometry is found in table 5.7.

Constructing the Calabi-Yau 4-fold \mathcal{Z} is then straightforward. By adding three additional projective coordinates x, y, z for the elliptic fiber \mathbb{P}_{231}^2 [6] and modifying the charges appropriately, one arrives at the toric data in table 5.8. The transversality condition on the two intersecting hypersurfaces will be explicitly investigated in the later section 7.1.1. Under the assumption of a smooth Weierstrass model, (5.16) gives

$$\chi^*(\mathcal{Z}) = 1728. \quad (5.54)$$

This value will later be used in chapter 7, when an explicit GUT model [88] is realized.

5.4.2 Gauge group enhancements and $SU(5)$ GUT ingredients

As before, the del Pezzo divisor $\mathcal{D}_w = \{w = 0\}$ of type dP_7 is of primary interest. Due to $c_1(\mathcal{B}) = P + X$ the Tate coefficients are again sections $a_n \in H^0(\mathcal{B}; \mathcal{O}(n(P+X)))$, such that along \mathcal{D}_w the generic Tate parametrization can be tuned to locally take the form

$$\left. \begin{aligned} a_1 &= P_{(1,1)}, & a_3 &= P_{(3,1)}w^2, \\ a_2 &= P_{(2,1)}w, & a_4 &= P_{(4,1)}w^3, \\ & & a_6 &= P_{(6,1)}w^5, \end{aligned} \right\} SU(5) \quad (5.55)$$

of an $SU(5)$ gauge group with overall vanishing degrees $(0, 1, 2, 3, 5)$, precisely the same as studied in (5.47). A look at the leading orders in w of the discriminant

$$\begin{aligned} \Delta = -w^5 & \left(\overbrace{P_{(1,1)}^4 Q_{(8,3)}}^{\text{order } w^5} + \overbrace{w P_{(1,1)}^2 (8P_{(2,1)} Q_{(8,3)} + P_{(1,1)} R_{(9,3)})}^{\text{order } w^6} \right) \\ & - \underbrace{w^2 (16P_{(3,1)}^2 P_{(2,1)}^2 + P_{(1,1)} S)}_{\text{order } w^7} + \mathcal{O}(w^3) \end{aligned} \quad (5.56)$$

with the abbreviation polynomials

$$\begin{aligned} Q_{(8,3)} &:= P_{(3,1)}^2 P_{(2,1)} - P_{(4,1)} P_{(3,1)} P_{(1,1)} + P_{(6,1)} P_{(1,1)}^2 \\ R_{(9,3)} &:= 4P_{(6,1)} P_{(2,1)} P_{(1,1)} - P_{(3,1)}^3 - P_{(4,1)}^2 P_{(1,1)} \end{aligned} \quad (5.57)$$

shows that the term in the parentheses does not in general factorize further. Generically, it yields the problematic I_1 remainder component \mathcal{D}_R along its vanishing locus, as discussed in sections 3.3 and 4.4.3. The divisor class of the entire discriminant vanishing locus of this setting therefore splits cohomologically as

$$[\{\Delta = 0\}] = 5[\mathcal{S}] + [\mathcal{D}_R] \in H^2(\mathcal{B}; \mathbb{Z}), \quad (5.58)$$

where $\mathcal{S} := \mathcal{D}_w$ is the del Pezzo divisor of the $SU(5)$ GUT brane.

As before, one can now systematically analyze the gauge group enhancements and relevant divisor intersections. Along the intersection of \mathcal{S} with $P_{(1,1)} = 0$ the Tate coefficient a_1 gains a further vanishing order, which leads to an $SO(10)$ enhancement curve

$$\mathcal{C}_{SO(10)} := \mathcal{S} \cap \{P_{(1,1)} = 0\}, \quad (5.59)$$

where matter in the $\mathbf{10}$ representation can be accommodated. Similarly, along the intersection of the GUT brane with $\{Q_{(8,3)} = 0\}$ the discriminant vanishing degree is

	sing. type	discr. deg(Δ)	gauge enh.		coeff. vanish. deg					object equation
			type	group	a_1	a_2	a_3	a_4	a_6	
GUT:	I_5^s	5	A_4	$SU(5)$	0	1	2	3	5	\mathcal{S} : $w = 0$
matter:	I_6^s	6	A_5	$SU(6)$	0	1	3	3	6	$\mathcal{C}_{SU(6)}$: $Q_{(8,3)} = 0$
	I_1^{*s}	7	D_5	$SO(10)$	1	1	2	3	5	$\mathcal{C}_{SO(10)}$: $P_{(1,1)} = 0$
Yukawa:	I_2^{*s}	8	D_6	$SO(12)$	1	1	3	3	5	$P_{(1,1)} = P_{(3,1)} = 0$
	IV^{*s}	8	E_6	E_6	1	2	2	3	5	$P_{(1,1)} = P_{(2,1)} = 0$
extra:	I_7^s	7	A_6	$SU(7)$	0	1	3	4	7	$Q_{(8,3)} = R_{(9,3)} = 0,$ $(P_{(1,1)}, P_{(2,1)}) \neq (0, 0)$

Table 5.9.: Relevant gauge enhancements for $SU(5)$ GUT model building in the considered geometry derived from $\mathbb{P}^4[4]$.

raised by one order, such that it follows from the (generic) non-vanishing of $P_{(1,1)}$ that by the Tate classification only the case of an $SU(6)$ enhancement along the curve

$$\mathcal{C}_{SU(6)} := \mathcal{S} \cap \{Q_{(8,3)} = 0\} \quad (5.60)$$

remains. This can localize matter in the $\mathbf{5}$ of $SU(6)$. However, generically this matter curve $\mathcal{C}_{SU(6)}$ does not factorize, which is phenomenologically undesired in the context of the doublet-triplet splitting problem, cf. section 3.8.2. At certain points along the $\mathbf{10}$ curve $\mathcal{C}_{SO(10)}$ the singularity type enhances further: At the codimension-3 intersection with $\{P_{(3,1)} = 0\}$, which is contained in $\mathcal{C}_{SU(6)}$ as well,

$$\mathcal{P}_{SO(12)} := \mathcal{C}_{SO(10)} \cap \{P_{(3,1)} = 0\} \subset \mathcal{C}_{SO(10)} \cap \mathcal{C}_{SU(6)}, \quad (5.61)$$

the singularity enhances to $SO(12)$. The subsequent decomposition then gives rise to the $\mathbf{10} \cdot \bar{\mathbf{5}}_m \cdot \bar{\mathbf{5}}_H$ Yukawa coupling. Likewise, at the intersection

$$\mathcal{P}_{E_6} := \mathcal{C}_{SO(10)} \cap \{P_{(2,1)} = 0\} \subset \mathcal{C}_{SO(10)} \cap \mathcal{C}_{SU(6)} \quad (5.62)$$

the $\mathbf{10} \cdot \mathbf{10} \cdot \mathbf{5}_H$ Yukawa coupling is localized at a point of E_6 enhancement. Those two enhancements correspond to a single and double zero of the polynomial $Q_{(8,3)}$ that defines $\mathcal{C}_{SU(6)}$ — yielding the respective number of $\mathbf{5}$ and $\bar{\mathbf{5}}$ representations localized at \mathcal{P}_{E_6} and $\mathcal{P}_{SO(12)}$. Furthermore, along the intersection of $\mathcal{C}_{SU(6)}$ with $\{R_{(9,3)} = 0\}$, where $P_{(1,1)}$ and $P_{(2,1)}$ are not simultaneously vanishing, there are enhancement points to $SU(7)$ at

$$\mathcal{P}_{SU(7)} := \mathcal{C}_{SU(6)} \cap \{R_{(9,3)} = 0 : (P_{(1,1)}, P_{(2,1)}) \neq (0, 0)\} \quad (5.63)$$

that realize the coupling $\mathbf{5}_H \cdot \bar{\mathbf{5}}_m \cdot \mathbf{1}$. For the convenience of the reader all those enhancements are listed in table 5.9.

Note that the intersection numbers for all three codimension-3 enhancements $\mathcal{P}_{SO(10)}$, \mathcal{P}_{E_6} and $\mathcal{P}_{SU(7)}$ are nonzero, i.e. in contrast to the geometries considered earlier the geometry arising from $\mathbb{P}^4[4]$ actually contains all important interactions and representations. Furthermore, all those promising ingredients follow entirely from 7-brane intersections, i.e. entirely without the help of extra ingredients like the M5-brane instantons discussed in chapter 4.

5.4.3 The $SO(10)$ matter curve

The distinct improvement of the geometry considered here is the actual presence of the top-quark Yukawa coupling $\mathbf{10} \cdot \mathbf{10} \cdot \mathbf{5}_H$ arising from \mathcal{P}_{E_6} , which is related to the non-generic del Pezzo transition performed on the quartic $\mathbb{P}^4[4]$. One can understand this from the weak coupling type IIB orientifold picture, where in the “upstairs” geometry the $\mathbf{10}$ matter curve arises from the intersection of the $SU(5)$ GUT brane with its mirror brane. Since this brane is wrapping a del Pezzo surface in the F-theory “downstairs” base, the “upstairs” geometry therefore has to have two intersecting del Pezzo surfaces—a highly non-generic situation. Furthermore, due to the rigidity of each del Pezzo surface both cannot be simultaneously shrunk to a point. This leads to the presence of a non-generic intersection curve to which both surfaces can be reduced [88, 99].

The presence of a non-generic del Pezzo surface within a “downstairs” F-theory basis is therefore corresponding to intersecting del Pezzo surfaces in the “upstairs” Calabi-Yau geometry—precisely the setting considered here. In particular, this circumvents a no-go theorem [157] that states the absence of the relevant couplings for generic del Pezzo $SU(5)$ GUT branes.

Ultimately, the bottom line is that the geometry arising from the non-generic del Pezzo transition of the quartic $\mathbb{P}^4[4]$ serves as a good starting point to construct a semi-realistic global F-theory $SU(5)$ GUT model. All the important matter representations and couplings have been accounted for in the previous analysis—even without the help of M5-brane instantons or other “extraordinary” ingredients. This makes the listed phenomenological properties in fact rather natural.

Chapter 6

Semi-Realistic Global F-theory GUT Model Building

BASED on the discovery of a promising geometry for $SU(5)$ GUT model building in F-theory from a non-generic del Pezzo transition of the quartic 3-fold hypersurface $\mathbb{P}^4[4]$, further investigation of the phenomenology is in order. The basic requirements like $\mathbf{5}$ and $\mathbf{10}$ matter curves as well as top- and bottom-quark Yukawa couplings — realized by suitable intersections between the allowed 7-brane divisors — have already been checked. However, it remains to describe an appropriate gauge flux that on the one hand breaks the GUT group $SU(5)$ to the MSSM group in the effective theory and on the other hand provides chiral matter.

The key to access worldvolume gauge fluxes is the spectral cover description, which was introduced via the heterotic/F-theory duality back in section 3.5. Due to the nature of many interesting GUT geometries, it is at first necessary to generalize this description to settings that lack a strict heterotic dual. One can then specialize to spectral cover descriptions in the particular context of F-theory $SU(5)$ GUTs.

This reveals that it is in fact necessary to apply a split spectral cover description to construct a viable model and establish a number of basic phenomenological requirements. More specifically, the split spectral cover will (like the name suggests) “split” the $\bar{\mathbf{5}}_m$ matter and the $\mathbf{5}_H + \bar{\mathbf{5}}_H$ Higgs states, which are localized on the same curve $\mathcal{C}_{SU(6)}$ of singularity enhancement in the discussed geometry. Ultimately, this separation allows to avoid the problematic $\mathbf{10} \cdot \bar{\mathbf{5}}_m \cdot \bar{\mathbf{5}}_m$ coupling that leads to the proton decay [182] while still generating the important $\mathbf{10} \cdot \mathbf{10} \cdot \mathbf{5}_H$ and $\mathbf{10} \cdot \bar{\mathbf{5}}_m \cdot \bar{\mathbf{5}}_H$ interactions. A further obstacle are the exotic gauge bosons $(\mathbf{3}, \mathbf{2})_{\pm 5}$ arising from the breaking of the $SU(5)$ GUT symmetry, that are being dealt with by a twisting procedure of the gauge breaking vector bundle. The chapter closes with a ready-to-use formula for the D3-brane tadpole in the context of the discussed model.

6.1 F-theory Spectral Covers without Heterotic Duals

6.1.1 Generic spectral cover construction

For F-theory models with heterotic duals the spectral cover construction from section 3.5 provides an explicit correspondence of the gauge breaking vector bundle V on the heterotic side to the singular structure of the geometry and G_4 flux on the F-theory side. In such models the 4-fold base \mathcal{B}_3 is itself \mathbb{P}^1 -fibered over \mathcal{B}_2 , such that one would aim to naturally identify the $SU(5)$ GUT brane divisor $\mathcal{S} \subset \mathcal{B}_3$ with \mathcal{B}_2 . But for generic F-theory models the required double fibration structure—elliptically and K3-fibered at the same time—is not given, i.e. no direct heterotic dual exists.

It has been shown that one can recover the major aspects of the spectral cover construction [144, 149] by locally viewing \mathcal{S} as the basis of an asymptotically local Euclidean (ALE) fibration that captures the singularity structure on \mathcal{S} as well [66, 69, 157]. The idea is therefore to extend the original spectral cover construction to F-theory settings that lack a heterotic dual in order to describe the localized gauge flux on the $SU(5)$ GUT brane and to produce chiral matter.

The starting point is to construct an auxiliary non-Calabi-Yau 3-fold space \mathcal{W} that takes the place of the heterotic compactification space \mathcal{Y}_3 in the original description, see section 3.5. Similar to the explicit description of the 4-fold base \mathcal{B}_3 , this space \mathcal{W} is explicitly given by a projectivization description

$$\mathcal{W} := \mathbb{P}(\mathcal{O}_{\mathcal{S}} \oplus K_{\mathcal{S}}) \xrightarrow{\pi} \mathcal{S}, \tag{6.1}$$

however, there is no conceptual relation to \mathcal{B}_3 . Note that while in the original construction the heterotic compactification space \mathcal{Y}_3 is elliptically fibered over \mathcal{B}_2 , the auxiliary space \mathcal{W} is a \mathbb{P}^1 -fibration over \mathcal{S} :

$$\begin{array}{ccc} \mathbb{E} \xrightarrow{\text{wavy}} \boxed{\mathcal{Y}_3} \supset \mathcal{C}^{(n)} & & \\ \downarrow \text{dotted} & \searrow & \downarrow \text{wavy} \\ \text{K3} \xrightarrow{\text{solid}} \boxed{\mathcal{Z}_4} \xrightarrow{\text{solid}} \mathcal{B}_2 & & \mathcal{B}_2 = \begin{cases} dP_n \\ \mathbb{F}_k \\ B(\mathbb{F}_k) \\ K3/\mathbb{Z}_2 \end{cases} \\ \downarrow \text{solid} & \downarrow \text{dotted} & \nearrow \text{dotted} \\ \mathbb{P}^1 \hookrightarrow \mathcal{B}_3 = \mathbb{P}(\mathcal{O} \oplus \mathcal{T}) & & \end{array}$$

original configuration, cf. section 3.5

$$\begin{array}{ccc} \mathbb{E} \xrightarrow{\text{wavy}} \boxed{\mathcal{W}} \supset \mathcal{C}^{(5)} & & \\ \downarrow \text{dotted} & \searrow & \downarrow \text{wavy} \\ \text{K3} \xrightarrow{\text{solid}} \boxed{\mathcal{Z}_4} \xrightarrow{\text{solid}} \mathcal{S} & & \mathcal{S} \\ \downarrow \text{dotted} & \downarrow \text{dotted} & \nearrow \text{dotted} \\ \mathbb{P}^1 \hookrightarrow \mathcal{B}_3 & & \mathcal{B}_3 \xrightarrow{\text{dotted}} \mathcal{S} \\ \text{ALE} \hookrightarrow \mathcal{B}_3 & & \text{local ALE fibration} \end{array}$$

configuration without heterotic duals

$$\tag{6.2}$$

The embedding of the base is provided by the section σ , satisfying the same relation

$$\sigma \cdot \sigma = -\sigma c_1(\mathcal{S}) \in H^4(\mathcal{W}; \mathbb{Z}) \tag{6.3}$$

as the original σ in (3.41). Since \mathcal{W} is not a Calabi-Yau space, its first Chern class turns out to be

$$c_1(\mathcal{W}) = 2\sigma + 2c_1(\mathcal{S}). \quad (6.4)$$

In addition, there is a spectral line bundle \mathcal{N} defined over the spectral surface $\mathcal{C}^{(n)} \subset \mathcal{W}$, which is entirely analogous to the one introduced in the original construction from section 3.5. As before, its primary property

$$(\tilde{\pi}_n)_*\mathcal{N} = V|_{\mathcal{S}} \quad (6.5)$$

describes the gauge breaking vector bundle and thus governs the gauge flux. The description (3.45) in terms of the first Chern class $c_1(\mathcal{N}) \in H^2(\mathcal{C}^{(n)}; \mathbb{Z})$ as well as the explicit form (3.47) remain unchanged here. Essentially, the big difference compared to the original construction is the usage of the auxiliary space \mathcal{W} , which for a strict heterotic dual is automatically provided by the heterotic compactification space \mathcal{Y}_3 . One also has to keep in mind that the spectral cover construction here rests upon the assumption of an ALE fibration, which is in general only locally valid. In contrast, the original spectral cover approach is a truly global description.

6.1.2 $SU(5)$ specifics

One then chooses homogeneous coordinates (M, N) to parameterize the fiber directions of \mathcal{W} , such that the restriction to each \mathbb{P}^1 -fiber $\mathcal{W}_p \cong \mathbb{P}^1$ gives the sections $\mathcal{O}(1) \otimes K_{\mathcal{S}}$ and $\mathcal{O}(1)$, respectively. The $SU(5)$ spectral cover surface $\mathcal{C}^{(5)}$ associated to the Tate parametrization (5.55) is described by the hypersurface condition¹

$$P'_{(6,1)}M^5 + P'_{(4,1)}M^3N^2 + P'_{(3,1)}M^2N^3 + P'_{(2,1)}MN^4 + P'_{(1,1)}N^5 = 0, \quad (6.6)$$

where each primed $P'_{(m,n)}$ is the restriction of the polynomials $P_{(m,n)}$ to \mathcal{S} , i.e.

$$P'_{(m,n)} := P_{(m,n)}|_{\mathcal{S}} = P_{(m,n)}|_{\{w=0\}}, \quad (6.7)$$

which are sections of powers of the anti-canonical bundle $K_{\mathcal{S}}^{-1} = K_{\mathcal{B}}^{-1}|_{\mathcal{S}} \otimes N_{\mathcal{S} \subset \mathcal{B}}^{-1}$ by the adjunction formula. Equation (6.6) can be treated as the projectivization of the hypersurface condition

$$P'_{(6,1)}s^5 + P'_{(4,1)}s^3 + P'_{(3,1)}s^2 + P'_{(2,1)}s + P'_{(1,1)} = 0 \quad (6.8)$$

¹One should keep in mind that the parametrization (5.55) rests on the assumption of $c_1(\mathcal{B}_3) = P + X$ with respect to the geometry in table 5.7, which fixes the polynomial charges in $P_{(m,n)}$. Nevertheless, the outlined procedure is easily generalized.

in the total space of the canonical line bundle $K_{\mathcal{S}}$, where $s = 0$ embeds the base \mathcal{S} into $K_{\mathcal{S}}$. The spectral surface $\mathcal{C}^{(5)} \subset \mathcal{W}$ defined in (6.6) then has the Poincaré-dual cohomology class

$$[\mathcal{C}^{(5)}] = 5\sigma + \pi^*\eta \in H^2(\mathcal{W}; \mathbb{Z}) \quad (6.9)$$

and with obvious similarity to (3.42) one finds

$$\eta = 6c_1(\mathcal{S}) + c_1(N_{\mathcal{S} \subset \mathcal{B}}) \in H^2(\mathcal{S}; \mathbb{Z}) \quad (6.10)$$

for the non-trivial part. The entire construction therefore is virtually identical in terms of the cohomological description. But one should keep in mind that whereas the original spectral cover construction is an equivalent global representation, the description here only applies locally to the GUT brane divisor \mathcal{S} .

6.2 Global $SU(5)$ GUT Models with Spectral Cover Fluxes

Equipped with the (local) spectral cover description for general F-theory models without a strict heterotic dual, one can now continue the analysis of the generic phenomenological properties of the $\mathbb{P}^4[4]$ model from section 5.4. However, it should be mentioned right from the start that this section is only an intermediate step, which requires further significant changes—a splitting of the entire spectral cover to deal with $\mathbf{5}_m$ and $\mathbf{5}_H$ separation—in order to produce a viable global F-theory model.

6.2.1 Matter curves in the spectral cover description

The ALE fibration assumes an underlying E_8 structure from the Weierstrass model used to describe the elliptic fibration of \mathcal{Z}_4 over the base \mathcal{B}_3 . Since one of the maximal subgroups of E_8 is $SU(5) \times SU(5)$, the structure group of the embedded vector bundle V on the heterotic side is $G = SU(5)^\perp \cong SU(5)$ and $H = SU(5)$ remains as the effective unbroken GUT gauge group. The massless matter representations therefore correspond to the irreducible representations in the decomposition of the E_8 's adjoint representation into $G \times H = SU(5) \times SU(5)$ representations

$$\mathbf{248} \rightarrow (\mathbf{24}, \mathbf{1}) \oplus (\mathbf{1}, \mathbf{24}) \oplus [(\mathbf{10}, \mathbf{5}) \oplus (\bar{\mathbf{5}}, \mathbf{10}) + \text{h. c.}]. \quad (6.11)$$

The matter curves and intersections on the GUT brane \mathcal{S} , that were analyzed in the previous chapter can be translated to the spectral cover description. With respect to the local $SU(5)$ parametrization (5.55) and the subsequently identified singularity enhancements, the $\mathbf{10}$ representation is localized on the $SO(10)$ curve $\mathcal{C}_{SO(10)} = \{w = P_{(1,1)} = 0\}$, cf. table 5.9 in section 5.4.2. By defining

$$\tilde{\mathcal{C}}_{\mathbf{10}} := \mathcal{C}^{(5)} \cap \sigma \subset \mathcal{W} \quad (6.12)$$

as the intersection of the $SU(5)$ spectral surface and the base embedding section, the matter curve $\mathcal{C}_{SO(10)} \subset \mathcal{S}$ can cohomologically be recovered as the restriction

$$\begin{aligned} [\mathcal{C}_{SO(10)}] &= [\tilde{\mathcal{C}}_{\mathbf{10}}]|_{\sigma} = (5\sigma + (\pi_5)^*\eta)|_{\sigma} \\ &= \eta - 5c_1(\mathcal{S}) \in H^2(\mathcal{S}; \mathbb{Z}) \end{aligned} \quad (6.13)$$

using (6.3). Therefore $\tilde{\mathcal{C}}_{\mathbf{10}}$ can roughly be understood as a sort of “uplift” of $\mathcal{C}_{SO(10)}$ to the 5-sheeted spectral surface $\mathcal{C}^{(5)}$ covering \mathcal{S} , where the used naming scheme highlights the $\mathbf{10}$ matter representation that is localized on this curve.^{II}

The corresponding spectral cover description of the $\bar{\mathbf{5}}$ matter representation is more complicated [146, 183, 184]. A detailed analysis in heterotic theory shows that one should regard it as the intersection

$$\mathcal{C}^{\Lambda^2 V} \cap \sigma, \quad (6.14)$$

where $\mathcal{C}^{\Lambda^2 V}$ is a 10-sheeted spectral surface associated to the antisymmetric $\mathbf{10}$ representation of $SU(5)$, which will not be introduced here. Instead, one can define a branched double cover

$$\begin{aligned} \tilde{\mathcal{C}}_{\bar{\mathbf{5}}} &:= \tau\mathcal{C}^{(5)} \cap \mathcal{C}^{(5)} - \mathcal{C}^{(5)} \cap \sigma - \mathcal{C}^{(5)} \cap \sigma_t \\ &= \mathcal{C}^{(5)} \cap (\tau\mathcal{C}^{(5)} - \sigma_{\tau}), \end{aligned} \quad (6.15)$$

where $\tau : N \mapsto -N$ is a \mathbb{Z}_2 -involution on the \mathbb{P}^1 -fibers of \mathcal{W} over \mathcal{S} , $\sigma_{\tau} := \sigma + \sigma_{\tau}$ is an abbreviation and $\sigma_t := 3(\sigma + \pi^*c_1(\mathcal{S}))$ a so-called trisection. The class of $\tilde{\mathcal{C}}_{\bar{\mathbf{5}}}$ can then be evaluated as

$$\begin{aligned} [\tilde{\mathcal{C}}_{\bar{\mathbf{5}}}] &= [\mathcal{C}^{(5)}] \cdot [\tau\mathcal{C}^{(5)} - \sigma_{\tau}] \\ &= \left(5\sigma + (\pi_5)^*\eta\right) \left(\sigma + (\pi_5)^*(\eta - 3c_1(\mathcal{S}))\right) \in H^4(\mathcal{W}; \mathbb{Z}). \end{aligned} \quad (6.16)$$

This completes the dictionary between the matter curves on \mathcal{S} identified in section 5.4.2 and the local spectral cover description introduced here.

One could now go on and identify the intersections between the matter curves in order to identify the couplings and interactions. Since $\mathbf{5}_H$, $\bar{\mathbf{5}}_H$ and $\bar{\mathbf{5}}_m$ are all localized on the same curve, one in particular finds the dangerous $\mathbf{10} \cdot \bar{\mathbf{5}}_m \cdot \bar{\mathbf{5}}_m$ coupling. This problem will be dealt with in the next section via the splitting approach.

^{II}For the readers convenience any curves on the spectral surface $\mathcal{C}^{(5)}$ will be denoted by tildes, e.g. $\tilde{\mathcal{C}}_{\mathbf{10}}$ or $\tilde{\mathcal{C}}_{\bar{\mathbf{5}}}$, in contrast to the matter curves $\mathcal{C}_{SO(10)} \subset \mathcal{S}$ of the GUT 7-brane divisor.

6.2.2 Gauge flux on the $SU(5)$ GUT and matter branes

The spectral cover description allows to handle the gauge flux on \mathcal{S} , such that chiral matter can be generated and the GUT symmetry be broken via an $U(1)_Y$ hypercharge flux, cf. section 3.8.3. Following section 2.5 such an internal flux would be described by an holomorphic line bundle L on the GUT brane \mathcal{S} in the perturbative theory [99], whereas the appropriate description in F-theory arises from a reduction of the G_4 flux along the singular locus of the GUT 7-brane, cf. section 3.4.3.

Aside from the gauge flux on the GUT brane one also has to take flux along the matter branes into account, which constitute the (generically) non-factorizing I_1 singularity part of the discriminant (5.56). Here one makes usage of the fact that the spectral cover description also takes the local neighborhood of the GUT brane \mathcal{S} into account, in particular the intersecting I_1 components that give rise to the matter curves and gauge enhancements.

The local flux along the I_1 components is described by a non-vanishing gauge field strength on \mathcal{S} , that is embedded into the complementary group $SU(5)^\perp$ on the GUT brane. As this reduces $SU(5)^\perp$ further, it leads to the complementary gauge enhancement along the matter curves in the realized gauge group. This flux is described via the spectral line bundle \mathcal{N} defined over the spectral surface $\mathcal{C}^{(5)}$, as introduced in sections 3.5 and 6.1. With respect to the discussed setting here, one has $n = 5$ for the $SU(5)$ group and $c_1(V) = 0$ for the gauge breaking bundle in the bulk, such that the integrality condition for $c_1(\mathcal{N})$ gives

$$\begin{aligned} 5\left(\frac{1}{2} + \lambda\right) &\in \mathbb{Z} \\ \left(\frac{1}{2} - \lambda\right)\eta + \left(5\lambda - \frac{1}{2}\right)c_1(\mathcal{S}) &\in H^2(\mathcal{S}; \mathbb{Z}) \end{aligned} \quad \text{for } \lambda \in \mathbb{Q} \quad (6.17)$$

using the explicit term (3.47). Together with the spectral surface $\mathcal{C}^{(5)}$ this allows to reconstruct the G_4 flux locally.

6.2.3 Chiral matter

Using the spectral cover description of the internal gauge flux on the GUT brane and (locally) the intersecting matter branes, one can systematically analyze the exact chiral matter spectrum arising from the geometry of section 5.4. The computation follows the principal ideas of section 2.5, i.e. by evaluating the chiral matter indices.

The spectrum in the $\mathbf{10}$ representation of $SU(5)$ arises in the sector of the spectral cover, where the zero section σ carries the trivial line bundle, denoted \mathcal{O}_σ . Let

$$\begin{aligned} i : \{\sigma = 0\} &\cong \mathcal{S} \hookrightarrow \mathcal{W} \\ j : \mathcal{C}^{(5)} &\hookrightarrow \mathcal{W} \end{aligned} \quad (6.18)$$

be the embedding mappings of the base \mathcal{S} and the spectral surface. The relevant extension groups are then [77, 157]

$$\begin{aligned} \text{Ext}^i(i_*\mathcal{O}_\sigma; j_*\mathcal{N}) &\cong H^{i-1}(\mathcal{C}^{(5)} \cap \sigma; \mathcal{N} \otimes K_{\mathcal{S}}|_{\mathcal{C}^{(5)} \cap \sigma}) \\ &= H^{i-1}(\tilde{\mathcal{C}}_{10}; \mathcal{N} \otimes K_{\mathcal{S}}|_{\tilde{\mathcal{C}}_{10}}). \end{aligned} \quad (6.19)$$

Analogous to (2.36) the chiral index of the **10** matter representation can be computed via the Riemann-Roch-Hirzebruch index theorem (A.28) as

$$\begin{aligned} \chi_{10} &= \sum_i (-1)^i \text{Ext}^i(i_*\mathcal{O}_\sigma; j_*\mathcal{N}) = \chi(\tilde{\mathcal{C}}_{10}; \mathcal{N} \otimes K_{\mathcal{S}}|_{\tilde{\mathcal{C}}_{10}}) \\ &= \int_{\tilde{\mathcal{C}}_{10}} \left(c_1(\mathcal{N}) + c_1(K_{\mathcal{S}}) + \frac{1}{2}c_1(\tilde{\mathcal{C}}_{10}) \right) \Big|_{\tilde{\mathcal{C}}_{10}} \\ &= \int_{\tilde{\mathcal{C}}_{10}} \left(\gamma - \frac{1}{2}c_1(\mathcal{C}^{(5)}) - \frac{1}{2}(\pi_5)^*c_1(\mathcal{S}) + \frac{1}{2}c_1(\tilde{\mathcal{C}}_{10}) \right) \Big|_{\tilde{\mathcal{C}}_{10}} = \int_{\tilde{\mathcal{C}}_{10}} \gamma, \end{aligned} \quad (6.20)$$

where the cancellation of the three terms in the second-last formula follows from the adjunction formula for the **10** matter curve $\tilde{\mathcal{C}}_{10} = \mathcal{C}^{(5)} \cap \sigma = \sigma|_{\mathcal{C}^{(5)}}$ and with the by now well-known identity $\sigma|_\sigma = \sigma \cdot \sigma = -\sigma c_1(\mathcal{S})$ from (6.3). Since γ depends only on the gauge flux, this reproduces the corresponding relationship in type IIB theory, where in (2.36) the chiral index likewise only depends on the fluxes. Using (6.13) this can be further evaluated to

$$\chi_{10} = \int_{\mathcal{W}} [\sigma] \cdot [\mathcal{C}^{(5)}] \cdot [\gamma] = -\lambda \int_{\mathcal{S}} \eta \cdot [\mathcal{C}_{SO(10)}] = -\lambda \int_{\mathcal{S}} \eta(\eta - 5c_1(\mathcal{S})). \quad (6.21)$$

Note that in general there will be non-chiral pairs invisible to this index computation. However, since negative degree line bundles over smooth curves have no global sections, all negative contributions vanish. The computed χ_{10} therefore directly gives the number of chiral **10** matter representations encountered in the considered geometry.

The computation for the massless $\bar{\mathbf{5}}$ representations is similar [77, 184]. The relevant extension groups here are formally analogous to (6.19)

$$\text{Ext}^i(i_*\mathcal{O}_\sigma; j_*\mathcal{N}^{\Lambda^2 V}) \cong H^{i-1}(\mathcal{C}^{\Lambda^2 V} \cap \sigma; \mathcal{N}^{\Lambda^2 V} \otimes K_{\mathcal{S}}|_{\mathcal{C}^{\Lambda^2 V} \cap \sigma}) \quad (6.22)$$

for $i = 1, 2$, where $(\mathcal{C}^{\Lambda^2 V}, \mathcal{N}^{\Lambda^2 V})$ refers to the 10-sheeted spectral cover of the antisymmetric representation mentioned in (6.14). Using the branched double cover curve $\tilde{\mathcal{C}}_{\bar{\mathbf{5}}}$ from (6.15), this can be rewritten to

$$\text{Ext}^i(i_*\mathcal{O}_\sigma; j_*\mathcal{N}^{\Lambda^2 V}) \cong H^{i-1}(\tilde{\mathcal{C}}_{\bar{\mathbf{5}}}/\tau; L \otimes K_{\mathcal{W}}^{-\frac{1}{2}}|_{\tilde{\mathcal{C}}_{\bar{\mathbf{5}}}/\tau}) \quad (6.23)$$

where the auxiliary line bundle L is fully specified cohomologically by its first Chern class

$$c_1(L)|_{\tilde{\mathcal{C}}_{\bar{5}}/\tau} = c_1(\mathcal{N} \otimes K_S^{\frac{1}{2}})|_{\tilde{\mathcal{C}}_{\bar{5}}} - \frac{R}{2}. \quad (6.24)$$

Here R refers to the number of ramification points of the double cover $\tilde{\mathcal{C}}_{\bar{5}} \rightarrow \tilde{\mathcal{C}}_{\bar{5}}/\tau$, which is given explicitly by the intersection number

$$R = \int_{\mathcal{W}} [\mathcal{C}^{(5)}] \cdot [\mathcal{C}^{(5)} - \sigma_\tau] \cdot [\sigma_\tau]. \quad (6.25)$$

Ultimately, this allows to compute the chiral index of the $\bar{5}$ representations to

$$\chi_{\bar{5}} = \int_{\tilde{\mathcal{C}}_{\bar{5}}} \left(c_1(\mathcal{N}) + \frac{1}{2}c_1(K_S) + \frac{1}{4}c_1(\mathcal{W}) \right) + \frac{1}{2}c_1(\tilde{\mathcal{C}}_{\bar{5}}/\tau)|_{\tilde{\mathcal{C}}_{\bar{5}}/\tau} - \frac{R}{2} = \int_{\tilde{\mathcal{C}}_{\bar{5}}} \gamma. \quad (6.26)$$

Like for χ_{10} , the number of chiral $\bar{5}$ representations $\chi_{\bar{5}}$ depends only on the flux along the intersection curve. One can also show [88] that $\chi_{10} = \chi_{\bar{5}}$ as required for a consistent bundle by anomaly cancellation.

6.2.4 GUT group breaking via hypercharge flux

After computing the number of 10 and $\bar{5}$ $SU(5)$ GUT group representations, one has to consider the breaking of the GUT group in order to obtain (or at least approximate) the well-established Standard Model matter content. The decomposition of the relevant GUT representations is listed in section 3.8.2. The attempt here is now to realize this kind of hypercharge flux GUT symmetry breaking consistently within the spectral cover description and dealing with two phenomenological obstacles:

- The first one of those problems involves the removal of the exotic gauge bosons $(\mathbf{3}, \mathbf{2})_5 \oplus (\mathbf{3}, \mathbf{2})_{-5}$ appearing in the decomposition of the $SU(5)$ adjoint representation, cf. (3.64). In a two-step breaking scheme akin to (2.35) like

$$E_8 \xrightarrow{V} SU(5) \times SU(5) \xrightarrow{L_Y} SU(5) \times SU(3) \times SU(2) \times U(1)_Y \quad (6.27)$$

those states are counted by $h^\bullet(\mathcal{S}; L_Y^{\pm 5})$ according to their respective $U(1)_Y$ charge. However, one can show that the line bundles \mathcal{L} over a del Pezzo- n surface S such that $H^\bullet(S; \mathcal{L}) = 0$ are in bijective correspondence to the roots α of E_n —which by definition implies that for linear scalings $\lambda\alpha$ only $\pm\alpha$ are in fact roots. Therefore, if the hypercharge flux line bundle L_Y is of this type, $L_Y^{\pm 5}$ cannot at the same time correspond to a root of E_n as well. The plain two-step breaking is therefore not suitable to achieve this kind of exotics elimination. Instead a certain twisting procedure borrowed from heterotic GUT model building [185, 186] is applied, such that one directly reduces the E_8 in a single step.

More precisely, the idea is to use a twisting line bundle \mathcal{L}_Y —which is conceptually to be distinguished from L_Y —and add it to a rank-5 spectral cover bundle V with non-trivial first Chern class $c_1(V) \neq 0$, which is similar to the gauge breaking $SU(5)$ vector bundle considered earlier. Then

$$V \oplus \mathcal{L}_Y \quad \text{such that} \quad c_1(V \oplus \mathcal{L}_Y) = c_1(V) + c_1(\mathcal{L}_Y) = 0 \quad (6.28)$$

is embedded as an $S[U(5) \times U(1)]$ -bundle into E_8 , which leads to the breaking of the gauge group like

$$E_8 \longrightarrow SU(5) \times SU(3) \times SU(2) \times U(1)_Y. \quad (6.29)$$

The Cartan generators of the $V \oplus \mathcal{L}_Y$ bundle structure group are embedded diagonally via

$$T = 1_{5 \times 5} \times (-5) = \text{diag}(1, 1, 1, 1, 1, -5) \quad (6.30)$$

into $S[U(5) \times U(1)] \subset SU(6) \subset E_8$, which effectively attributes the $U(1)_Y$ charge +1 to the fundamental representation of V and -5 to \mathcal{L}_Y . The decomposition of the 248-dimensional adjoint representation of E_8 then decomposes under (6.29) to

$$\begin{aligned} 248 \rightarrow & (\mathbf{24}; \mathbf{1}, \mathbf{1})_0 \oplus (\mathbf{1}; \mathbf{1}, \mathbf{1})_0 \oplus (\mathbf{1}; \mathbf{8}, \mathbf{1})_0 \oplus (\mathbf{1}; \mathbf{1}, \mathbf{3})_0 \\ & \oplus [(\mathbf{5}; \mathbf{3}, \mathbf{2})_1 \oplus (\mathbf{1}; \mathbf{3}, \mathbf{2})_5 \oplus \text{h.c.}] \\ & \oplus [(\mathbf{10}; \bar{\mathbf{3}}, \mathbf{1})_2 \oplus (\mathbf{5}; \bar{\mathbf{3}}, \mathbf{1})_{-4} \oplus \text{h.c.}] \\ & \oplus [(\mathbf{10}; \mathbf{1}, \mathbf{2})_{-3} \oplus (\mathbf{5}; \mathbf{1}, \mathbf{1})_6 \oplus \text{h.c.}], \end{aligned} \quad (6.31)$$

and the relevant representations of the Standard Model are identified in table 6.1. In particular, note that now the exotic matter representation $(\mathbf{3}, \mathbf{2})_5$ is associated to the bundle \mathcal{L}_Y^{-1} , i.e. an admissible power and thus easier to avoid.

- The second problem involves the $U(1)_Y$ -hypercharge gauge boson itself, which can potentially acquire a mass via the Chern-Simons couplings to the closed string background fields, i.e. the Stückelberg mechanism. Fortunately, within the F-theory framework this problem can be avoided by only considering internal Abelian gauge fluxes F_Y which correspond to the relative cohomology of $\mathcal{S} \subset \mathcal{Z}_4$, i.e. the Poincaré-dual 2-cycle $[F_Y] \in H^2(\mathcal{S}; \mathbb{Z})$ is non-trivial in \mathcal{S} but corresponds to a boundary—trivial cohomology—in the ambient 4-fold \mathcal{Z}_4 . This issue was already mentioned in section 3.8.3 and it can be shown that this topological requirement on \mathcal{S} , \mathcal{B}_3 and \mathcal{Z}_4 prohibits a double fibration structure as required for the heterotic/F-theory duality of section 3.5. It also raises certain problems with the gauge coupling unification that will be discussed later.

V	$(\mathbf{3}, \mathbf{2})_1$	Q_L	left-handed quark doublet
\mathcal{L}_Y^{-1}	$(\mathbf{3}, \mathbf{2})_5$	—	(exotic matter)
$\Lambda^2 V$	$(\mathbf{3}, \mathbf{1})_2$	$\bar{d}_L = (d_R)^c$	left-handed down-type anti-quark
$V \otimes \mathcal{L}_Y$	$(\bar{\mathbf{3}}, \mathbf{1})_{-4}$	$\bar{u}_L = (u_R)^c$	left-handed up-type anti-quark
$\Lambda^2 V \otimes \mathcal{L}_Y$	$(\mathbf{1}, \mathbf{2})_{-3}$	L_L	left-handed lepton doublet
$V \otimes \mathcal{L}_Y^{-1}$	$(\mathbf{1}, \mathbf{1})_6$	$\bar{e}_L = (e_R)^c$	left-handed anti-lepton

Table 6.1.: Standard model representations in $SU(5)$ GUTs resulting from the “twisted one-step breaking” of the GUT group. A single generation of left-handed matter is originally contained in the $\mathbf{10} \oplus \bar{\mathbf{5}}_m \oplus \mathbf{1}$ representation.

One can now go on and evaluate the D3-brane tadpole condition (3.50), which basically gives the required number of D3-branes that have to be added to the model. But since further refinements with subsequent changes to this computation are due, this computation is postponed.

6.3 Split Spectral Cover Refinements

While the $SU(5)$ spectral cover description manages to describe the G_4 flux, such that one can compute phenomenologically relevant quantities like the chiral indices, and the subsequent twisting to a $S[U(5) \times U(1)]$ spectral cover deals with the exotic GUT gauge bosons, it still remains to separate the conceptually different representation instances $\bar{\mathbf{5}}_m$ and $\mathbf{5}_H \oplus \bar{\mathbf{5}}_H$ — all of which are localized on the same matter curve. This is particularly unfavored due to the appearance of the dangerous $\mathbf{10} \cdot \bar{\mathbf{5}}_m \cdot \bar{\mathbf{5}}_m$ coupling, which leads to a rapid proton decay [68, 82, 182]. Even a separation of $\bar{\mathbf{5}}_m$ and $\mathbf{5}_H \oplus \bar{\mathbf{5}}_H$ on distinct matter curves is not entirely sufficient to deal with this aspect.

6.3.1 $S[U(4) \times U(1)_X]$ split spectral cover construction

It was realized that the entire spectral cover construction has to split into two components, which implies the replacement

$$\underbrace{SU(5)^\perp \cong SU(5)}_{\text{original spectral cover}} \rightsquigarrow \underbrace{S[U(4) \times U(1)_X]}_{\text{split spectral cover group}} \quad (6.32)$$

of the spectral cover group. Since $S[U(4) \times U(1)_X] \subset SU(5)$ is a maximal subgroup, the entire decomposition is then effectively of the form

$$E_8 \xrightarrow{V \oplus L} SU(4) \times SU(5) \times U(1)_X, \quad (6.33)$$

such that one in principle obtains the $SU(5)$ matter representations but with an additional massive Abelian $U(1)_X$ gauge factor. The Cartan generators of a subsequently defined rank- $(4 + 1)$ vector bundle are embedded diagonally via the matrix

$$T := 1_{4 \times 4} \times (-4) = \text{diag}(1, 1, 1, 1, -4), \quad (6.34)$$

that assigns the $U(1)_X$ charge $+1$ to the rank-4 sub-bundle and -1 to the line sub-bundle. The explicit decomposition of the E_8 's adjoint representation is then

$$\begin{aligned} 248 &\rightarrow (\mathbf{15}; \mathbf{1})_0 \\ &\oplus (\mathbf{1}; \mathbf{1})_0 \oplus (\mathbf{1}; \mathbf{10})_{-4} \oplus (\mathbf{1}; \bar{\mathbf{10}})_4 \oplus (\mathbf{1}; \mathbf{24})_0 \\ &\oplus (\mathbf{4}; \mathbf{1})_5 \oplus (\mathbf{4}; \bar{\mathbf{5}})_{-3} \oplus (\mathbf{4}; \mathbf{10})_1 \\ &\oplus (\bar{\mathbf{4}}; \mathbf{1})_{-5} \oplus (\bar{\mathbf{4}}; \bar{\mathbf{5}})_3 \oplus (\bar{\mathbf{4}}; \bar{\mathbf{10}})_{-1} \\ &\oplus (\mathbf{6}; \mathbf{5})_{-2} \oplus (\mathbf{6}; \bar{\mathbf{5}})_2, \end{aligned} \quad (6.35)$$

and the further breaking of the GUT $SU(5)$ group will be discussed later in section 6.3.4. Whereas the $\mathbf{10}_1$ representation of $SU(5) \times U(1)_X$ is required for the subsequent GUT model building, the $\mathbf{10}_{-4}$ leads to undesired additional states that one needs to remove.

From the geometrical point of view the factorization of the new group $SU(4) \times U(1)_X$ implies a corresponding splitting of the spectral surface in a quartic and linear piece

$$[\mathcal{C}^{(5)}] = [\mathcal{C}^{(4)}] + [\mathcal{C}^{(1)}], \quad \text{where} \quad \begin{aligned} \mathcal{C}^{(4)} &\xrightarrow{\pi_4} \mathcal{S}, \\ \mathcal{C}^{(1)} &\xrightarrow{\pi_1} \mathcal{S}. \end{aligned} \quad (6.36)$$

This corresponds to a factorization of the divisor, i.e. the original $SU(5)$ spectral cover surface (6.8) factorizes [159] like

$$\begin{aligned} &\overbrace{(c_0 s^4 + c_1 s^3 + c_2 s^2 + c_3 s + c_4)}^{\mathcal{C}^{(4)}} \overbrace{(d_0 s + d_1)}^{\mathcal{C}^{(1)}} \\ &= c_0 d_0 s^5 + (c_1 d_0 + c_0 d_1) s^4 + (c_2 d_0 + c_1 d_1) s^3 \\ &\quad + (c_3 d_0 + c_2 d_1) s^2 + (c_4 d_0 + c_3 d_1) s + c_4 d_1 \end{aligned} \quad (6.37)$$

where c_i and d_i are the coefficient functions of $\mathcal{C}^{(4)}$ and $\mathcal{C}^{(1)}$, respectively. In order to avoid the appearance of a second $\mathbf{10}$ representation curve—which can be associated to the aforementioned $\mathbf{10}_{-4}$ representation under $SU(5) \times U(1)_X$ —one sets d_1 to a non-zero constant, i.e. without loss of generality set $d_1 = 1$. Then

$$\underbrace{c_0 d_0}_{P'_{(6,1)}} s^5 + \underbrace{(c_1 d_0 + c_0)}_{\text{must vanish}} s^4 + \underbrace{(c_2 d_0 + c_1)}_{P'_{(4,1)}} s^3 + \underbrace{(c_3 d_0 + c_2)}_{P'_{(3,1)}} s^2 + \underbrace{(c_4 d_0 + c_3)}_{P'_{(2,1)}} s + \underbrace{c_4}_{P'_{(1,1)}} \quad (6.38)$$

leads to an identification with the coefficients from (6.8). Due to the absence of the s^4 power one therefore requires

$$c_1 d_0 = -c_0. \quad (6.39)$$

The two Poincaré-dual cohomology classes of the individual spectral surface components are

$$\begin{aligned} [\mathcal{C}^{(4)}] &= 4\sigma + \pi_4^* \tilde{\eta} & \text{where} & & \tilde{\eta} &= \eta - c_1(\mathcal{S}) \\ [\mathcal{C}^{(1)}] &= \sigma + \pi_1^* c_1(\mathcal{S}) & & & \eta &= 6c_1(\mathcal{S}) - c_1(N_{\mathcal{S} \subset B}), \end{aligned} \quad (6.40)$$

whose sum obviously gives the original results from (6.9) and (6.10).

The spectral cover line bundle \mathcal{N} over the spectral surface also has to split accordingly. Note that the $S[U(4) \times U(1)_X]$ gauge group considered here is structurally identical to the twisted gauge group $S[U(5) \times U(1)]$ from section 6.2.4. Whereas the $U(1)$ was localized on the GUT brane \mathcal{S} back there, it has now been attributed its own spectral cover piece $\mathcal{C}^{(1)}$. As before, one considers a split bundle

$$W = V \oplus L \quad \text{such that} \quad c_1(W) = c_1(V) + c_1(L) = 0. \quad (6.41)$$

Here V is a rank-4 vector bundle and L a line bundle, both of which are defined by the respective special push-forwards of the spectral cover line bundles, i.e.

$$\begin{aligned} (\tilde{\pi}_4)_* \mathcal{N}^{(4)} &= V|_{\mathcal{S}}, \\ (\tilde{\pi}_1)_* \mathcal{N}^{(1)} &= L|_{\mathcal{S}}. \end{aligned} \quad (6.42)$$

Due to the condition (6.41) on the first Chern class of the total vector bundle W it is helpful to define

$$\zeta := c_1(V) = -c_1(L). \quad (6.43)$$

As before, the spectral line bundle $\mathcal{N}^{(4)}$ is entirely specified by its first Chern class $c_1(\mathcal{N}^{(4)}) \in H^2(\mathcal{C}^{(4)}; \mathbb{Z})$, which can be explicitly given as

$$\begin{aligned} c_1(\mathcal{N}^{(4)}) &= \frac{r^{(4)}}{2} + \gamma_u^{(4)} + \frac{1}{4}(\pi_4)^* \zeta \\ &= (1 + 4\lambda)\sigma + \left(\frac{1}{2} - \lambda\right) (\pi_4)^* \tilde{\eta} \\ &\quad + \left(-\frac{1}{2} + 4\lambda\right) (\pi_4)^* c_1(\mathcal{S}) + \frac{1}{4}(\pi_4)^* \zeta. \end{aligned} \quad (6.44)$$

One might want to compare this to (3.47) for $n = 4$. The integrality requirement of this cohomology class then yields the conditions

$$\begin{aligned} 4\lambda &\in \mathbb{Z}, \\ \left(\frac{1}{2} - \lambda\right) \tilde{\eta} - \frac{1}{2} c_1(\mathcal{S}) + \frac{1}{4} \zeta &\in H^2(\mathcal{S}; \mathbb{Z}). \end{aligned} \quad (6.45)$$

Likewise, the first Chern class $c_1(\mathcal{N}^{(1)}) \in H^2(\mathcal{C}^{(1)}; \mathbb{Z})$ of the Abelian $U(1)_X$ gauge part can be evaluated to

$$c_1(\mathcal{N}^{(1)}) = (\tilde{\pi}_1)^*\zeta. \quad (6.46)$$

An interesting observation at this point can be derived from the second quantization condition in (6.45): it is impossible to have $\lambda = 0$ for an odd value of $c_1(\mathcal{S})$, i.e. if the GUT brane divisor does not support a spin structure. This is directly related to the Freed-Witten quantization condition [113] discussed in section 2.8.2. On non-spin GUT 7-branes it is therefore impossible to completely turn off the universal gauge flux γ if one wants to obtain a consistent model.

6.3.2 Factorization of matter curves and intersections

Using the factorization description (6.37) one can now again “uplift” the matter curves to the spectral cover surface components^{III} analogous to section 6.2.1. The **10** matter curve $\mathcal{C}_{SO(10)} \subset \mathcal{S}$ now corresponds to the locus

$$\hat{\mathcal{C}}_{10} := \{c_4 = 0\} \subset \mathcal{W}, \quad (6.47)$$

which is to be compared to (6.12) and has the cohomology class

$$[\hat{\mathcal{C}}_{10}]|_{\sigma} = \eta - 5c_1(\mathcal{S}) = \tilde{\eta} - 4c_1(\mathcal{S}) \in H^2(\mathcal{S}; \mathbb{Z}). \quad (6.48)$$

The $SU(6)$ enhancement curve $\mathcal{C}_{SU(6)} \subset \mathcal{S}$, where matter in the $\bar{\mathbf{5}}$ representation is localized, now factorizes thanks to the split spectral cover approach to

$$\underbrace{(c_3(c_2 + c_3d_0) - c_1c_4)}_{\hat{\mathcal{C}}_{\bar{\mathbf{5}}_H}} \underbrace{(c_2 + d_0(c_3 + c_4d_0))}_{\hat{\mathcal{C}}_{\bar{\mathbf{5}}_m}} = 0, \quad (6.49)$$

such that the $\mathbf{5}_H \oplus \bar{\mathbf{5}}_H$ Higgs representations live on $\hat{\mathcal{C}}_{\bar{\mathbf{5}}_H} \subset \mathcal{W}$ and the $\bar{\mathbf{5}}_m$ matter is accommodated on the curve $\hat{\mathcal{C}}_{\bar{\mathbf{5}}_m} \subset \mathcal{W}$. With some additional effort the cohomology classes of those curves can be computed to

$$\begin{aligned} [\hat{\mathcal{C}}_{\bar{\mathbf{5}}_H}] &= 2\sigma \cdot \pi^*(2\tilde{\eta} - 5c_1(\mathcal{S})) + \pi^*(\tilde{\eta} - c_1(\mathcal{S})) \cdot \pi^*(\tilde{\eta} - 2c_1(\mathcal{S})), \\ [\hat{\mathcal{C}}_{\bar{\mathbf{5}}_m}] &= \sigma \cdot \pi^*(\tilde{\eta} - 2c_1(\mathcal{S})) + \pi^*c_1(\mathcal{S}) + \pi^*(\tilde{\eta} - 2c_1(\mathcal{S})). \end{aligned} \quad (6.50)$$

A detailed analysis shows that $\hat{\mathcal{C}}_{\bar{\mathbf{5}}_H}$ derives from $\tau\mathcal{C}^{(4)} \cap \mathcal{C}^{(4)}$ and $\hat{\mathcal{C}}_{\bar{\mathbf{5}}_m}$ originates in the piece $\tau\mathcal{C}^{(1)} \cap \mathcal{C}^{(4)}$ similarly to (6.15). Furthermore, let $\hat{\mathcal{C}}_{\nu}$ be the intersection component of $\mathcal{C}^{(4)}$ and $\mathcal{C}^{(1)}$ away from \mathcal{S} , whose cohomology is given by

$$[\hat{\mathcal{C}}_{\nu}] = 2(\sigma + \pi^*c_1(\mathcal{S})) \cdot \pi^*c_1(\mathcal{S}). \quad (6.51)$$

^{III}In order to avoid confusion with the previous sections, all representation loci on the split spectral cover like $\hat{\mathcal{C}}_{10}$ are denoted with a hat.

V	$\mathbf{10}_1$	$(Q_L, (u_R)^c, (e_R)^c)$
L	$\mathbf{10}_{-4}$	—
$V \otimes L$	$\bar{\mathbf{5}}_{-3}$	$((d_R)^c, L_L)$
$\Lambda^2 V$	$\bar{\mathbf{5}}_{-2}$	$(H_u, H_d) \oplus (\bar{H}_u, \bar{H}_d)$
$V \otimes L^{-1}$	$\mathbf{1}_5$	$(\nu_R)^c$

Table 6.2.: Representations and bundles from the decomposition (6.35) in the $SU(5) \times U(1)_X$ representation.

This object cohomologically appears in the intersection

$$[\tau\mathcal{C}^{(1)} \cap \mathcal{C}^{(4)}] = [\hat{\mathcal{C}}_{\bar{\mathbf{5}}_m}] + [\hat{\mathcal{C}}_\nu] \in H^4(\mathcal{W}; \mathbb{Z}). \quad (6.52)$$

One can now study the intersections between those curves in order to identify the gauge enhancements—a task that was omitted at the end of section 6.2.1. The first intersection point

$$\hat{\mathcal{P}}_{SO(12)} := \{c_4 = 0\} \cap \{c_2 + c_3 d_0 = 0\} \subset \hat{\mathcal{C}}_{\bar{\mathbf{5}}_H} \cap \hat{\mathcal{C}}_{\bar{\mathbf{5}}_m} \quad (6.53)$$

leads to an $SO(12)$ gauge enhancement, whose adjoint representation's decomposition allows to associate it with the $\mathbf{10} \cdot \bar{\mathbf{5}}_H \cdot \bar{\mathbf{5}}_m$ Yukawa coupling. A second intersection at

$$\begin{aligned} \hat{\mathcal{P}}_{SU(7)} &:= \{c_1 + c_3(d_0)^2 = 0\} \cap \{c_2 + c_3 d_0 + c_4(d_0)^2 = 0\} \\ &\text{where } c_4 \neq 0 \text{ and } c_2 + c_3 d_0 \neq 0 \end{aligned} \quad (6.54)$$

gives the uplift of the $SU(7)$ enhancement identified in (5.63) and is therefore interpreted as the locus of the $\mathbf{5}_H \cdot \bar{\mathbf{5}}_m \cdot \mathbf{1}$ coupling. Furthermore, there is the point of E_6 enhancement

$$\hat{\mathcal{P}}_{E_6} := \{c_4 = 0\} \cap \{c_3 + c_4 d_0 = 0\} \quad (6.55)$$

that gives the top-quark Yukawa coupling $\mathbf{10} \cdot \mathbf{10} \cdot \mathbf{5}_H$. At this point one might want to reflect upon their respective phenomenological relevance as summarized in section 3.8.2.

6.3.3 Chiral matter

Equipped with an explicit description of the gauge breaking vector bundle $W = V \oplus L$ from (6.41) in terms of the split spectral cover description, one can directly associate the representations of the decomposition (6.35) with specific powers of V and L , see table 6.2. This is an intermediate identification step of the GUT representations

analogous to table 6.1. The breaking of the GUT group will be discussed afterwards in the next subsection.

Like in section 6.2.3, one can now go on and compute the chiral indices. Let again

$$i : \{\sigma = 0\} \hookrightarrow \mathcal{W} \quad \text{and} \quad \begin{aligned} j^{(4)} : \mathcal{C}^{(4)} &\hookrightarrow \mathcal{W} \\ j^{(1)} : \mathcal{C}^{(1)} &\hookrightarrow \mathcal{W} \end{aligned} \quad (6.56)$$

be the embedding mappings analogous to (6.18). For the remaining and relevant $\mathbf{10}_1$ matter curve $\hat{\mathcal{C}}_{10}$ the relevant extension groups can be expressed as

$$\begin{aligned} \text{Ext}^i(i_*\mathcal{O}_\sigma; (j^{(4)})_*\mathcal{N}^{(4)}) &\cong H^{i-1}(\mathcal{C}^{(4)} \cap \sigma; \mathcal{N}^{(4)} \otimes K_{\mathcal{S}}|_{\mathcal{C}^{(4)} \cap \sigma}) \\ &\cong H^{i-1}(\hat{\mathcal{C}}_{10}; \mathcal{N}^{(4)} \otimes K_{\mathcal{S}}|_{\hat{\mathcal{C}}_{10}}), \end{aligned} \quad (6.57)$$

such that the chiral index for the $\mathbf{10}$ representation via (A.28) is

$$\begin{aligned} \chi_{\mathbf{10}} &= \sum_i (-1)^i \text{Ext}^i(i_*\mathcal{O}_\sigma; (j^{(4)})_*\mathcal{N}^{(4)}) = \chi(\hat{\mathcal{C}}_{10}; \mathcal{N}^{(4)} \otimes K_{\mathcal{S}}|_{\hat{\mathcal{C}}_{10}}) \\ &= \int_{\hat{\mathcal{C}}_{10}} \left(\gamma_u^{(4)} + \frac{1}{4}(\pi_4)^*\zeta \right) = \int_{\mathcal{S}} \left(-\lambda\tilde{\eta} + \frac{1}{4}\zeta \right) (\tilde{\eta} - 4c_1(\mathcal{S})), \end{aligned} \quad (6.58)$$

which is to be compared to (6.20). The computation of the $\bar{\mathbf{5}}_m$ and $\bar{\mathbf{5}}_H$ chiral indices is a little bit more involved. Let $\mathcal{C}^{(n)}$ and $\mathcal{C}^{(m)}$ be two spectral covers and $V^{(n)} \otimes V^{(m)}$ be the bundles of an associated bi-fundamental matter representation. This is localized on the curve

$$\mathcal{C}_{V^{(n)} \otimes V^{(m)}} = \tau\mathcal{C}^{(n)} \cap \mathcal{C}^{(m)} - \underbrace{\tau\mathcal{C}^{(n)} \cap \mathcal{C}^R}_{\text{ramification correction}}, \quad (6.59)$$

where \mathcal{C}^R is introduced in order to account for ramification points. This ramification correction is necessary if the matter curve is singular over

$$R = \int_{\mathcal{W}} [\tau\mathcal{C}^{(n)}] \cdot ([\mathcal{C}^{(m)}] - [\mathcal{C}^R]) \cdot [\mathcal{C}^R] \quad (6.60)$$

points, similar to (6.25). It is then proposed that the massless matter states are counted by the cohomology groups

$$H^{i-1}(\mathcal{C}_{V^{(n)} \otimes V^{(m)}}; \mathcal{N}^{(n)} \otimes \mathcal{N}^{(m)} \otimes K_{\mathcal{S}} \otimes K_{\mathcal{W}}^{-\frac{1}{2}} \otimes \mathcal{O}(-\frac{R}{2})|_{\mathcal{C}_{V^{(n)} \otimes V^{(m)}}}). \quad (6.61)$$

For the case at hand—the $\bar{\mathbf{5}}_m$ matter curve $\hat{\mathcal{C}}_{\bar{\mathbf{5}}_m}$ specified in (6.50)—this reduces to

$$\begin{aligned} \text{Ext}^i(j_*^{(1)}(\mathcal{N}^{(1)})^\vee; j_*^{(4)}\mathcal{N}^{(4)}) \\ = H^{i-1}(\hat{\mathcal{C}}_{\bar{\mathbf{5}}_m}; \mathcal{N}^{(1)} \otimes \mathcal{N}^{(4)} \otimes K_{\mathcal{S}} \otimes K_{\mathcal{W}}^{-\frac{1}{2}} \otimes \mathcal{O}(-\frac{R}{2})|_{\hat{\mathcal{C}}_{\bar{\mathbf{5}}_m}}). \end{aligned} \quad (6.62)$$

The usage of the dual bundle $(\mathcal{N}^{(1)})^\vee$ implies a sign flip in the first Chern class, i.e. ζ is replaced by $-\zeta$. The chiral index then turns out to be

$$\begin{aligned}\chi_{\bar{\mathbf{5}}_m} &= \sum_i \text{Ext}^i(j_*^{(1)}(\mathcal{N}^{(1)})^\vee; j_*^{(4)}\mathcal{N}^{(4)}) = \chi(\hat{\mathcal{C}}_{\bar{\mathbf{5}}_m}; \mathcal{N}^{(1)} \otimes \mathcal{N}^{(4)} \otimes K_{\mathcal{S}}|_{\hat{\mathcal{C}}_{\bar{\mathbf{5}}_m}}) \\ &= \int_{\hat{\mathcal{C}}_{\bar{\mathbf{5}}_m}} \left(\gamma_u + \frac{1}{4}(\pi_4)^*\zeta - (\pi_1)^*\zeta \right) \\ &= \int_{\mathcal{S}} \left[\lambda \left(-\tilde{\eta}^2 + 6\tilde{\eta}c_1(\mathcal{S}) - 8c_1(\mathcal{S})^2 \right) + \frac{1}{4}\zeta \left(-3\tilde{\eta} + 6c_1(\mathcal{S}) \right) \right].\end{aligned}\tag{6.63}$$

Handling the number of $\bar{\mathbf{5}}_H$'s requires a similar treatment, but the resulting index is of a similar structure

$$\begin{aligned}\chi_{\bar{\mathbf{5}}_H} &= \int_{\hat{\mathcal{C}}_{\bar{\mathbf{5}}_H}} \left(\gamma_u + \frac{1}{4}(\pi_4)^*\zeta \right) \\ &= \int_{\mathcal{S}} \left[\lambda \left(-2\tilde{\eta}c_1(\mathcal{S}) + 8c_1(\mathcal{S})^2 \right) + \frac{1}{4}\zeta \left(4\tilde{\eta} - 10c_1(\mathcal{S}) \right) \right].\end{aligned}\tag{6.64}$$

As before, a consistent model requires the number of $\bar{\mathbf{5}}$ and $\mathbf{10}$ representations to be equal, and one can show that

$$\begin{aligned}\chi_{\bar{\mathbf{5}}_m} + \chi_{\bar{\mathbf{5}}_H} &= \int_{\mathcal{S}} \left[\lambda \left(-\tilde{\eta}^2 + 4\tilde{\eta}c_1(\mathcal{S}) \right) + \frac{1}{4}\zeta \left(\tilde{\eta} - 4c_1(\mathcal{S}) \right) \right] \\ &= \int_{\mathcal{S}} \left(-\lambda\tilde{\eta} + \frac{1}{4}\zeta \right) \left(\tilde{\eta} - 4c_1(\mathcal{S}) \right) = \chi_{\mathbf{10}}\end{aligned}\tag{6.65}$$

indeed agrees. The overall approach of a $S[U(4) \times U(1)_X]$ split spectral cover is therefore suitable for the construction of semi-realistic models.

A final comment related to those computations is in order for the $\mathbf{15}$ representations in table 6.2, which arise from the decomposition

$$\begin{aligned}SU(5) &\longrightarrow S[U(4) \times U(1)_X] \\ \mathbf{24} &\rightarrow \mathbf{15}_0 \oplus \mathbf{1}_0 \oplus \mathbf{4}_5 \oplus \bar{\mathbf{4}}_{-5}.\end{aligned}\tag{6.66}$$

The $U(1)_X$ charge allows the associated states to participate in the $\bar{\mathbf{5}}_m \cdot \mathbf{5}_H \cdot \mathbf{1}$ coupling that arises from the $SU(7)$ enhancement point (6.54), which makes them viable candidates for right-handed neutrinos $(\nu_R)^c$. The intersection component $\hat{\mathcal{C}}_\nu$ from (6.51) already highlights that they are localized off the GUT 7-brane \mathcal{S} . Using the proposed counting (6.61) the relevant cohomology groups are

$$\begin{aligned}\text{Ext}^i(j_*^{(1)}\mathcal{N}^{(1)}; j_*^{(4)}\mathcal{N}^{(4)}) \\ \cong H^{i-1}(\hat{\mathcal{C}}_\nu; (\mathcal{N}^{(1)})^\vee \otimes \mathcal{N}^{(4)} \otimes K_{\mathcal{S}} \otimes K_{\mathcal{W}}^{-\frac{1}{2}} \otimes \mathcal{O}(-\frac{R}{2})|_{\hat{\mathcal{C}}_\nu}),\end{aligned}\tag{6.67}$$

and the corresponding chiral index is

$$\begin{aligned}\chi_{(\nu_R)^c} &= \int_{\hat{\mathcal{C}}_\nu} \left(\gamma^{(4)} + \frac{1}{4}(\pi_4)^*\zeta + (\pi_1)^*\zeta \right) \\ &= \int_{\hat{\mathcal{C}}_\nu} \left(-\lambda\tilde{\eta} + \frac{5}{4}\zeta + 4\lambda c_1(\mathcal{S}) \right) 2c_1(\mathcal{S}).\end{aligned}\tag{6.68}$$

However, considering that the spectral cover approach used here is technically only valid locally in the vicinity of the GUT 7-brane \mathcal{S} , it remains unclear how to properly interpret those states from a fully global perspective.

6.3.4 GUT group breaking via hypercharge flux

It remains now to break the $SU(5)$ GUT symmetry down to the Standard Model gauge group $SU(3) \times SU(2) \times U(1)_Y$. In principle this task is analogous to the breaking in section 6.2.4, i.e. an additional bundle \mathcal{L}_Y is used as a twist in order to eliminate the exotic $(\mathbf{3}, \mathbf{2})_{\mathbf{5}} \oplus (\mathbf{3}, \mathbf{2})_{-\mathbf{5}}$ states from the spectrum and to break the GUT group. Due to the split bundle $W = V \oplus L$ used so far, the twisting of W has to affect V and L differently. More precisely, one redefines the bundles

$$\begin{aligned}V &= \mathcal{V} \otimes \mathcal{L}_Y^{-\frac{1}{5}} & \text{and} & & L_Y &= \mathcal{L}_Y^{\frac{1}{5}}, \\ L &= \mathcal{L} \otimes \mathcal{L}_Y^{\frac{4}{5}}\end{aligned}\tag{6.69}$$

which requires that the bundles V , L and L_Y are well-defined. This introduces a further Abelian gauge factor—the $U(1)_Y$ hypercharge—to the gauge group, such that one actually considers the gauge group

$$SU(3) \times SU(2) \times U(1)_X \times U(1)_Y.\tag{6.70}$$

As the $U(1)_X$ symmetry was originally used to single out the phenomenologically desirable $SU(5)$ GUT interactions, it does not prohibit any relevant Standard Model Yukawas. The relevant Standard Model-like representations are listed in table 6.3 along with the corresponding bundle choices, which agree with the expected representations of the Georgi-Glashow $SU(5)$ GUT in table 3.5.

The entire internal gauge flux on the branes is therefore described by the bundles in (6.69), more precisely:

- The GUT symmetry breaking $U(1)_Y$ hypercharge gauge flux on the GUT 7-brane \mathcal{S} is described by the line bundle \mathcal{L}_Y , which is specified by $c_1(\mathcal{L}_Y) \in H^2(\mathcal{S}; \mathbb{Z})$.
- The gauge flux on the intersecting I_1 -type matter 7-branes is described by an $S[U(4) \times U(1)_X]$ -bundle $\mathcal{V} \oplus \mathcal{L}$, which is constrained by the condition on the first Chern classes $c_1(\mathcal{V}) = -c_1(\mathcal{L}) \in H^2(\mathcal{S}; \mathbb{Z})$.

10	\mathcal{V}	$(\mathbf{3}, \mathbf{2})_{1_X, 1_Y}$	Q_L	left-handed quark doublet
	$\mathcal{V} \otimes \mathcal{L}_Y^{-1}$	$(\bar{\mathbf{3}}, \mathbf{1})_{1_X, -4_Y}$	$\bar{u}_L = (u_R)^c$	left-handed up-type anti-quark
	$\mathcal{V} \otimes \mathcal{L}_Y$	$(\mathbf{1}, \mathbf{1})_{1_X, 6_Y}$	$\bar{e}_L = (e_R)^c$	left-handed anti-lepton
$\bar{\mathbf{5}}_m$	$\mathcal{V} \otimes \mathcal{L} \otimes \mathcal{L}_Y$	$(\bar{\mathbf{3}}, \mathbf{1})_{-3_X, 2_Y}$	$\bar{d}_L = (d_R)^c$	left-handed down-type anti-quark
	$\mathcal{V} \otimes \mathcal{L}$	$(\mathbf{1}, \mathbf{2})_{-3_X, -3_Y}$	L_L	left-handed lepton doublet
$\mathbf{5}_H$	$\Lambda^2 \mathcal{V}$	$(\mathbf{3}, \mathbf{1})_{-2_X, -2_Y}$	T_u	up-type color triplet (GUT r.)
	$\Lambda^2 \mathcal{V} \otimes \mathcal{L}_Y^{-1}$	$(\mathbf{1}, \mathbf{2})_{-2_X, 3_Y}$	H_u	up-type Higgs doublet
1	$\mathcal{V} \otimes \mathcal{L}^{-1} \otimes \mathcal{L}_Y^{-1}$	$(\mathbf{1}, \mathbf{1})_{5_X, 0_Y}$	$(\nu_R)^c$	right-handed neutrino

Table 6.3.: Representations in $SU(3) \times SU(2) \times U(1)_X \times U(1)_Y$ following the GUT symmetry breaking induced from the bundles of (6.69).

6.3.5 Computing the Euler characteristic and 3-brane tadpole

As before, a central issue here is the computation of the proper Euler characteristic of the singular Calabi-Yau 4-fold \mathcal{Z} . However, one can derive an improved expression for $\chi(\mathcal{Z})$ compared to the formulas presented in section 5.2.3, which was originally conceived in the context of models with a heterotic dual.

In the heterotic $E_8 \times E_8$ theory one embeds the structure group of the two vector bundles V_1 and V_2 into the respective E_8 factor to reduce the gauge group, as discussed in section 3.5. By identifying 3-branes with M5-branes under the duality, the required number of M5-branes for anomaly cancellation on the heterotic side can be computed as

$$N_{M5} = \int_{\mathcal{B}_2} (c_2(\mathcal{Y}) - c_2(V_1) - c_2(V_2)) \quad (6.71)$$

if the embedding (3.48) is used. The second Chern classes of the vector bundles can be computed to

$$\begin{aligned} \int_{\mathcal{B}_2} c_2(V_1) &= \int_{\mathcal{B}_2} \eta_1 \sigma - \frac{1}{24} \chi_{SU(n)} - \frac{1}{2} \int_{\mathcal{B}_2} (\pi_n)_*(\gamma^2) \\ \int_{\mathcal{B}_2} c_2(V_2) &= \int_{\mathcal{B}_2} \eta_2 \sigma - \frac{1}{24} \chi_{E_8} \end{aligned} \quad (6.72)$$

for the expressions χ_G from table 6.4 where $\mathcal{S} = \mathcal{B}_2$. For the specific double-fibration geometry of the heterotic/F-theory duality, one can also compute the second Chern class of the heterotic compactification 3-fold \mathcal{Y} to

$$c_2(\mathcal{Y}) = 12\sigma c_1(\mathcal{B}_2) + 11c_1(\mathcal{B}_2)^2 + c_2(\mathcal{B}_2). \quad (6.73)$$

$H = E_8/G$	G	χ_G
$E_{9-n}, n \leq 5$	$SU(n)$	$\int_{\mathcal{S}} c_1(\mathcal{S})^2(n^3 - n) + 3n\eta(\eta - nc_1(\mathcal{S}))$
$SU(3)$	E_6	$72 \int_{\mathcal{S}} (\eta^2 - 7\eta c_1(\mathcal{S}) + 13c_1^2(\mathcal{S}))$
$SU(2)$	E_7	$18 \int_{\mathcal{S}} (8\eta^2 - 64\eta c_1(\mathcal{S}) + 133c_1^2(\mathcal{S}))$
-	E_8	$120 \int_{\mathcal{S}} (3\eta^2 - 27\eta c_1(\mathcal{S}) + 62c_1^2(\mathcal{S}))$

Table 6.4.: Redefined Euler characteristic for E_n -type gauge groups. Here η is given by $\eta = 6c_1(\mathcal{S}) + c_1(N_{\mathcal{S}})$ and one defines $E_5 := SO(10)$ as well as $E_4 := SU(5)$, which follows from a systematical shortening of the Dynkin diagram. Here G is the embedded structure group and $H = E_8/G$ the remaining gauge group.

Due to the embedding (3.48) the $\eta_i\sigma$ terms then cancel in the sum, and after identifying $N_{D3} = N_{M5}$ one finds

$$\begin{aligned}
N_{D3} &= \int_{\mathcal{B}_2} \left(11c_1(\mathcal{B}_2)^2 + c_2(\mathcal{B}_2) \right) && \text{(base geometry)} \\
&+ \frac{1}{24} \left(\chi_{SU(n)} + \chi_{E_8} \right) && \text{(singularity enhancement)} \\
&+ \frac{1}{2} \int_{\mathcal{B}_2} (\pi_n)_*(\gamma^2) && \text{(flux contribution)}
\end{aligned} \tag{6.74}$$

for the number of 3-branes. By (3.49) the third term can be directly identified with the G_4 flux contribution to the tadpole, such that via (3.50) one obtains

$$\begin{aligned}
\chi(\mathcal{Z}) &= 24 \left(N_{D3} + \frac{1}{2} \int_{\mathcal{Z}} G_4 \wedge G_4 \right) \\
&= 24 \int_{\mathcal{B}_2} \left(11c_1(\mathcal{B}_2)^2 + c_2(\mathcal{B}_2) \right) + \chi_{SU(n)} + \chi_{E_8}
\end{aligned} \tag{6.75}$$

for situations with a heterotic dual. The claim here is now that this computation remains valid even for models without a strict heterotic dual, i.e. where a local ALE fibration over \mathcal{S} following section 6.1 is applied instead.

Note that if both E_8 factors are entirely broken, no non-Abelian enhancement remains, such that for this case the 4-fold \mathcal{Z} is smooth, i.e. the Euler characteristic is uniquely defined. This allows to identify

$$\chi^*(\mathcal{Z}) = 24 \int_{\mathcal{B}_2} \left(11c_1(\mathcal{B}_2)^2 + c_2(\mathcal{B}_2) \right) + \chi_{E_8} + \chi_{E_8} \tag{6.76}$$

as the Euler characteristic of the I_1 case. However, for this case there is also the formula (5.16) in terms of the base $\mathcal{B} = \mathcal{B}_3$ of the elliptic fibration, i.e.

$$\chi^*(\mathcal{Z}) = 12 \int_{\mathcal{B}} c_1(\mathcal{B})c_2(\mathcal{B}) + 360 \int_{\mathcal{B}} c_1(\mathcal{B})^3, \quad (6.77)$$

which does not make any reference to the ALE fibration of the base space \mathcal{B} . One can now go on and replace one of the entirely broken E_8 factors, which leads to

$$\chi(\mathcal{Z}) = \chi^*(\mathcal{Z}) + \chi_{SU(n)} - \chi_{E_8}. \quad (6.78)$$

Using the above formula for $\chi^*(\mathcal{Z})$, this allows to determine the Euler characteristic for the singular case as well.

Initially it was hoped that (6.78) has general validity [88], but several counterexamples were found [162]. It turns out that there are certain subtleties when using spectral cover descriptions [182], in particular in the absence of a strict heterotic dual, which undermine the global validity. In fact, one can use the derived formula in reverse and check the computation against an explicit resolution of the non-Abelian singularity, where a match indicates the global validity of the spectral cover construction [119, 170].

After identifying the GUT brane divisor \mathcal{S} with the ALE fibration base \mathcal{B}_2 , one can now continue with the checking of further consistency conditions for the case at hand, specifically the 3-brane tadpole condition (3.50). Taking the split spectral cover into account, the number of required D3-branes can be computed to be

$$\begin{aligned} N_{D3} = & \frac{\chi^*(\mathcal{Z})}{24} - \frac{615}{2} \int_{\mathcal{S}} c_1(\mathcal{S})^2 - 15 \int_{\mathcal{S}} (\eta^2 - 9\eta c_1(\mathcal{S})) \\ & + \left(\frac{1}{2} - 2\lambda^2 \right) \int_{\mathcal{S}} \tilde{\eta} (\tilde{\eta} - 4c_1(\mathcal{S})) \\ & + \int_{\mathcal{S}} \left(\frac{5}{8} \zeta^2 + c_1(\mathcal{L}_Y)^2 - \zeta c_1(\mathcal{L}_Y) \right). \end{aligned} \quad (6.79)$$

The result has been successfully cross-checked with an entirely different method of computation [86, 177], which however is technically extremely involved.

Chapter 7

A Global F-theory $SU(5)$ GUT with Three Chiral Matter Generations

THE analysis and phenomenological tuning of the previous chapter paves the way for the explicit realization of a fully global F-theory $SU(5)$ GUT model with three chiral matter generations [88]. It is based on the non-generic del Pezzo transition of the quartic 3-fold $\mathbb{P}^4[4]$ and the generic topological structure of this geometry.

Since the described elliptically-fibered Calabi-Yau 4-fold arises as a complete intersection of two hypersurfaces [187–191], one has to establish the transversality of the intersection hypersurfaces. One also has to provide a full resolution of the non-Abelian singularities, more specifically of the $SU(5)$ enhancement over the GUT 7-brane, which yields codimension-2 singularities in the 4-fold. This can then be used to check the validity of the spectral cover description over the GUT brane. Fortunately, all those tasks can be carried out entirely within the realm of toric geometry.

One can then determine the necessary fluxes to produce three generations of chiral matter and realize the GUT breaking. The chapter culminates with a discussion of the phenomenological properties of the constructed model.

7.1 Construction of the Calabi-Yau 4-fold

7.1.1 Transversality of intersecting hypersurfaces

The geometry considered here is the non-generic del Pezzo transition of the quartic 3-fold hypersurface $\mathbb{P}^4[4]$ from section 5.4, which was introduced under the objective to use a Fano 3-fold as the base for F-theory models. The base geometry from table 5.7 can be successfully equipped with a $\mathbb{P}_{231}^2[6]$ -fibration, as has been carried out in table 5.8 by adding three additional coordinates x, y, z and a further hypersurface constraint. However, it was neglected to check the critical transversality of the intersection. If

nef part	vertices of the polyhedron / fan	coords	GLSM charges			divisor class
			Q^1	Q^2	Q^3	
∇_1	$\nu_1 = (1, 0, 0, 0, 0, 0)$	x	2	0	0	$2(\sigma + P + X)$
	$\nu_2 = (0, 1, 0, 0, 0, 0)$	y	3	0	0	$3(\sigma + P + X)$
	$\nu_3 = (-2, -3, 0, 0, 0, 0)$	z	1	-1	-1	σ
	$\nu_4 = (-2, -3, -1, -1, -1, -1)$	u_1	0	1	0	P
	$\nu_9 = (-2, -3, 0, 0, -1, -1)$	w	0	0	1	X
∇_2	$\nu_5 = (0, 0, 1, 0, 0, 0)$	u_2	0	1	0	P
	$\nu_6 = (0, 0, 0, 1, 0, 0)$	u_3	0	1	0	P
	$\nu_7 = (0, 0, 0, 0, 1, 0)$	u_4	0	1	1	$P + X$
	$\nu_8 = (0, 0, 0, 0, 0, 1)$	u_5	0	1	1	$P + X$
conditions:			6	0	0	
			0	4	2	

Stanley-Reisner ideal: $\langle xyz, u_1u_2u_3, u_4u_5w \rangle$

Table 7.1.: Nef-partitioned toric data for the elliptically-fibered Calabi-Yau 4-fold \mathcal{Z} arising from the non-generic del Pezzo transition of $\mathbb{P}^4[4]$.

two hypersurfaces are not intersecting transversally everywhere, different areas of the intersection are of different dimension, which introduces singularities of a very bad type to the space—in particular, one can no longer speak of an n -dimensional variety.

The transversality of the intersection of two hypersurfaces in a toric setting can be guaranteed if a nef partition—“numerically effective” partition—of the toric data can be found [187, 190]. It means that the set of lattice vectors ν_i spanning the toric fan Σ can be split up into two sets ∇_1 and ∇_2 , such that the Minkowski sum of those sets, which consists of all possible sums of one element from ∇_1 plus one element from ∇_2 , describes a reflexive polyhedron. This essentially means that the origin is the only interior lattice point of the Minkowski sum polyhedron. The well-defined complete intersection for a nef partition (∇_1, ∇_2) is then given by the intersection of the hypersurfaces arising from the sum of all divisors in each ∇_i , i.e.

$$\overbrace{\left(\sum_{\nu_i \in \nabla_1} D_{x_i} \right)}^{\text{partition } \nabla_1 \text{ hypersurface}} \cap \underbrace{\left(\sum_{\nu_j \in \nabla_2} D_{x_j} \right)}_{\text{partition } \nabla_2 \text{ hypersurface}}. \tag{7.1}$$

For the non-generic del Pezzo transition of $\mathbb{P}^4[4]$ this nef partition is provided by

$$\begin{aligned}\nabla_1 &:= \langle \nu_1, \nu_2, \nu_3, \nu_4, \nu_9 \rangle \\ \nabla_2 &:= \langle \nu_5, \nu_6, \nu_7, \nu_8 \rangle\end{aligned}\tag{7.2}$$

with respect to the vertices from table 5.8, which have been rearranged appropriately in table 7.1 for the reader's convenience.

7.1.2 Hypersurface constraints and monomials

Given the toric data in table 7.1, one can in fact explicitly derive the hypersurface constraints using a dual description [192]. For a nef partition (∇_1, ∇_2) there are dual Newton polyhedra (Δ_1, Δ_2) defined by

$$\langle \nu_i^{(n)}, \mu_j^{(m)} \rangle \geq -\delta_{mn} \quad \text{for all } \nu_i^{(n)} \in \nabla_n, \mu_j^{(m)} \in \Delta_m,\tag{7.3}$$

which is often denoted shortly as $\langle \nabla_n, \Delta_m \rangle \geq -\delta_{mn}$. Whereas the polyhedra of the nef partition are only consisting of a couple of points, the dual Newton polyhedra contain more than a thousand lattice points. The primary aspect of this dualization is the fact that those dual lattice points of the Newton polyhedron can be directly associated to monomials, whose collection then gives rise to the hypersurface polynomials of the complete intersection.

If the complete intersection is specified by two hypersurfaces like in the case considered here, the two hypersurface constraint polynomials are

$$f_m := \sum_{\mu_j \in \Delta_m} c_j^{(m)} \prod_{n=1}^2 \prod_{\nu_i \in \nabla_n} (x_i)^{\langle \nu_i, \mu_j \rangle + \delta_{mn}} \stackrel{!}{=} 0,\tag{7.4}$$

where according to table 7.1 the coordinates x_i are given by (x, y, z, u_1, w) for ∇_1 and (u_2, u_3, u_4, u_5) for ∇_2 . The coefficients $c_j^{(m)}$ correspond to the complex structure deformations of the described 4-fold \mathcal{Z} . If the blowup vertex ν_9 is removed, which implies that one considers an elliptic fibration over the Fano 3-fold $\mathbb{P}^4[4]$ instead of the del Pezzo transition thereof, the hypersurface constraint $f_1 = 0$ associated to ∇_1 in fact yields precisely (aside from a few signs) the full Tate parametrization (3.13) in the form

$$f_1 = x^3 - y^2 + a_1xyz + a_2x^2z^2 + a_3yz^3 + a_4xz^4 + a_6z^6 \stackrel{!}{=} 0.\tag{7.5}$$

The Tate coefficients a_i can therefore be directly expressed in terms of the toric data. Note that in this form the coefficient a_i appears in the term containing the factor z^i , which will be used to single out the coefficients. First define subsets of the Newton polyhedron by

$$A_r := \{\mu_j \in \Delta_1 : \langle \nu_3, \mu_j \rangle = r + 1\},\tag{7.6}$$

which contains all elements that generate monomials containing the power z^r due to the association of ν_3 to the coordinate z , cf. table 7.1. Based on this, one can see that the Tate coefficients can be expressed as

$$\begin{aligned} a_r &= \sum_{\mu_j \in A_r} c_j^{(1)} \prod_{n=1}^2 \prod_{\substack{\nu_i \in \nabla_n \\ i > 3}} (x_i)^{\langle \nu_i, \mu_j \rangle + \delta_{1n}} \\ &= \sum_{n=0}^r w^{r-n} \sum_{a=0}^n (u_4)^a (u_5)^{n-a} \tilde{f}_{r-n}^{(a,r)}(u_1, u_2, u_3) \end{aligned} \quad (7.7)$$

for the model considered here, where $\tilde{f}_{r-n}^{(a,r)}$ are generic polynomials of degree $r - n$ in the indicated base coordinates. Note that the underlying approach is entirely general and can be applied to other complete intersection nef partitions as well.

7.1.3 Resolving the $SU(5)$ GUT brane singularity

Singling out the coordinate w in (7.7) was of course in the foresight of dealing with the $SU(5)$ gauge enhancement localized on the GUT 7-brane del Pezzo divisor $\mathcal{S} = \mathcal{D}_w = \{w = 0\}$. From the Tate classification it is known that the vanishing degrees

$$SU(5) : \quad \deg(a_1, a_2, a_3, a_4, a_6) = (0, 1, 2, 3, 5) \quad (7.8)$$

are indicating the presence of such an $SU(5)$ singularity, which leads to the explicit parametrization (5.55). Using the monomials that arise from lattice points in the dual Newton polytope, one can systematically eliminate the points which admit powers w^k with $k < (0, 1, 2, 3, 5)$ for the respective Tate coefficient. This defines new sets $A_r^{SU(5)} \subset A_r$ and in particular a new Newton polytope

$$\Delta_1^{SU(5)} := \bigcup_r A_r^{SU(5)} \subset \Delta_1 \quad (7.9)$$

that intrinsically encodes the $SU(5)$ enhancement over \mathcal{S} . Naturally, this procedure can also be used to handle the other singularity enhancements from the Tate list in table 3.6. The toric resolution to those singularities then arises by performing the dualization (7.3) in reverse, i.e. via

$$\langle \nabla_n^{SU(5)}, \Delta_m^{SU(5)} \rangle \geq -\delta_{mn} \quad \text{for } \Delta_2^{SU(5)} := \Delta_2 \quad (7.10)$$

one obtains the resolved nef partition $(\nabla_1^{SU(5)}, \nabla_2^{SU(5)})$ of the resolved geometry. Since the dual Newton polytope $\Delta_1^{SU(5)}$ is a subset of Δ_1 , the normal polyhedron $\nabla_1^{SU(5)}$ instead gains additional vectors $\tilde{\nu}_i$ of the toric resolution.

nef part	vertices of the polyhedron / fan	coords	GLSM charges		
			Q^1	Q^2	Q^3
$\nabla_1^{SU(5)}$	$\nu_1 = (1, 0, 0, 0, 0, 0)$	x	2	0	0
	$\nu_2 = (0, 1, 0, 0, 0, 0)$	y	3	0	0
	$\nu_3 = (-2, -3, 0, 0, 0, 0)$	z	1	-1	-1
	$\nu_4 = (-2, -3, -1, -1, -1, -1)$	u_1	0	1	0
	$\nu_9 = (-2, -3, 0, 0, -1, -1)$	w	0	0	1
	$\tilde{\nu}_1 = (-1, -2, 0, 0, -1, -1)$	$\tilde{\nu}_1$	0	0	0
	$\tilde{\nu}_2 = (-1, -1, 0, 0, -1, -1)$	$\tilde{\nu}_2$	0	0	0
	$\tilde{\nu}_3 = (0, -1, 0, 0, -1, -1)$	$\tilde{\nu}_3$	0	0	0
	$\tilde{\nu}_4 = (0, 0, 0, 0, -1, -1)$	$\tilde{\nu}_4$	0	0	0
$\nabla_2^{SU(5)}$	$\nu_5 = (0, 0, 1, 0, 0, 0)$	u_2	0	1	0
	$\nu_6 = (0, 0, 0, 1, 0, 0)$	u_3	0	1	0
	$\nu_7 = (0, 0, 0, 0, 1, 0)$	u_4	0	1	1
	$\nu_8 = (0, 0, 0, 0, 0, 1)$	u_5	0	1	1

Table 7.2.: Nef-partitioned toric data for the resolved Calabi-Yau 4-fold $\tilde{\mathcal{Z}}^{SU(5)}$ based on the singular elliptically-fibered 4-fold in table 7.1. Note that the four blow-up vertices $\tilde{\nu}_1, \dots, \tilde{\nu}_4$ of the resolution also introduce four additional projective relations between the coordinates, which are not show above. In particular, those relations break apart the elliptic fibration.

For the discussed elliptically-fibered del Pezzo transition of $\mathbb{P}^4[4]$ the original singular 4-fold described in table 7.1 gains the new vectors $\tilde{\nu}_1, \dots, \tilde{\nu}_4$ that have been added in table 7.2. This defines a new complete-intersection Calabi-Yau 4-fold $\tilde{\mathcal{Z}}^{SU(5)}$, where the non-Abelian $SU(5)$ singularity is resolved [129]. With all singularities in $\tilde{\mathcal{Z}}^{SU(5)}$ removed, the ambiguities in the topological quantities are avoided as well. The Euler characteristic turns out to be

$$\chi(\tilde{\mathcal{Z}}^{SU(5)}) = 918. \quad (7.11)$$

Using the previously computed Euler characteristic $\chi^*(\mathcal{Z}) = 1728$ from (5.54), one can now apply (6.78) for the case of an $SU(5)$ singularity. Using the data in (7.12) one finds the correction term $\chi_{SU(5)} - \chi_{E_8} = -810$, which gives precisely the above result (7.11). The spectral cover for \mathcal{S} is therefore globally valid, and since the subsequently used split spectral cover is a factorization thereof, it is equally valid.

7.2 Gauge fluxes for three chiral matter generations

7.2.1 Realizing the split spectral cover

The generic $S[U(4) \times U(1)_X]$ split spectral cover introduced in chapter 6 can now be made explicit. This implies in particular to show that appropriate sections for the various coefficients c_i and d_i can indeed be found, such that the non-trivial relationship (6.39) responsible for the vanishing of the s^4 power in (6.39) is satisfied. The topology and required intersection data of the GUT 7-brane divisor \mathcal{S} is given by

$$\begin{aligned} \text{total Chern class:} \quad & c(\mathcal{S}) = 1 + P + (6P^2 + 6PX + X^2) \\ \text{normal bundle:} \quad & c_1(N_{\mathcal{S} \subset \mathcal{B}}) = -X, \\ \text{intersection form:} \quad & I(\mathcal{S}) = 2P^2 - 2X^2, \end{aligned} \tag{7.12}$$

i.e. one finds $c_1(\mathcal{S}) = P$ with respect to the divisor basis implied in the geometry in table 7.2. Thus one has

$$\begin{aligned} \eta &= 6c_1(\mathcal{S}) - c_1(N_{\mathcal{S} \subset \mathcal{B}}) = 6P + X, \\ \tilde{\eta} &= \eta - c_1(\mathcal{S}) = 5P + X. \end{aligned} \tag{7.13}$$

Coming back to the coefficient functions of the split spectral cover, those are sections

$$\begin{aligned} c_n &\in H^0(\mathcal{W}; \mathcal{O}_{\mathcal{W}}(\pi^*(\eta - (1+n)c_1(\mathcal{S})))), \\ d_0 &\in H^0(\mathcal{W}; \pi^*T_{\mathcal{S}}), \\ d_1 &\in H^0(\mathcal{W}; \mathcal{O}_{\mathcal{W}}), \end{aligned} \tag{7.14}$$

such that the relevant ones for the condition (6.39) are cohomologically explicitly described by

$$\begin{aligned} [c_0]_{\sigma} &= \eta - c_1(\mathcal{S}) = 5P + X, \\ [c_1]_{\sigma} &= \eta - 2c_1(\mathcal{S}) = 4P + X, \\ [d_0]_{\sigma} &= c_1(\mathcal{S}) = P. \end{aligned} \tag{7.15}$$

Using the monomial description for global sections implied by the algorithm in appendix A, the most general ansatz for those sections can be formulated as

$$\begin{aligned} c_0 &= wP_5(u_1, u_2, u_3) + Q_1(u_4, u_5)R_4(u_1, u_2, u_3), \\ c_1 &= wP_4(u_1, u_2, u_3) + S_1(u_4, u_5)T_3(u_1, u_2, u_3), \\ d_0 &= P_1(u_1, u_2, u_3), \end{aligned} \tag{7.16}$$

where P_i , Q_1 , R_4 , S_1 and T_3 are independent polynomials of the denoted total power of the coordinates, cf. the GLSM charges of the coordinates in table 7.2. Finding polynomials such that the factorization condition is met is therefore indeed possible.

7.2.2 Tuning of three chiral matter generations

In order to find an appropriate gauge flux for the matter branes, a suitable ansatz for the spectral line bundle $\mathcal{N}^{(4)}$ has to be chosen. Its first Chern class is provided in (6.44) as well as the integrality conditions (6.45), which immediately yields $\lambda \in \frac{1}{4}\mathbb{Z}$. The most general ansatz is therefore provided by

$$\begin{aligned} \zeta &= aX + bP \\ \lambda &= \frac{x}{4} \end{aligned} \quad \text{for } a, b, x \in \mathbb{Z}. \quad (7.17)$$

Using (7.13), the second part of the integrality condition gives

$$\begin{aligned} &\left(\frac{1}{2} - \lambda\right) \tilde{\eta} - \frac{1}{2}c_1(\mathcal{S}) + \frac{1}{4}\zeta \in H^2(\mathcal{B}; \mathbb{Z}) \\ &= \left(2 + \frac{1}{4}(b - 5x)\right) P + \frac{1}{4}(2 - x + a)X \quad \rightsquigarrow \quad \begin{cases} b - 5x \in 4\mathbb{Z} \\ 2 - x + a \in 4\mathbb{Z} \end{cases} \end{aligned} \quad (7.18)$$

in order to have a well-defined gauge flux. The second phenomenological requirement is to have three chiral matter generations, which using (6.58) requires

$$\begin{aligned} \chi_{\mathbf{10}} &= \int_{\mathcal{S}} \left(-\lambda\tilde{\eta} + \frac{1}{4}\zeta\right) (\tilde{\eta} - 4c_1(\mathcal{S})) \\ &= \int_{\mathcal{S}} \frac{1}{4} \left[(a - x)PX + (b - 5x)P^2 + (a - x)X^2 + (b - 5x)PX \right] \\ &= \frac{1}{2}(b - a - 4x) = \pm 3. \end{aligned} \quad (7.19)$$

On the other hand — which was one of the main reasons to employ the split spectral cover approach in the first place — the number of $\bar{\mathbf{5}}_H$ states should vanish, which by (6.64) means

$$\chi_{\bar{\mathbf{5}}_H} = -2a + 5b - x = 0. \quad (7.20)$$

Following (6.65) this indeed implies $\chi_{\bar{\mathbf{5}}_m} = \chi_{\mathbf{10}} = \pm 3$, i.e. the presence of three chiral matter generations while avoiding additional Higgses.

A suitable solution to the two conditions (7.19) and (7.20), that at the same time fulfills the integrability requirements (7.18), is given by

$$\begin{aligned} \text{3 chiral generations} \\ \text{gauge flux solution:} \end{aligned} \quad \begin{cases} a = 10 \\ b = 4 \\ x = 0 \end{cases} \quad \rightsquigarrow \quad \begin{cases} \zeta = 10X + 4P \\ \lambda = 0 \end{cases} \quad (7.21)$$

For those values the chiral index of the right-handed neutrinos in (6.68) gives

$$\chi_{(\nu_R)^c} = 5, \quad (7.22)$$

suggesting more neutrino generations than matter generations. Overall, this indeed shows that it is possible to construct a global model supporting three chiral generations of $SU(5)$ GUT matter.

7.2.3 Tuning of the GUT breaking hypercharge flux

After fixing the gauge flux on the matter branes, one has to consider the GUT group breaking $U(1)_Y$ hypercharge flux. This requires a better understanding of the GUT 7-brane topology. From table 3.4 it is clear that a del Pezzo-7 surface has $b^2 = 8$ non-trivial 2-cycles. However, due to the non-generic nature of the particular dP_7 that is considered in the geometry here, only a sub-lattice corresponding to E_6 of $H^2(\mathcal{S})$ contains 2-cycles that are trivial in the cohomology of the base \mathcal{B} . This is required to keep the Stückelberg mechanism for the $U(1)_Y$ in check, recall section 3.8.3. The basis for the cohomology of a dP_n is usually chosen to be (ℓ, E_1, \dots, E_n) , where ℓ can be considered to correspond to the unique original $\mathbb{P}^1 \subset \mathbb{P}^2$ divisor class and each exceptional divisor class E_i arises from a further blowup [99]. The intersection numbers are then conveniently given by

$$\ell^2 = 1, \quad E_i E_j = -\delta_{ij}, \quad \ell E_i = 0 \quad \text{for all } i = 1, \dots, n. \quad (7.23)$$

By analyzing the highly restricted structure of curves on a del Pezzo surface, one can identify two curves in terms of the ambient space, i.e.

$$\begin{aligned} \text{genus 1: } C_1 &:= P|_{\mathcal{S}} && \rightsquigarrow 3\ell - \sum_{i=1}^7 E_i = -f \\ \text{genus 0: } C_2 &:= (P + X)|_{\mathcal{S}} && \rightsquigarrow \ell - E_7, \end{aligned} \quad (7.24)$$

which allow a partial identification of the standard dP_7 cohomology generators (7.23) and the inherited cohomology base of the considered geometry. One can express the split spectral cover “uplift” matter curves (6.48) and (6.50) cohomologically by

$$\begin{aligned} [\hat{\mathcal{C}}_{10}]|_{\sigma} &= [c_4]|_{\sigma} = \eta - 5c_1(\mathcal{S}) = P + X, \\ [\hat{\mathcal{C}}_{\bar{5}_H}]|_{\sigma} &= [c_3(c_2 + c_3 d_0) - c_1 c_4]|_{\sigma} = 2\eta - 7c_1(\mathcal{S}) = 5P + 2X, \\ [\hat{\mathcal{C}}_{\bar{5}_m}]|_{\sigma} &= [c_2 + d_0(c_3 + c_4 d_0)]|_{\sigma} = \eta - 3c_1(\mathcal{S}) = 3P + X. \end{aligned} \quad (7.25)$$

In order to gain a better understanding of the matter curves on the GUT 7-brane \mathcal{S} , one could now “restrict” (i.e. pullback via the inclusion mapping) those to the cohomology

$H^2(\mathcal{S}; \mathbb{Z})$. The matter curves (7.25) then correspond cohomologically to

$$\begin{aligned} [\mathcal{C}_{10}] &= \ell - E_7 \\ [\mathcal{C}_{\mathfrak{5}_H}] &= -3f + 2(\ell - E_7) \\ [\mathcal{C}_{\mathfrak{5}_m}] &= -2f + (\ell - E_7) \end{aligned} \quad (7.26)$$

in terms of the standard dP_7 divisor base. This terminology and conventions allow for a convenient comparison to the literature.

The $U(1)_Y$ hypercharge gauge flux that breaks the $SU(5)$ GUT symmetry can then be chosen corresponding to the E_6 root, i.e.

$$c_1(\mathcal{L}_Y) = E_1 - E_2 \in H^2(\mathcal{S}; \mathbb{Z}). \quad (7.27)$$

Following the earlier remark, this choice guarantees that the described flux indeed leads to a massless $U(1)_Y$ gauge boson upon GUT breaking. Moreover, this restricts trivially on the matter curves (7.26), such that the previously computed chiral indices do not change. Ultimately, this allows the GUT group to be broken by the $U(1)_Y$ hypercharge flux, while generating three generations of chiral matter.

7.3 Evaluating the Consistency Conditions

7.3.1 D-term condition

In order to ensure D-flatness for the vector bundle \mathcal{V} , the corresponding Fayet-Iliopoulos D-term has to vanish, which can be easily checked using the Kähler cone of \mathcal{B} . However, since for the choice of divisor class basis (P, X) and (\tilde{P}, X) in table 5.8 neither intersection form is positive definite, one has to define a third base by

$$\left. \begin{aligned} K_1 &:= P + X \\ K_2 &:= P \end{aligned} \right\} \rightsquigarrow I(\mathcal{B}) = 4(K_2)^3 + 4K_1(K_2)^2 + 2(K_1)^2 K_2. \quad (7.28)$$

If the Kähler form $J \in H^{1,1}(\mathcal{B}; \mathbb{Z})$ is then expanded as $J = r^1 K_1 + r^2 K_2$, all physical volumes will be positive in the Kähler cone given by $r^i > 0$. The Fayet-Iliopoulos term for the vector bundle then reads

$$\begin{aligned} \mu(\mathcal{V}) &= \int_{\mathcal{S}} J \wedge \zeta = \int_{\mathcal{S}} \left(r_1(P + X) + r_2 P \right) (10X + 4P) \\ &= \int_{\mathcal{S}} \left[(14r_1 + 10r_2)PX + 10r_1 X^2 + (4r_1 + 4r_2)P^2 \right] = -12r_1 + 8r_2. \end{aligned} \quad (7.29)$$

The vanishing of $\mu(\mathcal{V})$ can then obviously be achieved achieved for $r^i > 0$ such that $3r_1 = 2r_2$, i.e. within the Kähler cone.

7.3.2 3-brane tadpole condition

The last consistency check relevant here is the 3-brane tadpole condition (3.50), that was already specialized to this setting in section 6.3.5. The “smooth” I_1 prediction for the Euler characteristic of the elliptically-fibered Calabi-Yau 4-fold \mathcal{Z} of this model is

$$\begin{aligned}\chi^*(\mathcal{Z}) &= 12 \int_{\mathcal{B}} c_1(\mathcal{B})c_2(\mathcal{B}) + 360 \int_{\mathcal{B}} c_1(\mathcal{B})^3 \\ &= \int_{\mathcal{B}} \left(432P^3 + 1236P^2X + 1176PX^2 + 372X^3 \right) = 1728\end{aligned}\quad (7.30)$$

according to (5.16). Of course, this neglects the $SU(5)$ gauge enhancement along \mathcal{S} as well as the further gauge enhancements along the matter curves and triple intersection points. The first two lines of (6.79) now essentially compute the Euler characteristic that takes all enhancements into account, i.e.

$$\begin{aligned}\frac{\chi(\mathcal{Z})}{24} &= \frac{\chi^*(\mathcal{Z})}{24} - \frac{615}{2} \int_{\mathcal{S}} c_1(\mathcal{S})^2 - 15 \int_{\mathcal{S}} \left(\eta^2 - 9\eta c_1(\mathcal{S}) \right) \\ &\quad + \left(\frac{1}{2} - 2\lambda^2 \right) \int_{\mathcal{S}} \left(\tilde{\eta}^2 - 4\tilde{\eta} c_1(\mathcal{S}) \right) \\ &= \frac{1728}{24} - \frac{615}{2} \int_{\mathcal{S}} P^2 - 15 \int_{\mathcal{S}} \left[(36P^2 + 12PX + X^2) - (54P^2 + 9PX) \right] \\ &\quad + \frac{1}{2} \int_{\mathcal{S}} \left[(25P^2 + 10PX + X^2) - (20P^2 + 4PX) \right] \\ &= 72 - 615 + 570 + 4 = 31\end{aligned}\quad (7.31)$$

is the geometry-dependent part of the 3-brane tadpole. It should be noted that $\chi(\mathcal{Z}) = 744$ differs from $\chi(\tilde{\mathcal{Z}}^{SU(5)}) = 918$, where only the $SU(5)$ -brane divisor was taken into account.

The gauge flux dependent contribution in the third line of (6.79) is given by

$$\begin{aligned}-\frac{1}{2} \int_{\mathcal{S}} G_4 \wedge G_4 &= \frac{1}{2} \int_{\mathcal{S}} (\pi_4)_*(\gamma_{(4)}^2) = \int_{\mathcal{S}} \left(\frac{5}{8} \zeta^2 + c_1(\mathcal{L}_Y)^2 - \zeta c_1(\mathcal{L}_Y) \right) \\ &= -105 - 2 + 0 = -107\end{aligned}\quad (7.32)$$

from the choices in (7.21) and (7.27). The required total number of 3-branes to saturate the tadpole condition is therefore

$$N_{D3} = \frac{\chi(\mathcal{Z})}{24} - \frac{1}{2} \int_{\mathcal{Z}} G_4 \wedge G_4 = 31 - 107 = -76,\quad (7.33)$$

which is—unfortunately—negative. The chosen gauge bundle leads to an considerable overshooting of the tadpole, which means that the model would have to include anti-D3-branes in order to cancel the tadpole. This is, however, a very undesirable situation and

considering the overall success of the described approach it stands to reason that this overshooting can be attributed to the rather simple geometry considered here, which yields comparably small values for the Euler characteristic.

In fact, using simple extensions of this setup and the base $\mathbb{P}^4[3]$ instead of $\mathbb{P}^4[4]$ to start with, the 3-brane tadpole can indeed be satisfied [119, 161]. This provides sufficient evidence that the general approach is quite fruitful and at this point only spoiled due to the choice of an unsuitable geometry. It should also be mentioned that the integrality of (7.33) and in particular (7.32) provides a further non-trivial consistency check.

7.4 Phenomenological Properties

The described model provides the first example of a global F-theory model that leads to three generations of chiral Standard Model matter obtained from the breaking of the $SU(5)$ GUT representation $\mathbf{10} \oplus \bar{\mathbf{5}}_m$. The only drawback is the apparent overshooting of the flux contribution to the geometry-dependent part of the 3-brane tadpole. While this is not a dramatic failure, it is certainly undesired. Fortunately, as mentioned, a slight change in the geometry remedies this issue. It is therefore in order to analyze the phenomenological properties of the specified model constructed here.

- *Proton decay*: The model contains the $\mathbf{10} \cdot \mathbf{10} \cdot \mathbf{5}_H$ and $\mathbf{10} \cdot \bar{\mathbf{5}}_m \cdot \bar{\mathbf{5}}_H$ couplings, while preventing the dimension-4 proton decay operators $\mathbf{10} \cdot \bar{\mathbf{5}}_m \cdot \bar{\mathbf{5}}_m$ and $\mathbf{10} \cdot \bar{\mathbf{5}}_H \cdot \bar{\mathbf{5}}_H$ due to the extra $U(1)_X$ symmetry [159]. However, the “missing partner mechanism”, that is effectively realized by the $U(1)_X$, does not affect dimension-5 operators, which ultimately lead to the same problem. A potential way out could be provided by a further splitting of the Higgs curve.
- *Higgs sector*: The particular form of the (split) spectral cover is known to produce some problematic effects in the Higgs sector [159]: Both the H_u and H_d localize as a vector-like pair on the Higgs curve $\mathcal{C}_{\bar{\mathbf{5}}_H}$. However, this naturally leads to the generation of a Higgs mass term $\mu H_u H_d$ in the superpotential. Phenomenologically, the Higgs mass μ is expected to be of the order of the weak scale, but in the context of GUT theories it can be of much higher value. Keeping the μ -term small—generally known as the μ -problem of supersymmetric theories—requires therefore a high level of fine-tuning unless other modifications can be applied to the proposed Higgs curve.
- *Right-handed neutrinos*: For the three-generation gauge flux solution (7.21) used in the model, the number of right-handed neutrinos is $\chi_{(\nu_R)^c} = 5$. It is known that in general the usage of a $U(1)_X$ “selection symmetry” is in conflict with realistic neutrino structures [79, 82, 159]. Most importantly, the selection rules prohibit

Majorana mass terms for the neutrinos, leaving only the Dirac mass terms¹ derived from the $\bar{\mathbf{5}}_m \cdot \mathbf{5}_H \cdot \mathbf{1}$ coupling, which implies different anti-neutrinos. However, using M5-brane instantons there exists a possibility for generating Majorana masses based on known type IIB E3-brane mechanisms for right-handed neutrinos. One could also consider a direct breaking of the $U(1)_X$ symmetry.

- *Gauge coupling unification:* Whereas supersymmetric field theories usually lead to a perfect gauge coupling unification, the breaking of the GUT symmetry via a $U(1)_Y$ flux only preserves this unification at leading order in α' from the perturbative type IIB perspective [69]. Due to the Chern-Simons action (2.18) term

$$\mu_7 \int_{\mathbb{R}^{1,3} \times \mathcal{S}} C_0 \wedge \text{tr}(F^4) \quad (7.34)$$

for the GUT 7-brane there are further corrections from the $U(1)_Y$ flux to the gauge coupling unification. However, due to the varying axio-dilaton in F-theory, the Chern-Simons action is not strictly applicable. In order to continue the discussion, one therefore replaces the varying g_s with the F-theory mass scale

$$M_*^4 = \frac{1}{g_s \ell_s^4}, \quad (7.35)$$

which can be shown to stay constant over the base \mathcal{B} . For the discussed model the $U(1)_Y$ flux is encoded in the line bundle \mathcal{L}_Y . The $U(1)_X$ flux on the other hand is encoded in the split spectral cover line bundle and should not contribute to the GUT brane's Chern-Simons term. A suitable ansatz for the gauge field strength is then given by

$$F := \sum_{a=1}^8 F_{SU(3)}^a \begin{pmatrix} \frac{\lambda_a}{2} & 0 \\ 0 & 0 \end{pmatrix} + \sum_{i=1}^3 F_{SU(2)}^i \begin{pmatrix} 0 & 0 \\ 0 & \frac{\sigma_i}{2} \end{pmatrix} + \frac{1}{6} F_Y \begin{pmatrix} (-2)_{3 \times 3} & 0 \\ 0 & (3)_{2 \times 2} \end{pmatrix} + \frac{1}{5} \mathcal{F}_Y \begin{pmatrix} (-2)_{3 \times 3} & 0 \\ 0 & (3)_{2 \times 2} \end{pmatrix}, \quad (7.36)$$

¹Recall that Majorana particles – which correspond to a real spinor representation, i.e. they are conjugation-invariant – and Dirac particles are essentially distinguished by the question if the particle is truly different from its associated anti-particle. While the answer is obvious for charged particles due to the flipped charged sign of anti-particles, it is not clear in the case of neutral particles. Furthermore, the distinction only becomes apparent if the particles are massive. This applies in particular to neutrinos, which are usually only observed by indirect means and are not yet known to have a nonzero mass. From a phenomenological point of view Majorana and Dirac neutrinos behave differently under the CP transformation and a massive neutrino has both an electric dipole as well as magnetic moment, that could in principle be experimentally detected.

where λ_a are the Gellmann matrices and σ_i are the Pauli matrices, i.e. the canonical adjoint representation generators of $SU(3)$ and $SU(2)$. By inserting this ansatz into the Chern-Simons term (7.34) and extracting the relevant $F \wedge F$ terms, the MSSM gauge couplings can be determined to be

$$\begin{aligned}\frac{1}{\alpha_s} &= M_*^4 \left(\text{vol}(\mathcal{S}) - \frac{4}{50} \ell_s^4 \int_{\mathcal{S}} c_1(\mathcal{L}_Y)^2 \right) \\ \frac{1}{\alpha_w} &= M_*^4 \left(\text{vol}(\mathcal{S}) - \frac{9}{50} \ell_s^4 \int_{\mathcal{S}} c_1(\mathcal{L}_Y)^2 \right) \\ \frac{1}{\alpha_Y} &= \frac{5}{3} M_*^4 \left(\text{vol}(\mathcal{S}) - \frac{7}{50} \ell_s^4 \int_{\mathcal{S}} c_1(\mathcal{L}_Y)^2 \right),\end{aligned}\tag{7.37}$$

where according to the choice (7.27) one has $\int_{\mathcal{S}} c_1(\mathcal{L}_Y)^2 = -2$. While the corrected gauge couplings do not unify perfectly—as desired—one can at least find a relation

$$\frac{1}{\alpha_Y} = \frac{1}{\alpha_w} + \frac{2}{3} \frac{1}{\alpha_s}\tag{7.38}$$

between the four-dimensional couplings [74]. This can be roughly be made compatible with the running of the gauge couplings, provided that a threshold $M_{\mathbf{3}\bar{\mathbf{3}}} < M_X$ of the Higgs color triplets $(\mathbf{3}, \mathbf{1})_{-\frac{2}{3}} \oplus (\bar{\mathbf{3}}, \mathbf{1})_{\frac{2}{3}}$ exists.

A very important issue is the explicit determination of the exact matter spectrum, i.e. including the vector-like states that are not counted by the chiral indices. This would also help to clarify the situation of the Higgs sector mentioned above.

Overall, one can acknowledge that the construction of this model is a significant step forward in the construction of semi-realistic grand unified theories within the F-theory framework. While certain aspects like the overshooting 3-brane tadpole and some of the aforementioned phenomenological problems are certainly unsatisfactory from the current point of view, there exist various constructive approaches to remedy those drawbacks. On the other hand, the successful construction of this model together with the handling of a non-trivial gauge flux opens the door for further theoretical study of this manifestly non-perturbative approach to GUT model building in string theory.

Chapter 8

Summary and Outlook

F-THEORY as a non-perturbative framework provides a unified perspective on various aspects of string model building. While the actual theory itself is only indirectly defined via various dualities discussed in section 3.4, one is nevertheless able to access all the relevant information for the construction of non-trivial compactifications and to determine the phenomenological properties of the described setup [71–85]. As it was shown in section 3.5 and chapters 6 and 7, the spectral cover description provides an invaluable tool to get a handle on the gauge flux. At the moment it provides the only feasible access to obtain chiral matter states or to break the GUT symmetry. In the end, this tool suffices for the purpose considered in this thesis. In the following two sections the contents and results of part III are summarized and an overview of several unsolved issues in F-theory model building is given.

8.1 Obtained Results

It was shown in chapter 4 that it is possible to understand non-perturbative E3-brane instantons from (perturbative) type IIB superstring theory directly within the genuinely non-perturbative F-theory in terms of vertical M5-branes. In fact, one can explicitly relate the E3-brane Hodge diamond to the M5-brane Hodge diamond and identify the precise correspondence between the respective bosonic and fermionic zero-mode structures. An important point here is the fact, that one does not necessarily require a fundamental quantization or understanding from first principles on the F-theory side, in order to arrive at those conclusions. A careful uplifting of the perturbative type IIB orientifold setup to F-theory in the Sen limit already provides sufficient evidence to support those findings. Conceptually, one essentially relates the open strings on E3-branes to open membranes ending on M5-branes.

The first indication of non-perturbative effects on the F-theory side was observed in the uplifting of a self-invariant $O(1)$ instanton compared to a $U(1)$ instanton E3-

brane/image brane pair. As long as the instanton intersects with the O-plane, an automatic recombination to the more generic $O(1)$ case is triggered. Only in specifically chosen geometries one can therefore find true $U(1)$ instantons in F-theory. This corresponds to an automatic uplifting of the $\bar{\tau}_\alpha$ zero-mode and geometrically translates to the statement that the $\bar{\tau}_\alpha$ zero-modes only survive non-perturbatively if they correspond to 1-cycles of the M5-brane.

Understanding charged matter zero-modes in F-theory proved to be technically challenging due to the abundance of singularities appearing both on the IIB and F-theory side. The particularly troublesome—yet generic—case arises from the intersection of the M5-brane with the generic I_1 remainder component \mathcal{D}_R of the discriminant locus. The results indicate that a part of the IIB zero-modes is non-perturbatively lifted when one moves away from the perturbative Sen limit. Moreover, an investigation of the 1-loop determinant contributions of the M5-brane to the superpotential—along with a type IIB interpretation—revealed that an E3-brane instanton contains more potentially harmful moduli than the naive zero-mode structure analysis suggests. Based on this observation, a refined and sufficient criterion for E3-branes in IIB to generate an uncharged, nowhere vanishing superpotential was derived.

In the type IIB theory instantons serve a further very important purpose, as they can be used to generate certain Yukawa couplings required for realistic GUT model building, specifically the $\mathbf{10} \cdot \mathbf{10} \cdot \mathbf{5}_H$ interaction. The fact that this coupling can only be generated non-perturbatively in type IIB suggests to investigate the entire problem of GUT model building from the perspective of the F-theory framework. Here one has direct access to 7-branes with exceptional gauge groups, such that couplings and interactions like the $\mathbf{10} \cdot \mathbf{10} \cdot \mathbf{5}_H$ are much easier to obtain. Via the $U(1)_Y$ hypercharge flux one can break the GUT symmetry of such models. However, this requires a specific structure of the GUT 7-brane geometry. In order to utilize the elegant decoupling principle that allows to effectively detach the GUT 7-brane with its intersections from the entire global setting, a shrinkable rigid divisor is required—a del Pezzo surface. Moreover, a suitable $U(1)_Y$ gauge flux requires the presence of 2-cycles in the GUT 7-brane, which are trivial in the ambient base of the F-theory 4-fold.

In chapter 5 several example geometries were constructed that satisfy both requirements. But a realistic GUT model naturally requires appropriate matter curves and interactions, which are realized by singularity enhancements localized on curves and points of the GUT 7-brane. The construction of those particular geometries was essentially based on an earlier study of suitable GUT geometries from the type IIB perspective. Therefore, the first considered geometries of chapter 5 were direct F-theory uplifts of known type IIB setups. However, a subsequent analysis revealed that all those geome-

tries have profound shortcomings in specific basic requirements, like missing singularity enhancements or no interaction point intersections.

Ultimately, those intermediate steps led to the construction of a true F-theory geometry without an explicit underlying type IIB orientifold. As shown in section 5.4, a non-generic del Pezzo transition of the quartic Fano 3-fold $\mathbb{P}^4[4]$ provides an F-theory Kähler 3-fold base with an acceptable enhancement and intersection structure to support a non-trivial $SU(5)$ GUT model. A key observation is that the existence of a suitable $\mathbf{10}$ matter curve requires the presence of a non-generic del Pezzo surface GUT 7-brane, which can only be shrunk to a curve instead of a point. From a perturbative IIB orientifold perspective this would correspond to two intersecting del Pezzo surfaces, each of which restricts the other's ability to fully shrink.

In the next step the spectral cover description — originally only defined for F-theory settings with a heterotic dual — was extended to be applicable to the aforementioned geometry. The overall discussion in chapter 6 was, however, kept rather general to allow for easy customization to other settings. This provided the means to describe the gauge flux on the GUT 7-brane as well as the gauge flux on the intersecting matter branes — at least locally — such that both chiral matter and a $U(1)_Y$ hypercharge flux for the breaking of the GUT group could be obtained. However, a central problem was the localization of both the $\mathbf{5}_H$ and $\mathbf{5}_m$ representations on the same curve, which easily leads to rapid proton decay via the $\mathbf{10} \cdot \bar{\mathbf{5}}_m \cdot \bar{\mathbf{5}}_m$ Yukawa coupling.

To avoid this issue, the generic $SU(5)$ spectral cover was replaced by an $S[U(4) \times U(1)_X]$ split spectral cover, that effectively introduced a further Abelian $U(1)_X$ symmetry, which is used to distinguish the two conceptually different $\mathbf{5}$ representations of $SU(5)$. In this approach the quantization conditions in fact forced to turn on a non-trivial universal gauge flux. The split spectral cover also allowed to bypass a sort of no-go theorem for the construction of global F-theory GUT models with three chiral matter generations [154, 157]. Having a global description of F-theory and the G_4 flux then allowed to check those consistency conditions that are not available from a purely local perspective, for example the 3-brane tadpole cancellation condition. Furthermore, a formula for the computation of the (singular) 4-fold's Euler characteristic was presented, which can — in reverse — also be used to test the global validity of a spectral cover description in the absence of a strict heterotic dual.

In chapter 7 the rather general constructions from chapter 6 were explicitly realized for the geometry arising from the non-generic del Pezzo transition of the $\mathbb{P}^4[4]$ hypersurface. The elliptically-fibered Calabi-Yau 4-fold was then explicitly constructed as a complete intersection of two hypersurfaces in a toric 6-fold ambient space. In fact, using the dual polytopes of the associated nef partition, the $SU(5)$ enhancement over

the del Pezzo divisor of the GUT 7-brane—responsible for codimension-2 singularities in the 4-fold—can be entirely resolved.

Following the construction of the geometry, it was shown that one can indeed find a suitable flux solution to satisfy both the three generation criterion and the $U(1)_Y$ hypercharge breaking of the GUT group that satisfies the required quantization condition. Furthermore, the intersection structure of the matter curves on the GUT brane provides gauge enhancements to $SU(6)$, $SU(7)$ and E_6 , which yield the vital $\mathbf{10} \cdot \mathbf{10} \cdot \mathbf{5}_H$ and $\mathbf{10} \cdot \mathbf{\bar{5}}_m \cdot \mathbf{\bar{5}}_H$ Yukawa couplings along with a $\mathbf{\bar{5}}_m \cdot \mathbf{5}_H \cdot \mathbf{1}$ coupling that can be associated to right-handed neutrinos. As mentioned earlier, the usage of the split spectral cover prohibited the appearance of dangerous dimension-4 proton decay operators.

A further analysis of the phenomenological properties of this model revealed that indeed most of the basic requirements for semi-realistic GUT models have been met. The only serious drawback stems from an overshooting of the 3-brane tadpole, i.e. the flux contribution is significantly larger than the geometry contribution, such that in principle a negative number of D3-branes would be required to saturate the tadpole. While this is in principle possible using anti-D3-branes, it presents a rather undesired situation. Fortunately, subsequent investigations [161] of slightly different geometries based on $\mathbb{P}^4[3]$ instead of $\mathbb{P}^4[4]$ indeed showed that the approach pursued here is productive. While there is still a lot of phenomenological fine-tuning left to do, various known mechanisms are available to deal with those issues at least in principle.

The result of chapter 7 is therefore the construction of the first global F-theory $SU(5)$ GUT model that also takes gauge flux into account and contains three chiral matter generations of $\mathbf{10} \oplus \mathbf{\bar{5}}_m$ as well as providing a $U(1)_Y$ hypercharge gauge flux for GUT symmetry breaking—accompanied by overall semi-realistic phenomenological structures.

8.2 Future Outlook and Open Questions

Clearly, despite the aforementioned successes the abundant number of issues throughout this thesis has shown that a lot of problems remain open or at least require a significant improvement. In the following, several problems are listed which directly concern the material within this work.

- *Improving the IIB/F-theory uplifting:* In chapter 5 several known type IIB orientifold geometries were uplifted to F-theory, a task which already required considerable effort [87, 126, 152, 153]. Considering that those models are of a rather simple structure, it becomes clear that at the moment there is no such thing as a true and universally applicable uplifting procedure for general type IIB orien-

tifolds, in particular if complicated D-brane matter content is present as well. Considering the results of chapters 4 and 5, one can truly gain from the intrinsically non-perturbative perspective that F-theory offers. Usually the problems stem from the difficulties in constructing a suitable elliptically-fibered Calabi-Yau 4-fold, which requires quite sophisticated techniques from algebraic and toric geometry—even for the rather simple examples that are considered to be “accessible”. It would therefore be quite important to improve the dictionary between the perturbative type IIB string theory and F-theory.

- *Developing a new model building paradigm:* Most (perturbative) model builders are accustomed to a step-by-step approach in handling the various phenomenological requirements. Since most properties are geometrically encoded in the elliptic fibration of the 4-fold, everything related to the geometry and D-brane content has to be dealt with in a single step in F-theory model building. This is one of the reasons that so far almost exclusively F-theory settings that are at least remotely based on perturbative setups have been studied in detail.
- *Describing global G_4 fluxes:* The spectral cover description provides a description of the gauge flux only for settings that have a strict heterotic dual. While the extensions of chapter 6 are promising, this treatment of gauge fluxes is still rather cumbersome. Only recently some partial results on the flux quantization in F-theory have appeared [140, 141, 193]. Ultimately, the problem originates in the huge number of 4-cycles that a typical elliptically-fibered Calabi-Yau 4-fold contains. In terms of the base geometry only a small fraction of those can be easily described, leaving the vast majority untouched. Due to the importance of gauge fluxes for the generation of chiral matter and several other crucial tasks a better description is required.
- *Instantons in the presence of fluxes:* Once the description of global G_4 fluxes in F-theory has been improved, one could revisit the analysis carried out in chapter 4 and study vertical M5-brane instantons in the presence of fluxes [103, 194–198]. Considering the insights of the flux-less case obtained herein, there is a significant potential for further refinements.

A speculative further project would be a study of the phenomenological structure of the F-theory part of the string landscape [199–201], once the G_4 flux is better understood. More precisely, an observation that can be derived from chapter 5 is a decrease in the value of the Euler characteristic $\chi(\mathcal{Z})$ of the elliptically-fibered Calabi-Yau 4-fold, when more complicated gauge enhancements and brane intersections are considered. This is not really a surprise, as more and more complex structure moduli are fixed in the process, which are related to the 4-cycles of the geometry—thus the decreasing $\chi(\mathcal{Z})$.

In the estimation of the number of flux vacua the 4th Betti number $b_4(\mathcal{Z})$ takes a critical role in the determination of the exponent, which leads to such large numbers like 10^{500} to 10^{1500} flux vacua, which have appeared in the literature. Provided that the aforementioned observation holds true for the majority of F-theory compactification manifolds, one could—based on phenomenological requirements—systematically analyze how the size of the landscape shrinks, as more and more conditions are enforced. In particular, if for basic assumptions the number of flux vacua falls short of the critical value 10^{120} of the (apparent) level of fine-tuning of the cosmological constant Ω , this would significantly impact the statistical arguments “explaining” the observed value of Ω , which have gained popularity in recent years [202]. Nevertheless, there are significant obstacles to be tackled at first before one can turn to such an analysis.

IV Appendices

Appendix A

Toric Geometry and Algorithmic Cohomology Computations

ONE major technical obstacle in string model building and many other areas of theoretical physics lies in the computation of cohomology groups for certain geometric ingredients of the theory. The common methods usually try to relate the problem at hand via a chain of isomorphisms back to known results in order to avoid the cumbersome computations of the cohomology groups from the ground up. However, this makes it difficult to generalize results that were derived for a specific configuration and rules out automated scans over a wide range of geometries, where each instance would require an individual treatment.

In this chapter an algorithmic method [90, 91] to compute the dimensions of sheaf cohomology groups for line bundles over toric varieties is presented. Via the induced long exact cohomology sequence of the Koszul complex or the monad / extension construction one can derive the cohomology of more complicated bundles over subspaces of toric varieties, like compact Calabi-Yau hypersurfaces and their divisors. Furthermore, a brief overview of the basic definitions of toric geometry [203–205] is presented as well as several tools [206–209] to deal with equivariant cohomologies.

A.1 Toric Varieties and Fans

The framework of toric geometry is directly related to gauged linear σ -models (GLSMs) in physics [117, 210, 211]. A toric variety X is a generalization of a projective space, which consists of a set of homogeneous coordinates x_1, \dots, x_n and R projective equivalence relations

$$(x_1, \dots, x_n) \sim (\lambda_r^{Q_1^{(r)}} x_1, \dots, \lambda_r^{Q_n^{(r)}} x_n) \quad \text{for } \lambda_r \in \mathbb{C}^\times. \quad (\text{A.1})$$

Here $Q_1^{(r)}$ for $r = 1, \dots, R$ are the projective weights that can be treated as the Abelian $U(1)$ charges in the associated GLSM, where the homogeneous coordinates act as chiral superfields in a $\mathcal{N}=(2,2)$ supersymmetric gauge theory. The Fayet-Iliopoulos parameters ξ_r of those $U(1)$ s can be interpreted as the Kähler parameters of the geometric space. A vanishing of the D-terms associated to the GLSM then splits the parameter space of $\vec{\xi} \in \mathbb{R}^R$ into R -dimensional cones in which the D-flatness conditions can be solved and which correspond to the geometrical Kähler cones. For each cone—usually referred to as a geometric phase—there are sets of collections of coordinates

$$\mathcal{S}_\rho = \{x_{\rho_1}, x_{\rho_2}, \dots, x_{\rho_{|\mathcal{S}_\rho|}}\} \quad \text{for } \rho = 1, \dots, N \quad (\text{A.2})$$

that are not allowed to vanish simultaneously. All those sets form the Stanley-Reisner ideal

$$\text{SR}(X) = \langle \mathcal{S}_1, \dots, \mathcal{S}_N \rangle. \quad (\text{A.3})$$

It is Alexander-dual to the irrelevant ideal B_Σ , which is often used in the mathematical literature. The toric variety X of dimension $d = n - R$ for this geometric phase can then be described as the coset space

$$X = (\mathbb{C}^n - Z) / (\mathbb{C}^\times)^R. \quad (\text{A.4})$$

Here Z is the set of removed points given by

$$Z = \bigcup_{\rho=1}^N \{x_{\rho_1} = x_{\rho_2} = \dots = x_{\rho_{|\mathcal{S}_\rho|}} = 0\}, \quad (\text{A.5})$$

which encodes precisely the information of the Stanley-Reisner ideal $\text{SR}(X)$. Basically, the set Z is the generalization of the removed origin in projective spaces

$$\mathbb{C}\mathbb{P}^n = (\mathbb{C}^{n+1} - \{0\}) / \mathbb{C}^\times. \quad (\text{A.6})$$

Another perspective on toric geometry is formulated in terms of toric fans, cones and triangulations, which allows for a combinatorial treatment of the subject. In this language a geometric phase corresponds to the choice of a triangulation for a given set of lattice vectors ν_i . Those vertices satisfy the R linear relations

$$\sum_{i=1}^n Q_i^{(r)} \nu_i = 0 \quad \text{for } r = 1, \dots, R. \quad (\text{A.7})$$

Therefore, associating ν_i to x_i shows that the linear relations (A.7) between the lattice vectors encode the projective equivalences (A.1) between the homogeneous coordinates. From this perspective the Stanley-Reisner ideal consists of all square-free monomials whose coordinates are not contained in any cone of the toric fan Σ_X .

A.2 Dimensions of Sheaf Cohomology Groups for Line Bundles

Given a toric variety X , the geometric input data of the algorithm [91, 212, 213] are the GLSM charges of the homogeneous coordinates and the Stanley-Reisner ideal generators. The algorithm counts the number of monomials where the total GLSM charge is equal to the divisor class of D , the divisor that specifies the line bundle $\mathcal{O}_X(D)$. The form of those monomials is restricted by the Stanley-Reisner ideal $\text{SR}(X)$. Negative integer exponents are only admissible for the coordinates contained in subsets of the Stanley-Reisner ideal generators. One therefore determines in the first step the set of square-free monomials \mathcal{Q} that arise from unions of the coordinates in any subset of $\text{SR}(X)$ generators, i.e. the set of negative exponents. For each such set of negative exponents—or square-free monomials \mathcal{Q} —there is an associated weighting factor $\mathfrak{h}_i(\mathcal{Q})$ that specifies to which cohomology group’s dimension $h^i(X; \mathcal{O}_X(D))$ the number of monomials $\mathcal{N}_D(\mathcal{Q})$ with GLSM charge D contributes. The total cohomology group dimension formula is then

$$\dim H^i(X; \mathcal{O}_X(D)) = \sum_{\mathcal{Q}} \overbrace{\mathfrak{h}_i(\mathcal{Q})}^{\text{multiplicity factor}} \cdot \underbrace{\mathcal{N}_D(\mathcal{Q})}_{\text{number of monomials}} \tag{A.8}$$

where the sum ranges over all square-free monomials that can be obtained from unions of Stanley-Reisner ideal generators.

A.2.1 Computation of multiplicity factors

The multiplicity factors are given as the group dimensions of an intermediate relative homology [90, 212]. As before, let X be a toric variety and let (A.3) be the Stanley-Reisner ideal that is generated by N square-free monomials. Let $[N] := \{1, \dots, N\}$ be the set of indices for those generators. For each subset

$$S_\rho := \{\mathcal{S}_{\rho_1}, \dots, \mathcal{S}_{\rho_k}\} \subset \{\mathcal{S}_1, \dots, \mathcal{S}_N\} \tag{A.9}$$

of generators let $\mathcal{Q}(S_\rho)$ denote the square-free monomial that arises from the union of all coordinates in each generator \mathcal{S}_{ρ_i} of the subset. Now construct a relative complex $\Gamma^\mathcal{Q}$ of the full simplex on $[N]$ by extracting only those subsets $\rho \subset [N]$ with $\mathcal{Q}(S_\rho) = \mathcal{Q}$, i.e. all combinations of Stanley-Reisner ideal generators leading to the same square-free monomial \mathcal{Q} . For some fixed cardinality $|\rho| = k$ this defines the set of $(k-1)$ -dimensional faces $F_{k-1}(\mathcal{Q})$ of $\Gamma^\mathcal{Q}$, i.e.

$$F_k(\mathcal{Q}) := \left\{ \rho \subset [N] : \begin{array}{l} |\rho| = k + 1 \\ \mathcal{Q}(S_\rho) = \mathcal{Q} \end{array} \right\}. \tag{A.10}$$

Let $\mathbb{C}^{F_k(\mathcal{Q})}$ be the complex vector space with basis vectors e_ρ corresponding to k -faces $\rho \in F_k(\mathcal{Q})$. The (relative) complex

$$F_\bullet(\mathcal{Q}) : \quad 0 \longrightarrow F_{N-1}(\mathcal{Q}) \xrightarrow{\phi_{N-1}} \cdots \xrightarrow{\phi_1} F_0(\mathcal{Q}) \xrightarrow{\phi_0} F_{-1}(\mathcal{Q}) \longrightarrow 0, \quad (\text{A.11})$$

where $F_{-1}(\mathcal{Q}) = \{\emptyset\}$ is a face of dimension -1 in this formalism, is then given by the mappings

$$\begin{aligned} \phi_k : F_k(\mathcal{Q}) &\longrightarrow F_{k-1}(\mathcal{Q}) \\ e_\rho &\mapsto \sum_{s \in \rho} \text{sign}(s, \rho) e_{\rho - \{s\}}. \end{aligned} \quad (\text{A.12})$$

A basis vector $e_{\rho - \{s\}}$ vanishes if ρ with the element s removed is not contained in $\Gamma^\mathcal{Q}$. Furthermore, $\text{sign}(s, \rho) := (-1)^{\ell-1}$ when s is the ℓ th element of $\rho \subset [N]$ written in increasing order. Then define the relabeling

$$\mathfrak{C}_i(\mathcal{Q}) := F_{|\mathcal{Q}|-i}(\mathcal{Q}) \quad (\text{A.13})$$

while leaving the mappings (A.12) untouched. The dimensions $\mathfrak{h}_i(\mathcal{Q}) := \dim H^i(\mathfrak{C}_\bullet(\mathcal{Q}))$ of the relabeled complex then gives the multiplicity factors for the square-free monomial \mathcal{Q} . Note that the $\mathfrak{h}_i(\mathcal{Q})$ only depend on the geometry of the toric variety.

A.2.2 Counting monomials

The second part of the algorithm depends on the GLSM charges of the homogeneous coordinates and the specific line bundle $\mathcal{O}_X(D)$. Let $I = (i_1, \dots, i_k, \dots, i_n)$ be an index relabeling such that the product of the first k coordinates $\mathcal{Q} = x_{i_1} \cdots x_{i_k}$ is a square-free monomial. For each \mathcal{Q} one counts monomials of the form

$$\begin{aligned} R^\mathcal{Q}(x_1, \dots, x_n) &:= (x_{i_1})^{-1-a} (x_{i_2})^{-1-b} \cdots (x_{i_k})^{-1-c} (x_{i_{k+1}})^d \cdots (x_{i_n})^e \\ &= \frac{T(x_{i_{k+1}}, \dots, x_{i_n})}{x_{i_1} \cdots x_{i_k} \cdot W(x_{i_1}, \dots, x_{i_k})}, \end{aligned} \quad (\text{A.14})$$

where T and W are monomials and $a, b, c, d, e \in \mathbb{N}_0$. Obviously, the coordinates of \mathcal{Q} are found in the denominator whereas their complements are in the numerator. Then define

$$\mathcal{N}_D(\mathcal{Q}) := \dim\{R^\mathcal{Q} : \deg_{\text{GLSM}}(R^\mathcal{Q}) = D\}, \quad (\text{A.15})$$

which counts the number of monomials of the specific form (A.14) that have the same GLSM degree as the divisor that specifies the line bundle $\mathcal{O}_X(D)$.

After completing the computation of the multiplicities $\mathfrak{h}^i(\mathcal{Q})$ in section A.2.1, the monomial counting only has to be carried out for those square-free monomials \mathcal{Q} where at least one factor $\mathfrak{h}^i(\mathcal{Q})$ is non-vanishing. All aforementioned steps have been conveniently implemented in a high-performance cross-platform package called **cohomCalc** [214].

A.5 Equivariant Cohomology

In orientifold and orbifold settings the internal part of the space-time is usually specified by a discrete symmetry acting on the “upstairs” geometry. This induces a corresponding splitting of the cohomology groups as the generating p -cycles can be either invariant or non-invariant under the symmetry:

$$H^i(X) = H_{\text{inv}}^i(X) \oplus H_{\text{non-inv}}^i(X). \quad (\text{A.25})$$

Furthermore, if a bundle is defined on the upstairs geometry, one has to specify the induced action on the bundle. A so-called equivariant structure [90, 216, 217] uplifts the action on the base geometry to the bundle and preserves the group structure. More precisely, for a generic group G , each element $g \in G$ induces a mapping $g : X \rightarrow X$ on the base geometry and has a corresponding uplift $\phi_g : V \rightarrow V$ compatible with the bundle structure, i.e. it makes the diagram

$$\begin{array}{ccc} V & \xrightarrow{\phi_g} & V \\ \pi \downarrow & & \downarrow \pi \\ X & \xrightarrow{g} & X \end{array} \quad \rightsquigarrow \quad g \circ \pi = \pi \circ \phi_g \quad (\text{A.26})$$

commutative. This G -structure on V is called an equivariant structure if it preserves the group structure, i.e. if $\phi_g \circ \phi_h = \phi_{gh}$ holds such that $g \mapsto \phi_g$ is a group homomorphism.

The case of primary interest here concerns line bundles L in orientifold settings, i.e. a \mathbb{Z}_2 -symmetry acting on the upstairs Calabi-Yau geometry X . In general, it is rather complicated to determine the invariant and non-invariant p -cycles of a geometry. A very useful tool is the Lefschetz theorem [89, 90, 217, 218]

$$\chi^\sigma(X; L) = \int_{X^\sigma} \text{ch}_\sigma(L) \frac{\text{Td}(T_{X^\sigma})}{\text{ch}_\sigma(\Lambda_{-1}(\bar{N}_{X^\sigma}))} \quad (\text{A.27})$$

that depends on the fixpoint set X^σ of the involution $\sigma : X \rightarrow X$ and generalizes the Riemann-Roch-Hirzebruch theorem [90, 117, 215]

$$\chi(X; L) = \int_X \text{ch}(L) \text{Td}(T_X). \quad (\text{A.28})$$

Here $\text{ch}(V)$ refers to the Chern character of V , a polynomial expression of the Chern classes

$$\begin{aligned} \text{ch}(V) := & \dim(V) + c_1(V) + \frac{1}{2} [c_1(V)^2 - c_2(V)] \\ & + \frac{1}{6} [c_1(V)^3 - 3c_1(V)c_2(V) + 3c_3(V)] + \dots, \end{aligned} \quad (\text{A.29})$$

satisfying $\text{ch}(V \oplus W) = \text{ch}(V) + \text{ch}(W)$ as well as $\text{ch}(V \otimes W) = \text{ch}(V) \text{ch}(W)$ and $\text{Td}(X) := \text{Td}(T_X)$ is the Todd class of the base space's tangent bundle, which can for a holomorphic vector bundle also be represented by a Chern class polynomial

$$\text{Td}(E) = 1 + \frac{1}{2}c_1(E) + \frac{1}{12}[c_1(E)^2 + c_2(E)] + \dots \quad (\text{A.30})$$

Note that for line bundles the Chern character simplifies to the simple Taylor expansion

$$\text{ch}(L) = e^{c_1(L)} = \sum_m \frac{c_1(L)^m}{m!} = 1 + c_1(L) + \frac{c_1(L)^2}{2} + \dots \quad (\text{A.31})$$

that naturally truncates at the dimension of the base space, leaving only a finite number of non-zero terms in the sum.

For the special case of the group \mathbb{Z}_2 (i.e. orientifold symmetries) both index theorems allow to compute the Euler characteristics of the invariant (“+”) and anti-invariant (“−”) part of the cohomology:

$$\begin{aligned} \chi(X/\sigma; L) = \chi_+(X; L) &= \sum_{i=0}^n (-1)^i h_+^i(X; L) = \frac{\chi(X; L) + \chi^\sigma(X; L)}{2} \\ \chi_-(X; L) &= \sum_{i=0}^n (-1)^i h_-^i(X; L) = \frac{\chi(X; L) - \chi^\sigma(X; L)}{2}. \end{aligned} \quad (\text{A.32})$$

Since $h_+^i + h_-^i = h^i$ has to hold for all i , the vanishing of the upstairs cohomology groups (i.e. $h^i = 0$ for some i) together with the values of χ_+ and χ_- often suffices to uniquely determine all h_+^i and h_-^i . However, evaluating (A.28) and in particular (A.27) for more involved geometries quickly becomes complicated.

Using the monomial representatives (A.14) of the algorithm presented in section A.2 one can formulate the following proposal [90, 217] for an alternative method of computation:

Conjecture for \mathbb{Z}_2 -equivariant line bundle sheaf cohomology: Given a toric variety X , an involution mapping $\sigma : X \rightarrow X$ as well as an equivariant structure on a line bundle L , the lifted involution mapping ϕ_σ can be directly applied to the monomials counted in the cohomology algorithm. The overall sign that a monomial picks up under the bundle involution determines whether it contributes to the invariant or anti-invariant cohomology group, and non-trivial multiplicities apply canonically in this counting.

The simplicity of this method stems from the fact that the involution mapping specified for the homogeneous coordinates of the toric base space X can be directly applied to

the monomials representing the sheaf cohomology. This conjecture can be generalized to allow for more general groups and has been successfully tested on numerous examples [90].

Backmatter

Figures & Tables

List of Figures

4.1	Generic geometric setting of E3-branes in IIB and M5-branes in F-theory	98
4.2	Self-intersecting D7-brane vs. factorized D7-brane/image brane pair	103
4.3	Invariant $O(1)$ instanton E3-brane and $U(1)$ instanton E3 brane/image brane pair	103
4.4	Intersection of E3-brane with $SU(n)$ 7-branes	108
4.5	Matter zero-modes (σ -invariant IIB / F-theory / IIB) depending on E3-brane divisor degree	113

List of Tables

2.1	Massless closed string spectrum of type II superstring theory	47
2.2	Massless open string spectrum of type II superstring theory	49
2.3	Hodge diamond of a Calabi-Yau 3-fold	53
2.4	Signs of the type IIB fields under the orientifold mapping	55
2.5	Multiplicities, bundles and representations arising from D-brane/O-plane intersections	57
2.6	Zero-modes of a $U(1)$ -instanton	62
2.7	Zero-modes of an $O(1)$ -instanton	62
3.1	Monodromies arising from combinations of non-perturbative A , B and C 7-branes	72
3.2	Kodaira classification of singular fibers in elliptically-fibered surfaces	75
3.3	Hodge diamond of a Calabi-Yau 4-fold and non-trivial relations between the Hodge numbers	78
3.4	Hodge diamonds of the del Pezzo surfaces	90

3.5	Standard Model representations in $SU(5)$ GUTs	91
3.6	Kodaira classification resulting from Tate's algorithm	94
4.1	Toric data for the F-theory uplift 4-fold over \mathbb{P}^3	99
4.2	Type IIB and F-theory zero-modes for an $O(1)$ instanton	105
4.3	Toric data for the resolution of an $SU(2)$ -enhancement singularity	109
4.4	Matching of the M5-brane Hodge diamond to the "upstairs" E3-brane topology and resolved matter curve	116
5.1	Toric data for the single del Pezzo transition of the quintic Calabi-Yau 3-fold $\mathbb{P}^4[5]$	123
5.2	Toric data for the downstairs Kähler 3-fold base $\mathcal{B} = \mathcal{X}/\sigma$ of the quintic's single del Pezzo transition	125
5.3	Toric data for the elliptically-fibered Calabi-Yau 4-fold \mathcal{Z} arising from the quintic's single del Pezzo transition	126
5.4	Enhancement pattern for an $SU(5)$ and $SO(10)$ gauge group	129
5.5	Toric data for the double del Pezzo transition of the quintic	133
5.6	Toric data for the downstairs Kähler 3-fold base \mathcal{B} of the quintic's double del Pezzo transition	135
5.7	Toric data for the downstairs Kähler 3-fold base \mathcal{B} of the quartic's non-generic del Pezzo transition	139
5.8	Toric data for the elliptically-fibered Calabi-Yau 4-fold \mathcal{Z} arising from the quartic's non-generic del Pezzo transition	140
5.9	Relevant gauge enhancements for $SU(5)$ GUT model building in the geometry derived from $\mathbb{P}^4[4]$	142
6.1	Standard model representations in $SU(5)$ GUTs resulting from the "twisted one-step breaking" of the GUT group	154
6.2	Representations and bundles in the $SU(5) \times U(1)_X$ representation	158
6.3	Representations in $SU(3) \times SU(2) \times U(1)_X \times U(1)_Y$ following the GUT symmetry breaking	162
6.4	Redefined Euler characteristic for E_n -type gauge groups	163
7.1	Nef-partitioned toric data for the elliptically-fibered Calabi-Yau 4-fold \mathcal{Z} arising from the non-generic del Pezzo transition of $\mathbb{P}^4[4]$	166
7.2	Nef-partitioned toric data for the resolved Calabi-Yau 4-fold	169

Curriculum Vitæ

Personal Information

Surname, Given Name: Jurke, Benjamin (Helmut Friedrich)

Date and Place of Birth: March 6, 1984 in Rheda-Wiedenbrück, NRW, Germany

Citizenship: German

Academic Background

- 06/2008 – 02/2011: PhD in Theoretical Physics at Max-Planck-Institut für Physik & Ludwig-Maximilians-Universität München, Germany
- 10/2002 – 05/2008: Diploma in Mathematics at Universität Bielefeld, Germany
- 10/2002 – 07/2007: Diploma in Physics at Universität Bielefeld, Germany
- 08/1994 – 06/2002: Abitur at Ratsgymnasium, Rheda-Wiedenbrück, Germany

Bibliography

- [1] K. Nakamura and P. D. Group, “Review of Particle Physics,” *Journal of Physics G: Nuclear and Particle Physics* **37** no. 7A, (2010) 075021.
- [2] T. Schücker, “Higgs-mass predictions,” [arXiv:0708.3344](https://arxiv.org/abs/0708.3344) [[hep-ph](#)].
- [3] A. A. Geraci, S. B. Papp, and J. Kitching, “Short-Range Force Detection Using Optically Cooled Levitated Microspheres,” *Phys. Rev. Lett.* **105** no. 10, (Aug, 2010) 101101.
- [4] M. Milgrom, “A modification of the Newtonian dynamics as a possible alternative to the hidden mass hypothesis,” *The Astrophysical Journal* **270** (1983) 365–370.
- [5] M. Milgrom, “A modification of the Newtonian dynamics-Implications for galaxies,” *The Astrophysical Journal* **270** (1983) 371–389.
- [6] J. D. Bekenstein, “The Modified Newtonian Dynamics: MOND and its implications for new physics,” *Contemp. Phys.* **47** (2007) 387, [arXiv:astro-ph/0701848](https://arxiv.org/abs/astro-ph/0701848) [[ASTRO-PH](#)].
- [7] J. Moffat, “Scalar–tensor–vector gravity theory,” *Journal of Cosmology and Astroparticle Physics* **2006** (2006) 004.
- [8] B. J. Carr, K. Kohri, Y. Sendouda, and J. Yokoyama, “New cosmological constraints on primordial black holes,” *Phys. Rev. D* **81** no. 10, (May, 2010) 104019, [arXiv:0912.5297](https://arxiv.org/abs/0912.5297) [[astro-ph.CO](#)].
- [9] S. Coleman and J. Mandula, “All Possible Symmetries of the S Matrix,” *Phys. Rev.* **159** (1967) 1251–1256.
- [10] R. Haag, J. T. Lopuszański, and M. Sohnius, “All possible generators of supersymmetries of the S-matrix,” *Nucl. Phys.* **B88** (Mar., 1975) 257–274.
- [11] Z. Bern, L. J. Dixon, and R. Roiban, “Is $N = 8$ Supergravity Ultraviolet Finite?,” *Phys. Lett.* **B644** (2007) 265–271, [arXiv:hep-th/0611086](https://arxiv.org/abs/hep-th/0611086).
- [12] R. Kallosh, “ $N=8$ Supergravity on the Light Cone,” *Phys. Rev.* **D80** (2009) 105022, [arXiv:0903.4630](https://arxiv.org/abs/0903.4630) [[hep-th](#)].
- [13] H. Georgi and S. L. Glashow, “Unity of All Elementary-Particle Forces,” *Phys. Rev. Lett.* **32** (Feb., 1974) 438–441.
- [14] H. Fritzsch and P. Minkowski, “Unified interactions of leptons and hadrons,” *Annals of Physics* **93** (Sept., 1975) 193–266.

-
- [15] M. B. Green, J. H. Schwarz, and E. Witten, *Superstring Theory: Vol. 1: Introduction*. Cambridge University Press, 1988.
- [16] M. B. Green, J. H. Schwarz, and E. Witten, *Superstring Theory: Vol. 2: Loop Amplitudes, Anomalies and Phenomenology*. Cambridge University Press, 1988.
- [17] D. Lüst and S. Theisen, *Lectures on String Theory (Lecture Notes in Physics)*. Springer, 1989.
- [18] D. Bailin and A. Love, *Supersymmetric Gauge Field Theory and String Theory*. Taylor & Francis, 1994.
- [19] M. Kaku, *Introduction to Superstrings and M-Theory*. Springer, 1998.
- [20] M. Kaku, *Strings, Conformal Fields, and M-Theory*. Springer, 2000.
- [21] P. Deligne *et al.*, *Quantum Fields and Strings: A Course for Mathematicians (2 Volume Set)*. American Mathematical Society, 1999.
- [22] J. Polchinski, *String Theory, Vol. 1: An Introduction to the Bosonic String*. Cambridge University Press, 2005.
- [23] J. Polchinski, *String Theory, Vol. 2: Superstring Theory and Beyond*. Cambridge University Press, 2005.
- [24] C. V. Johnson, *D-Branes*. Cambridge University Press, 2006.
- [25] K. Becker, M. Becker, and J. H. Schwarz, *String Theory and M-Theory: A Modern Introduction*. Cambridge University Press, 2007.
- [26] E. Kiritsis, *String Theory in a Nutshell*. Princeton University Press, 2007.
- [27] P. H. Ginsparg, “Applied Conformal Field Theory,” [arXiv:hep-th/9108028](https://arxiv.org/abs/hep-th/9108028) [[hep-th](https://arxiv.org/abs/hep-th)].
- [28] M. R. Gaberdiel, “An introduction to conformal field theory,” *Rept. Prog. Phys.* **63** (2000) 607–667, [arXiv:hep-th/9910156](https://arxiv.org/abs/hep-th/9910156).
- [29] P. Francesco, P. Mathieu, and D. Senechal, *Conformal Field Theory*. Springer, 1996.
- [30] M. Schottenloher, *A Mathematical Introduction to Conformal Field Theory*. Springer, 2008.
- [31] R. Blumenhagen and E. Plauschinn, *Introduction to Conformal Field Theory: With Applications to String Theory*. Springer, 2009.
- [32] D. Lüst, S. Stieberger, and T. R. Taylor, “The LHC String Hunter’s Companion,” *Nucl. Phys.* **B808** (2009) 1–52, [arXiv:0807.3333](https://arxiv.org/abs/0807.3333) [[hep-th](https://arxiv.org/abs/hep-th)].
- [33] D. Lüst, O. Schlotterer, S. Stieberger, and T. R. Taylor, “The LHC String Hunter’s Companion (II): Five-Particle Amplitudes and Universal Properties,” *Nucl. Phys.*

- B828** (2010) 139–200, [arXiv:0908.0409](#) [hep-th].
- [34] W.-Z. Feng, D. Lüst, O. Schlotterer, S. Stieberger, and T. R. Taylor, “Direct Production of Lightest Regge Resonances,” *Nucl. Phys.* **B843** (2011) 570–601, [arXiv:1007.5254](#) [hep-th].
- [35] F. Gliozzi, J. Scherk, and D. I. Olive, “Supergravity and the Spinor Dual Model,” *Phys. Lett.* **B65** (1976) 282.
- [36] F. Gliozzi, J. Scherk, and D. I. Olive, “Supersymmetry, Supergravity Theories and the Dual Spinor Model,” *Nucl. Phys.* **B122** (1977) 253–290.
- [37] M. B. Green and J. H. Schwarz, “Supersymmetrical Dual String Theory,” *Nucl. Phys.* **B181** (1981) 502–530.
- [38] M. B. Green and J. H. Schwarz, “Supersymmetrical Dual String Theory. 2. Vertices and Trees,” *Nucl. Phys.* **B198** (1982) 252–268.
- [39] M. B. Green and J. H. Schwarz, “Supersymmetrical Dual String Theory. 3. Loops and Renormalization,” *Nucl. Phys.* **B198** (1982) 441–460.
- [40] M. B. Green and J. H. Schwarz, “Supersymmetrical String Theories,” *Phys. Lett.* **B109** (1982) 444–448.
- [41] J. Polchinski, “Dirichlet Branes and Ramond-Ramond charges,” *Phys. Rev. Lett.* **75** (1995) 4724–4727, [arXiv:hep-th/9510017](#) [hep-th].
- [42] R. Blumenhagen, M. Cvetič, P. Langacker, and G. Shiu, “Toward realistic intersecting D-brane models,” *Ann. Rev. Nucl. Part. Sci.* **55** (2005) 71–139, [arXiv:hep-th/0502005](#).
- [43] R. Blumenhagen, B. Körs, D. Lüst, and S. Stieberger, “Four-dimensional String Compactifications with D-Branes, Orientifolds and Fluxes,” *Phys. Rept.* **445** (2007) 1–193, [arXiv:hep-th/0610327](#).
- [44] A. Strominger, “Quantum gravity and string theory: What have we learned?,” [arXiv:hep-th/9110011](#).
- [45] S. R. Wadia, “String Theory: A Framework for Quantum Gravity and Various Applications,” [arXiv:0809.1036](#) [gr-qc].
- [46] A. Strominger and C. Vafa, “Microscopic Origin of the Bekenstein-Hawking Entropy,” *Phys. Lett.* **B379** (1996) 99–104, [arXiv:hep-th/9601029](#).
- [47] S. D. Mathur, “The fuzzball proposal for black holes: An elementary review,” *Fortsch. Phys.* **53** (2005) 793–827, [arXiv:hep-th/0502050](#).
- [48] S. D. Mathur, “Fuzzballs and the information paradox: a summary and conjectures,” [arXiv:0810.4525](#) [hep-th].

-
- [49] S. D. Mathur, “The quantum structure of black holes,” *Class. Quant. Grav.* **23** (2006) R115, [arXiv:hep-th/0510180](#).
- [50] L. Randall and R. Sundrum, “A large mass hierarchy from a small extra dimension,” *Phys. Rev. Lett.* **83** (1999) 3370–3373, [arXiv:hep-ph/9905221](#).
- [51] L. Randall and R. Sundrum, “An alternative to compactification,” *Phys. Rev. Lett.* **83** (1999) 4690–4693, [arXiv:hep-th/9906064](#).
- [52] N. Arkani-Hamed, S. Dimopoulos, and G. R. Dvali, “The hierarchy problem and new dimensions at a millimeter,” *Phys. Lett.* **B429** (1998) 263–272, [arXiv:hep-ph/9803315](#).
- [53] T. Kaluza, “On the Problem of Unity in Physics,” *Sitzungsber. Preuss. Akad. Wiss. Berlin (Math. Phys.)* **1921** (1921) 966–972.
- [54] P. Candelas, G. T. Horowitz, A. Strominger, and E. Witten, “Vacuum configurations for superstrings,” *Nucl. Phys.* **B258** (1985) 46–74.
- [55] P. Horava and E. Witten, “Heterotic and type I string dynamics from eleven dimensions,” *Nucl. Phys.* **B460** (1996) 506–524, [arXiv:hep-th/9510209](#).
- [56] P. K. Townsend, “Four lectures on M-theory,” [arXiv:hep-th/9612121](#).
- [57] M. Haack, B. Körs, and D. Lüst, “Recent developments in string theory: From perturbative dualities to M-theory,” [arXiv:hep-th/9904033](#).
- [58] M. Dine, “TASI lectures on M theory phenomenology,” [arXiv:hep-th/0003175](#).
- [59] C. Vafa, “Evidence for F-Theory,” *Nucl. Phys.* **B469** (1996) 403–418, [arXiv:hep-th/9602022](#).
- [60] M. R. Gaberdiel and B. Zwiebach, “Exceptional groups from open strings,” *Nucl. Phys.* **B518** (1998) 151–172, [arXiv:hep-th/9709013](#) [[hep-th](#)]. (Revised in September 1997).
- [61] M. R. Gaberdiel, T. Hauer, and B. Zwiebach, “Open string-string junction transitions,” *Nucl. Phys.* **B525** (1998) 117–145, [arXiv:hep-th/9801205](#) [[hep-th](#)].
- [62] T. Hauer, “Equivalent string networks and uniqueness of BPS states,” *Nucl. Phys.* **B538** (1999) 117–136, [arXiv:hep-th/9805076](#) [[hep-th](#)].
- [63] O. DeWolfe, “Affine Lie algebras, string junctions and seven-branes,” *Nucl. Phys.* **B550** (1999) 622–637, [arXiv:hep-th/9809026](#) [[hep-th](#)].
- [64] O. DeWolfe, T. Hauer, A. Iqbal, and B. Zwiebach, “Uncovering the symmetries on [p,q] seven-branes: Beyond the Kodaira classification,” *Adv. Theor. Math. Phys.* **3** (1999) 1785–1833, [arXiv:hep-th/9812028](#) [[hep-th](#)].

- [65] O. DeWolfe, T. Hauer, A. Iqbal, and B. Zwiebach, “Uncovering infinite symmetries on [p, q] 7-branes: Kac-Moody algebras and beyond,” *Adv. Theor. Math. Phys.* **3** (1999) 1835–1891, [arXiv:hep-th/9812209](#) [hep-th].
- [66] R. Donagi and M. Wijnholt, “Model Building with F-Theory,” [arXiv:0802.2969](#) [hep-th].
- [67] C. Beasley, J. J. Heckman, and C. Vafa, “GUTs and Exceptional Branes in F-theory - I,” *JHEP* **0901** (2009) 058, [arXiv:0802.3391](#) [hep-th].
- [68] C. Beasley, J. J. Heckman, and C. Vafa, “GUTs and Exceptional Branes in F-theory - II: Experimental Predictions,” *JHEP* **0901** (2009) 059, [arXiv:0806.0102](#) [hep-th].
- [69] R. Donagi and M. Wijnholt, “Breaking GUT Groups in F-Theory,” [arXiv:0808.2223](#) [hep-th].
- [70] R. Blumenhagen, M. Cvetič, D. Lüst, . Richter, Robert, and T. Weigand, “Non-perturbative Yukawa Couplings from String Instantons,” *Phys. Rev. Lett.* **100** (2008) 061602, [arXiv:0707.1871](#) [hep-th].
- [71] J. J. Heckman and C. Vafa, “F-theory, GUTs, and the Weak Scale,” *JHEP* **09** (2009) 079, [arXiv:0809.1098](#) [hep-th].
- [72] A. Font and L. E. Ibanez, “Yukawa Structure from U(1) Fluxes in F-theory Grand Unification,” *JHEP* **02** (2009) 016, [arXiv:0811.2157](#) [hep-th].
- [73] J. J. Heckman and C. Vafa, “Flavor Hierarchy From F-theory,” *Nucl. Phys.* **B837** (2010) 137–151, [arXiv:0811.2417](#) [hep-th].
- [74] R. Blumenhagen, “Gauge Coupling Unification in F-Theory Grand Unified Theories,” *Phys. Rev. Lett.* **102** (2009) 071601, [arXiv:0812.0248](#) [hep-th].
- [75] J. J. Heckman, A. Tavanfar, and C. Vafa, “Cosmology of F-theory GUTs,” *JHEP* **04** (2010) 054, [arXiv:0812.3155](#) [hep-th].
- [76] J. L. Bourjaily, “Local Models in F-Theory and M-Theory with Three Generations,” [arXiv:0901.3785](#) [hep-th].
- [77] H. Hayashi, T. Kawano, R. Tatar, and T. Watari, “Codimension-3 Singularities and Yukawa Couplings in F- theory,” *Nucl. Phys.* **B823** (2009) 47–115, [arXiv:0901.4941](#) [hep-th].
- [78] J. J. Heckman, G. L. Kane, J. Shao, and C. Vafa, “The Footprint of F-theory at the LHC,” *JHEP* **10** (2009) 039, [arXiv:0903.3609](#) [hep-ph].
- [79] V. Bouchard, J. J. Heckman, J. Seo, and C. Vafa, “F-theory and Neutrinos: Kaluza-Klein Dilution of Flavor Hierarchy,” *JHEP* **01** (2010) 061, [arXiv:0904.1419](#) [hep-ph].

- [80] L. Randall and D. Simmons-Duffin, “Quark and Lepton Flavor Physics from F-Theory,” [arXiv:0904.1584](#) [hep-ph].
- [81] J. J. Heckman and C. Vafa, “CP Violation and F-theory GUTs,” [arXiv:0904.3101](#) [hep-th].
- [82] R. Tatar, Y. Tsuchiya, and T. Watari, “Right-handed Neutrinos in F-theory Compactifications,” *Nucl. Phys.* **B823** (2009) 1–46, [arXiv:0905.2289](#) [hep-th].
- [83] J. Jiang, T. Li, D. V. Nanopoulos, and D. Xie, “Flipped $SU(5)XU(1)_X$ Models from F-Theory,” *Nucl. Phys.* **B830** (2010) 195–220, [arXiv:0905.3394](#) [hep-th].
- [84] T. Li, “ $SU(5)$ and $SO(10)$ Models from F-Theory with Natural Yukawa Couplings,” *Phys. Rev.* **D81** (2010) 065018, [arXiv:0905.4563](#) [hep-th].
- [85] J. J. Heckman, “Particle Physics Implications of F-theory,” [arXiv:1001.0577](#) [hep-th].
- [86] B. Andreas and G. Curio, “From Local to Global in F-Theory Model Building,” *J. Geom. Phys.* **60** (2010) 1089–1102, [arXiv:0902.4143](#) [hep-th].
- [87] R. Blumenhagen, T. W. Grimm, B. Jurke, and T. Weigand, “F-theory uplifts and GUTs,” *JHEP* **0909** (2009) 053, [arXiv:0906.0013](#) [hep-th].
- [88] R. Blumenhagen, T. W. Grimm, B. Jurke, and T. Weigand, “Global F-theory GUTs,” *Nucl. Phys.* **B829** (2010) 325–369, [arXiv:0908.1784](#) [hep-th].
- [89] R. Blumenhagen, A. Collinucci, and B. Jurke, “On Instanton Effects in F-theory,” *JHEP* **1008** (2010) 079, [arXiv:1002.1894](#) [hep-th].
- [90] R. Blumenhagen, B. Jurke, T. Rahn, and H. Roschy, “Cohomology of Line Bundles: Applications,” [arXiv:1010.3717](#) [hep-th].
- [91] R. Blumenhagen, B. Jurke, T. Rahn, and H. Roschy, “Cohomology of Line Bundles: A Computational Algorithm,” *J. Math. Phys.* **51** (2010) 103525, [arXiv:1003.5217](#) [hep-th].
- [92] R. Bohm, H. Gunther, C. Herrmann, and J. Louis, “Compactification of type IIB string theory on Calabi-Yau threefolds,” *Nucl. Phys.* **B569** (2000) 229–246, [arXiv:hep-th/9908007](#).
- [93] G. Dall’Agata, “Type IIB supergravity compactified on a Calabi-Yau manifold with H-fluxes,” *JHEP* **11** (2001) 005, [arXiv:hep-th/0107264](#).
- [94] J. Louis and A. Micu, “Type II theories compactified on Calabi-Yau threefolds in the presence of background fluxes,” *Nucl. Phys.* **B635** (2002) 395–431, [arXiv:hep-th/0202168](#).
- [95] A. Dabholkar and J. Park, “Strings on Orientifolds,” *Nucl. Phys.* **B477** (1996)

- 701–714, [arXiv:hep-th/9604178](#).
- [96] I. Brunner, K. Hori, K. Hosomichi, and J. Walcher, “Orientifolds of Gepner models,” *JHEP* **02** (2007) 001, [arXiv:hep-th/0401137](#).
- [97] T. W. Grimm and J. Louis, “The effective action of $N = 1$ Calabi-Yau orientifolds,” *Nucl. Phys.* **B699** (2004) 387–426, [arXiv:hep-th/0403067](#).
- [98] S. H. Katz and E. Sharpe, “D-branes, open string vertex operators, and Ext groups,” *Adv. Theor. Math. Phys.* **6** (2003) 979–1030, [arXiv:hep-th/0208104](#).
- [99] R. Blumenhagen, V. Braun, T. W. Grimm, and T. Weigand, “GUTs in Type IIB Orientifold Compactifications,” *Nucl. Phys.* **B815** (2009) 1–94, [arXiv:0811.2936 \[hep-th\]](#).
- [100] R. Blumenhagen, M. Cvetič, S. Kachru, and T. Weigand, “D-Brane Instantons in Type II Orientifolds,” *Ann. Rev. Nucl. Part. Sci.* **59** (2009) 269–296, [arXiv:0902.3251 \[hep-th\]](#).
- [101] M. Billo *et al.*, “Classical gauge instantons from open strings,” *JHEP* **02** (2003) 045, [arXiv:hep-th/0211250](#).
- [102] E. Witten, “Non-Perturbative Superpotentials In String Theory,” *Nucl. Phys.* **B474** (1996) 343–360, [arXiv:hep-th/9604030](#).
- [103] J. Park, “D3 instantons in Calabi-Yau orientifolds with(out) fluxes,” *Eur. Phys. J.* **C67** (2010) 263–271, [arXiv:hep-th/0507091](#).
- [104] D. Lüst, S. Reffert, W. Schulgin, and P. K. Tripathy, “Fermion Zero Modes in the Presence of Fluxes and a Non-perturbative Superpotential,” *JHEP* **08** (2006) 071, [arXiv:hep-th/0509082](#).
- [105] R. Blumenhagen, M. Cvetič, R. Richter, 2, and T. Weigand, “Lifting D-Instanton Zero Modes by Recombination and Background Fluxes,” *JHEP* **10** (2007) 098, [arXiv:0708.0403 \[hep-th\]](#).
- [106] S. Coleman and S. L. Glashow, “Departures from the Eightfold Way: Theory of Strong Interaction Symmetry Breakdown,” *Phys. Rev.* **134** no. 3B, (May, 1964) B671–B681.
- [107] S. Gukov, C. Vafa, and E. Witten, “CFT’s from Calabi-Yau four-folds,” *Nucl. Phys.* **B584** (2000) 69–108, [arXiv:hep-th/9906070](#).
- [108] J. M. Maldacena and C. Nunez, “Supergravity description of field theories on curved manifolds and a no go theorem,” *Int. J. Mod. Phys.* **A16** (2001) 822–855, [arXiv:hep-th/0007018](#).
- [109] M. Grana, “Flux compactifications in string theory: A comprehensive review,” *Phys. Rept.* **423** (2006) 91–158, [arXiv:hep-th/0509003](#).

-
- [110] S. Sethi, C. Vafa, and E. Witten, “Constraints on low-dimensional string compactifications,” *Nucl. Phys.* **B480** (1996) 213–224, [arXiv:hep-th/9606122](#).
- [111] A. Collinucci, F. Denef, and M. Esole, “D-brane Deconstructions in IIB Orientifolds,” *JHEP* **02** (2009) 005, [arXiv:0805.1573 \[hep-th\]](#).
- [112] E. Plauschinn, “The Generalized Green-Schwarz Mechanism for Type IIB Orientifolds with D3- and D7-Branes,” *JHEP* **05** (2009) 062, [arXiv:0811.2804 \[hep-th\]](#).
- [113] D. S. Freed and E. Witten, “Anomalies in string theory with D-branes,” [arXiv:hep-th/9907189](#).
- [114] E. Witten, “D-branes and K-theory,” *JHEP* **12** (1998) 019, [arXiv:hep-th/9810188](#).
- [115] A. M. Uranga, “D-brane probes, RR tadpole cancellation and K-theory charge,” *Nucl. Phys.* **B598** (2001) 225–246, [arXiv:hep-th/0011048](#).
- [116] J. Evslin, “What does(n’t) K-theory classify?,” [arXiv:hep-th/0610328](#).
- [117] F. Denef, “Les Houches Lectures on Constructing String Vacua,” [arXiv:0803.1194 \[hep-th\]](#).
- [118] R. Blumenhagen, “Basics of F-theory from the Type IIB Perspective,” *Fortsch. Phys.* **58** (2010) 820–826, [arXiv:1002.2836 \[hep-th\]](#).
- [119] T. Weigand, “Lectures on F-theory compactifications and model building,” *Class. Quant. Grav.* **27** (2010) 214004, [arXiv:1009.3497 \[hep-th\]](#).
- [120] B. R. Greene, A. Shapere, C. Vafa, and S. Yau, “Stringy cosmic strings and noncompact Calabi-Yau manifolds,” *Nucl. Phys.* **B337** (June, 1990) 1–36.
- [121] A. P. Braun, A. Hebecker, and H. Triendl, “D7-Brane Motion from M-Theory Cycles and Obstructions in the Weak Coupling Limit,” *Nucl. Phys.* **B800** (2008) 298–329, [arXiv:0801.2163 \[hep-th\]](#).
- [122] J. H. Schwarz, “An $SL(2, Z)$ multiplet of type IIB superstrings,” *Phys. Lett.* **B360** (1995) 13–18, [arXiv:hep-th/9508143](#).
- [123] E. Witten, “Bound states of strings and p-branes,” *Nucl. Phys.* **B460** (1996) 335–350, [arXiv:hep-th/9510135](#).
- [124] A. Sen, “F-theory and Orientifolds,” *Nucl. Phys.* **B475** (1996) 562–578, [arXiv:hep-th/9605150](#).
- [125] A. Sen, “F-theory and the Gimon-Polchinski orientifold,” *Nucl. Phys.* **B498** (1997) 135–155, [arXiv:hep-th/9702061](#).
- [126] A. Sen, “Orientifold limit of F-theory vacua,” *Nucl. Phys. Proc. Suppl.* **68** (1998) 92–98, [arXiv:hep-th/9709159](#).

- [127] P. Mayr, “Mirror symmetry, $N = 1$ superpotentials and tensionless strings on Calabi-Yau four-folds,” *Nucl. Phys.* **B494** (1997) 489–545, [arXiv:hep-th/9610162](#).
- [128] A. Klemm, B. Lian, S. S. Roan, and S.-T. Yau, “Calabi-Yau fourfolds for M- and F-theory compactifications,” *Nucl. Phys.* **B518** (1998) 515–574, [arXiv:hep-th/9701023](#).
- [129] P. Candelas, E. Peveralov, and G. Rajesh, “Toric geometry and enhanced gauge symmetry of F- theory/heterotic vacua,” *Nucl. Phys.* **B507** (1997) 445–474, [arXiv:hep-th/9704097](#).
- [130] S. H. Katz and C. Vafa, “Matter from geometry,” *Nucl. Phys.* **B497** (1997) 146–154, [arXiv:hep-th/9606086](#).
- [131] S. H. Katz and C. Vafa, “Geometric engineering of $N = 1$ quantum field theories,” *Nucl. Phys.* **B497** (1997) 196–204, [arXiv:hep-th/9611090](#).
- [132] M. Bershadsky, K. A. Intriligator, S. Kachru, D. R. Morrison, V. Sadov, *et al.*, “Geometric singularities and enhanced gauge symmetries,” *Nucl. Phys.* **B481** (1996) 215–252, [arXiv:hep-th/9605200](#) [hep-th].
- [133] J. Tate, “Algorithm for determining the type of a singular fiber in an elliptic pencil,” in *Modular Functions of One Variable IV*, B. Birch and W. Kuyk, eds., vol. 476 of *Lecture Notes in Mathematics*, pp. 33–52. Springer Berlin / Heidelberg, 1975.
- [134] P. Aluffi and M. Esole, “New Orientifold Weak Coupling Limits in F-theory,” *JHEP* **02** (2010) 020, [arXiv:0908.1572](#) [hep-th].
- [135] K. Kodaira, “On compact analytic surfaces,” *Annals of Math.* **71** (1960) 111–152.
- [136] K. Kodaira, “On compact analytic surfaces: II,” *Annals of Math.* **77** (1963) 563–626.
- [137] K. Becker and M. Becker, “M-Theory on Eight-Manifolds,” *Nucl. Phys.* **B477** (1996) 155–167, [arXiv:hep-th/9605053](#).
- [138] K. Dasgupta, G. Rajesh, and S. Sethi, “M theory, orientifolds and G-flux,” *JHEP* **08** (1999) 023, [arXiv:hep-th/9908088](#).
- [139] M. Haack and J. Louis, “M-theory compactified on Calabi-Yau fourfolds with background flux,” *Phys. Lett.* **B507** (2001) 296–304, [arXiv:hep-th/0103068](#).
- [140] J. Marsano, N. Saulina, and S. Schafer-Nameki, “A Note on G-Fluxes for F-theory Model Building,” *JHEP* **11** (2010) 088, [arXiv:1006.0483](#) [hep-th].
- [141] A. Collinucci and R. Savelli, “On Flux Quantization in F-Theory,” [arXiv:1011.6388](#) [hep-th].
- [142] D. R. Morrison and C. Vafa, “Compactifications of F theory on Calabi-Yau threefolds. 1,” *Nucl. Phys.* **B473** (1996) 74–92, [arXiv:hep-th/9602114](#) [hep-th].

-
- [143] D. R. Morrison and C. Vafa, “Compactifications of F theory on Calabi-Yau threefolds. 2.,” *Nucl. Phys.* **B476** (1996) 437–469, [arXiv:hep-th/9603161](#) [[hep-th](#)].
- [144] R. Friedman, J. Morgan, and E. Witten, “Vector bundles and F theory,” *Commun. Math. Phys.* **187** (1997) 679–743, [arXiv:hep-th/9701162](#).
- [145] G. Curio and R. Y. Donagi, “Moduli in $N = 1$ heterotic/F-theory duality,” *Nucl. Phys.* **B518** (1998) 603–631, [arXiv:hep-th/9801057](#).
- [146] H. Hayashi, R. Tatar, Y. Toda, T. Watari, and M. Yamazaki, “New Aspects of Heterotic–F Theory Duality,” *Nucl. Phys.* **B806** (2009) 224–299, [arXiv:0805.1057](#) [[hep-th](#)].
- [147] T. W. Grimm, T.-W. Ha, A. Klemm, and D. Klevers, “Five-Brane Superpotentials and Heterotic/F-theory Duality,” *Nucl. Phys.* **B838** (2010) 458–491, [arXiv:0912.3250](#) [[hep-th](#)].
- [148] H. Jockers, P. Mayr, and J. Walcher, “On $N=1$ 4d Effective Couplings for F-theory and Heterotic Vacua,” [arXiv:0912.3265](#) [[hep-th](#)].
- [149] R. Y. Donagi, “Principal bundles on elliptic fibrations,” [arXiv:alg-geom/9702002](#).
- [150] K. Dasgupta and S. Mukhi, “F-theory at constant coupling,” *Phys. Lett.* **B385** (1996) 125–131, [arXiv:hep-th/9606044](#).
- [151] C.-h. Ahn and S. Nam, “Compactifications of F theory on Calabi-Yau threefolds at constant coupling,” *Phys. Lett.* **B419** (1998) 132–138, [arXiv:hep-th/9701129](#) [[hep-th](#)].
- [152] A. Collinucci, “New F-theory lifts,” *JHEP* **08** (2009) 076, [arXiv:0812.0175](#) [[hep-th](#)].
- [153] A. Collinucci, “New F-theory lifts II: Permutation orientifolds and enhanced singularities,” *JHEP* **04** (2010) 076, [arXiv:0906.0003](#) [[hep-th](#)].
- [154] C. Cordova, “Decoupling Gravity in F-Theory,” [arXiv:0910.2955](#) [[hep-th](#)].
- [155] S. Cecotti, M. C. N. Cheng, J. J. Heckman, and C. Vafa, “Yukawa Couplings in F-theory and Non-Commutative Geometry,” [arXiv:0910.0477](#) [[hep-th](#)].
- [156] E. Dudas and E. Palti, “On hypercharge flux and exotics in F-theory GUTs,” *JHEP* **09** (2010) 013, [arXiv:1007.1297](#) [[hep-ph](#)].
- [157] R. Donagi and M. Wijnholt, “Higgs Bundles and UV Completion in F-Theory,” [arXiv:0904.1218](#) [[hep-th](#)].
- [158] J. Marsano, N. Saulina, and S. Schäfer-Nameki, “F-theory Compactifications for Supersymmetric GUTs,” *JHEP* **0908** (2009) 030, [arXiv:0904.3932](#) [[hep-th](#)].

- [159] J. Marsano, N. Saulina, and S. Schäfer-Nameki, “Monodromies, Fluxes, and Compact Three-Generation F-theory GUTs,” *JHEP* **0908** (2009) 046, [arXiv:0906.4672 \[hep-th\]](#).
- [160] J. Marsano, N. Saulina, and S. Schäfer-Nameki, “Compact F-theory GUTs with $U(1)_{PQ}$,” *JHEP* **1004** (2010) 095, [arXiv:0912.0272 \[hep-th\]](#).
- [161] T. W. Grimm, S. Krause, and T. Weigand, “F-Theory GUT Vacua on Compact Calabi-Yau Fourfolds,” *JHEP* **07** (2010) 037, [arXiv:0912.3524 \[hep-th\]](#).
- [162] C.-M. Chen, J. Knapp, M. Kreuzer, and C. Mayrhofer, “Global $SO(10)$ F-theory GUTs,” [arXiv:1005.5735 \[hep-th\]](#).
- [163] R. Blumenhagen, B. Körs, D. Lüst, and T. Ott, “The standard model from stable intersecting brane world orbifolds,” *Nucl. Phys.* **B616** (2001) 3–33, [arXiv:hep-th/0107138](#).
- [164] R. Blumenhagen, M. Cvetič, and T. Weigand, “Spacetime instanton corrections in 4D string vacua - the seesaw mechanism for D-brane models,” *Nucl. Phys.* **B771** (2007) 113–142, [arXiv:hep-th/0609191](#).
- [165] L. E. Ibanez and A. M. Uranga, “Neutrino Majorana masses from string theory instanton effects,” *JHEP* **03** (2007) 052, [arXiv:hep-th/0609213](#).
- [166] L. E. Ibanez, A. N. Schellekens, and A. M. Uranga, “Instanton Induced Neutrino Majorana Masses in CFT Orientifolds with MSSM-like spectra,” *JHEP* **06** (2007) 011, [arXiv:0704.1079 \[hep-th\]](#).
- [167] M. Cvetič, I. Garcia-Etxebarria, and R. Richter, 2, “Branes and instantons intersecting at angles,” *JHEP* **01** (2010) 005, [arXiv:0905.1694 \[hep-th\]](#).
- [168] M. Cvetič, I. Garcia-Etxebarria, and R. Richter, “Branes and instantons at angles and the F-theory lift of $O(1)$ instantons,” *AIP Conf. Proc.* **1200** (2010) 246–260, [arXiv:0911.0012 \[hep-th\]](#).
- [169] E. Witten, “Five-brane effective action in M-theory,” *J. Geom. Phys.* **22** (1997) 103–133, [arXiv:hep-th/9610234](#).
- [170] T. W. Grimm and T. Weigand, “On Abelian Gauge Symmetries and Proton Decay in Global F-theory GUTs,” *Phys. Rev.* **D82** (2010) 086009, [arXiv:1006.0226 \[hep-th\]](#).
- [171] S. Kachru, R. Kallosh, A. D. Linde, and S. P. Trivedi, “De Sitter vacua in string theory,” *Phys. Rev.* **D68** (2003) 046005, [arXiv:hep-th/0301240](#).
- [172] J. Marsano, N. Saulina, and S. Schäfer-Nameki, “Gauge Mediation in F-Theory GUT Models,” *Phys. Rev.* **D80** (2009) 046006, [arXiv:0808.1571 \[hep-th\]](#).

-
- [173] J. J. Heckman, J. Marsano, N. Saulina, S. Schafer-Nameki, and C. Vafa, “Instantons and SUSY breaking in F-theory,” [arXiv:0808.1286](#) [[hep-th](#)].
- [174] J. Marsano, N. Saulina, and S. Schafer-Nameki, “An Instanton Toolbox for F-Theory Model Building,” *JHEP* **01** (2010) 128, [arXiv:0808.2450](#) [[hep-th](#)].
- [175] T. W. Grimm and A. Klemm, “U(1) Mediation of Flux Supersymmetry Breaking,” *JHEP* **10** (2008) 077, [arXiv:0805.3361](#) [[hep-th](#)].
- [176] P. Aluffi and M. Esole, “Chern class identities from tadpole matching in type IIB and F-theory,” *JHEP* **03** (2009) 032, [arXiv:0710.2544](#) [[hep-th](#)].
- [177] B. Andreas and G. Curio, “On discrete twist and four-flux in $N = 1$ heterotic/F-theory compactifications,” *Adv. Theor. Math. Phys.* **3** (1999) 1325–1413, [arXiv:hep-th/9908193](#).
- [178] V. A. Iskovskih, “Fano 3-folds. I,” *Mathematics of the USSR-Izvestiya* **11** no. 3, (1977) 485.
- [179] V. A. Iskovskih, “Fano 3-folds. II,” *Mathematics of the USSR-Izvestiya* **12** no. 3, (1978) 469.
- [180] S. Mori and S. Mukai, “Classification of Fano 3-folds with $b_2 \geq 2$,” *manuscripta mathematica* **36** (1981) 147–162.
- [181] S. Mori and S. Mukai, “On Fano 3-folds with $b_2 \geq 2$.” Algebraic varieties and analytic varieties, Proc. Symp., Tokyo 1981, Adv. Stud. Pure Math. 1, 101-129 (1983)., 1983.
- [182] H. Hayashi, T. Kawano, Y. Tsuchiya, and T. Watari, “More on Dimension-4 Proton Decay Problem in F-theory – Spectral Surface, Discriminant Locus and Monodromy,” *Nucl. Phys.* **B840** (2010) 304–348, [arXiv:1004.3870](#) [[hep-th](#)].
- [183] R. Donagi, Y.-H. He, B. A. Ovrut, and R. Reinbacher, “The particle spectrum of heterotic compactifications,” *JHEP* **12** (2004) 054, [arXiv:hep-th/0405014](#).
- [184] R. Blumenhagen, S. Moster, R. Reinbacher, and T. Weigand, “Massless spectra of three generation U(N) heterotic string vacua,” *JHEP* **05** (2007) 041, [arXiv:hep-th/0612039](#).
- [185] R. Blumenhagen, G. Honecker, and T. Weigand, “Loop-corrected compactifications of the heterotic string with line bundles,” *JHEP* **06** (2005) 020, [arXiv:hep-th/0504232](#).
- [186] R. Blumenhagen, S. Moster, and T. Weigand, “Heterotic GUT and standard model vacua from simply connected Calabi-Yau manifolds,” *Nucl. Phys.* **B751** (2006) 186–221, [arXiv:hep-th/0603015](#).
- [187] L. Borisov, “Towards the Mirror Symmetry for Calabi-Yau Complete intersections in Gorenstein Toric Fano Varieties,” [arXiv:alg-geom/9310001](#).

- [188] V. V. Batyrev and L. A. Borisov, “Dual cones and mirror symmetry for generalized Calabi-Yau manifolds,” [arXiv:alg-geom/9402002](#).
- [189] V. V. Batyrev and L. A. Borisov, “On Calabi-Yau Complete Intersections in Toric Varieties,” [arXiv:alg-geom/9412017](#).
- [190] M. Kreuzer, E. Riegler, and D. A. Sahakyan, “Toric complete intersections and weighted projective space,” *Journal of Geometry and Physics* **46** no. 2, (2003) 159 – 173.
- [191] A. Klemm, M. Kreuzer, E. Riegler, and E. Scheidegger, “Topological string amplitudes, complete intersection Calabi-Yau spaces and threshold corrections,” *JHEP* **05** (2005) 023, [arXiv:hep-th/0410018](#).
- [192] D. A. Cox and S. Katz, *Mirror Symmetry and Algebraic Geometry*. American Mathematical Society, 1999.
- [193] D. Robbins and S. Sethi, “A barren landscape,” *Phys. Rev.* **D71** (2005) 046008, [arXiv:hep-th/0405011](#).
- [194] R. Kallosh, A.-K. Kashani-Poor, and A. Tomasiello, “Counting fermionic zero modes on M5 with fluxes,” *JHEP* **06** (2005) 069, [arXiv:hep-th/0503138](#).
- [195] E. Bergshoeff, R. Kallosh, A.-K. Kashani-Poor, D. Sorokin, and A. Tomasiello, “An index for the Dirac operator on D3 branes with background fluxes,” *JHEP* **10** (2005) 102, [arXiv:hep-th/0507069](#).
- [196] P. K. Tripathy and S. P. Trivedi, “D3 Brane Action and Fermion Zero Modes in Presence of Background Flux,” *JHEP* **06** (2005) 066, [arXiv:hep-th/0503072](#).
- [197] N. Saulina, “Topological constraints on stabilized flux vacua,” *Nucl. Phys.* **B720** (2005) 203–210, [arXiv:hep-th/0503125](#).
- [198] D. Tsimpis, “Fivebrane instantons and Calabi-Yau fourfolds with flux,” *JHEP* **03** (2007) 099, [arXiv:hep-th/0701287](#).
- [199] L. Susskind, “The anthropic landscape of string theory,” [arXiv:hep-th/0302219](#).
- [200] C. Vafa, “The string landscape and the swampland,” [arXiv:hep-th/0509212](#).
- [201] H. Ooguri and C. Vafa, “On the Geometry of the String Landscape and the Swampland,” *Nucl. Phys.* **B766** (2007) 21–33, [arXiv:hep-th/0605264](#) [[hep-th](#)].
- [202] R. Bousso and J. Polchinski, “Quantization of four-form fluxes and dynamical neutralization of the cosmological constant,” *JHEP* **06** (2000) 006, [arXiv:hep-th/0004134](#).
- [203] W. Fulton, *Introduction to Toric Varieties*. Princeton University Press, 1993.

- [204] K. Hori, S. Katz, A. Klemm, R. Pandharipande, R. Thomas, C. Vafa, R. Vakil, and E. Zaslow, *Mirror Symmetry*, vol. 1 of *Clay Mathematics Monograph*, ch. Toric Geometry for String Theory. AMS Clay Mathematics Institute, 2003.
- [205] D. A. Cox, J. B. Little, and H. Schenck, *Toric Varieties*. American Mathematical Society, 2011. <http://www.cs.amherst.edu/~dac/toric.html>. Scheduled for publication in spring 2011.
- [206] M. Kreuzer and H. Skarke, “PALP: A Package for Analyzing Lattice Polytopes with Applications to Toric Geometry,” *Comput. Phys. Commun.* **157** (2004) 87–105, [arXiv:math/0204356](https://arxiv.org/abs/math/0204356).
- [207] J. Rambau, “TOPCOM: Triangulations of Point Configurations and Oriented Matroids,” in *Mathematical Software—ICMS 2002*, A. M. Cohen, X.-S. Gao, and N. Takayama, eds., pp. 330–340. World Scientific, 2002.
- [208] W. Stein *et al.*, *Sage Mathematics Software*. The Sage Development Team, 2010. <http://www.sagemath.org>.
- [209] D. R. Grayson and M. E. Stillman, “Macaulay2, a software system for research in algebraic geometry.” <http://www.math.uiuc.edu/Macaulay2/>.
- [210] M. Kreuzer, “Toric Geometry and Calabi-Yau Compactifications,” *Ukr. J. Phys.* **55** (2010) 613, [arXiv:hep-th/0612307](https://arxiv.org/abs/hep-th/0612307).
- [211] S. Reffert, “The Geometer’s Toolkit to String Compactifications,” [arXiv:0706.1310](https://arxiv.org/abs/0706.1310) [hep-th].
- [212] T. Rahn and H. Roschy, “Cohomology of Line Bundles: Proof of the Algorithm,” *J. Math. Phys.* **51** (2010) 103520, [arXiv:1006.2392](https://arxiv.org/abs/1006.2392) [hep-th].
- [213] S.-Y. Jow, “Cohomology of toric line bundles via simplicial Alexander duality,” [arXiv:1006.0780](https://arxiv.org/abs/1006.0780) [math.AG].
- [214] “**cohomCalg** package.” Download link, 2010. <http://wwwth.mppmu.mpg.de/members/blumenha/cohomcalg/>. High-performance line bundle cohomology computation based on [91].
- [215] P. Griffiths and J. Harris, *Principles of Algebraic Geometry*. Wiley-Interscience, 1994.
- [216] V. Braun, “On Free Quotients of Complete Intersection Calabi-Yau Manifolds,” [arXiv:1003.3235](https://arxiv.org/abs/1003.3235) [hep-th].
- [217] M. Cvetič, I. Garcia-Etxebarria, and J. Halverson, “On the computation of non-perturbative effective potentials in the string theory landscape – IIB/F-theory perspective,” [arXiv:1009.5386](https://arxiv.org/abs/1009.5386) [hep-th].
- [218] P. Shanahan, *The Atiyah-Singer Index Theorem*. Springer, Berlin, 1978.